Investigating the evolution and function of LWY effectors in *Phytophthora* pathogens

Yufei Li

Thesis submitted to the University of East Anglia for the Degree of

Doctor of Philosophy

Jan 2025

Table of Contents

Abstract

Successful colonization on hosts depends on pathogen secreted virulence proteins, termed effectors. For the devastating *Phytophthora* pathogens, many effectors are composed of tandem repeats of the (L)WY motif. Each (L)WY unit forms a conserved 3 or 5 α-helical bundle. Multiple units can be concatenated through a conserved linkage to form the WY1-(LWY)n architecture. Despite the structural conservation, the (L)WY units are sequence-wise variable, leading to the hypothesis that they may mediate diverse interactions with host molecules. Shuffling of these (L)WY units further promotes functional diversification. In this thesis, I examined the role of (L)WY tandem repeats in promoting effector evolution in *Phytophthora*.

I identified (L)WY-encoding sequences across five *Phytophthora* species, revealing 73-173 LWY effector genes per genome. 15%-63% of these LWY genes encode proteins lacking the N-terminal secretion Signal Peptide (SP), with a subset also missing the host-targeting RxLR motif. This suggests these variants may serve as a genetic reservoir for unit recombination or be secreted through non-canonical mechanisms. The LWY genes form multi-gene clusters, potentially facilitating recombination. I identified a recombination event in which two (L)WY effectors recombined to form a hybrid effector. Analysis of host targets revealed both shared and unique host interactors with the “parent” and hybrid effectors, demonstrating recombination as a mechanism that drives the evolution of novel virulence activity in (L)WY effectors.

I classified the (L)WY units based on their surface residues and identified specific (L)WY-LWY combinations as potential functional modules using a co-occurrence analysis. Selected LWY effectors that carry these modules were further characterized for host interactors in *Nicotiana benthamiana* using immunoprecipitation and mass-spectrometry. In addition to the known PP2A-interacting module, this analysis revealed additional modules that may recruit E2 ligases in the host.

This thesis provides important insights into the modularity-driven evolution of pathogen effectors and reveals novel virulence mechanisms in *Phytophthora*.

List of Figures

List of Tables

Abbreviations

ACS	Acetyl-coenzyme A synthetase
ADP	Adenosine diphosphate
ADR1	Activated Disease Resistance 1
AIM	ATG8-interaction motif
ATG8	Host autophagy-related 8
ATP	Adenosine triphosphate
Avh	Avirulence homolog
AVR	Avirulence
BAK1	BRI1-associated receptor kinase 1
bHLH	basic Helix-Loop-Helix
BR	Brassinosteroid
CC	Coiled-coil
CD	Conditionally dispensable
DNA	Deoxyribonucleic acid
EDS1	Enhanced disease susceptibility 1
EFR	Elongation factor-thermo unstable receptor
elf18	Epitope of the bacterial elongation factor Tu
ETI	Effector-triggered immunity
flg22	Flagellin 22
FLS2	Flagellin-sensing 2
FOLD	Fol dual-domain
GSR	Gene sparse regions
HDAC5	Histone deacetylase 5
HMA	Heavy metal-associated
HMM	Hidden Markov model
HR	Hypersensitive response
IP-MS	Immunoprecipitation-Mass Spectrometry
LARS	Leptosphaeria Avirulence and Suppressing
LRR	Leucine-rich repeat
LS	Lineage-specific
LysM	Lysin motif
MAMP	Microbe-associated molecular pattern
MAPK	Mitogen-activated protein kinase
MAPKKKK	Mitogen-activated protein kinase kinase kinases
MAX	*Magnaporthe* Avrs and ToxB-like
miRNA	microRNA
MLA	Mildew locus A

MPMI	Microbe-plant molecular interactions
Nep1	Necrosis and Ethylene-inducing Peptide 1
NLP20	Necrosis and Ethylene-inducing peptide 1-like protein 20
NLR	Nucleotide-binding LRR receptors
NRC	NLR required for cell death
PAD4	Phytoalexin deficient 4
PAMP	Pathogen-associated molecular pattern
PBL17	PBS1-like 17
PBL8	PBS1-like 8
PERU	Pep-13 receptor unit
PP2A	Protein phosphatase 2A
PRR	Pattern recognition receptor
PSR1	*Phytophthora* suppressors of RNA silencing *1*
PSR2	*Phytophthora* suppressors of RNA silencing *2*
R gene	Resistance gene
RALPH	RNase-like Proteins Associated with Haustoria
RLCK	Receptor-like cytoplasmic kinase
RLK	Receptor-like kinase
RLP	Receptor-like protein
RNA	Ribonucleic acid
ROS	Reactive oxygen species
Rps	Resistance to *Phytophthora* sojae
RVDs	Repeat variable diresidues
S gene	Susceptibility gene
SP	Signal peptide
TAL effector	Transcription activator-like effector
TIR	Toll/Interleukin-1 receptor
TOL9a	Target of Myb 1-like protein 9a
UBC	Ubiquitin conjugation
WT	wildtype

Acknowledgments

First and foremost, I would like to thank my supervisor, Dr. Wenbo Ma. Your mentorship has been transformative through your patience in training me and the many opportunities you've provided for collaborations and conferences. You've helped me grow not just as a researcher but also introduced me to a wonderful scientific community I never thought I'd be part of.

I am grateful to my second supervisor, Dr. Sophien Kamoun. Your insights about what makes science exciting and your career guidance have been invaluable in shaping my scientific journey.

To my previous mentors Dr. Yuanchao Wang, Dr. Suomeng Dong, Dr. Wenwu Ye, Dr. Long Lin, and Dr. Ruqiang Cui, thank you for laying the foundation of my academic journey. Your early encouragement gave me the confidence to pursue this path.

Thank you to my collaborators, Dr. Jonathan Jones, Dr. Suomeng Dong, Dr. Wenwu Ye, Dr. Xiao Lin, Dr. Haidong Shu, Dr. Zhichao Zhang, Dr. Robert Heal and Dr. Fan Zhang for sharing your data and insights. Particular thanks go to Jan Sklenar and Dr. Frank Menke from the proteomics team for their wonderful collaboration and support.

My time at UC Riverside and The Sainsbury Laboratory has been shaped by amazing colleagues. I'm grateful to Dr. Yi Zhai for helping me settle in and always being there, you're amazing. Thanks to Dr. Min Qiu, Dr. Li Feng, Dr. Min Wang, Dr. Bozeng Tang, Dr. Xiaodong Fang, Dr. Hui Li, Dr. Nicola Atkinson, Dr. He Zhao, Dr. Jianhua Huang, Dr. Guanghao Guo, Dr. Amelia Lovelace, Dr. Michelle Hulin, and Dr. Yingnan Hou for being both mentors and friends. To our postdocs Dr. Agustina de Francesco, Dr. Kelley Clark, Dr. Eva Hawara, Dr. Morgan Halane, Dr. Alexandre Leary, and Dr. Danxia He, thanks for all the enriching discussions. And to Jennie Yang, Dr. Jessica Trinh, Dr. Fan Qi, Dr. Ben Koch, Rita Archibong, and Renzo Villena-Gaspar, your kindness made the lab feel like home.

Special thanks to Dr. Wenbo Ma, Dr. Min Wang, Dr. Alexander Joseph McClelland, AmirAli Toghani, and Dr. Bozeng Tang for reviewing my thesis drafts and helping improve this work.

The TSL community has been wonderful. Thanks to my student buddy Dr. Mauricio P. Contreras for the smooth start, to Dr. Joe Win for always making time for scientific discussions, and to Hsuan Pai and Adeline Harant for sharing both plants and laughter. I would like to acknowledge everyone at TSL and all the support teams who have made this work possible.

A big shout out to Room 200 (Mamoun office), your friendship, and positive energy made every day brighter. From scientific discussions to Cork Cup Ball games, from the infamous shame wall to inappropriate jokes, you all made our office a place of joy. Thanks to Shuang Yang, Xue Lve, Dr. Min Wang, Dr. Xinyu Zhang, Dr. Alexander Joseph McClelland, Josh Bennett, Lena Knorr, Dr. Diana Gómez de la Cruz, Dr. Sara Dorhmi, Attilio Pascucci, AmirAli Toghani, Dr. Mauricio P. Contreras and Andy Posbeyikian. Your company and friendship made this journey special.

To my family, Dad, thank you for your constant support. Mom, you bring so much joy to my life. My aunts, uncles, and especially grandma, your love and support mean everything to me.

To my dear housemates and friends, Dr. Shujuan Xu, Dr. Jianjun Zhu, Dr. Chen Ji and Dr. Yang Yue, our shared meals, TV shows, and laughter made our house truly feel like home.

To my friends back home Meiqing, Lan, Min, Yaning, Yuyin, Jiawei, Long, Dan, and Xiaohong, thank you for keeping our friendship strong across the distance.

As I conclude, I am profoundly grateful to have been on this remarkable journey and to have met such extraordinary people whom I admire, trust, and regard as role models. You are all like stars in my universe, each one bringing your unique light to my path. Let's keep shining together!

Chapter 1: General introduction

1.1 Phytophthora pathogens pose threat to food security.

The human population is projected to increase to 9.7 billion by 2050 with the food gap to be filled with at least 50% more for human consumption than from 2000 to 2050 (Bruinsma 2012). The dramatic demand for food, driven by population growth, increasing gaps in food supply and demand, and changing dietary patterns, puts immense pressure on agricultural systems and natural resources. Meeting this demand sustainably requires significant advances in improving agricultural productivity, farming practices, and food storage systems.

However, plant diseases exert a major burden on food security and agricultural productivity gains, leading to up to 30% yield loss in the five major crops (wheat, rice, maize, potato and soybean) globally (Savary et al. 2019). These losses significantly widen the gap between food supply and demand, particularly affecting staple crops that feed billions.

A particularly devastating group of plant pathogens are *Phytophthora* species, including many destructive pathogens, which infect a great variety of economically important crops and horticulture plants (Brasier et al. 2022). Together with advanced molecular tools, more than 200 *Phytophthora* species have been identified (Brasier et al. 2022). Each year, billions of dollars are lost worldwide due to *Phytophthora* diseases in the field.

Phytophthora infestans for instance, is the most devastating pathogen for potato yield loss, leading to 5% loss globally and can go up to 10% in specific regions, like the Indo-Gangetic Plain (Savary et al. 2019). This pathogen is historically notorious for triggering the infamous Irish Famine in 1845, killing approximately 1 million people. The population in Ireland nowadays remains less than three quarters of the pre-famine population. *Phytophthora sojae*, for example, causes stem and root rot on soybeans and is responsible for over 1 million tonnes loss of soybean production worldwide annually (Tyler 2007; Wrather and Koenning 2006). *Phytophthora capsici* was first described from infected chili pepper in 1922 but now is an important causative agent of disease on many

solanaceous, cucurbitaceous and malvaceous plants (Parada-Rojas et al. 2021). *Phytophthora ramorum* causes sudden oak death in the United States, which is responsible for $135 million in residential property losses over the past ten years (Kovacs et al. 2011).

How diseases develop depends on how fast pathogens adapt to hosts and environments, which depends on several layers of factors, such as disease spread, agriculture practice, climate, fungicide and cultivars used.

Trade and transport help pathogens to reach new geographic regions rapidly. Many *Phytophthora* species are reported to transmit via nursery trade. Surveys in Maryland revealed 15 *Phytophthora* species on plants imported from West Coast suppliers (Bienapfl 2013). Similarly, UK nursery monitoring identified 63 species, including quarantine organisms and novel species, with *P. ramorum* dominating (Green et al. 2021). The identification of *Phytophthora pachypleura* on French-imported *Aucuba japonica* in Italian nurseries further illustrates how commercial plant movement enables cross-border *Phytophthora* spread (Henricot et al. 2014). The global spread of *Phytophthora* pathogens through trade and transport intensifies economic impacts across both established and newly colonized regions.

Besides globalization, monoculture also facilitates the fast adaptation of pathogens to the agricultural ecosystem by maintaining the uniformity of the host population and environment. In the agricultural ecosystem, crop pathogens favour specific domesticated hosts and transmit more easily than in the natural eco-system. Therefore, the dispersal of pathogens causes epidemics of disease globally (McDonald and Stukenbrock 2016). Soybeans are more frequently monocultured than other crops, causing a great reduction in the soybean yield (de Groot et al. 2021). In consecutive five-year trials, *Phytophthora megasperma* infection caused progressive yield decline in monoculture systems, with susceptible cultivars showing a 39.2% reduction and tolerant cultivars experiencing a 16.7% decrease in yield by the fifth year (T. Anderson, R. 1985). Therefore, the monocultural agriculture system allows *Phytophthora* pathogens to better adapt to hosts, therefore further reducing crop yield.

Current agricultural disease management relies heavily on two approaches: the application of single-site antifungal compounds and the deployment of crop varieties carrying individual major resistance (R) genes to recognize pathogen virulence factors, namely effectors. Plant R genes provide immunity against *Phytophthora* species through

recognition of specific pathogen effectors. In soybean, R genes Rps1a (Resistance to *Phytophthora sojae 1a*) and Rps1k confer resistance to *P. sojae* by detecting the effectors Avr1a, Avr1k, and Avr1b (Qutob et al. 2009; T. Song et al. 2013). Similarly, Solanum R genes Rpi-blb1, Rpi-blb2, Rpi-amr1, and Rpi-amr3 recognize corresponding *P. infestans* effectors Avr-blb1, Avr-blb2, Avramr1, and Avramr3, respectively (Champouret et al. 2009; X. Lin et al. 2020; X. Lin et al. 2022; Oh et al. 2009; Witek et al. 2021). However, such resistance can be broken down when plant pathogens evolve to evade or suppress R gene recognition. This is evident in *Phytophthora* species, as demonstrated by three widely deployed Rps genes losing efficacy against *P. sojae* in three of the four major soybean-producing nations: United States, Argentina, and Canada (McCoy et al. 2023). *Phytophthora* effectors recognized by R genes escape such recognition via various mechanisms such as sequence polymorphisms, gene silencing, gene deletions and frameshift mutations (Dong et al. 2011; Na et al. 2013; Qutob et al. 2013; T. Song et al. 2013; Wang. et al. 2020).

Additionally, chemical pesticides demand increasing costs annually due to the emergence of pesticide-resistant populations (Kovacs et al. 2011). Therefore, understanding the interactions between *Phytophthora* pathogens and hosts is the key to bringing in a new strategy for disease management, which will eventually improve food security.

1.2 Infection process of *Phytophthora* pathogens.

The *Phytophthora* genus belongs to the *Oomycota* phylum and *Peronospora* order, with the vast majority of species being plant pathogens (Beakes et al. 2012; Hardham and Blackman 2018). Despite having similar filamentous hyphae and overall similar lifestyles with fungi, *Phytophthora* pathogens are classified as stramenopiles together with diatoms and brown algae, which are evolutionarily distinct from fungi.

Phytophthora species can reproduce both sexually and asexually. *Phytophthora* pathogens can be self-fertile (homothallic) or require two compatible mating types A1 and A2 (heterothallic) to reproduce sexually. A1 and A2 are bisexual and can both act as male or female during outcrossing or selfing (Anna-Liisa Fabritius 1997). Oospores, the thick-walled sexual spores, are formed when the oogonium (female organ) is fertilized by an antheridium (male organ) in heterothallic *Phytophthora* species (Figure 1.1). For homothallic pathogens, the oospores will come from a single mating type. These resilient structures can persist in soil for years.

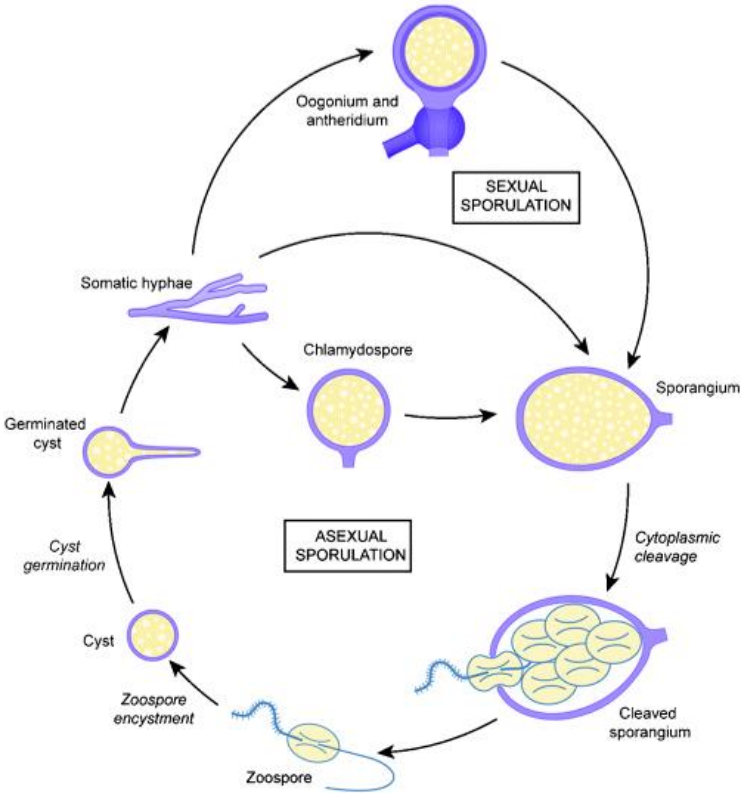

Figure 1.1 Lifecycle of *Phytophthora* species.

Here the lifecycle of *Phytophthora cinamomi* was used to illustrate the development of sexual and asexual reproduction. Figure was adapted from Hardham (2005).

Another thick-wall structure for long-term survival is the chlamydospore, an asexual spore that can survive in extreme environments (such as low temperatures) and germinate in conducive conditions for reproduction during asexual propagation. Besides that, the asexual life cycle requires other asexual spores like sporangia and zoospores to complete. In the presence of water, chlamydospores germinate to form sporangia, which are multinucleate spores that can disperse by wind and water.

Sporangia can either directly germinate or release one-celled swimming zoospores to attach to root surfaces. These zoospores can disperse with flood and rain or be transmitted by living hosts. When encountering compatible hosts, zoospores will stop swimming and land on hosts to form cysts. Following germination, cysts develop germ tubes that subsequently differentiate into appressoria, specialized structures that facilitate host cell penetration.

Many *Phytophthora* pathogens are hemi-biotrophic, meaning the infection initiates from the biotrophic stage for nutrition up-taking using invasive hyphae and switches to the necrotrophic phase by killing the host cells. To establish successful infections, *Phytophthora* pathogens form specialized haustoria that deliver effectors to suppress plant immunity, thereby evading host immune responses.

1.3 The plant immune system.

Plants are exposed to biotic stresses from various pathogens, including bacteria, viruses, fungi, oomycetes and nematodes. However, plants remain healthy in most scenarios, attributed to a robust plant immune system based on efficient recognition of potential pathogens.

Indeed, plants have developed a sophisticated two-layered immune system to combat pathogen infections, namely pattern-triggered immunity (PTI) and effector-triggered immunity) (ETI). PTI is activated when cell surface pattern recognition receptors (PRRs) detect conserved pathogen- or microbe- associated molecular patterns (PAMPs or MAMPs), while ETI occurs when intracellular receptors recognize pathogen-secreted virulence factors known as effectors.

PRR genes encode either receptor-like kinases (RLKs) or receptor-like proteins (RLPs) that lack a kinase domain. The first identified cell surface receptor was Arabidopsis flagellin-sensing 2 (FLS2), which responds to a 22-amino-acid bacterial flagellin peptide flg22. FLS2 is a RLK, comprising an extracellular leucine-rich-repeat (LRR) domain, a trans-membrane domain and an intracellular serine/threonine protein kinase domain (Bleecker 2001; Gomez-Gomez and Boller 2000). The perception of flg22 induces a heteromeric complex with FLS2 and a co-receptor BAK1, another LRR-RLK brassinosteroid (BR) insensitive 1-associated kinase 1, initiating the plant innate immunity (Chinchilla et al. 2007; Heese et al. 2007). Most PRRs show one-to-one recognition of ligands, like FLS2 and flg22, the epitope of the bacterial elongation factor Tu (elf18) to ELONGATION FACTOR-THERMO UNSTABLE RECEPTOR (EFR), NECROSIS AND ETHYLENE-INDUCING PEPTIDE1-LIKE PROTEIN 20 (NLP20) to RECEPTOR-LIKE PROTEIN 23 (RLP23) and Pep-13 to Pep-13 receptor unit (PERU), etc (Albert et al. 2015; Ascurra et al. 2023; Gomez-Gomez and Boller 2000; Zipfel et al. 2006). The downstream signalling induced by PTI includes reactive oxygen species (ROS) production, mitogen-activated protein kinase (MAPK) cascades, callose deposition, calcium influx, plant hormone signalling and the production of antimicrobial compounds (Y. Peng et al. 2018; Thulasi Devendrakumar et al. 2018; Tsuda and Katagiri 2010).

To establish a successful colonization, pathogens secrete diverse effector repertoires to suppress PTI (Boller and He 2009; Bouwmeester et al. 2011; Hogenhout et

al. 2009; Irieda et al. 2019; Shan et al. 2008; Zheng et al. 2018). In response, plants employ intracellular nucleotide-binding domain leucine-rich repeat-containing receptors (NLRs) that recognize these effectors directly or indirectly, activating ETI and localized hypersensitive response (HR) that effectively blocks disease progression (J. D. Jones and Dangl 2006). Additional ETI outputs converge with PTI on many downstream signalling outputs, such as Ca^{2+} influx, MAPK cascades, ROS burst, etc, suggesting the intricate interactions of PRR and NLR-mediated immune responses. For example, a recent study indicated the mutual potentiation of PTI and ETI, showing that PTI is indispensable for bacteria-triggered ETI while ETI restores and enhances PTI (Ngou et al. 2021; Ngou et al. 2022b; Ngou et al. 2022a; Yuan et al. 2021). A new Zig-Zag model was proposed to incorporate the two-layer crosstalk (J. D. Jones and Dangl 2006; Ngou et al. 2022a). This multi-layered immune system enhances the robustness of plant immunity, effectively countering co-evolving pathogen effectors. The knowledge of PRR and NLR functions and crosstalk increases our capacity to discover more ways to engineer durable resistance (J. D. G. Jones et al. 2024; Ngou et al. 2022b).

1.4 *Phytophthora* pathogens employ fast-evolving effectors to overcome the plant immune system.

The “Gene-for-gene” model was initially proposed by H.H. Flor suggesting that for a gene that confers to resistance in the host (R gene), there will be another dominant gene in the pathogen contributing to pathogenicity, termed avirulence gene (FLOR 1971). After that, the first avirulence factor was cloned from *Pseudomonas syringae* (Staskawicz et al. 1984). While AVR genes trigger plant immunity when recognized by corresponding R genes, many also function as virulence factors promoting infection in plants lacking R genes. For instance, the *P. syringae* AVR gene avrBs2 enhances bacterial growth in susceptible hosts but triggers resistance in plants carrying the Bs2 resistance gene (Kearney and Staskawicz 1990). This dual role explains why pathogens maintain AVR genes despite their potential to be recognized by host immune system.

Effectors are classified into two distinct groups based on their localization: cytoplasmic effectors that function within host cells and apoplastic effectors that operate in the extracellular space between cells (Blackman et al. 2015; Dye and Bostock 2021; Judelson and Ah-Fong 2019; S. Wang et al. 2017). *Phytophthora* pathogens secrete apoplast effectors like plant cell wall-degrading enzymes, extracellular protease inhibitors and small cysteine-rich (SCR) proteins (Hein et al. 2009; Z. Ma et al. 2015; Z. Ma et al. 2017; M. Tian et al. 2004; M. Tian et al. 2005). The cytoplasmic effectors in *Phytophthora* mainly include RxLR effectors and CRN effectors (Fabro 2022). RxLR effectors contain an N-terminal Signal Peptide (SP), a conserved RxLR motif (Arg–any residue–Leu–Arg), a downstream Glu–Glu–Arg motif (EER) motif and an effector domain (R. G. Anderson et al. 2015; McGowan and Fitzpatrick 2017). CRN effectors encode an SP, the LxLFLAK domain and the HVLVVVP motif in a DWL domain (Haas et al. 2009; Win et al. 2007).

These effector arsenals actively interfere with host defense to promote pathogen proliferation (Bos et al. 2010; Latorre et al. 2020; Qutob et al. 2013; Sanchez-Vallet et al. 2018; B. Yang et al. 2017). Indeed, numerous cases of rapid breakdown of disease resistance have been observed (Fry 2008; McCoy et al. 2023). These effectors tend to locate in repeat-rich genome regions. According to the proposed two-speed genome, the essential genes are shielded in the core genome to avoid deleterious mutations

while the effectors are located in a specific genome compartment (repeat-enriched and gene-sparse regions) to facilitate fast evolution (Croll and McDonald 2012; Dong et al. 2015; Haas et al. 2009). The compartmentalized distribution of effector genes in gene-sparse regions enables *P. infestans* and its three sister species to accumulate adaptive mutations at higher rates without compromising essential gene functions (Raffaele et al. 2010).

A wealth of RxLR effectors located within these regions, and the RxLR effectors adopt diversified strategies to overcome the host recognition by gene duplication/recombination, deletion/insertion, and point polymorphisms (Goss et al. 2013; F. Zhang et al. 2021). For instance, a *P. sojae* RxLR effector Avh238 displayed the sequence polymorphism in isolates P6497 and P7076. PsAvh238^{P6497} can trigger cell death in *N. benthamiana*, while Avh238^{P7076} cannot. Amino acid sequence comparison indicates a 79th residue is essential for the PsAvh238^{P6497} triggered HR (Hypersensitive Response) (B. Yang et al. 2017). These virulence factors display high sequence polymorphisms and normally show high nonsynonymous to synonymous mutation rates (dN/dS ratio), which contributes to the gain or loss of function of these effectors. For example, 13 residue polymorphisms in PiAVR2 and PiAVR2-like, a *P. infestans* effector recognized by the potato R2 gene, contribute to the escape of R2 recognition (Oh et al. 2009). Some AVRs also undertake mutation but do not necessarily result in a significant loss in pathogenicity. One of the reasons is that effectors can function redundantly, or another new allele emerges to replace the function.

Effectors can rapidly adapt to the host not only in a sequence-based manner but also by employing post-transcriptional and epigenetic regulation. Avr3a undergoes small RNA-mediated gene silencing and regain virulence in Rps3a plants (Qutob et al. 2013). A subunit of the H3K27me3 methyltransferase complex was reported to be involved in the suppression of Avr1b transcription (Wang. et al. 2020). The post-transcriptional and epigenetic regulation benefit the pathogen by evading host recognition while maintaining the effectors in the gene pool. These reversible regulations may lower the cost of loss-of-function mutations of AVRs and therefore increase the plasticity of the effector evolution.

Dynamic repertoires of secreted proteins can vary between *Phytophthora* sister species, indicating effector fast evolution benefit pathogens for better colonization (McGowan and Fitzpatrick 2017). Therefore, understanding the effector evolution will

enable us to dissect the emergence of effector novel functions, which can ultimately be leveraged to establish sustainable resistance in crops.

1.5 RxLR effectors are important models to study effector biology.

All the currently known AVRs belong to the RxLR effector family (R. G. Anderson et al. 2015; McGowan and Fitzpatrick 2017). RxLR effectors consist of a SP, a conserved RxLR-EER motif and an effector domain (Figure 1.3A) (R. G. Anderson et al. 2015; McGowan and Fitzpatrick 2017). Using sequence features in the N termini, RxLR effectors can be accurately predicted from *Phytophthora* genomes. Analysis of six *Phytophthora* species reveals about 2,000 RxLR effectors (Ai et al. 2020; Haas et al. 2009; Jiang et al. 2008; Lamour et al. 2012; Studholme et al. 2019; Ye et al. 2016). Some of these effectors have been investigated for virulence functions and evolution. As such, *Phytophthora* RxLR effectors have served as an important model to advance our understanding of plant-pathogen interaction at the molecular level. Here, I summarized the modes of action of RxLR effectors.

1.5.1 RxLR effectors modulate plant gene expression and silencing.

Plant transcriptional regulation of defence gene expression is a hallmark of PTI and ETI during pathogen infection. To manipulate this process, oomycete pathogens secrete RxLR effectors to manipulate defence gene expression or induce the expression of susceptible genes by targeting transcription factors, transcriptional regulators and RNA silencing machinery.

The *P. infestans* effector AVR2 enhances pathogen virulence by upregulating the potato bHLH transcription factor StCHL1, which is a brassinosteroid (BR) signalling marker gene (Turnbull et al. 2017). The *Hyaloperonospora arabidopsidis* effector HaRxLL470 suppresses plant immunity by interfering with the DNA-binding capacity of HY5, a transcription factor that activates defence gene expression (S. Chen et al. 2021). The *P. sojae* effector PsAvh113 promotes infection by targeting the soybean transcription factor GmDPB for proteasomal degradation, thereby suppressing the expression of the immunity-related gene GmCAT1 (Zhu et al. 2023). *Phytophthora* effectors manipulate host transcription through multiple mechanisms, targeting both transcription factors

directly and modulating their regulatory complexes to suppress plant immunity. The *P. sojae* effector PsAvh110 suppresses immunity by disrupting nuclear complex assembly, specifically preventing the interaction between transcriptional regulators GmLHP1-2 and GmPHD6 to block defence gene activation (Qiu et al. 2023).

Phytophthora species deploy RxLR effectors to interfere with defence gene expression via the disruption of the RNA interference (RNAi) pathway to enhance susceptibility. RNA interference (RNAi) is a conserved biological process in which small RNA molecules, including siRNAs and miRNAs, deplete specific messenger RNAs in a sequence-dependent manner to regulate gene expression (Huppi et al. 2005; Rosa et al. 2018). Two *P. sojae* RxLR effectors PSR1 (*Phytophthora* suppressors of RNA silencing) 1 and PSR2 promote infection by interfering with RNA silencing through distinct mechanisms, with PSR1 interfering with miRNA maturation while PSR2 inhibits secondary small RNA biogenesis (He et al. 2019; Hou et al. 2019; Qiao et al. 2015; Xiong et al. 2014).

1.5.2 RxLR effectors manipulate plant protein cell trafficking.

Pathogen effectors frequently target host vesicle trafficking to prevent the secretion of defence molecules, as demonstrated by multiple *Phytophthora* effectors. The *P. infestans* PexRD12/31 effector family targets VAMP72 R-SNARE proteins, promoting endosome accumulation in infected tissues (Petre et al. 2021). A *P. capsici* effector RXLR242 suppresses immunity by targeting RAB GTPases to disrupt protein trafficking, preventing both pathogenesis-related protein secretion and membrane receptor localization through interference of RAB protein interactions (T. Li et al. 2022). The *P. sojae* effector PsAvh181 suppresses apoplastic immunity by disrupting vesicle trafficking through binding to GmSNAP-1, thereby interfering with its interaction with GmNSF and blocking the secretion of defence-related proteins (H. Wang et al. 2021).

1.5.3 RxLR effectors interfere with immune regulators.

Plant immunity against pathogens operates through multiple recognition layers. Plants detect conserved PAMPs from oomycetes, including transglutaminase (Pep13), β-glucans, cellulose-binding elicitor lectins, elicitins and the glycoside hydrolase XEG1 (Brunner et al. 2002; Gaulin et al. 2006; Klarzynski et al. 2000; Z. Ma et al. 2015; Sharp et al. 1984; L. M. YU 1995; L. Zhang et al. 2014). Additionally, plant R genes provide a second layer of defense by recognizing specific pathogen AVR factors, as exemplified by several well-characterized interactions in *Phytophthora* species. These include the recognition of *P. infestans* AVR3a by potato R3a and AVRblb1 by Rpi-blb1(Armstrong et al. 2005; Huang et al. 2005; van der Vossen et al. 2003; Vleeshouwers et al. 2008). Recent studies have identified potato R genes with broader recognition capacity, such as Rpi-amr1 and Rpi-amr3, which recognize conserved RxLR effectors across multiple *Phytophthora* species, demonstrating the evolution of more comprehensive resistance mechanisms (Ahn et al. 2023; X. Lin et al. 2022; Witek et al. 2016; Witek et al. 2021).

In response to plant immune surveillance, *Phytophthora* pathogens have evolved sophisticated strategies to suppress host defence responses. These effectors target multiple components of the immune signalling network (S. Wang et al. 2023c). For instance, three *P. infestans* effectors (SFI5, SFI6, and SFI7) suppress flg22-triggered immunity by interfering with MAP kinase activation in tomato (Zheng et al. 2014). Multiple effectors including a *P. infestans* RxLR effector AVRcap1b were reported to suppress the helper NLR required for cell death (NRCs), which are the central nodes of NRC networks (Derevnina et al. 2021; M. Y. Wang et al. 2023a). Enhanced Disease Susceptibility 1 (EDS1), a lipase-like protein in Arabidopsis, forms an immune complex with Phytoalexin Deficient 4 (PAD4) and Activated Disease Resistance 1 (ADR1) helper proteins to activate plant immunity (Feehan et al. 2020; Lapin et al. 2020; Pruitt et al. 2021). The *P. capsici* effector PcAvh103 disrupts plant immunity by binding to the EDS1 lipase domain, preventing EDS1-PAD4 complex formation (Q. Li et al. 2020). This highlights how pathogens have adapted to compromise key nodes in plant defence networks.

1.5.4 RxLR effectors modulate plant protein degradation.

Ubiquitination acts as a crucial regulator in plant immunity. The *P. sojae* effector Avr1d promotes *Phytophthora* infection by binding to and stabilizing the E3 ubiquitin ligase GmPUB13 in soybean, specifically competing with E2 enzymes to prevent GmPUB13 self-ubiquitination and subsequent degradation (Y. Lin et al. 2021b). The *P. infestans* effector Pi06432 suppresses salicylic acid-mediated immunity by stabilizing StUDP in potato, which in turn promotes degradation of the proteasome subunit StRPT3b, ultimately leading to reduced proteasome activity and decreased stability of the SA biosynthesis regulator StSARD1 (Z. Wang et al. 2023d). The *P. sojae* effector PsAvh238 suppresses plant immunity by destabilizing Type2 Acetyl-coenzyme A synthetase (ACS), thereby inhibiting ethylene biosynthesis which is essential for defence against *Phytophthora* infection (B. Yang et al. 2019). The *P. infestans* effector PITG20303, a virulent variant of AVRblb2, promotes infection by stabilizing the potato MAPK cascade protein StMKK1, which functions as a negative regulator of PTI (Du et al. 2021).

1.5.5 RxLR effectors manipulate plant protein phosphorylation.

Protein phosphorylation plays a central role in plant immune signalling, making it a key target for pathogen effectors. For example, the *P. capsici* effector RXLR25 compromises PTI by inhibiting phosphorylation of RLCK-VII proteins such as BIK1, PBL8, and PBL17, which serve as essential kinases in immune receptor complexes (Liang et al. 2021). Similarly, the *P. infestans* effector PexRD2 promotes infection by disrupting MAPK phosphorylation cascades, specifically targeting MAPKKK to prevent activation of downstream immune components (King et al. 2014). These examples illustrate how pathogens have evolved sophisticated mechanisms to manipulate host phosphorylation events and suppress defence responses.

1.6 (L) WY motif is prevalent in RxLR effectors.

Although many research efforts have been invested to understand the functions of RxLR effectors, the mechanisms by which RxLR effectors evolve such diverse modes of action remain unclear. This challenge is further complicated by the high variability in effector sequences. Gaining a deeper understanding of the evolutionary trajectories of these virulence factors will uncover how novel functions emerge.

Recently, comparative structure analysis has emerged as a powerful strategy to investigate sequence-unrelated but structurally similar effectors in fungal and oomycete pathogens. Conserved structural folds, like *Magnaporthe oryzae* Avrs and ToxB (MAX), Fol dual-domain (FOLD), the RNase-like Proteins Associated with Haustoria (RALPH), Leptosphaeria Avirulence and Suppressing (LARS) and ToxA have been found to be enriched in specific pathogens (de Guillen et al. 2015; De la Concepcion et al. 2018; Di et al. 2017; Franceschetti et al. 2017; Lazar et al. 2022; Ortiz et al. 2017; Outram et al. 2022; Sarma et al. 2005; Seong and Krasileva 2021; Spanu 2017; Teulet et al. 2023). AlphaFold-based structural prediction can be applied to proteomes to identify similar motifs from candidate effectors (Jumper et al. 2021).

Phytophthora species also were found to encode a repertoire of RxLR effectors with a conserved structural fold, called (L)WY (Figure 1.2). Hundreds of RxLR effectors encode single or tandem repeats of (L)WY motifs in the effector domains. Each motif folds into a 3 or 5-α-helical bundle with conserved W and Y residues or L, W, and Y residues in the buried backbones, therefore known as WY or LWY motifs, respectively (Figure 1.2) (Boutemy et al. 2011; X. R. Chen et al. 2019; Chou et al. 2011; B. Guo et al. 2019; He et al. 2019; Jiang et al. 2008; Lovelace et al. 2023; Maqbool et al. 2016; Win et al. 2012; Wood et al. 2020). Structural analysis reveals high similarity between WY and LWY motifs, as demonstrated by their superimposition. The key architectural difference lies in the LWY motifs containing two additional α-helices that constitute the L motif.

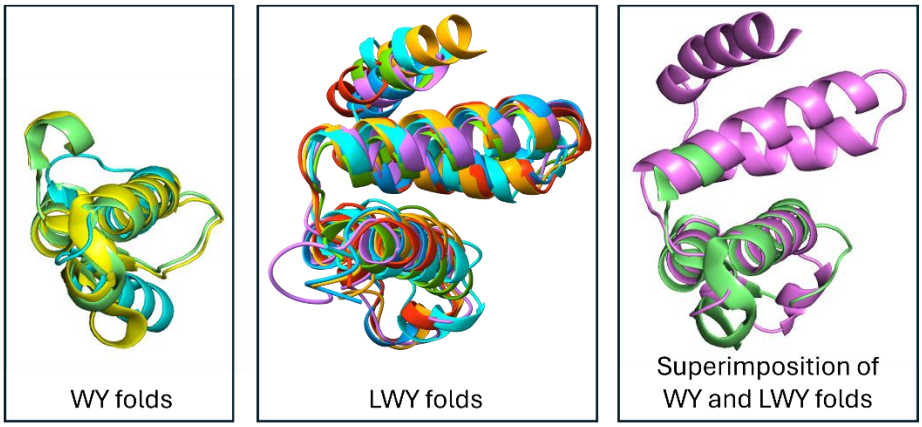

Figure 1.2 Conserved (L)WY folds are adopted by (L)WY effectors.

WY folds and LWY folds were extracted from PexRD54 and PsPSR2, respectively. WY folds contain a 3-α-helical bundle (left panel, RMSD=1.353 Å), while LWY folds feature a 5-α-helical bundle (center panel, RMSD=1.530 Å). Superimposition of WY1 from PexRD54 (in green) and LWY2 unit from PSR2 (in purple) (right panel, RMSD=1.090 Å).

1.7 Concatemeric organization of (L)WY motifs in RxLR effector domains.

Tandem repeats forming elongated WY1-(WY)n or WY1-(LWY)n architectures are named as WY effectors or LWY effectors, respectively. N represents the additional WY or LWY units following the initial one. WY effectors contain consecutive WY motifs throughout their length (Figure 1.3A). The majority (86%) of the WY effectors show two or three units while less than 4% have more than six WY units. Here, I showed a *P. infestans* WY effector PexRD54, which consists of five WY units and an AIM (ATG8-interaction motif) domain (Figure 1.3B) (Dagdas et al. 2016). The AIM domain of PexRD54 is responsible for the interaction with host ATG8. PexRD54 promotes pathogen nutrition by interacting with host ATG8 to redirect Rab8a-mediated vesicle trafficking toward pathogen feeding sites, effectively hijacking cellular resources (Pandey et al. 2021). Other than that, no additional WY effectors have been characterized with adopted domains, suggesting that WY units or unit combinations might be responsible for host manipulation (Boutemy et al. 2011; King et al. 2014).

In addition to the conserved helical bundle structure in (L)WY motifs, WY or LWY motifs are concatenated with adjacent LWY tandem repeats to form an elongated WY1-(LWY)n architecture through a conserved mechanism in LWY effectors (Figure 1.3A). LWY effectors typically contain more repeating units than WY effectors, with 31% harbouring four to five (L)WY units, suggesting these extended structures provide expanded interfaces for host protein interactions. A typical RxLR effector, PsPSR2 (*Phytophthora* suppressor of RNA silencing 2 in *P. sojae*) has the WY1-(LWY)6 architecture (Figure 1.3B) (He et al. 2019; Xiong et al. 2014). In PSR2, the presence of the "L" in LWY units forms conserved hydrophobic interactions with adjacent (L)WY units to enable the interunit connection, leading to the formation of a rigid, stick-like overall shape with a fixed orientation (Figure 1.3C) (He et al. 2019; H. Li et al. 2023). Despite sharing conserved WY residues that stabilize intra-unit structure, PexRD54 exhibits greater conformational flexibility compared to PSR2 due to the lack of inter-unit connections provided by the L motif found in LWY units (Figure 1.3C) (He et al. 2019; Maqbool et al. 2016). Like WY effectors, no additional protein domains were found in LWY effectors beyond the (L)WY motifs, suggesting these conserved units may serve as functional modules in host interactions. The rigid stick-like architecture of LWY effectors

can possibly provide an expanded molecular surface that facilitate interactions with multiple host proteins.

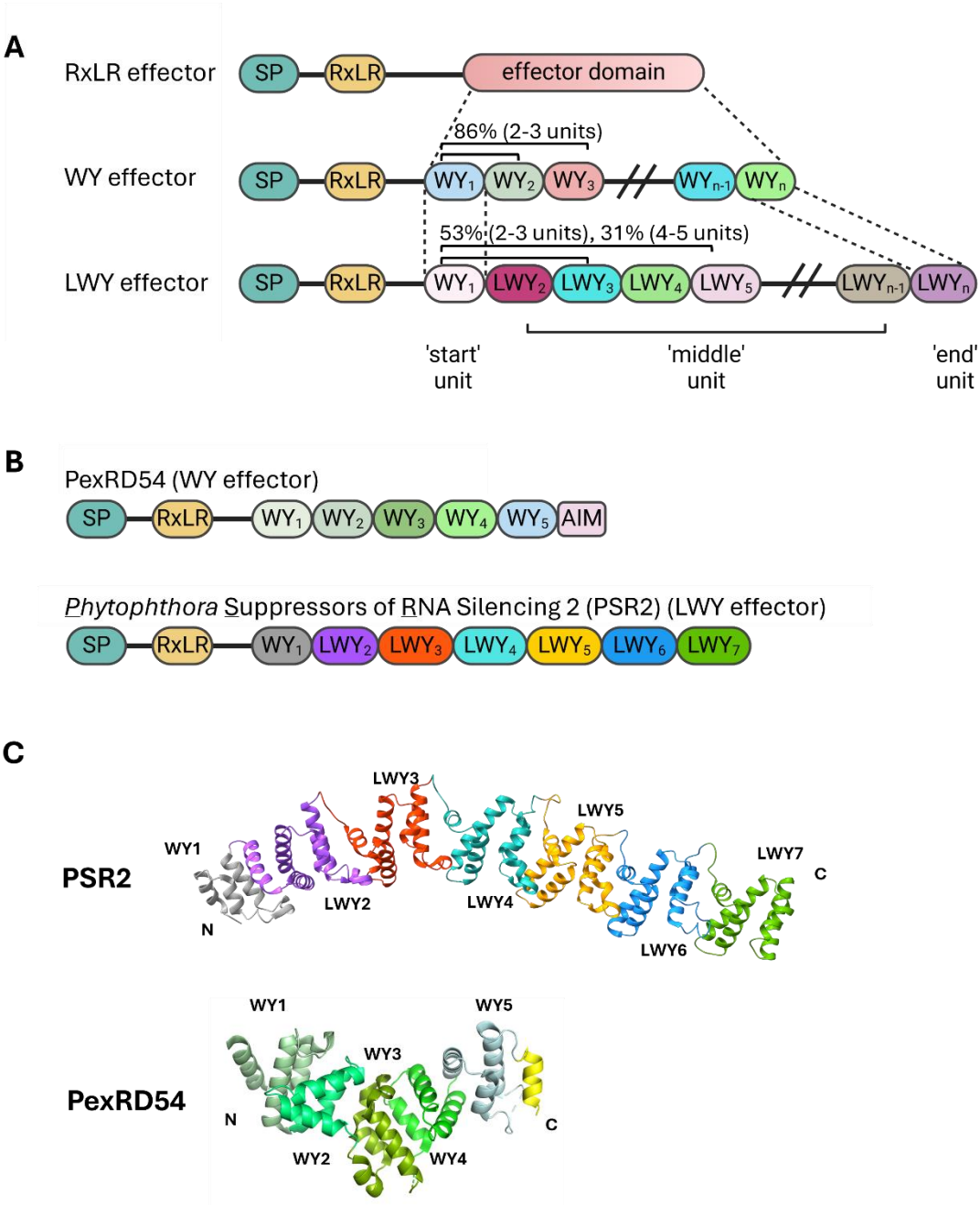

Figure 1.3 Domain and structural arrangement of RxLR effectors, WY effectors and LWY effectors.

(**A**) Domain organization of RxLR effectors containing WY and LWY motifs in their effector domains. LWY effectors possess a characteristic arrangement: an N-terminal WY1 motif (start unit), followed by multiple LWY motifs in the middle region, and terminating with a C-terminal LWY motif (end unit). In contrast, WY effectors contain consecutive WY

motifs throughout their length. All effectors include a signal peptide (SP) at their N-terminus. The distribution of repeating units for each effector type is indicated above their respective domain architectures. (**B**) PexRD54 and PsPSR2 are chosen to represent WY and LWY effector arrangement. The AIM (ATG8-interaction motif) domain in PexRD54 is responsible for host ATG8 protein interaction. (**C**) Crystal structure of PSR2 (5GNC) and PexRD54 (5L7S) were downloaded from PDB database. Individual (L)WY unit was labeled with different colors.

1.8 (L)WY units display diverse combinations in RxLR effectors.

To indicate the residue conservations in (L)WY units, the WebLogo shows the sequences extracted from each (L)WY unit from all predicted LWY effectors (Figure 1.4A) (He et al. 2019). The L, W and Y motifs were initially identified from avirulence homolog (*Avh*) genes in *P. sojae* and *P. ramorum* using protein sequences (Jiang et al. 2008). Structural analysis of the RxLR effectors PexRD2 and AVR3a11 revealed that while these proteins maintain a conserved core α-helical bundle containing a single WY module, they exhibit conformational flexibility in their overall structure (Boutemy et al. 2011). Notably, PexRD2 forms homodimers and displays surface variations compared to its *P. mirabilis* homolog, suggesting evolutionary adaptability while maintaining core structural integrity (Boutemy et al. 2011).

The crystal structure of PSR2 later demonstrated structural homology between its LWY motif and the WY motif from PcAVR3a11, while also revealing an extended L motif newly characterized by four conserved leucine residues (L1-L4) (Figure 1.4A). These L pocket residues show strong conservation in middle units but exhibit more variation in end units. This architectural pattern appears consistent across *Phytophthora* LWY-containing effectors, which typically feature a WY motif at their N-terminus (start unit) and a degenerated LWY motif at their C-terminus (end unit).

Although (L)WY units share similar structural features, their amino acid sequences exhibit considerable diversity. Sequence clustering of individual (L)WY units reveals different patterns of (L)WY unit combinations across LWY effectors (Figure 1.4B) (He et al. 2019). LWY effectors incorporate varying numbers of (L)WY units while maintaining conserved inter-unit interactions through hydrophobic contacts. This architectural diversity, combined with sequence variation between (L)WY units, may influence their capacity for host protein recruitment.

The (L)WY units with different sequences may possess different abilities to interact with host targets. Thus, (L)WY effectors adopting these varied unit combinations may recruit different host targets and promote functional diversification of (L)WY effectors (Figure 1.4B). This is supported by characterized (L)WY effectors that display distinct molecular functions. 13 LWY effectors, including PSR2, were reported to hijack host PP2A (serine/threonine protein phosphatase 2A) core enzymes to promote disease

(H. Li et al. 2023). The *P. infestans* LWY effector, AVRCap1b, encodes seven (L)WY tandem repeats formatting as WY1-(LWY)6 and associates with a membrane-bound protein NbTOL9a (Target of Myb 1-like protein 9a) to suppress NRC responses (Derevnina et al. 2021). The second WY unit in a *H. arabidopsidis* WY effector ATR1 is recognized by structurally distinct NLR receptors (Goritschnig et al. 2016). The *P. sojae* effector PSR1 relies on its single WY unit for suppressing host RNA silencing and binding to its target PINP1 (Qiao et al. 2015; P. Zhang et al. 2019).

Additionally, WY effectors can form homodimers to function. PexRD2 promotes *P. infestans* infection by targeting the host kinase MAPKKK. Mutations in variable regions in one WY fold simultaneously disrupt MAPKKK binding and abolish enhanced pathogen growth in *Nicotiana benthamiana*, suggesting that the WY unit in PexRD2 is a unit of function (King et al. 2014). The *P. sojae* WY effector PsAvh240 contains two WY units, where the first WY unit (WY1) determines effector plasma membrane localization and its second WY unit (WY2) mediates effector dimerization, both contribute to preventing host target secretion. Specifically, mutations on WY1 unit abolish the interaction with GmAP1 (soybean-resistant aspartic protease 1) and compromise pathogen virulence in soybean hairy roots, highlighting that WY1 in PsAvh240 is a functional unit (B. Guo et al. 2019).

Together, these examples demonstrate how sequence variations within conserved WY1-(LWY)n architectures enable diverse effector functions, suggesting (L)WY units may function as fundamental modules for different host target associations.

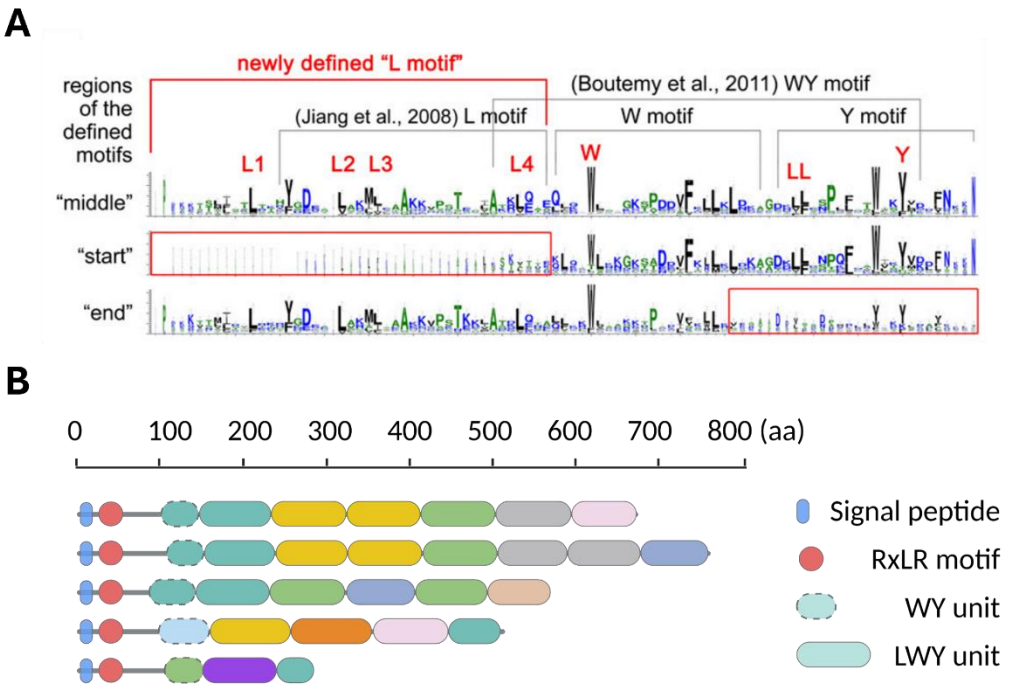

Figure 1.4 LWY effectors display mosaic patterns of tandem repeats by adopting varied (L)WY units.

(**A**) Sequence conservation analysis of start, middle, and end LWY units based on multiple sequence alignments of (L)WY units from predicted LWY effectors. Stack height represents the degree of sequence conservation at each position. Conserved leucine (L), tryptophan (W), and tyrosine (Y) residues that define each LWY unit are highlighted in red. Previously identified L, W, and Y motifs were labelled with the corresponding publications, while a novel L motif was newly characterized based on the PSR2 crystal structure from (He et al. 2019). (**B**) Unit compositions of the LWY effectors were labelled correspondingly. (L)WY units were clustered based on sequence similarity and labeled with different colors if belonging to different clusters. The starting WY units and the following LWY units are outlined with dashed and solid lines, respectively. Signal peptides and RxLR motifs are labeled as blue and red, respectively.

1.9 PP2A-interacting LWY effectors regulate host protein phosphorylation.

LWY effectors are composed of structurally similar, but surface residue diversified (L)WY units. It's likely that the diversity in different (L)WY units might determine the effector capacity of host protein interactions.

Our laboratory investigates effector host protein interactions using PsPSR2 as a probe. This effector contains seven tandem (L)WY repeats organized in a WY1-(LWY)6 arrangement. By analysing how different combinations of these (L)WY units mediate specific host protein interactions, we can identify what we term functional modules, which represent the (L)WY units or unit combinations required for recognizing and binding particular host targets (H. Li et al. 2023).

PsPSR2 targets the host PP2A holoenzyme, a key eukaryotic phosphatase that regulates diverse biological processes. PP2A requires a scaffolding A subunit, a regulatory B subunit, and a catalytic C subunit to form a heterotrimeric holoenzyme, which dephosphorylates phospho-peptides as substrates (Figure 1.5) (Bian et al. 2020; Brautigan 2013; O'Connor et al. 2018). PsPSR2 can effectively hijack the host protein phosphatase 2A (PP2A) A subunit and mimic the B subunit to form a functional effector-PP2A holoenzyme and promote disease (Figure 1.5). Importantly, the module combination LWY2-LWY3 in PSR2 forms an interaction interface with the PP2A A subunit. This PP2A-interacting pocket is also adopted by 12 other LWY effectors in *P. sojae* and *P. infestans*. Despite the interaction with the PP2A A subunit, the C terminal LWY units in the PP2A-interacting effectors have a high level of diversity in sequence and structure, suggesting a functional diversification of the effector-PP2A holoenzymes that may dephosphorylate different substrates. To investigate different effector-PP2A interactions, we conducted a comparative phospho-proteomic analysis of transgenic Arabidopsis lines expressing two PP2A-interacting effectors: PSR2 and PITG_15142. While both effectors interact with PP2A, PITG_15142 contains five tandem repeats (WY1-(LWY)4) and specifically uses its WY1-LWY2 region as the PP2A-binding interface. The results indicate peptides that have reduced phosphorylation in PsPSR2 and PITG_15142 are distinct, suggesting these two LWY effectors regulate phosphorylation in different sets of host proteins (Figure 1.5). This proves that PSR2 LWY2-LWY3 represents a functional

module that mediates the interactions with PP2A A subunits while the varied C terminal LWY modules recruit different substrates.

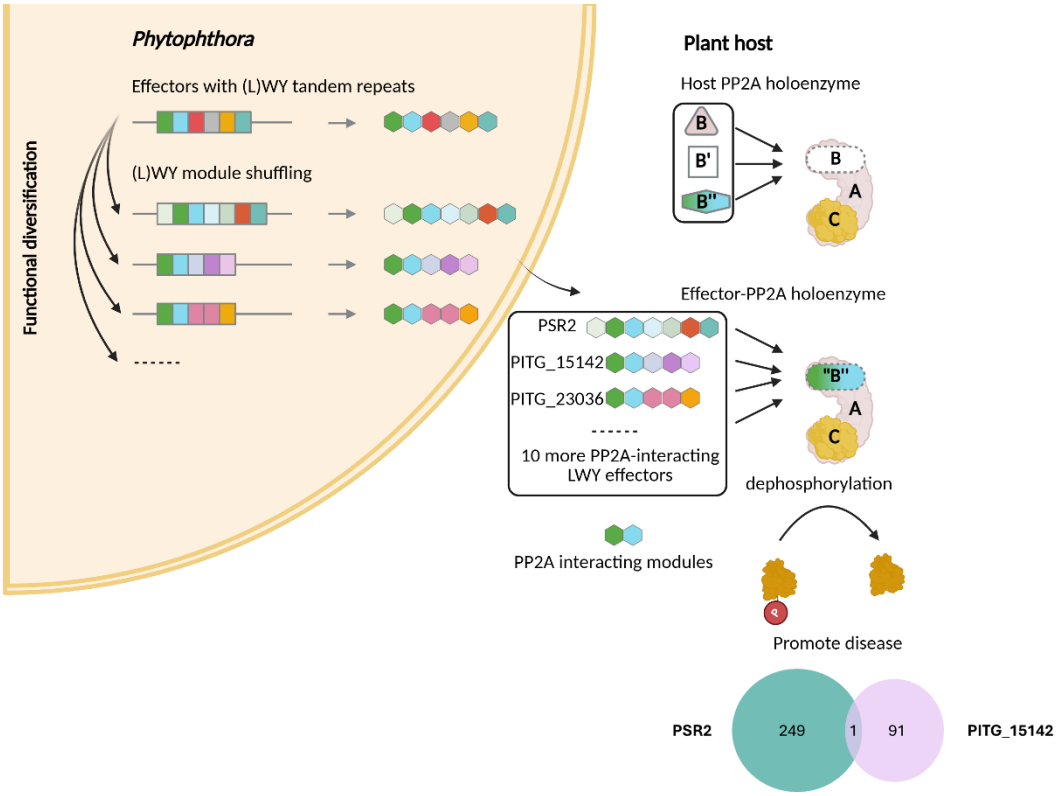

Figure 1.5 LWY effectors interact with host PP2A A subunit but regulate distinct phospho-peptides.

All the contents in this figure were modified from H. Li et al. (2023). The scheme shows PSR2, PITG_15142 and 11 other PP2A-interacting LWY effectors efficiently hijacking host PP2A core enzymes to form effector-PP2A holoenzymes, thus mimicking the host PP2A B subunit. The interface detected between the PP2A A subunit and effectors resides in two adjacent LWY units. PP2A phosphatases regulate cellular processes through targeted dephosphorylation of specific protein substrates. However, phospho-peptides that are down-regulated in PSR2- and PITG_15142-expressing *Arabidopsis* lines are distinct, suggesting the functional divergence of two PP2A-interacting effectors. Corresponding structural PDB files can be found with 7XVK (PSR2) and 7XVI (PITG_15142). This figure was generated using Biorender.

1.10 Hypothesis and main objectives of the thesis.

1.10.1 Hypothesis 1: The LWY effector repertoire can expand through domain shuffling.

Fungal pathogens provide compelling evidence for the presence of recombination hotspots, which are enriched with effector genes (Croll et al. 2015; Muller et al. 2019; Pierre et al. 2000; Stukenbrock and Dutheil 2018). Nonhomologous recombination of repeated fragments can give rise to sequence polymorphisms (de Jonge et al. 2013; Goss et al. 2013). We hypothesized that recombination may drive the shuffling of (L)WY units that embed different exposed residues in LWY effectors and lead to the mosaic patterns of (L)WY tandem repeats for each LWY effector.

Shuffling of these units with variable host-interacting capacities would then lead to effector multi-functionality and/or neo-functionality by forming dynamic protein complexes. The mosaic patterns of (L)WY units in the PP2A-interacting LWY effectors can serve as an initial indication for potential module shuffling events. To test if LWY effectors undergo recombination, the following objectives will be pursued:

1.10.1.1 Predict LWY repertoires in Phytophthora species.

LWY effectors have been predicted from RxLR effectors in five *Phytophthora* species based on sequence similarity (He et al. 2019). In this thesis, we aim to expand our knowledge of the LWY repertoires in *Phytophthora* using a new bioinformatic pipeline by excluding SP and RxLR filters. The predicted LWY proteins were then classified as effectors and non-effectors based on the presence of SP and/or RxLR motifs.

1.10.1.2 Characterize LWY sequence features.

All predicted LWY domain proteins were analyzed for sequence diversification and (L)WY unit numbers. The loci of predicted LWY genes were extracted and mapped to *Phytophthora* genomes to determine whether forming gene clusters in the genomes.

1.10.1.3 Identify LWY unit shuffling events and determine their functional significance.

We hypothesized that LWY tandem repeats may be evolving through recombination. This leads to our priority of identifying potential recombination events in LWY proteins with shuffled LWY units. The identified effectors were then investigated for their host interacting proteins using co-IP followed by mass spectrometry.

1.10.2 Hypothesis 2: LWY effectors with common functional modules can recruit common host targets.

Our previous research indicates that 13 LWY effectors contain a PP2A-interacting module, which is composed of two adjacent (L)WY units (H. Li et al. 2023). Therefore, we hypothesized that specific (L)WY-(L)WY combinations might serve as functional modules to mediate interactions with specific host components. To test the hypothesis, I identified potential functional modules that are enriched in LWY effectors and characterized their host targets through immuno-precipitation mass-spectrometry (IP-MS).

1.10.2.1 Identify potential functional modules in LWY effectors.

To understand if there are “popular” (L)WY units or unit combinations in LWY effectors that may mediate specific host protein interactions, the exposed residues on each (L)WY unit were extracted and subsequently clustered based on sequence similarities. The corresponding cluster for each (L)WY unit was mapped back to every LWY sequence. The combinations of every two adjacent units were extracted to

determine the enrichment of each combination. Specific combinations that are over-represented in LWY effectors are considered candidate functional modules.

1.10.2.2 Characterize host interactors for LWY effectors with potential functional modules.

Since historically notorious *P. infestans* imposes a great threat to food security, we decided to focus on *P. infestans* LWY effectors that contain potential functional modules for functional characterization. Individual effectors were fused to a GFP tag and transiently expressed in *N. benthamiana*. Effector proteins were enriched using GFP beads, and their interacting proteins were analysed by mass spectrometry. Co-IP was used for validation of effector-host protein interactions.

1.11 Reference

Ahn, H. K., et al. (2023), 'Effector-dependent activation and oligomerization of plant NRC class helper NLRs by sensor NLR immune receptors Rpi-amr3 and Rpi-amr1', *EMBO J,* 42 (5), e111484.

Ai, G., et al. (2020), 'Prediction and Characterization of RXLR Effectors in Pythium Species', *Mol Plant Microbe Interact,* 33 (8), 1046-58.

Albert, I., et al. (2015), 'An RLP23-SOBIR1-BAK1 complex mediates NLP-triggered immunity', *Nat Plants,* 1, 15140.

Anderson, R. G., et al. (2015), 'Recent Progress in RXLR Effector Research', *Mol Plant Microbe Interact,* 28 (10), 1063-72.

Anderson, T, R. (1985), 'Plant Losses and Yield Responses to Monoculture of Soybean Cultivars Susceptible, Tolerant and Resistant to Phytophthora megasperma f. sp. glycinea', *Plant Disease,* 70.

Anna-Liisa Fabritius, Howard S. Judelson (1997), 'Mating-type loci segregate aberrantly in Phytophthora infestans but normally in Phytophthora parasitica: implications for models of mating-type determination', *Curr Genet,* 32.

Armstrong, M. R., et al. (2005), 'An ancestral oomycete locus contains late blight avirulence gene Avr3a, encoding a protein that is recognized in the host cytoplasm', *PNAS,* 102.

Ascurra, Yerisf C. Torres., et al. (2023), 'Functional diversification of a wild potato immune receptor at its center of origin', *Science,* 381.

Beakes, G. W., Glockling, S. L., and Sekimoto, S. (2012), 'The evolutionary phylogeny of the oomycete "fungi"', *Protoplasma,* 249 (1), 3-19.

Bian, C., et al. (2020), 'Protein phosphatase 2A promotes stomatal development by stabilizing SPEECHLESS in Arabidopsis', *Proc Natl Acad Sci U S A,* 117 (23), 13127-37.

Bienapfl , J. C. and Balci, Y. (2013), 'Movement of Phytophthora spp. in Maryland's Nursery Trade', *Plant Disease,* 98.

Blackman, L. M., et al. (2015), 'RNA-Seq Analysis of the Expression of Genes Encoding Cell Wall Degrading Enzymes during Infection of Lupin (Lupinus angustifolius) by Phytophthora parasitica', *PLoS One,* 10 (9), e0136899.

Bleecker, Shin-Han Shiu and Anthony B. (2001), 'Receptor-like kinases from Arabidopsis form a monophyletic gene family related to animal receptor kinases', *PNAS,* 98.

Boller, T. and He, S. Y. (2009), 'Innate immunity in plants: an arms race between pattern recognition receptors in plants and effectors in microbial pathogens', *Science,* 324 (5928), 742-4.

Bos, J. I., et al. (2010), 'Phytophthora infestans effector AVR3a is essential for virulence and manipulates plant immunity by stabilizing host E3 ligase CMPG1', *Proc Natl Acad Sci U S A,* 107 (21), 9909-14.

Boutemy, L. S., et al. (2011), 'Structures of Phytophthora RXLR effector proteins: a conserved but adaptable fold underpins functional diversity', *J Biol Chem,* 286 (41), 35834-42.

Bouwmeester, K., et al. (2011), 'The lectin receptor kinase LecRK-I.9 is a novel Phytophthora resistance component and a potential host target for a RXLR effector', *PLoS Pathog,* 7 (3), e1001327.
Brasier, C., et al. (2022), 'Phytophthora: an ancient, historic, biologically and structurally cohesive and evolutionarily successful generic concept in need of preservation', *IMA Fungus,* 13 (1), 12.
Brautigan, D. L. (2013), 'Protein Ser/Thr phosphatases--the ugly ducklings of cell signalling', *FEBS J,* 280 (2), 324-45.
Bruinsma, Nikos Alexandratos and Jelle (2012), 'WORLD AGRICULTURE TOWARDS 2030/2050'.
Brunner, FreÂdeÂric., Rosahl, Sabine., and Lee, Justin. (2002), 'Pep-13, a plant defense-inducing pathogenassociated pattern from Phytophthora transglutaminases', *EMBO J,* 21.
Champouret, Nicolas., Bouwmeester, Klaas., and Rietman, Hendrik. (2009), 'Phytophthora infestans Isolates Lacking Class I ipiO Variants Are Virulent on Rpi-blb1 Potato', *MPMI,* 22.
Chen, S., et al. (2021), 'Arabidopsis downy mildew effector HaRxLL470 suppresses plant immunity by attenuating the DNA-binding activity of bZIP transcription factor HY5', *New Phytol,* 230 (4), 1562-77.
Chen, X. R., et al. (2019), 'The RXLR Effector PcAvh1 Is Required for Full Virulence of Phytophthora capsici', *Mol Plant Microbe Interact,* 32 (8), 986-1000.
Chinchilla, D., et al. (2007), 'A flagellin-induced complex of the receptor FLS2 and BAK1 initiates plant defence', *Nature,* 448 (7152), 497-500.
Chou, S., et al. (2011), 'Hyaloperonospora arabidopsidis ATR1 effector is a repeat protein with distributed recognition surfaces', *Proc Natl Acad Sci U S A,* 108 (32), 13323-8.
Croll, D. and McDonald, B. A. (2012), 'The accessory genome as a cradle for adaptive evolution in pathogens', *PLoS Pathog,* 8 (4), e1002608.
Croll, D., et al. (2015), 'The Impact of Recombination Hotspots on Genome Evolution of a Fungal Plant Pathogen', *Genetics,* 201 (3), 1213-28.
Dagdas, Y. F., et al. (2016), 'An effector of the Irish potato famine pathogen antagonizes a host autophagy cargo receptor', *Elife,* 5.
de Groot, Grecia Stefanía, et al. (2021), 'Large-scale monoculture reduces honey yield: The case of soybean expansion in Argentina', *Agriculture, Ecosystems & Environment,* 306.
de Guillen, K., et al. (2015), 'Structure Analysis Uncovers a Highly Diverse but Structurally Conserved Effector Family in Phytopathogenic Fungi', *PLoS Pathog,* 11 (10), e1005228.
de Jonge, R., et al. (2013), 'Extensive chromosomal reshuffling drives evolution of virulence in an asexual pathogen', *Genome Res,* 23 (8), 1271-82.
De la Concepcion, J. C., et al. (2018), 'Polymorphic residues in rice NLRs expand binding and response to effectors of the blast pathogen', *Nat Plants,* 4 (8), 576-85.
Derevnina, L., et al. (2021), 'Plant pathogens convergently evolved to counteract redundant nodes of an NLR immune receptor network', *PLoS Biol,* 19 (8), e3001136.

Di, X., et al. (2017), 'Structure-function analysis of the Fusarium oxysporum Avr2 effector allows uncoupling of its immune-suppressing activity from recognition', *New Phytol,* 216 (3), 897-914.
Dong, S., Raffaele, S., and Kamoun, S. (2015), 'The two-speed genomes of filamentous pathogens: waltz with plants', *Curr Opin Genet Dev,* 35, 57-65.
Dong, S., et al. (2011), 'Sequence variants of the Phytophthora sojae RXLR effector Avr3a/5 are differentially recognized by Rps3a and Rps5 in soybean', *PLoS One,* 6 (7), e20172.
Du, Y., et al. (2021), 'Phytophthora infestans RXLR effector PITG20303 targets a potato MKK1 protein to suppress plant immunity', *New Phytol,* 229 (1), 501-15.
Dye, Sara M. and Bostock, Richard M. (2021), 'Eicosapolyenoic fatty acids induce defense responses and resistance to Phytophthora capsici in tomato and pepper', *Physiological and Molecular Plant Pathology,* 114.
Fabro, G. (2022), 'Oomycete intracellular effectors: specialised weapons targeting strategic plant processes', *New Phytol,* 233 (3), 1074-82.
Feehan, J. M., et al. (2020), 'Plant NLRs get by with a little help from their friends', *Curr Opin Plant Biol,* 56, 99-108.
FLOR, H. H. (1971), 'CURRENT STATUS OF THE GENE-FOB-GENE CONCEPT', *Annu. Rev. Phytopathol,* 9.
Franceschetti, M., et al. (2017), 'Effectors of Filamentous Plant Pathogens: Commonalities amid Diversity', *Microbiol Mol Biol Rev,* 81 (2).
Fry, W. (2008), 'Phytophthora infestans: the plant (and R gene) destroyer', *Mol Plant Pathol,* 9 (3), 385-402.
Gaulin, E., et al. (2006), 'Cellulose binding domains of a Phytophthora cell wall protein are novel pathogen-associated molecular patterns', *Plant Cell,* 18 (7), 1766-77.
Gomez-Gomez, Lourdes . and Boller, Thomas. (2000), 'FLS2: An LRR Receptor–like Kinase Involved in the Perception of the Bacterial Elicitor Flagellin in Arabidopsis', *Molecular Cell,* 5.
Goritschnig, S., et al. (2016), 'Structurally distinct Arabidopsis thaliana NLR immune receptors recognize tandem WY domains of an oomycete effector', *New Phytol,* 210 (3), 984-96.
Goss, E. M., Press, C. M., and Grunwald, N. J. (2013), 'Evolution of RXLR-class effectors in the oomycete plant pathogen Phytophthora ramorum', *PLoS One,* 8 (11), e79347.
Green, Sarah, et al. (2021), 'PHYTO-THREATS: Addressing Threats to UK Forests and Woodlands from Phytophthora; Identifying Risks of Spread in Trade and Methods for Mitigation', *Forests,* 12 (12).
Guo, B., et al. (2019), 'Phytophthora sojae Effector PsAvh240 Inhibits Host Aspartic Protease Secretion to Promote Infection', *Mol Plant,* 12 (4), 552-64.
Haas, B. J., et al. (2009), 'Genome sequence and analysis of the Irish potato famine pathogen Phytophthora infestans', *Nature,* 461 (7262), 393-8.
Hardham, A. R. (2005), 'Phytophthora cinnamomi', *Mol Plant Pathol,* 6 (6), 589-604.

Hardham, A. R. and Blackman, L. M. (2018), 'Phytophthora cinnamomi', *Mol Plant Pathol,* 19 (2), 260-85.
He, J., et al. (2019), 'Structural analysis of Phytophthora suppressor of RNA silencing 2 (PSR2) reveals a conserved modular fold contributing to virulence', *Proc Natl Acad Sci U S A,* 116 (16), 8054-59.
Heese, Antje ., et al. (2007), 'The receptor-like kinase SERK3/BAK1 is a central regulator of innate immunity in plants', *PNAS,* 104.
Hein, I., et al. (2009), 'The zig-zag-zig in oomycete-plant interactions', *Mol Plant Pathol,* 10 (4), 547-62.
Henricot, B., Pérez Sierra, A., and Jung, T. (2014), 'Phytophthora pachypleura sp. nov., a new species causing root rot of Aucuba japonica and other ornamentals in the United Kingdom', *Plant Pathology,* 63 (5), 1095-109.
Hogenhout, Saskia A., Hoorn, Renier A. L. Van der., and Terauchi, Ryohei and Sophien Kamoun4 (2009), 'Emerging Concepts in Effector Biology of Plant-Associated Organisms', *MPMI,* 22.
Hou, Y., et al. (2019), 'A Phytophthora Effector Suppresses Trans-Kingdom RNAi to Promote Disease Susceptibility', *Cell Host Microbe,* 25 (1), 153-65 e5.
Huang, S., et al. (2005), 'Comparative genomics enabled the isolation of the R3a late blight resistance gene in potato', *Plant J,* 42 (2), 251-61.
Irieda, H., et al. (2019), 'Conserved fungal effector suppresses PAMP-triggered immunity by targeting plant immune kinases', *Proc Natl Acad Sci U S A,* 116 (2), 496-505.
Jiang, H. Y., et al. (2008), 'RXLR effector reservoir in two Phytophthora species is dominated by a single rapidly evolving superfamily with more than 700 members', *PNAS,* 105 (12).
Jones, J. D. and Dangl, J. L. (2006), 'The plant immune system', *Nature,* 444 (7117), 323-9.
Jones, J. D. G., Staskawicz, B. J., and Dangl, J. L. (2024), 'The plant immune system: From discovery to deployment', *Cell,* 187 (9), 2095-116.
Judelson, H. S. and Ah-Fong, A. M. V. (2019), 'Exchanges at the Plant-Oomycete Interface That Influence Disease', *Plant Physiol,* 179 (4), 1198-211.
Jumper, J., et al. (2021), 'Highly accurate protein structure prediction with AlphaFold', *Nature,* 596 (7873), 583-89.
Kearney, Brain. and Staskawicz, B. J. (1990), 'Widespread distribution and fitness contribution of Xanthomonas campestris avirulence gene avrBs2', *Nature,* 346.
King, S. R., et al. (2014), 'Phytophthora infestans RXLR effector PexRD2 interacts with host MAPKKK epsilon to suppress plant immune signaling', *Plant Cell,* 26 (3), 1345-59.
Klarzynski, Olivier., et al. (2000), 'Linear β-1,3 Glucans Are Elicitors of Defense Responses in Tobacco', *plant Physiol,* 124.
Kovacs, K., et al. (2011), 'Predicting the economic costs and property value losses attributed to sudden oak death damage in California (2010-2020)', *J Environ Manage,* 92 (4), 1292-302.
Lamour, K. H., et al. (2012), 'Genome sequencing and mapping reveal loss of heterozygosity as a mechanism for rapid adaptation in the vegetable

pathogen Phytophthora capsici', *Mol Plant Microbe Interact,* 25 (10), 1350-60.
Lapin, D., Bhandari, D. D., and Parker, J. E. (2020), 'Origins and Immunity Networking Functions of EDS1 Family Proteins', *Annu Rev Phytopathol,* 58, 253-76.
Latorre, S. M., et al. (2020), 'Differential loss of effector genes in three recently expanded pandemic clonal lineages of the rice blast fungus', *BMC Biol,* 18 (1), 88.
Lazar, N., et al. (2022), 'A new family of structurally conserved fungal effectors displays epistatic interactions with plant resistance proteins', *PLoS Pathog,* 18 (7), e1010664.
Li, H., et al. (2023), 'Pathogen protein modularity enables elaborate mimicry of a host phosphatase', *Cell,* 186 (15), 3196-207 e17.
Li, Q., et al. (2020), 'A Phytophthora capsici effector suppresses plant immunity via interaction with EDS1', *Mol Plant Pathol,* 21 (4), 502-11.
Li, T., et al. (2022), 'A Phytophthora capsici RXLR effector manipulates plant immunity by targeting RAB proteins and disturbing the protein trafficking pathway', *Mol Plant Pathol,* 23 (12), 1721-36.
Liang, X., et al. (2021), 'A Phytophthora capsici RXLR effector targets and inhibits the central immune kinases to suppress plant immunity', *New Phytol,* 232 (1), 264-78.
Lin, X., et al. (2020), 'Identification of Avramr1 from Phytophthora infestans using long read and cDNA pathogen-enrichment sequencing (PenSeq)', *Mol Plant Pathol,* 21 (11), 1502-12.
Lin, X., et al. (2022), 'A potato late blight resistance gene protects against multiple Phytophthora species by recognizing a broadly conserved RXLR-WY effector', *Mol Plant,* 15 (9), 1457-69.
Lin, Y., et al. (2021), 'Phytophthora sojae effector Avr1d functions as an E2 competitor and inhibits ubiquitination activity of GmPUB13 to facilitate infection', *Proc Natl Acad Sci U S A,* 118 (10).
Lovelace, A. H., et al. (2023), 'Effector Identification in Plant Pathogens', *Phytopathology,* 113 (4), 637-50.
Ma, Z., et al. (2017), 'A paralogous decoy protects Phytophthora sojae apoplastic effector PsXEG1 from a host inhibitor', *Science,* 355.
Ma, Z., et al. (2015), 'A Phytophthora sojae Glycoside Hydrolase 12 Protein Is a Major Virulence Factor during Soybean Infection and Is Recognized as a PAMP', *Plant Cell,* 27 (7), 2057-72.
Maqbool, A., et al. (2016), 'Structural Basis of Host Autophagy-related Protein 8 (ATG8) Binding by the Irish Potato Famine Pathogen Effector Protein PexRD54', *J Biol Chem,* 291 (38), 20270-82.
McCoy, A. G., et al. (2023), 'A global-temporal analysis on Phytophthora sojae resistance-gene efficacy', *Nat Commun,* 14 (1), 6043.
McDonald, B. A. and Stukenbrock, E. H. (2016), 'Rapid emergence of pathogens in agro-ecosystems: global threats to agricultural sustainability and food security', *Philos Trans R Soc Lond B Biol Sci,* 371 (1709).
McGowan, Jamie. and Fitzpatrick, David. A. (2017), 'Genomic, Network, and Phylogenetic Analysis of the Oomycete Effector Arsenal', *mSphere,* 2 (6).

Muller, M. C., et al. (2019), 'A chromosome-scale genome assembly reveals a highly dynamic effector repertoire of wheat powdery mildew', *New Phytol,* 221 (4), 2176-89.
Na, R., et al. (2013), 'Deletion of the Phytophthora sojae avirulence gene Avr1d causes gain of virulence on Rps1d', *Mol Plant Microbe Interact,* 26 (8), 969-76.
Ngou, B. P. M., Jones, J. D. G., and Ding, P. (2022a), 'Plant immune networks', *Trends Plant Sci,* 27 (3), 255-73.
Ngou, B. P. M., Ding, P., and Jones, J. D. G. (2022b), 'Thirty years of resistance: Zig-zag through the plant immune system', *Plant Cell,* 34 (5), 1447-78.
Ngou, B. P. M., et al. (2021), 'Mutual potentiation of plant immunity by cell-surface and intracellular receptors', *Nature,* 592 (7852), 110-15.
O'Connor, C. M., et al. (2018), 'Therapeutic targeting of PP2A', *Int J Biochem Cell Biol,* 96, 182-93.
Oh, S. K., et al. (2009), 'In planta expression screens of Phytophthora infestans RXLR effectors reveal diverse phenotypes, including activation of the Solanum bulbocastanum disease resistance protein Rpi-blb2', *Plant Cell,* 21 (9), 2928-47.
Ortiz, D., et al. (2017), 'Recognition of the Magnaporthe oryzae Effector AVR-Pia by the Decoy Domain of the Rice NLR Immune Receptor RGA5', *Plant Cell,* 29 (1), 156-68.
Outram, M. A., et al. (2022), 'Seeing is believing: Exploiting advances in structural biology to understand and engineer plant immunity', *Curr Opin Plant Biol,* 67, 102210.
Pandey, P., et al. (2021), 'An oomycete effector subverts host vesicle trafficking to channel starvation-induced autophagy to the pathogen interface', *Elife,* 10.
Parada-Rojas, Camilo H., et al. (2021), 'A Diagnostic Guide for Phytophthora capsici Infecting Vegetable Crops', *Plant Health Progress,* 22 (3), 404-14.
Peng, Y., van Wersch, R., and Zhang, Y. (2018), 'Convergent and Divergent Signaling in PAMP-Triggered Immunity and Effector-Triggered Immunity', *Mol Plant Microbe Interact,* 31 (4), 403-09.
Petre, B., et al. (2021), 'Host-interactor screens of Phytophthora infestans RXLR proteins reveal vesicle trafficking as a major effector-targeted process', *Plant Cell,* 33 (5), 1447-71.
Pierre, M., Noël , L., and Bonas, T. Lahaye · A. Ballvora J. Veuskens · M. Ganal · U. (2000), 'High-resolution genetic mapping of the pepper resistance locus Bs3governing recognition of the Xanthomonas campestris pv vesicatora AvrBs3 protein', *Theor Appl Genet,* 101.
Pruitt, R. N., et al. (2021), 'The EDS1-PAD4-ADR1 node mediates Arabidopsis pattern-triggered immunity', *Nature,* 598 (7881), 495-99.
Qiao, Y., et al. (2015), 'Phytophthora effector targets a novel component of small RNA pathway in plants to promote infection', *Proc Natl Acad Sci U S A,* 112 (18), 5850-5.
Qiu, X., et al. (2023), 'The Phytophthora sojae nuclear effector PsAvh110 targets a host transcriptional complex to modulate plant immunity', *Plant Cell,* 35 (1), 574-97.

Qutob, D., Chapman, B. P., and Gijzen, M. (2013), 'Transgenerational gene silencing causes gain of virulence in a plant pathogen', *Nat Commun,* 4, 1349.

Qutob, D., et al. (2009), 'Copy number variation and transcriptional polymorphisms of Phytophthora sojae RXLR effector genes Avr1a and Avr3a', *PLoS One,* 4 (4), e5066.

Raffaele, Sylvain., Farrer, Rhys A. ., and Liliana M. Cano, 1* David J. Studholme, 1‡ Daniel MacLean,1 Marco Thines,1,2,3 Rays H. Y. Jiang,4 Michael C. Zody,4 Sridhara G. Kunjeti,5 Nicole M. Donofrio,5 Blake C. Meyers,5 Chad Nusbaum,4 Sophien Kamoun1§ (2010), 'Genome Evolution Following Host Jumps in the Irish Potato Famine

Pathogen Lineage', *Science,* 330.

Sanchez-Vallet, A., et al. (2018), 'The Genome Biology of Effector Gene Evolution in Filamentous Plant Pathogens', *Annu Rev Phytopathol,* 56, 21-40.

Sarma, G. N., et al. (2005), 'Structure of Ptr ToxA: an RGD-containing host-selective toxin from Pyrenophora tritici-repentis', *Plant Cell,* 17 (11), 3190-202.

Savary, S., et al. (2019), 'The global burden of pathogens and pests on major food crops', *Nat Ecol Evol,* 3 (3), 430-39.

Seong, K. and Krasileva, K. V. (2021), 'Computational Structural Genomics Unravels Common Folds and Novel Families in the Secretome of Fungal Phytopathogen Magnaporthe oryzae', *Mol Plant Microbe Interact,* 34 (11), 1267-80.

Shan, L., et al. (2008), 'Bacterial effectors target the common signaling partner BAK1 to disrupt multiple MAMP receptor-signaling complexes and impede plant immunity', *Cell Host Microbe,* 4 (1), 17-27.

Sharp, J. K., Valent, B., and Albersheim, P. (1984), 'Purification and partial characterization of a beta-glucan fragment that elicits phytoalexin accumulation in soybean', *Journal of Biological Chemistry,* 259 (18), 11312-20.

Song, T., et al. (2013), 'Two RxLR avirulence genes in Phytophthora sojae determine soybean Rps1k-mediated disease resistance', *Mol Plant Microbe Interact,* 26 (7), 711-20.

Spanu, P. D. (2017), 'Cereal immunity against powdery mildews targets RNase-Like Proteins associated with Haustoria (RALPH) effectors evolved from a common ancestral gene', *New Phytol,* 213 (3), 969-71.

Staskawicz, Brian. J., Dahlbeck, Douglas., and Keen, Noel T. (1984), 'Cloned avirulence gene of Pseudomonas syringae pv. glycinea determines race-specific incompatibility on Glycine max (L.) Merr.', *PNAS,* 81.

Studholme, D. J., et al. (2019), 'Genome sequencing of oomycete isolates from Chile supports the New Zealand origin of Phytophthora kernoviae and makes available the first Nothophytophthora sp. genome', *Mol Plant Pathol,* 20 (3), 423-31.

Stukenbrock, E. H. and Dutheil, J. Y. (2018), 'Fine-Scale Recombination Maps of Fungal Plant Pathogens Reveal Dynamic Recombination Landscapes and Intragenic Hotspots', *Genetics,* 208 (3), 1209-29.

Teulet, A., et al. (2023), 'A pathogen effector FOLD diversified in symbiotic fungi', *New Phytol,* 239 (3), 1127-39.
Thulasi Devendrakumar, K., Li, X., and Zhang, Y. (2018), 'MAP kinase signalling: interplays between plant PAMP- and effector-triggered immunity', *Cell Mol Life Sci,* 75 (16), 2981-89.
Tian, M., Benedetti, B., and Kamoun, S. (2005), 'A Second Kazal-like protease inhibitor from Phytophthora infestans inhibits and interacts with the apoplastic pathogenesis-related protease P69B of tomato', *Plant Physiol,* 138 (3), 1785-93.
Tian, M., et al. (2004), 'A Kazal-like extracellular serine protease inhibitor from Phytophthora infestans targets the tomato pathogenesis-related protease P69B', *J Biol Chem,* 279 (25), 26370-7.
Tsuda, K. and Katagiri, F. (2010), 'Comparing signaling mechanisms engaged in pattern-triggered and effector-triggered immunity', *Curr Opin Plant Biol,* 13 (4), 459-65.
Turnbull, D., et al. (2017), 'RXLR Effector AVR2 Up-Regulates a Brassinosteroid-Responsive bHLH Transcription Factor to Suppress Immunity', *Plant Physiol,* 174 (1), 356-69.
Tyler, B. M. (2007), 'Phytophthora sojae: root rot pathogen of soybean and model oomycete', *Mol Plant Pathol,* 8 (1), 1-8.
van der Vossen, E., et al. (2003), 'An ancient R gene from the wild potato species Solanum bulbocastanum confers broad-spectrum resistance to Phytophthora infestans in cultivated potato and tomato', *Plant J,* 36 (6), 867-82.
Vleeshouwers, V. G., et al. (2008), 'Effector genomics accelerates discovery and functional profiling of potato disease resistance and phytophthora infestans avirulence genes', *PLoS One,* 3 (8), e2875.
Wang, H., et al. (2021), 'An atypical Phytophthora sojae RxLR effector manipulates host vesicle trafficking to promote infection', *PLoS Pathog,* 17 (11), e1010104.
Wang, M. Y., et al. (2023a), 'The plant immune receptor SNC1 monitors helper NLRs targeted by a bacterial effector', *Cell Host Microbe,* 31 (11), 1792-803 e7.
Wang, S., et al. (2023b), 'RxLR Effectors: Master Modulators, Modifiers and Manipulators', *Mol Plant Microbe Interact,* 36 (12), 754-63.
Wang, S., et al. (2017), 'Delivery of cytoplasmic and apoplastic effectors from Phytophthora infestans haustoria by distinct secretion pathways', *New Phytol,* 216 (1), 205-15.
Wang, Z., et al. (2023c), 'A Phytophthora infestans RXLR effector targets a potato ubiquitin-like domain-containing protein to inhibit the proteasome activity and hamper plant immunity', *New Phytol,* 238 (2), 781-97.
Wang., et al. (2020), 'Effector gene silencing mediated by histone methylation underpins host adaptation in an oomycete plant pathogen', *Nucleic Acids Res,* 48 (4), 1790-99.

Win, J., et al. (2012), 'Sequence divergent RXLR effectors share a structural fold conserved across plant pathogenic oomycete species', *PLoS Pathog,* 8 (1), e1002400.
Win, J., et al. (2007), 'Adaptive evolution has targeted the C-terminal domain of the RXLR effectors of plant pathogenic oomycetes', *Plant Cell,* 19 (8), 2349-69.
Witek, K., et al. (2016), 'Accelerated cloning of a potato late blight-resistance gene using RenSeq and SMRT sequencing', *Nat Biotechnol,* 34 (6), 656-60.
Witek, K., et al. (2021), 'A complex resistance locus in Solanum americanum recognizes a conserved Phytophthora effector', *Nat Plants,* 7 (2), 198-208.
Wood, K. J., et al. (2020), 'Effector prediction and characterization in the oomycete pathogen Bremia lactucae reveal host-recognized WY domain proteins that lack the canonical RXLR motif', *PLoS Pathog,* 16 (10), e1009012.
Wrather, J. A and Koenning, S.R. (2006), 'Estimates of Disease Effects on Soybean Yields in the United States 2003 to 2005', *JOURNAL OF NEMATOLOGY,* 38.
Xiong, Q., et al. (2014), 'Phytophthora suppressor of RNA silencing 2 is a conserved RxLR effector that promotes infection in soybean and Arabidopsis thaliana', *Mol Plant Microbe Interact,* 27 (12), 1379-89.
Yang, B., et al. (2017), 'Distinct regions of the Phytophthora essential effector Avh238 determine its function in cell death activation and plant immunity suppression', *New Phytol,* 214 (1), 361-75.
Yang, B., et al. (2019), 'The Phytophthora sojae RXLR effector Avh238 destabilizes soybean Type2 GmACSs to suppress ethylene biosynthesis and promote infection', *New Phytol,* 222 (1), 425-37.
Ye, W., et al. (2016), 'Sequencing of the Litchi Downy Blight Pathogen Reveals It Is a Phytophthora Species With Downy Mildew-Like Characteristics', *Mol Plant Microbe Interact,* 29 (7), 573-83.
YU, LLOYD M. (1995), 'Elicitins from Phytophthora and basic resistance in tobacco', *PNAS,* 92.
Yuan, M., et al. (2021), 'PTI-ETI crosstalk: an integrative view of plant immunity', *Curr Opin Plant Biol,* 62, 102030.
Zhang, F., et al. (2021), 'Genome Analysis of Two Newly Emerged Potato Late Blight Isolates Sheds Light on Pathogen Adaptation and Provides Tools for Disease Management', *Phytopathology,* 111 (1), 96-107.
Zhang, L., et al. (2014), 'Fungal endopolygalacturonases are recognized as microbe-associated molecular patterns by the arabidopsis receptor-like protein RESPONSIVENESS TO BOTRYTIS POLYGALACTURONASES1', *Plant Physiol,* 164 (1), 352-64.
Zhang, P., et al. (2019), 'The WY domain in the Phytophthora effector PSR1 is required for infection and RNA silencing suppression activity', *New Phytol,* 223 (2), 839-52.

Zheng, X., et al. (2018), 'Phytophthora infestans RXLR effector SFI5 requires association with calmodulin for PTI/MTI suppressing activity', *New Phytol,* 219 (4), 1433-46.
Zheng, X., et al. (2014), 'Functionally redundant RXLR effectors from Phytophthora infestans act at different steps to suppress early flg22-triggered immunity', *PLoS Pathog,* 10 (4), e1004057.
Zhu, X., et al. (2023), 'Phytophthora sojae effector PsAvh113 associates with the soybean transcription factor GmDPB to inhibit catalase-mediated immunity', *Plant Biotechnol J,* 21 (7), 1393-407.
Zipfel, C., et al. (2006), 'Perception of the bacterial PAMP EF-Tu by the receptor EFR restricts Agrobacterium-mediated transformation', *Cell,* 125 (4), 749-60.

Chapter 2: Genome analysis of (L)WY repertoires in *Phytophthora* species

2.1 Introduction

Food security faces mounting challenges due to the ongoing evolutionary arms race between crop plants and plant pathogens. Plant diseases cause substantial agricultural losses as pathogens continuously evolve to overcome host immunity. To counter this threat, extensive pathogen genome sequencing has revealed crucial insights into their adaptation mechanisms, particularly through the study of secreted virulence factors (effectors). Large-scale genome sequencing initiatives, such as the 1000 Fungal Genomes and GetGenome projects, continue to expand our understanding of pathogen genomic diversity (Canham et al. 2024).

Plant pathogens encode arsenals of effectors that rapidly evolve to interfere with host processes. The regulation, function and evolution of effector genes are tightly associated with genome compartments. A well-known model in oomycete is the “two-speed genomes”, which describes bipartite genomes that undergo uneven evolutionary rates (Dong et al. 2015). Effectors tend to be located in gene-poor and repeat-rich genomic regions, which may facilitate fast evolution while the core genes distribute in regions with higher gene densities and less transposable elements. Despite of different effector repertoires employed in different microorganisms, similar genomic compartmentalization for virulence factors is a shared feature observed in comparative genome analysis of pathogens, known as accessory chromosomes, AT isochores, TE-rich genomic islands, conditionally dispensable (CD), lineage-specific (LS), supernumerary and mini chromosomes (Bao et al. 2017; Goodwin et al. 2011; Grandaubert et al. 2014; Langner et al. 2021; L. J. Ma et al. 2010; Miao et al. 1991; Z. Peng et al. 2019; Rouxel et al. 2011; Schmidt et al. 2013; Schotanus et al. 2015; Temporini and VanEtten 2004; Vlaardingerbroek et al. 2016). This bipartite genome architecture not only shields the core genes from deleterious mutations but also provides regions that allow higher mutation rates. Despite that, mechanisms driving the evolution of new effectors or effector neo-functionality remain unclear.

These expanded families of repeat-containing effectors were proposed to be the product of gene duplication and recombination (Jiang et al. 2008; Prince and Pickett 2002; Reams and Neidle 2004). Analysis of the RxLR effectors revealed a prevalent presence of (L)WY effectors across the *Peronospora* genus with each containing multiple (L)WY units (Boutemy et al. 2011; Chou et al. 2011; Dagdas et al. 2016; Derevnina et al. 2021; B. Guo et al. 2019; He et al. 2019; H. Li et al. 2023; Maqbool et al. 2016; Win et al. 2012; Wood et al. 2020). The (L)WY units form structurally conserved hydrophobic bundles consisting of either 3 α-helices (WY units) or 5 α-helices (LWY units). WY effectors adopt WY1-(WY)n domain arrangements while these structural similar (L)WY units in LWY effectors are concatenated with adjacent (L)WY units to form elongated WY1-(LWY)n architectures. The value "n" indicates how many additional WY or LWY units follow the initial unit.

While these units maintain their core structural architecture, they exhibit sequence variations on their surfaces, resulting in diverse tandem repeat patterns within each effector. This structural conservation coupled with sequence diversity suggests that (L)WY units represent a genetic reservoir that could facilitate the evolution of novel functions through recombination events. PSR2 and 12 LWY effectors were reported to adopt a common combination in the N terminal region for mediating the interaction with host PP2A A subunits while the LWY repeats at the C terminal region remain varied, indicating rearrangement might occur and determine the binding specificity of different host targets in the shuffled regions (H. Li et al. 2023).

This chapter aims to systematically investigate whether LWY effectors can undergo module shuffling. I predicted the LWY repertories in five *Phytophthora* species and found 568 proteins that contain LWY units (henceforth LWYs or LWY effectors). I then utilized Signal Peptide (SP) and the RxLR motif to classify the LWY proteins, which revealed that 22%-54% of LWYs contain both the SP and RxLR motifs. 4%-30% of LWYs have SP but lack RxLR motifs while 15%-63% of LWYs lack SPs and/ or RxLR motifs. These LWY genes physically co-localize with each other to form multi-gene clusters that are independent of their SP and RxLR motif composition. This suggests that LWY tandem repeats could serve as a reservoir to provide genetic materials for recombination, which will promote the generation of new module combinations in LWY effectors to evolve novel functions.

2.2 Results

2.2.1 Predicting LWY effectors in *P. infestans*, *P. mirabilis*, *P. sojae*, *P. melonis* and *P. pisi*.

Investigating the evolution of LWY effectors through recombination requires a comprehensive analysis of all LWY domain proteins across *Phytophthora* species, as these may serve as potential sources of genetic variations to effector evolution. Previous studies have focused exclusively on LWY domains within RxLR effectors, leaving the broader evolutionary landscape unexplored.

To explore the role of recombination in LWY effector evolution more comprehensively, I developed a computational pipeline for comparative analysis across five *Phytophthora* species. This study sought to identify LWY domain proteins and investigate whether rearrangement and shuffling may have driven functional diversification of these tandem repeats.

To begin with, I constructed a Hidden Markov Model (HMM) using previously published LWY effector protein sequences from two reference isolates: 60 sequences from *P. sojae* P6497 and 79 from *P. infestans* T30-4. This model was then used to screen proteomes using HMMsearch from five *Phytophthora* species selected from two distant subclades: subclade 1c (*P. infestans* and its sister species *P. mirabilis*) and subclade 7b (*P. sojae* and its closely related species *P. melonis* and *P. pisi*). The reason for choosing *P. sojae*, *P. infestans* and the sister species from these two *Phytophthora* species derived from one pair of potential recombination candidates PsPSR2 (formatting as WY1-(LWY)6) and PiPSR2 (formatting as WY1-(LWY)7) (He et al. 2019). The homologs PSR2 from *P. sojae* and *P. infestans* differ in one unit: PiPSR2 contains an additional LWY7 unit that does not align with any unit in PsPSR2, while their other units show clear correspondence (WY1 through LWY6 in both proteins and LWY7 in PsPSR2 aligning with LWY8 in PiPSR2). This LWY7 unit in PiPSR2 likely originated through recombination from other LWY proteins. However, the extensive sequence divergence between these distantly related species prevents nucleotide-level verification of this recombination event. Therefore, I expanded the investigation to compare *P. sojae* and *P. infestans* with

their closely related species, where sequence conservation would be better preserved to enable the detection of recombination events.

LWY candidate sequences identified through HMM searches were further analyzed using MEME (Multiple Em for Motif Elicitation) and validated through protein secondary structure prediction to confirm the presence of the characteristic 3 α-helical bundle in the WY units (Each unit consists of approximately 50 amino acid residues) and 5 α-helical bundle in the LWY units (each LWY unit comprises approximately 100 amino acid residues). I defined LWY domain proteins (LWYs or LWY effectors) as those displaying the WY1-(LWY)n architecture. Notably, it's acceptable if the first unit lacked a tryptophan (W) residue or the last unit lacked a tryptophan-tyrosine (WY) sequence, as these terminal units often degenerate (He et al. 2019).

The importance of WY domains extends beyond RxLR-containing effectors, as research has demonstrated that WY effectors lacking the RxLR motif can also induce cell death, indicating host recognition of WY domain proteins (Wood et al. 2020). Building on these findings, I developed a computational pipeline that retains and categorizes LWY sequences based on both the presence and absence of Signal Peptide (SP) and RxLR motifs, rather than excluding sequences that lack these canonical signals (Figure 2.1). This pipeline therefore classified LWY effectors into three groups based on the presence and absence of Signal Peptide (SP) and RxLR motifs: SP+RxLR LWYs, SP only LWYs and No SP LWYs.

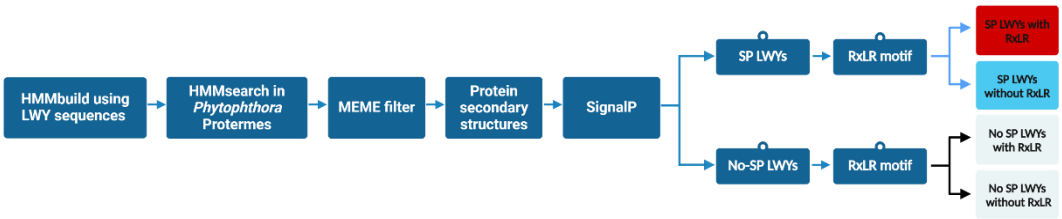

Figure 2.1 HMM pipeline for LWY effector prediction.

HMM pipeline was used for LWY effector prediction. Blue, red, and white colors represent three categories based on N-terminal features including SP and the RxLR motif.

Importantly, this new pipeline not only successfully identified previously characterized LWY effectors but also revealed novel LWY sequences in the *P. infestans* genome that haven't been explored in earlier studies (Figure 2.2). This demonstrates the pipeline's effectiveness in detecting LWY proteins across the *Phytophthora* species and suggests its potential applicability to other oomycetes.

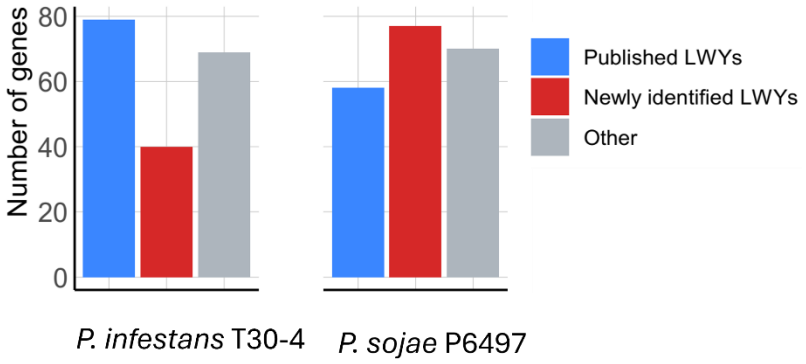

Figure 2.2 Current pipeline validates published results and identifies new LWY effectors.

The current pipeline was tested with two *Phytophthora* species analyzed in previous publications. The prediction output overlaps with published LWY effectors, and the newly identified LWY proteins are labelled accordingly. Others represent sequences that lack LWY units or have degenerated LWY domain structures after confirming the presence of LWY units using MEME motif scanning and the helical α-bundle using protein secondary structures.

This analysis identified diverse LWY repertoires across the five *Phytophthora* species, ranging from 73 to 173 proteins per species (568 total), using an e-value cutoff of 1.00E-17 (Figure 2.3). Approximately 89% of the proteins above this cutoff contained LWY-effector-like sequences, with a false positive rate of less than 0.1% among non-LWY proteins (Table 1.1).

The distribution of Signal Peptide (SP) and RxLR motifs varied substantially among predicted LWY sequences across the five *Phytophthora* species.

Collectively, 300 LWY genes contain SPs. 22%-54% of LWYs contain both the signal peptide and RxLR motif (34% in *P. mirabilis*, 54% in *P. infestans*, 22% in *P.pisi*, 47% in *P. sojae* and 34% in *P. melonis*). Up to 63% of LWY genes in each species lack SPs (90 in *P. mirabilis* (52%), 18 in *P. infestans* (15%), 48 in *P. pisi* (63%), 54 in *P. sojae* (41%) and 45 in *P. melonis* (61%)) (Figure 2.3). The presence of both SP and RxLR motifs in approximately 40% of LWY effectors suggests they are likely cytoplasmic effectors. Notably, LWY effectors without SP and/or RxLR motifs (No SP LWYs) represent a previously understudied category, as all the earlier analyses implemented the SP and RxLR filters. These No SP LWYs may 1:) be secreted using non-canonical SP. 2:) function endogenously in *Phytophthora* species. 3:) contribute to effector evolution by serving as genetic reservoirs for LWY module shuffling within *Phytophthora* species.

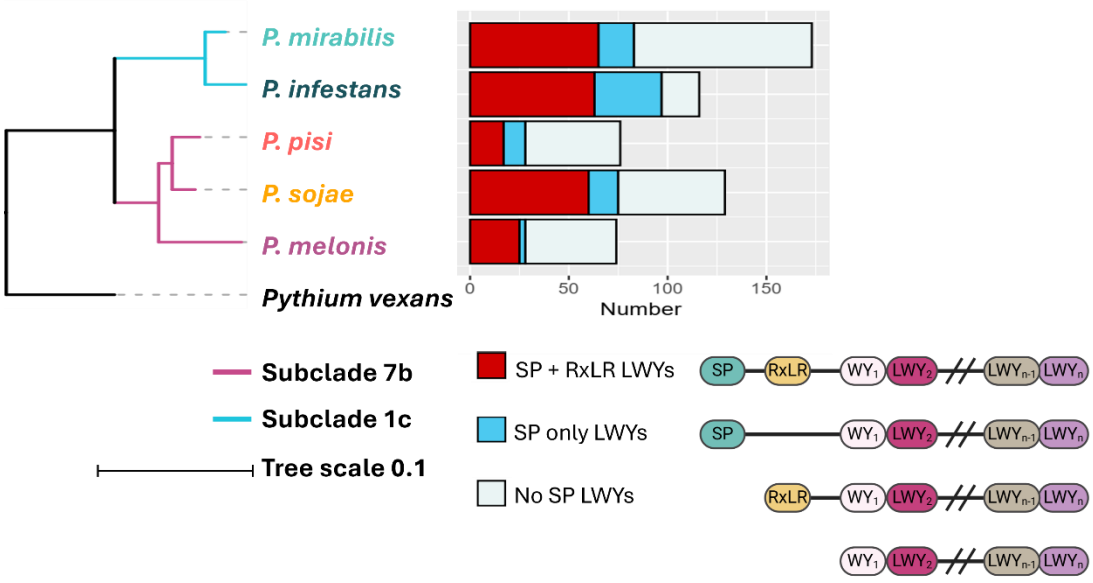

Figure 2.3 *Phytophthora* species encode numerous LWY effectors.

Phylogeny tree was used to indicate the five species from *Phytophthora* species tree 1c and 7b in this study. *Pythium vexans* served as the outgroup. The stacked bar plot represents the composition of predicted LWYs from the three categories based on the presence and absence of SP and/ or RxLR motifs. The domain architecture for each category is also illustrated.

Table 1.1 Numbers of *Phytophthora* proteins in the LWY/non-LWY proteomes that score above/below the HMM threshold 1E-17

Species	LWY effectors, above the cutoff	LWY effectors, below the cutoff	Non-LWYs, above the cutoff	Non-LWYs, below the cutoff
P. infestans T30-4	95	24	4	17793
P. mirabilis Pm3010	167	6	55	24749
P. sojae P6497	110	23	16	26473
P. sojae JS2	112	19	18	26889
P. pisi OSU-2014	67	9	14	18905
P. melonis OSU-2014	72	1	26	21682
Total: *Phytophthora spp.*	623 (88.37%)	82 (11.63%)	133 (0.10%)	136491 (99.90%)

Analysis of encoded LWY gene numbers revealed no significant correlation between LWY gene count and either genome size, RxLR effectors or host range (Table 1.2). Rather, the diversification of LWY repertoires appears to be primarily influenced by species-specific host interactions.

Table 1.2 Genomes of *Phytophthora* pathogens discussed in this chapter.

Species	Host(s)	Genome size	No. LWYs	No. RxLR effectors	Reference
P. infestans T30-4	Solanaceae: *Solanum* spp. (potato) and *Lycopersicon esculentum* (tomato).	228.5 Mb	114	563	(Haas et al. 2009)
P. mirabilis Pm3010	*Mirabilis jalapa* (four O' clock weed)	200 Mb	173	397	Unpublished data from Dr. Suomeng Dong in NJAU
P. sojae JS2	*Glycine max* (soybean)	85.1 Mb	131	456	(Z. Zhang et al. 2024)
P. pisé OSU-2014	*Pisum sativum* (pea) and *Vicia faba* (faba bean)	58.9 Mb	76	~300	(Kronmiller et al. 2023)
P. melonis OSU-2014	*Cucumus sativus* (cucumber), *Citrullus lanatus* and *Pistacia vera*	73.4 Mb	73	~400	(Kronmiller et al. 2023)

Note: The number of RxLR effectors in *P. pisi* and *P. melonis* was estimated from the figure presented in the cited paper.

2.2.2 *Phytophthora spp.* encode LWY repertoires varied in unit numbers and sequences.

Analysis of LWY effectors across five *Phytophthora* species revealed significant variations in (L)WY unit numbers, ranging from 1 to 12 units, with proteins reaching lengths exceeding 1,000 amino acids (each LWY unit comprising approximately 100 amino acids) (Figure 2.4A). To further analyse unit number preference in LWY proteins, I compared the abundance of LWY proteins based on encoded (L)WY unit numbers in the *Phytophthora spp*. The majority (77%) of LWY effectors contain between two to five (L)WY units, with 46% harbouring two to three units and 31% containing four to five units. The frequency distribution of LWY proteins peaked at three units, with declining abundance as the unit number increased. Comparative analysis of LWY unit numbers across the five species consistently showed three-unit LWY proteins as the most prevalent (Figure 2.4B). Notably, three species (*P. infestans*, *P. mirabilis*, and *P. melonis*) exhibited a trend with higher frequencies of odd-numbered units compared to even-numbered units (Figure 2.4B). To explore the correlation between such odd unit number peaks and LWY protein categories, (L)WY unit numbers were investigated based on the presence and absence of the SP and RxLR motifs. Interestingly, LWYs with SP and RxLR motifs follow a similar distribution pattern of unit number preference (Figure 2.4C), suggesting a potential advantage for odd-numbered units in virulence functions, host protein recruitment, protein stabilization and secretion. More experiments will be needed to test this hypothesis.

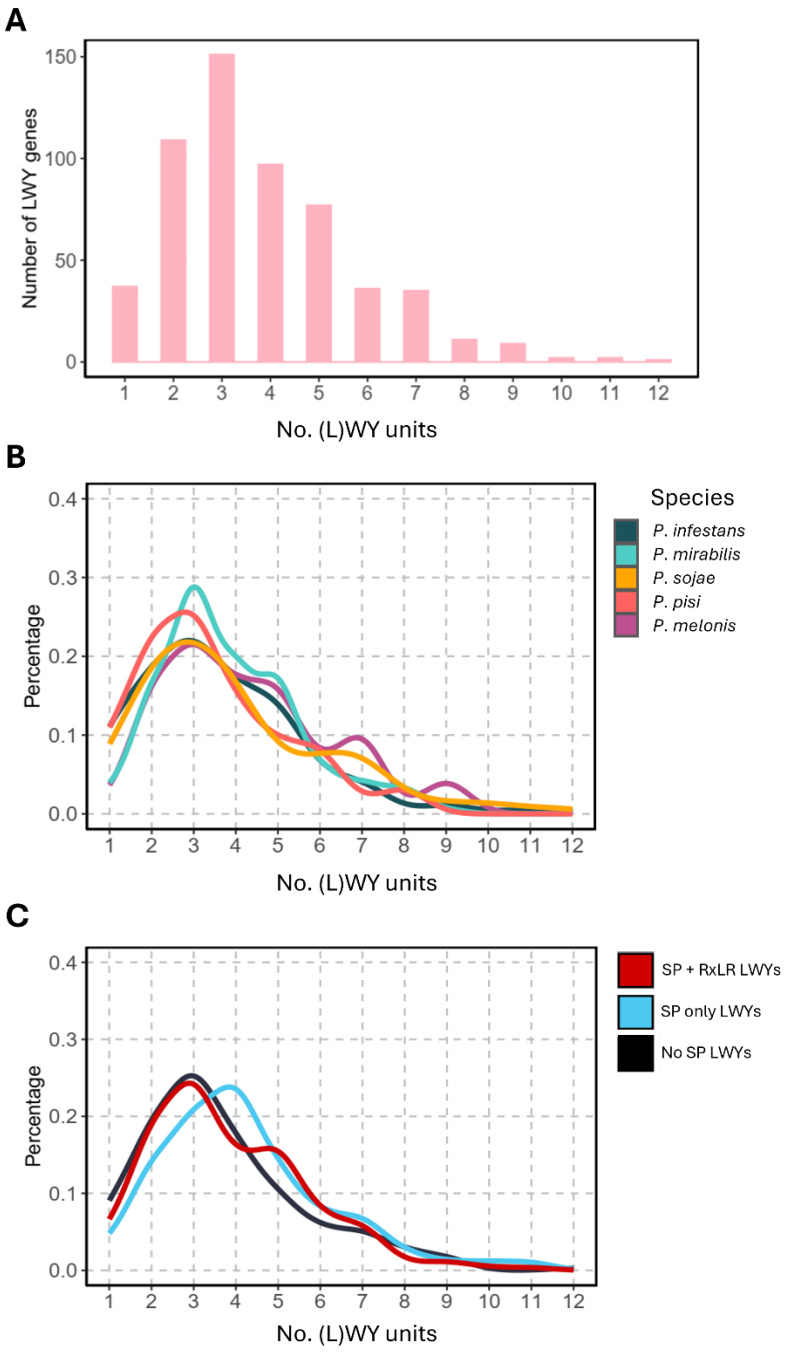

Figure 2.4 *Phytophthora* species enrich LWY effectors with odd number (L)WY units.

(**A**) The bar plot was performed to visualize the distribution of No. tandem repeats from each LWY protein. (**B**) The distribution of (L)WY unit numbers normalized by the total number of LWY proteins in different *Phytophthora* species. (**C**) The percentage of encoded unit numbers was characterized in LWY genes according to the presence and absence of SP and/ or RxLR motifs.

Next, I determined the correlation between LWY unit number, N-terminal SP/RxLR features, and phylogenetic variation of the LWY proteins. The 568 LWY proteins were used to construct a phylogeny tree that revealed 11 clades (Figure 2.5). While most clades contain LWY effectors from all five species, clade 11 predominantly comprised sequences from *P. infestans* and *P. mirabilis*, indicating lineage-specific gene evolution in these sister species. Comparison among phylogenetically related LWY genes revealed a variation in the N-terminal secretion signal peptide and RxLR motif and unit numbers. This implies that LWY proteins share homology within one subgroup but still exhibit variability in N-terminal signal segments and C-terminal tandem repeats. The dynamics of secretion signals, translocation signals, and unit numbers in LWY indicate that the modular architecture of these proteins might reflect their roles in effector evolution and function.

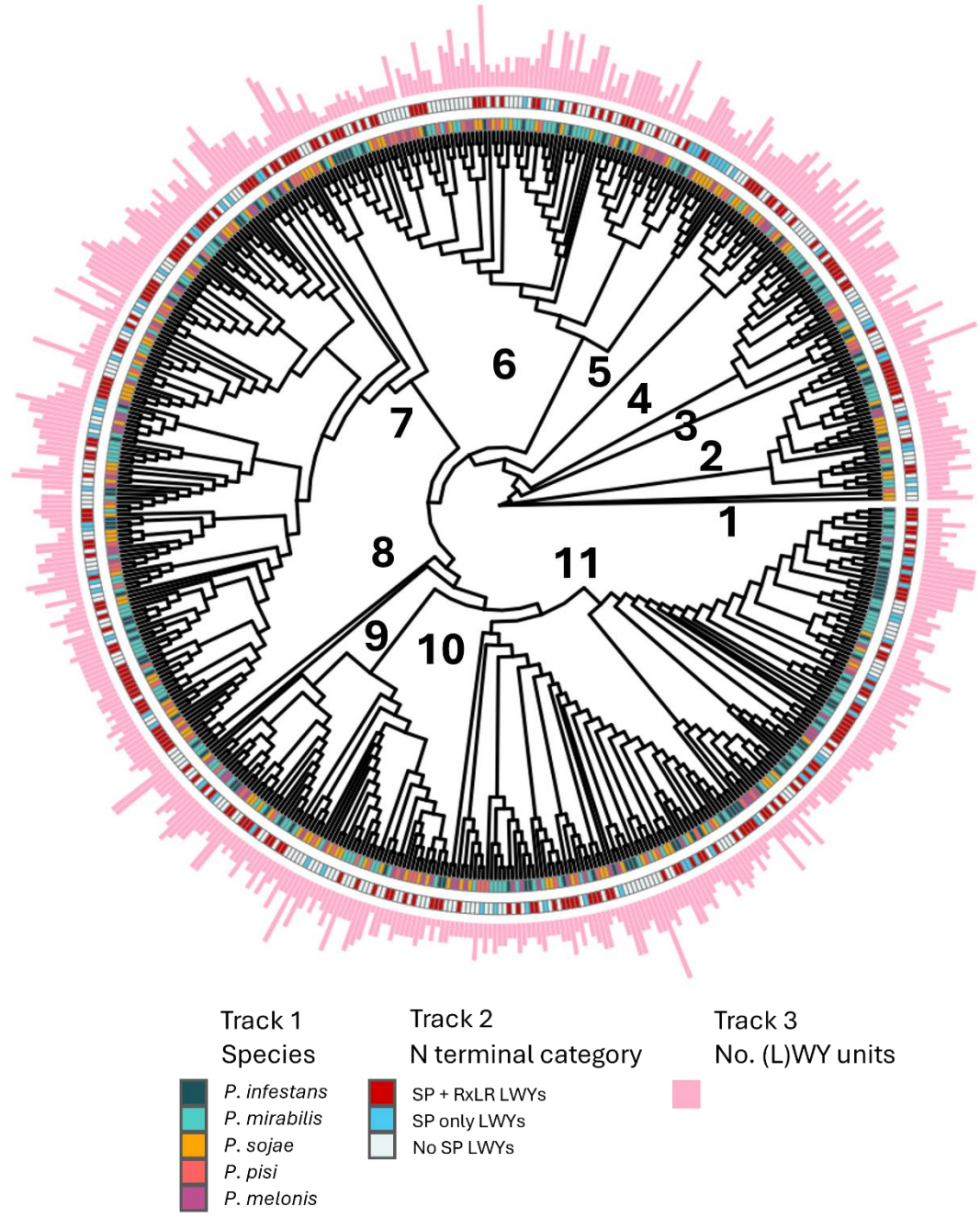

Figure 2.5 LWY unit number varies in phylogenetically related LWY sequences.

A phylogeny tree was built with LWY protein sequences using maximum-likelihood (ML) analysis and categorized into 11 clades. Tracks 1, 2, and 3 present *Phytophthora* species, N terminal signal category, and (L)WY unit number, respectively.

2.2.3 LWYs contribute to sequence and unit number diversification in *Phytophthora* species.

I next investigated the conservation of LWY repertoires in the five *Phytophthora* species. For this purpose, I analyzed the protein sequences of LWY homologs using protein Basic Local Alignment Search Tool (BlastP). 1e-5 was applied as the e-value for BlastP. Each pair of genes identified as best reciprocal hits was considered a candidate for ortholog finding. The results show that only seven LWY genes have homologous genes in all these five species, which are named “core” LWYs (Figure 2.6).

Overall, the five *Phytophthora* species encode more than 63% (359 out of 568) of lineage-specific LWYs, indicating a substantial divergence of LWYs after species speciation. 174/568 (31%) LWYs are shared by two to four *Phytophthora* species, reflecting the sequence divergence of these LWY repertoires (Figure 2.6).

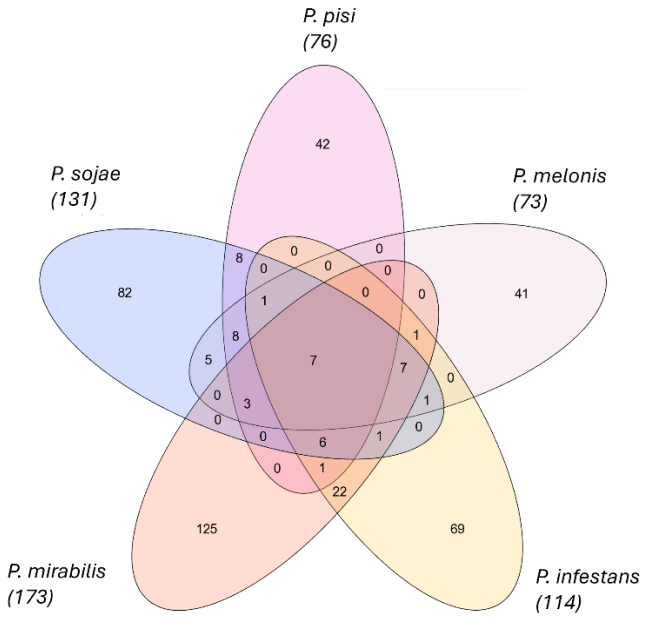

Figure 2.6 The comparison of paralogs in five *Phytophthora* species.

LWY gene conservation in *P. infestans*, *P. mirabilis*, *P. sojae*, *P. melonis* and *P. pisi* was investigated using Orthofinder and BlastP. The overlapping region represents the number of shared paralogs in different species. The numbers of predicted LWY genes in each species are shown accordingly.

Three functionally characterized RxLR effectors are present within the "core" LWY set (Figure 2.7). This includes two PP2A-interacting LWY effectors *PsPSR2* and *PITG_15032* (Core set 1 and 2). PsPSR2 is a *P. sojae* effector with seven (L)WY tandem repeats, which was initially found to suppress defence-related small RNA biogenesis (He et al. 2019; Hou et al. 2019; Qiao et al. 2013; Xiong et al. 2014). More recently, LWY2-LWY3 in PsPSR2 were shown to be responsible for hijacking Arabidopsis PP2A core enzyme to promote disease (H. Li et al. 2023). The *P. infestans* effector PITG_15032 also contains the PP2A-interacting (L)WY-LWY module as in PsPSR2, and similar to PsPSR2, also hijacks the host PP2A core enzyme (H. Li et al. 2023). PITG_16705, also known as AVRcap1b, consists of seven (L)WY units, which was reported to suppress the activity of two NRCs by recruiting a trafficking-associated protein NbTOL9a in *N. benthamiana* (Derevnina et al. 2021). It is therefore intriguing that these effectors with key virulence functions are conserved in evolutionarily divergent *Phytophthora* species.

Most importantly, unit number variation has been observed in these "core" LWYs. For example, *PSR2* paralogs (Core set 1) and *PITG_15032* (Core set 2) have one unit difference in the *Phytophthora* species while core sets 3, 4, 5, 6 and 7 have shown a difference of up to three LWY units (Figure 2.7). Therefore, I concluded that LWY repertoires may undergo constant evolution in unit arrangements, effector delivery and translocation into plants.

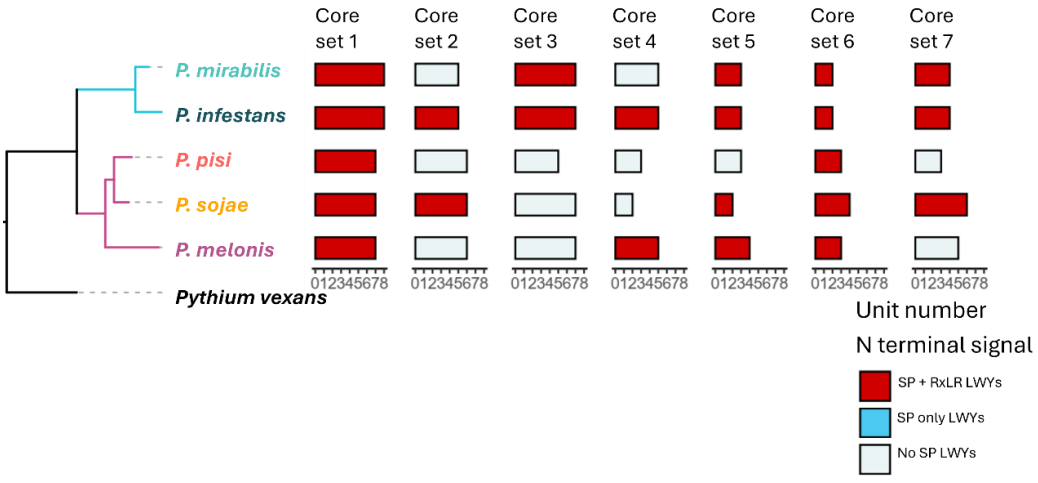

Figure 2.7 "Core" LWY sequences undergo variations in N terminal signals and unit numbers.

Bar plot together with species tree summarizes the presence and absence of SP and RxLR motifs at N termini and (L)WY unit numbers at the C terminal in seven “core” LWYs five *Phytophthora* species.

To examine potential co-evolution between "core" LWY effectors and *Phytophthora* species, I compared phylogenetic relationships across seven sets of "core" LWY effectors with the established species tree (Figure 2.8). The phylogenies of four “core” LWYs (core set 1, 4, 5 and 7) are congruent with the species, indicating these LWY effectors were present before the speciation of these species and kept in the species, reflecting potential virulence contributions to *Phytophthora* pathogens.

During co-evolution, hosts may have evolved to recognize functional modules from these “core” LWY effectors. Consequently, host recognition may lead to mutations in SP, RxLR motif, and effector domains. Indeed, some of the members in the conserved LWY family seem to undergo SP and RxLR motif gain and loss and unit number variation at the C-termini of the paralogs in different *Phytophthora* species (Figure 2.7).

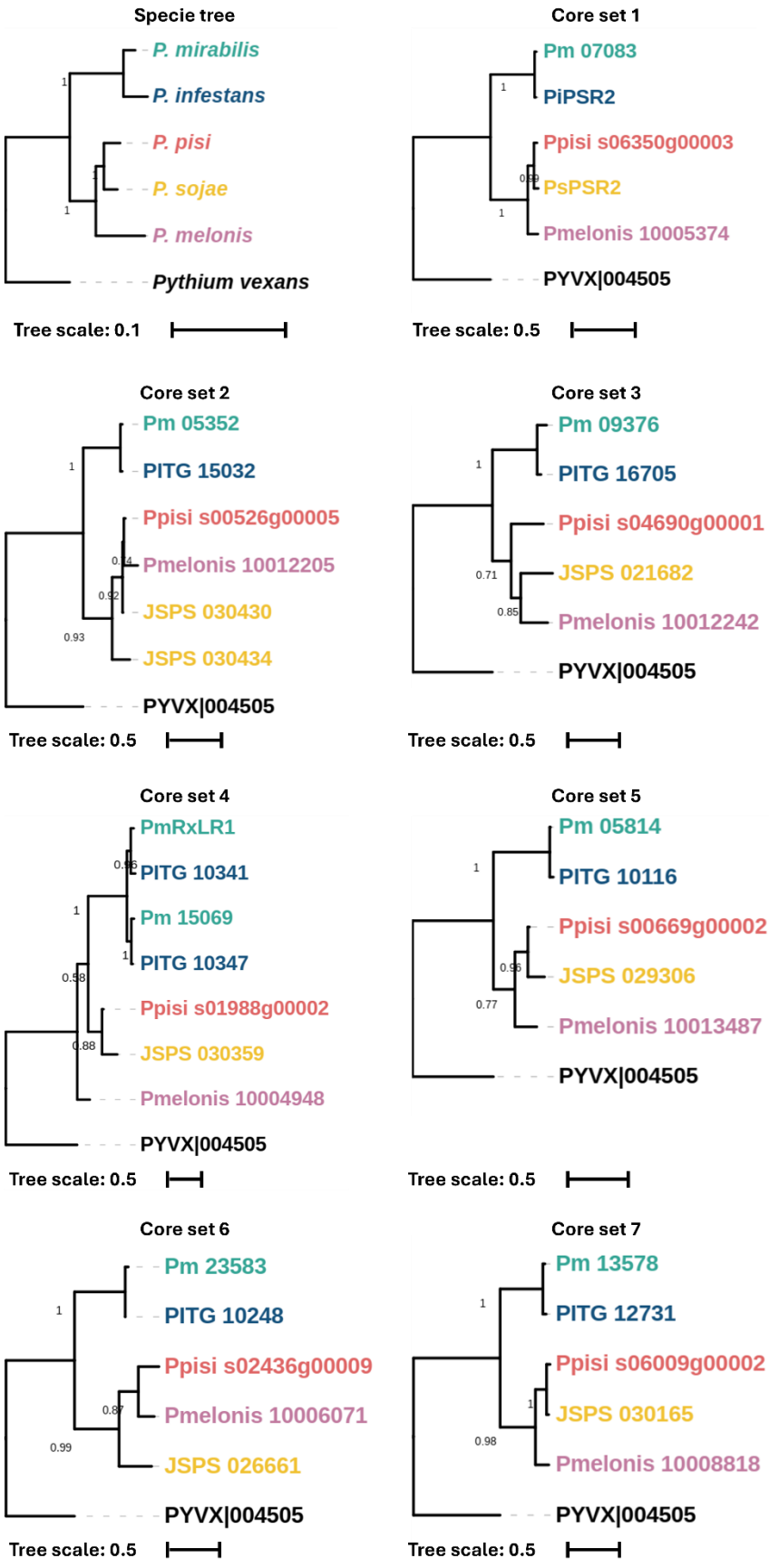

Figure 2.8 Co-evolutionary patterns of "Core" LWY effectors and *Phytophthora* species.

The species tree was constructed using neighbor-joining (NJ) analysis with five important genetic marker genes in *Phytophthora*. Protein sequences of each LWY gene from each "core" set were aligned for constructing phylogeny trees using maximum-likelihood (ML)analysis. Gene IDs from different species were labeled with their corresponding species-specific colors. *Pythium vexans* and *PYVX_004505* were the outgroups for species tree and "core" sets gene trees.

Since many RxLR effectors contain LWY tandem repeats, it is important to investigate whether LWY effectors evolve at different rates compared to RxLR effectors without LWY units by analysing sequence similarity of homologous LWY or non-LWY RxLR gene pairs either in closely related species (*P. infestans* and *P. mirabilis*) or two *P. sojae* isolates. Using BlastP, I conducted pairwise sequence comparisons of both LWY effectors and non-LWY RxLR effectors across these evolutionary distances to assess their relative conservation patterns. Sequence homology for a gene and its best hits in the other genome was assessed by combining sequence identity and sequence coverage.

A total of 397 *P. mirabilis* RxLR effectors were predicted using a combination of BlastP, HMM search, and RxLR-dEER string analysis. Among these, 70 were identified as containing LWY tandem repeats. Consequently, the comparative dataset includes 490 non-LWY RxLR effectors from *P. infestans* and 340 from *P. mirabilis*. In the two *P. sojae* strains, 206 non-LWY RxLR effectors were analyzed in P6497 and 293 in JS2.

The pairwise comparisons revealed significantly lower sequence similarity in LWY proteins compared to non-LWY RxLR effectors between *P. sojae* isolates (Figure 2.9A). However, this divergence pattern was not observed between *P. infestans* and *P. mirabilis* (Figure 2.9B). To further elucidate if different categories of LWYs might be evolving at different paces due to their different roles in functions and evolutions, LWY sequences were further analyzed by categories based on the presence or absence of SP and/or RxLR motifs.

Across both *P. sojae* isolates and in *P. infestans* and *P. mirabilis*, LWYs lacking signal peptides (No SP LWYs) showed significantly higher sequence variation compared to LWYs containing both SP and RxLR motifs (SP+RxLR LWYs), suggesting that No SP LWYs may experience reduced evolutionary constraints (Figure 2.9C and 2.9D). The lack

of selective pressure on LWY proteins without signal peptides suggests these genes may be undergoing pseudogenization.

In addition, non-LWY RxLR effectors (RxLR effectors that lack LWY units) have significantly higher sequence identity than all three subsets of LWYs in the two *P. sojae* isolates, implying that the (L)WY tandem arrays facilitate sequence variations and potentially drive the functional divergence even within strains than non-LWY RxLR effectors (Figure 2.9C). All these observations suggested that LWY repertoires play a significant role in driving effector variation within species. The lack of a similar pattern when comparing *P. infestans* and *P. mirabilis* may be attributed to species-specific differentiation, where factors other than (L)WY module shuffling serve as the primary drive of effector sequence variation (Figure 2.9E).

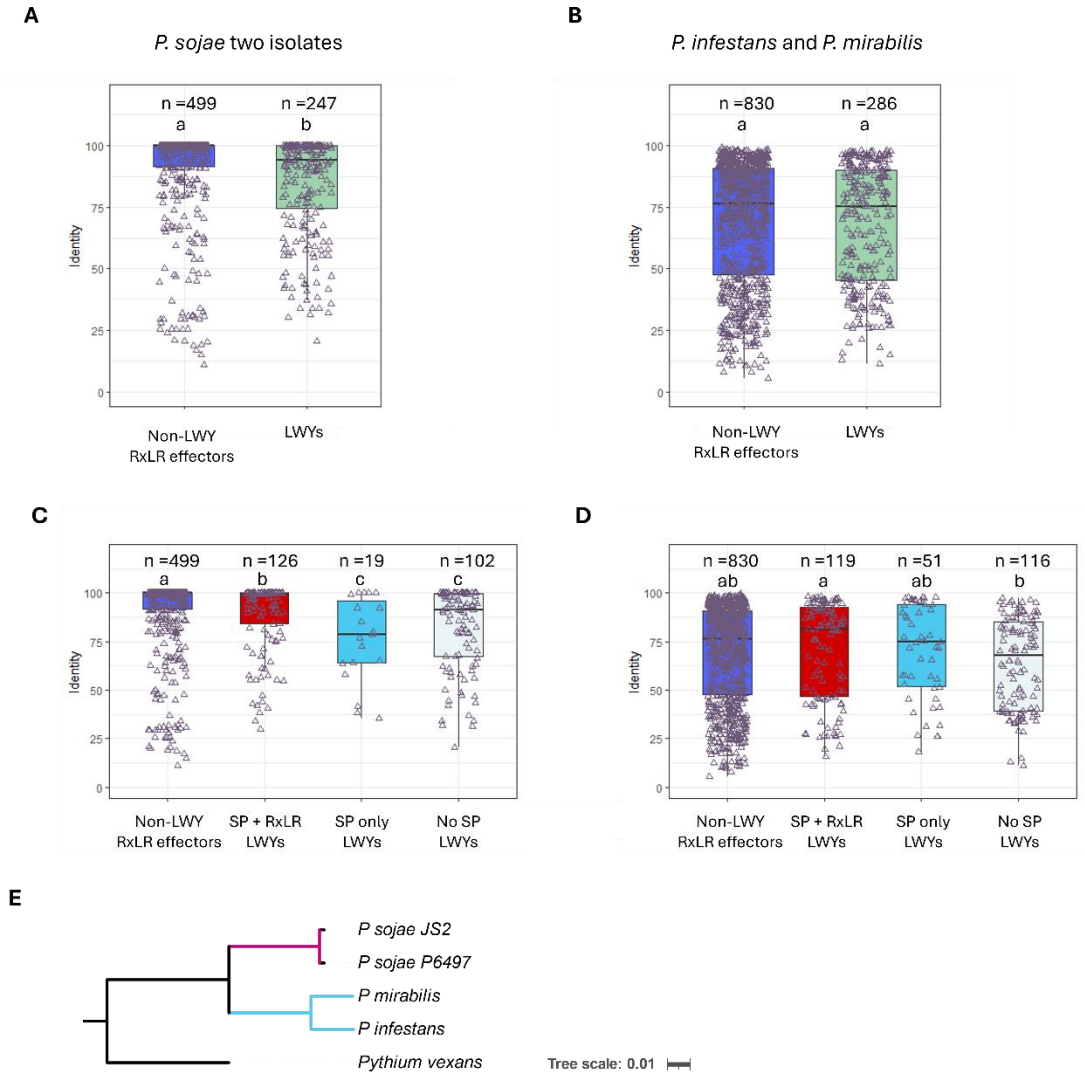

Figure 2.9 Sequence divergence of non-LWY RxLR effectors and LWY effectors.

Protein sequence identity in RxLR effectors lacks LWY units and LWYs were evaluated in two *P. sojae* isolates (**A**) or between *P. infestans* and its sister specie *P. mirabilis* (**B**). The number of genes in each set is labeled as "n." The statistical significance of sequence similarity was assessed using the Kruskal-Wallis test. Sequence similarities of non-LWY RxLR effectors, SP + RxLR LWYs, SP only LWYs and No SP LWYs were compared in two *P. sojae* strains (**C**) or between *P. infestans* and *P. mirabilis* (**D**). 2.2.4 *P. sojae* LWYs form multi-gene clusters in the genome, independent of the presence of SP and/or RxLR motifs.

To investigate the genomic organization of LWY effector genes, I mapped their distribution across the high-quality *P. sojae* JS2 genome assembly. This genome was selected for its high-quality assembly, enabling accurate characterization of gene locations and potential clustering patterns. The result revealed the distribution of LWY effector genes across all 13 chromosomes, occurring in genomic regions where RxLR effectors are also found, indicating similar genomic localization patterns in these two groups on the same genome (Figure 2.10A).

Noticeably, chromosomes 2, 8, 10, and 11 exhibited significantly higher LWY gene density, collectively harboring approximately 67% of all LWY genes encoded in JS2. Such LWY-dense regions are composed of LWY genes independent of the presence of SP and/or RxLR motifs, which may form a genomic environment that is conducive to rapid evolution (Figure 2.10A).

We hypothesized that LWY tandem repeat diversity might arise through unit rearrangement. Since recombination events are not uniformly distributed across the genome, it's crucial to identify genome regions that promote LWY effector shuffling (Matson et al. 2022; Tsai et al. 2010).

To better quantify whether LWYs can form multi-gene clusters, pairwise distances of adjacent LWY genes were calculated. Flanking distance with adjacent LWY genes within 15 kb is considered gene clustering. Measurement of physical distance in every two adjacent LWY genes from *the P. sojae* genome revealed four relatively large clusters (>- 4 LWY genes per cluster) in Chr 8, 9, and 11 and seventeen small LWY gene blocks (2-3 LWY genes) spanning the whole genome (Table 1.3). Noticeably, 58% of the LWY genes on Chr 2, 8, 10, and 11 are located in gene clusters, suggesting that these genomic environments may facilitate LWY unit rearrangements (Figure 2.10B).

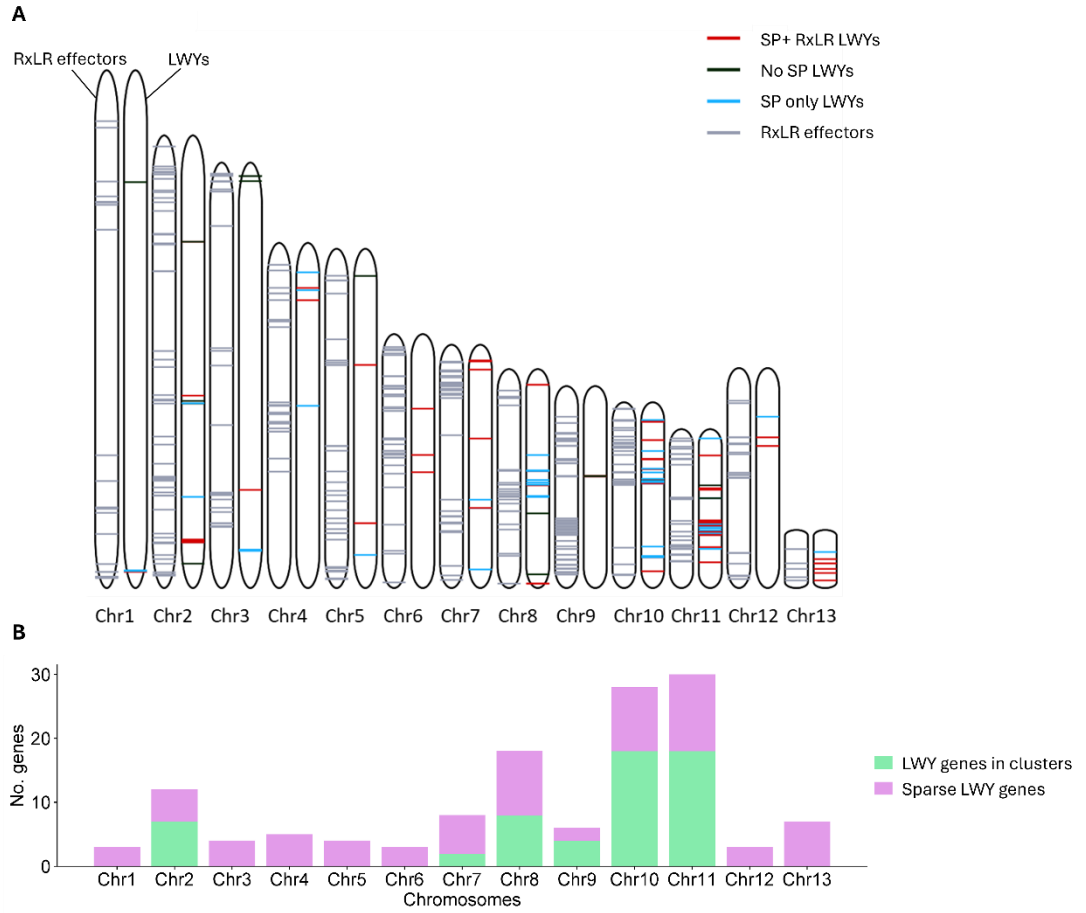

Figure 2.10 LWY effector genes form multi-gene clusters in *P. sojae* genome.

(**A**) The gene loci of RxLR effectors and LWY genes (different colors represent different categories with or without SP and/or RxLR motifs) in *P. sojae*. (**B**) A stacked bar plot displays the number of LWY genes organized into multi-gene clusters or dispersed across the genome.

Interestingly, one pair of LWY genes in *P. sojae* isolate JS2, *JSPS_021759* and *JSPS_021762,* located on a large cluster on Chr 8, share similar sequences in the N terminal three (L)WY units while exhibiting variation in the remaining four units (Figure 2.11). Another gene pair, JSPS_030430 and JSPS_030434, located in a cluster on chromosome 11, demonstrates similar unit variations that share four N-terminal units but diverge in their two C-terminal units. The homologs of JSPS_030430 and JSPS_030434 in *P. sojae* isolate P6497 were previously identified as the PP2A-interacting effectors PsAvh144 and PsAvh145 (Figure 2.11) (H. Li et al. 2023). However, while common N-terminal sequences are shared within each pair of LWY genes, their C-terminal regions show no detectable homology to any annotated genes or genomic

sequences in *P. sojae* strain JS2, suggesting rapid sequence divergence within these clustered LWY genes.

Most gene clusters consist of a mixture of LWY genes, including LWY effectors with both SP and RxLR motifs, as well as those lacking either SP, RxLR motif, or both signal features (Table 1.3). The Cluster 15 in Chr 11 contains primarily LWY effectors with SP and RxLR motifs while the Cluster 6 in Chr 8 harbors mainly No SP LWYs (Figure 2.11).

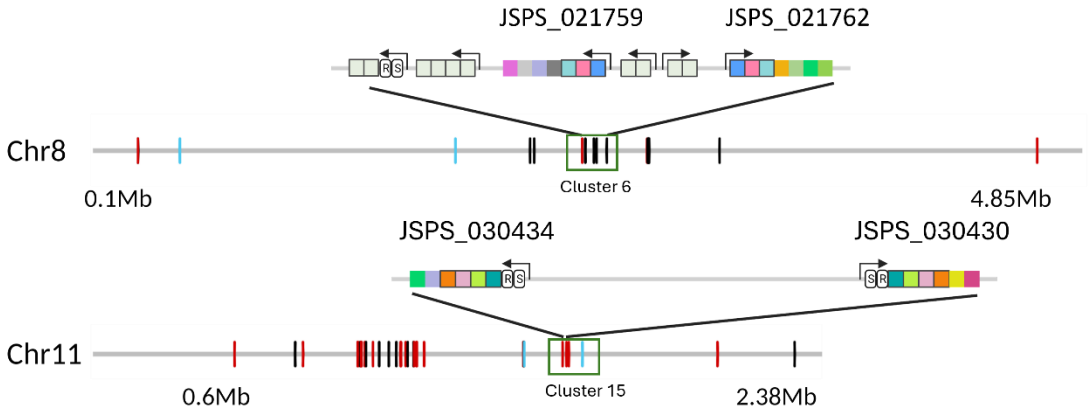

Figure 2.11 *P. sojae* genome contains LWY multi-gene clusters.

Two gene clusters in Chr8 and Chr11 harbor genes with potential recombination events. Architectures of putative protein products of LWY effector genes are illustrated with similar colored blocks representing LWY units with similar sequences. LWY genes with grey blocks are within the same gene clusters but don't share similar (L)WY units. The arrows represent the DNA strand orientation of corresponding genes. LWY genes in Cluster 6 and Cluster 15 are boxed in green.

Table 1.3 LWY multi-gene clusters.

Chromosome	Clusters	LWY genes	Category
Chr 2	Cluster1	JSPS_009323 JSPS_009324 JSPS_009325	No SP LWYs SP+RxLR LWYs SP+RxLR LWYs
Chr 2	Cluster2	JSPS_010350 JSPS_010353	SP only LWYs No SP LWYs
Chr 2	Cluster3	JSPS_011671 JSPS_011672	SP+RxLR LWYs SP only LWYs
Chr 7	Cluster4	JSPS_025484 JSPS_025486	No SP LWYs SP+RxLR LWYs
Chr 8	Cluster5	JSPS_021651 JSPS_021654	No SP LWYs No SP LWYs
Chr 8	Cluster6	JSPS_021757 JSPS_021758 JSPS_021759 JSPS_021760 JSPS_021761 JSPS_021762	SP+RxLR LWYs No SP LWYs No SP LWYs No SP LWYs No SP LWYs No SP LWYs
Chr 9	Cluster7	JSPS_027569 JSPS_027570 JSPS_027571 JSPS_027572	No SP LWYs SP only LWYs SP+RxLR LWYs SP only LWYs
Chr 10	Cluster8	JSPS_028522 JSPS_028523	SP+RxLR LWYs No SP LWYs
Chr 10	Cluster9	JSPS_029099 JSPS_029100	No SP LWYs SP+RxLR LWYs
Chr 10	Cluster10	JSPS_029103 JSPS_029107	No SP LWYs No SP LWYs
Chr 10	Cluster11	JSPS_029124 JSPS_029125	No SP LWYs No SP LWYs
Chr 10	Cluster12	JSPS_029131 JSPS_029134 JSPS_029135	SP only LWYs SP+RxLR LWYs No SP LWYs
Chr 10	Cluster13	JSPS_029218 JSPS_029219 JSPS_029220 JSPS_029222	No SP LWYs SP+RxLR LWYs SP+RxLR LWYs No SP LWYs
Chr 10	Cluster14	JSPS_029306 JSPS_029307 JSPS_029308	SP+RxLR LWYs SP+RxLR LWYs SP+RxLR LWYs
Chr 11	Cluster15	JSPS_030153	SP+RxLR LWYs

		JSPS_030154 JSPS_030158 JSPS_030159 JSPS_030160 JSPS_030161	SP+RxLR LWYs No SP LWYs SP+RxLR LWYs SP+RxLR LWYs SP+RxLR LWYs
Chr 11	Cluster16	JSPS_030165 JSPS_030166	SP+RxLR LWYs No SP LWYs
Chr 11	Cluster17	JSPS_030223 JSPS_030224	SP+RxLR LWYs SP+RxLR LWYs
Chr 11	Cluster18	JSPS_030229 JSPS_030232	SP+RxLR LWYs No SP LWYs
Chr 11	Cluster19	JSPS_030241 JSPS_030242	No SP LWYs SP+RxLR LWYs
Chr 11	Cluster20	JSPS_030244 JSPS_030245	SP+RxLR LWYs SP+RxLR LWYs
Chr 11	Cluster21	JSPS_030359 JSPS_030360	No SP LWYs SP only LWYs

2.2.4 Gene expression patterns of LWYs in *P. infestans*.

To dissect how LWY effector secretion, unit numbers play a role in plant-pathogen interaction, the transcriptome of *P. infestans* LWY genes was explored. Five stages of *P. infestans* strain 1306 transcriptomic data were analysed, with two from vegetative growth (Early rye and late rye) and three from different infection time points (1.5 dpi, 2.5 dpi and 4 dpi) (Ah-Fong et al. 2017). The CPM (counts per million reads mapped) values were normalized according to the length of the encoded LWY genes since CPM may bring bias that longer genes might produce more reads (Figure 2.12). Transcriptomic changes were visualized using a heatmap based on log10-transformed CPM values, with expression patterns clustered by similarity. The transcriptome from another *P. infestans* strain 3928A was also included. The heatmap was annotated with two additional columns indicating the number of (L)WY units and N-terminal features for each LWY gene.

Transcripts from 98 of these *P. infestans* LWY genes could be detected in the transcriptomic data (Figure 2.12). 47 LWY genes with the presence of SP are upregulated during infection in at least one of the two *P. infestans* strains. Notably, seven LWY genes lacking SP in studied two isolates can also be induced during infection, indicating a potential role in *P. infestans* endogenously (Figure 2.12).

Using a two-color system to differentiate between LWY proteins with fewer than three tandem units and those with three or more units, I observed that LWY genes encoding longer proteins (≥3 units) were preferentially upregulated during infection (Figure 2.12).

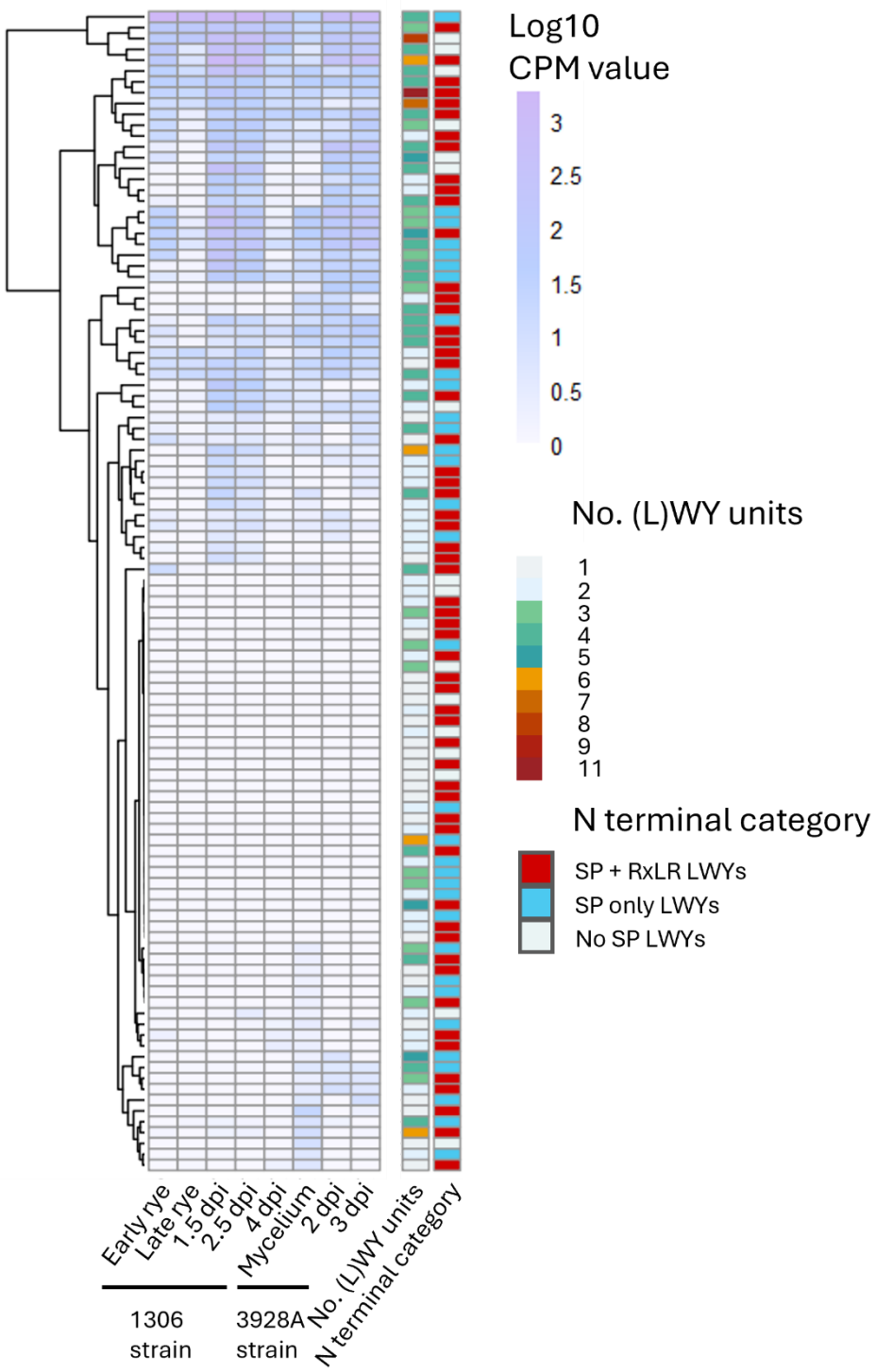

Figure 2.12 Transcriptomic analysis of vegetative growth and *P. infestans*-infected tubers, correlating (L)WY unit numbers with three LWY categories based on SP and RxLR motifs.

The transcriptome data was clustered to reveal expression patterns of vegetative (Early rye, late rye and mycelium) and infective stages (1.5 dpi, 2.5 dpi, 4 dpi, 2 dpi and 3 dpi) in two *P. infestans* isolates. The transcriptome data of *P. infestans* strain 1306 was

downloaded from (Ah-Fong et al. 2017). CPM values were normalized by sequence length, and the log10 of CPM (counts per million reads mapped) values was used as input. The transcriptome data of 3928A strain was from Dr. Suomeng Dong. No. (L)WY units and three LWY categories based on N-terminal signals were labelled accordingly.

2.3 Methods

2.3.1 HMM search, MEME motif finding, prediction of protein secondary structure, Signal Peptide and RxLR motifs

A comprehensive computational pipeline was developed to identify and characterize LWY effectors across five *Phytophthora* species. First, I constructed a Hidden Markov Model (HMM) using previously published LWY unit sequences (He et al. 2019). This model was used to search proteomes of *P. infestans*, *P. mirabilis*, *P. sojae*, *P. melonis*, and *P. pisi* for potential LWY-containing proteins.

Initial HMM candidates were further validated using MEME motif analysis with an E-value threshold of 1E-9. MEME parameters were optimized for LWY unit detection following established protocols: mod = zoops, nmotifs = 100, minsites = 50, minw = 15, maxw = 100, and maxsize = 1000000 (Boutemy et al. 2011). The false positive rate of our predictions was calculated using the standard formula: False Positive Rate = Number of False Positives / (Number of False Positives + Number of True Negatives).

Confirmed LWY proteins were then analyzed for additional features using specialized tools. Secondary structure predictions were performed using NetSurfP 3.0 (Hoie et al. 2022). Signal peptides were predicted using SignalP 5.0 (Nielsen et al. 2019), and RxLR motifs within the first 100 amino acids were identified using HMM searches following established protocols (Wood et al. 2020). This multi-step analysis enabled classification of LWY proteins based on the presence or absence of signal peptides and RxLR motifs.

2.3.2 Phylogeny tree

Phylogenetic analyses were conducted using MEGA11 (Tamura et al. 2021) through multiple approaches. For species tree construction, I concatenated sequences from five *Phytophthora* genetic markers and aligned them using the ClustalW algorithm. A Neighbor-Joining (NJ) tree was then constructed with 1,000 bootstrap replicates to establish species relationships.

For protein-level analyses, LWY sequences were aligned using ClustalW and analyzed using Maximum-Likelihood (ML) methods with 1,000 bootstrap replicates. A separate analysis of LWY genes showing evidence of recombination was performed at the nucleotide level using NJ analysis with 1,000 bootstrap replicates.

This multi-tiered phylogenetic approach enabled us to examine evolutionary relationships at different molecular levels - from species relationships to specific patterns of protein and gene evolution.

2.3.3 Ortholog search

Ortholog identification and analysis were conducted through a multi-step process. First, I performed all-against-all BlastP searches of 568 LWY proteins (Altschu et al. 1990) to identify potential homologous relationships. The best hits for each LWY sequence were then manually curated to verify their presence in orthologous groups. To compare evolutionary patterns, I conducted separate BlastP analyses of non-LWY RxLR effectors and LWY effectors to assess sequence identity levels between these protein classes.

The relationships between orthologous groups and BlastP results were visualized using the VennDiagram package in R (H. Chen and Boutros 2012). This integrated approach enabled comprehensive identification of orthologous relationships while providing insights into the evolutionary dynamics of different protein classes.

2.3.4 Genome loci analysis

Genomic analyses were conducted using genome assemblies from multiple *Phytophthora* species. The *P. sojae* isolate P6497 and JS2 genomes, *P. infestans* T30-4 genome, *P. pisi* genome, and *P. melonis* genome were obtained from NCBI (Haas et al. 2009; Kronmiller et al. 2023; Tyler 2007; Z. Zhang et al. 2024). The *P. mirabilis* genome was provided by the Suomeng Dong laboratory prior to publication.

To visualize the genomic distribution of these genes, I constructed an integrated chromosome plot displaying the locations of RxLR genes and LWY genes on opposite sides. The LWY genes were further categorized based on their structural features,

specifically the presence or absence of signal peptides and RxLR motifs, to examine potential patterns in their genomic organization.

2.3.5 Transcriptome analysis

Transcriptome analysis was conducted using publicly available *P. infestans* RNA-seq data from vegetative growth and infection stages. Expression levels were quantified using CPM (counts per million reads mapped) values and normalized by gene length to account for transcript differences in *P. infestans* 1306 isolate (Ah-Fong et al. 2017). The transcriptome data of another *P. infestans* isolate 3928A was from Dr. Suomeng Dong. I then generated heatmaps to visualize potential correlations between expression patterns and three key features of LWY genes: presence/absence of signal peptides, presence/absence of RxLR motifs, and the number of LWY units. This analysis enabled us to examine how structural characteristics of LWY genes might influence their transcriptional regulation during different developmental stages.

2.4 Discussion

In this chapter, I aimed to investigate whether LWY effectors can undergo unit rearrangement by analysing *Phytophthora* genome sequences. I identified two pairs of LWY genes in *P. sojae* localized in multi-gene clusters that might undergo module shuffling. Additionally, I found diverse resources of LWY fragments in the five *Phytophthora* genomes I studied, with up to 64% of LWYs lacking SP and/ or RxLR motifs (Figure 2.13). These LWY tandem repeats physically form multi-gene clusters (Figure 2.13). Interestingly, these gene clusters comprise a combination of LWY effectors that lack N terminal secretion and/ or translocation signals, potentially representing a reservoir for (L)WY module shuffling (Figure 2.13). Genomic regions in which these dynamic LWY gene clusters are embedded may create genomic environments that facilitate LWY module shuffling and generate new combinations.

Additionally, LWY genes contain repeated (L)WY units up to 12, with 63% being lineage-specific. Such a diversity indicates the sequence variation of embedded LWY effectors, which may confer the ability to recruit distinct host molecules, thereby driving functional divergence of effectors. In summary, my research highlights that *Phytophthora* genomes contain a reservoir of LWY sequences that may serve as a cradle for effector evolution.

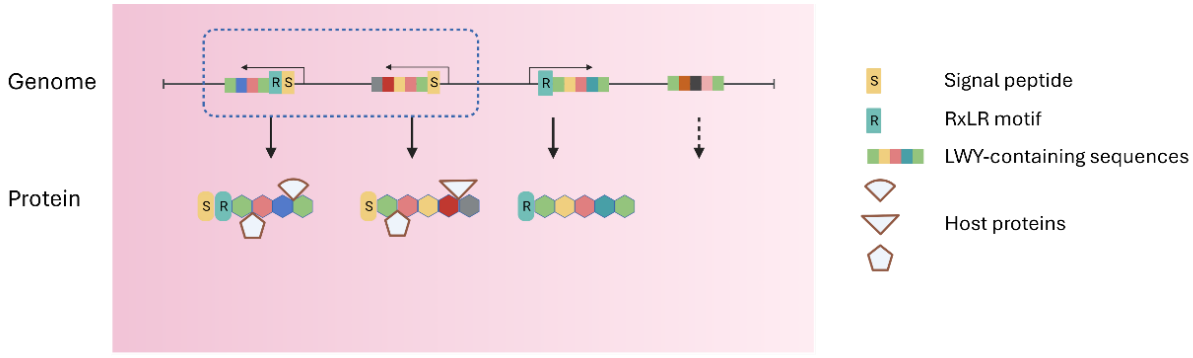

Figure 2.13 Model for (L)WY module shuffling.

Effector biology has traditionally relied on SP and RxLR motifs as key features for secretion and plant entry, potentially underestimating the diversity of virulence factors. This limitation is exemplified by downy mildew, where approximately half of the secreted WY domain proteins lack RxLR motifs yet retain RxLR effector-like functions, including PTI response suppression and cell death elicitation. These findings suggest that WY units themselves serve as robust predictive features for effector identification (Wood, Nur et al. 2020).

Given the structural similarities between WY and LWY units and their common occurrence as tandem repeats in effector domains, our identification of numerous LWY effectors lacking SP and/or RxLR motifs (No SP and SP only LWYs) is particularly significant. Transcriptome analysis indicated some No SP LWYs are induced during *P. infestans* infection, indicating their potential roles as virulence factors. Notably, I cataloged a more extensive repertoire of LWY domain proteins than previous studies using SP and RxLR motifs as criteria instead of filters. Thus, I propose that (L)WY units should be considered predictive features for studying *Phytophthora* effector repertoires.

Pathogens encode effector genes, which are rapidly evolving, in the regions of the genome that enrich repetitive elements. These genome compartments are referred to as gene sparse regions (GSR) in two-speed genomes, accessory genomes, AT isochores, mini-chromosomes, etc, which are linked to higher rates of point mutations and sequence rearrangements, therefore driving effector diversification (Chuma et al. 2011; Croll and McDonald 2012; Langner et al. 2021; L. J. Ma et al. 2010; Rouxel et al. 2011). Particularly, some of these effectors are organized in gene clusters and confer virulence in bacteria, fungi and oomycete (Brefort et al. 2014; Doehlemann et al. 2009; Ji et al. 2016; Jiang et al. 2008; Kamper et al. 2006). *Ustilago maydis* display an attenuation of disease after deleting a large effector gene cluster comprising 24 effectors (Brefort et al. 2014).

Gene duplication and genome arrangement are hypothesized to be the origin of gene cluster assemblies (Dutheil et al. 2016; Fouché et al. 2018). Thus, the presence of gene clusters can be an indicator of gene duplication and recombination events. Indeed, I identified LWY genes that may result from recombination in LWY cluster assemblies. These tandem duplicated gene structures on genomes could promote the expansion of the LWY repertoires and host adaptation. Therefore, it's likely that the shuffling of LWY effectors facilitates functional divergence of the expanded effector arsenals. We

previously observed that the mosaic patterns of tandem arrays in PP2A-interacting LWY effectors (H. Li et al. 2023). Additionally, I found two pairs of LWY genes in *P. sojae* that show the combinations of common and varied (L)WY units, indicating that unit shuffling might be a common strategy used by LWY effectors for diversifying protein-binding specificities.

In summary, this chapter systematically characterized LWY effectors and discovered the genome environment suitable for (L)WY module shuffling and potential candidates that may undergo tandem repeat rearrangement, paving the way for the identification of LWY effectors undergoing recombination. This leads to Chapter 4, where I'll report the discovery of recombined LWY effectors and their functional divergence.

2.5 Reference

Ah-Fong, A. M. V., Shrivastava, J., and Judelson, H. S. (2017), 'Lifestyle, gene gain and loss, and transcriptional remodeling cause divergence in the transcriptomes of *Phytophthora* infestans and Pythium ultimum during potato tuber colonization', *BMC Genomics,* 18 (1), 764.

Altschu, Stephen. F. , et al. (1990), 'Basic Local Alignment Search Tool', *J Mol Biol,* 215.

Bao, J., et al. (2017), 'PacBio Sequencing Reveals Transposable Elements as a Key Contributor to Genomic Plasticity and Virulence Variation in Magnaporthe oryzae', *Mol Plant,* 10 (11), 1465-68.

Boutemy, L. S., et al. (2011), 'Structures of *Phytophthora* RXLR effector proteins: a conserved but adaptable fold underpins functional diversity', *J Biol Chem,* 286 (41), 35834-42.

Brefort, T., et al. (2014), 'Characterization of the largest effector gene cluster of Ustilago maydis', *PLoS Pathog,* 10 (7), e1003866.

Canham, J., et al. (2024), 'GetGenome: Overcoming inequalities in access to genomics technology', *PLoS Biol,* 22 (8), e3002804.

Chen, Hanbo. and Boutros, Paul. C. (2012), 'VennDiagram: a package for the generation of highly-customizable Venn and Euler diagrams in R', *BMC Bioinformatics,* 12.

Chou, S., et al. (2011), 'Hyaloperonospora arabidopsidis ATR1 effector is a repeat protein with distributed recognition surfaces', *Proc Natl Acad Sci U S A,* 108 (32), 13323-8.

Chuma, I., et al. (2011), 'Multiple translocation of the AVR-Pita effector gene among chromosomes of the rice blast fungus Magnaporthe oryzae and related species', *PLoS Pathog,* 7 (7), e1002147.

Croll, D. and McDonald, B. A. (2012), 'The accessory genome as a cradle for adaptive evolution in pathogens', *PLoS Pathog,* 8 (4), e1002608.

Dagdas, Y. F., et al. (2016), 'An effector of the Irish potato famine pathogen antagonizes a host autophagy cargo receptor', *Elife,* 5.

Derevnina, L., et al. (2021), 'Plant pathogens convergently evolved to counteract redundant nodes of an NLR immune receptor network', *PLoS Biol,* 19 (8), e3001136.

Doehlemann, G., et al. (2009), 'Pep1, a secreted effector protein of Ustilago maydis, is required for successful invasion of plant cells', *PLoS Pathog,* 5 (2), e1000290.

Dong, S., Raffaele, S., and Kamoun, S. (2015), 'The two-speed genomes of filamentous pathogens: waltz with plants', *Curr Opin Genet Dev,* 35, 57-65.

Dutheil, J. Y., et al. (2016), 'A Tale of Genome Compartmentalization: The Evolution of Virulence Clusters in Smut Fungi', *Genome Biol Evol,* 8 (3), 681-704.

Fouché, Simone., Plissonneau, Clémence., and Croll, Daniel. (2018), 'The birth and death of effectors in rapidly evolving filamentous pathogen genomes', *Current Opinion in Microbiology,* 46.

Goodwin, S. B., et al. (2011), 'Finished genome of the fungal wheat pathogen Mycosphaerella graminicola reveals dispensome structure, chromosome plasticity, and stealth pathogenesis', *PLoS Genet,* 7 (6), e1002070.

Grandaubert, Jonathan., Lowe, Rohan. GT., and Soyer, Jessica. L. (2014), 'Transposable element-assisted evolution and adaptation to host plant within the Leptosphaeria maculans-Leptosphaeria biglobosa species complex of fungal pathogens', *BMC Genomics,* 15.

Guo, B., et al. (2019), '*Phytophthora* sojae Effector PsAvh240 Inhibits Host Aspartic Protease Secretion to Promote Infection', *Mol Plant,* 12 (4), 552-64.

Haas, B. J., et al. (2009), 'Genome sequence and analysis of the Irish potato famine pathogen *Phytophthora* infestans', *Nature,* 461 (7262), 393-8.

He, J., et al. (2019), 'Structural analysis of *Phytophthora* suppressor of RNA silencing 2 (PSR2) reveals a conserved modular fold contributing to virulence', *Proc Natl Acad Sci U S A,* 116 (16), 8054-59.

Hoie, M. H., et al. (2022), 'NetSurfP-3.0: accurate and fast prediction of protein structural features by protein language models and deep learning', *Nucleic Acids Res,* 50 (W1), W510-W15.

Hou, Y., et al. (2019), 'A *Phytophthora* Effector Suppresses Trans-Kingdom RNAi to Promote Disease Susceptibility', *Cell Host Microbe,* 25 (1), 153-65 e5.

Ji, Z., et al. (2016), 'Interfering TAL effectors of Xanthomonas oryzae neutralize R-gene-mediated plant disease resistance', *Nat Commun,* 7, 13435.

Jiang, H. Y., et al. (2008), 'RXLR effector reservoir in two *Phytophthora* species is dominated by a single rapidly evolving superfamily with more than 700 members', *PNAS,* 105 (12).

Kamper, J., et al. (2006), 'Insights from the genome of the biotrophic fungal plant pathogen Ustilago maydis', *Nature,* 444 (7115), 97-101.

Kronmiller, B. A., et al. (2023), 'Comparative Genomic Analysis of 31 *Phytophthora* Genomes Reveals Genome Plasticity and Horizontal Gene Transfer', *Mol Plant Microbe Interact,* 36 (1), 26-46.

Langner, T., et al. (2021), 'Genomic rearrangements generate hypervariable mini-chromosomes in host-specific isolates of the blast fungus', *PLoS Genet,* 17 (2), e1009386.

Li, H., et al. (2023), 'Pathogen protein modularity enables elaborate mimicry of a host phosphatase', *Cell,* 186 (15), 3196-207 e17.

Ma, L. J., et al. (2010), 'Comparative genomics reveals mobile pathogenicity chromosomes in Fusarium', *Nature,* 464 (7287), 367-73.

Maqbool, A., et al. (2016), 'Structural Basis of Host Autophagy-related Protein 8 (ATG8) Binding by the Irish Potato Famine Pathogen Effector Protein PexRD54', *J Biol Chem,* 291 (38), 20270-82.

Matson, M. E. H., et al. (2022), 'Karyotype variation, spontaneous genome rearrangements affecting chemical insensitivity, and expression level polymorphisms in the plant pathogen *Phytophthora* infestans revealed using its first chromosome-scale assembly', *PLoS Pathog,* 18 (10), e1010869.

Miao, VIVIAN. P., Covert, SARAH. F. , and Vanetten, HANs. D. (1991), 'A Fungal Gene for Antibiotic Resistance on a Dispensable ("B") Chromosome', *Science,* 254.
Nielsen, H., et al. (2019), 'A Brief History of Protein Sorting Prediction', *Protein J,* 38 (3), 200-16.
Peng, Z., et al. (2019), 'Effector gene reshuffling involves dispensable mini-chromosomes in the wheat blast fungus', *PLoS Genet,* 15 (9), e1008272.
Prince, V. E. and Pickett, F. B. (2002), 'Splitting pairs: the diverging fates of duplicated genes', *Nat Rev Genet,* 3 (11), 827-37.
Qiao, Y., et al. (2013), 'Oomycete pathogens encode RNA silencing suppressors', *Nat Genet,* 45 (3), 330-3.
Reams, A. B. and Neidle, E. L. (2004), 'Selection for gene clustering by tandem duplication', *Annu Rev Microbiol,* 58, 119-42.
Rouxel, T., et al. (2011), 'Effector diversification within compartments of the Leptosphaeria maculans genome affected by Repeat-Induced Point mutations', *Nat Commun,* 2, 202.
Schmidt, Sarah. M., Houterman, Petra. M., and Schreiver, Ines. (2013), 'MITEs in the promoters of effector genes allow prediction of novel virulence genes in Fusarium oxysporum', *BMC Genomics,* 14.
Schotanus, K., et al. (2015), 'Histone modifications rather than the novel regional centromeres of Zymoseptoria tritici distinguish core and accessory chromosomes', *Epigenetics Chromatin,* 8, 41.
Tamura, K., Stecher, G., and Kumar, S. (2021), 'MEGA11: Molecular Evolutionary Genetics Analysis Version 11', *Mol Biol Evol,* 38 (7), 3022-27.
Temporini, E. D. and VanEtten, H. D. (2004), 'An analysis of the phylogenetic distribution of the pea pathogenicity genes of Nectria haematococca MPVI supports the hypothesis of their origin by horizontal transfer and uncovers a potentially new pathogen of garden pea: Neocosmospora boniensis', *Curr Genet,* 46 (1), 29-36.
Tsai, I. J., Burt, A., and Koufopanou, V. (2010), 'Conservation of recombination hotspots in yeast', *Proc Natl Acad Sci U S A,* 107 (17), 7847-52.
Tyler, B. M. (2007), '*Phytophthora* sojae: root rot pathogen of soybean and model oomycete', *Mol Plant Pathol,* 8 (1), 1-8.
Vlaardingerbroek, I., et al. (2016), 'Dispensable chromosomes in Fusarium oxysporum f. sp. lycopersici', *Mol Plant Pathol,* 17 (9), 1455-66.
Win, J., et al. (2012), 'Sequence divergent RXLR effectors share a structural fold conserved across plant pathogenic oomycete species', *PLoS Pathog,* 8 (1), e1002400.
Wood, K. J., et al. (2020), 'Effector prediction and characterization in the oomycete pathogen Bremia lactucae reveal host-recognized WY domain proteins that lack the canonical RXLR motif', *PLoS Pathog,* 16 (10), e1009012.
Xiong, Q., et al. (2014), '*Phytophthora* suppressor of RNA silencing 2 is a conserved RxLR effector that promotes infection in soybean and Arabidopsis thaliana', *Mol Plant Microbe Interact,* 27 (12), 1379-89.

Zhang, Z., et al. (2024), 'Complete telomere-to-telomere genomes uncover virulence evolution conferred by chromosome fusion in oomycete plant pathogens', *Nat Commun,* 15 (1), 4624.

Chapter 3 Identification of specific (L)WY unit combinations as potential functional modules

3.1 Introduction

As stated in Chapter 1, (L)WY effectors contain structurally conserved folds but sequence variable surface residues. Recent studies demonstrate that WY units play crucial roles in effector functions through specific interactions with host proteins. Two key examples illustrate this functional importance:

First, the *P. infestans* WY effector PexRD2 targets host MAPKKK to suppress phosphorylation of downstream MAPKs, thereby promoting disease progression (King et al. 2014). Mutation of two surface residues on only one WY unit abolishes the interaction of PexRD2 and its target MAPKKK. This is further supported by two PexRD2-like proteins, which present varied residues in the WY domains has attenuated interactions with MAPKKK. This illustrates that the WY unit in PexRD2 is a functional unit to interacts with MAPKKK.

Second, the *P. sojae* effector PsAvh240, which contains two WY units, prevents secretion of the soybean-resistant aspartic protease 1 (GmAP1) into the apoplast apoplast (Guo et al. 2019). Deletion of two α-helices in the WY1 unit compromises GmAP1 interaction, indicating that WY1 serves as a functional module for target binding.

Based on these findings, it's likely that, similar to WY units, LWY units or unit combinations can associate with specific host interactors. Therefore, we hypothesize that LWY effectors adopt (L)WY units or unit combinations to recruit host targets for effector functions. These host-target interacting units are defined as functional modules. Additionally, the majority of WY effectors in the previous study had two to three WY units while in Chapter 2, I found the majority (77%) of LWY effectors contain between two to five (L)WY units. This suggests enhanced compacity for LWY effectors to encode multiple functional modules for target binding, resulting in the association of different host proteins into protein complexes for effector novel functions.

Our recent research provides compelling evidence for this functional module hypothesis through the characterization of the *P. sojae* effector PSR2. We discovered that PSR2 interacts with the plant protein phosphatase 2A (PP2A) core enzyme (PP2A A and C subunits) by mimicking PP2A B subunits. Structural analysis of the PSR2-PP2A complex revealed that the LWY2-LWY3 region of PSR2 directly interacts with the Arabidopsis PP2A A subunit PDF1, demonstrating that this LWY2-LWY3 combination functions as a specific recruitment module for the PP2A A subunit.

Significantly, we identified a similar (L)WY-LWY module combination in 12 additional LWY effectors from *P. sojae* and *P. infestans*. These effectors also associate with the plant PP2A core enzyme to form effector-PP2A holoenzymes (H. Li et al. 2023). Notably, mutations of key interacting residues revealed by the PSR2-PDF1 complex structure abolished the interaction and reduced the effectors' virulence activity. This study defined a functional module from two adjacent (L)WY units.

PSR2 exhibits a domain architecture comprising seven tandem repeats arranged as WY1-(LWY)6, with the PP2A-interacting modules specifically located within LWY2-LWY3 (Figure 3.1). Since the human PP2A B subunit shows close association with the C subunit for substrate binding, the PSR2 as the mimicry of PP2A B subunits in plants may recruit substrates through C terminal LWY units. However, the sequences and structures of PP2A-interacting effectors in the C terminal are quite diverse, suggesting the potential of recruiting different substrates by PP2A-interacting effectors.

To investigate this hypothesis, we analyzed the crystal structure of PITG_15142, another PP2A-interacting effector that displays a WY1-(LWY)4 architecture. Our structural comparison revealed the high conservation between PSR2 and PITG_15142 in N-terminal (L)WY units responsible for PP2A interaction. However, their C-terminal regions exhibit structural diversity, which might reflect on divergence in substrate binding. Indeed, phospho-proteomics analysis in Arabidopsis transgenic lines revealed distinct patterns of phospho-peptide regulation by these two effectors (Figure 3.1). Furthermore, interactome analyses demonstrated that, while both effectors maintain their interaction with PP2A core enzymes, they associate with distinct sets of host targets. These findings demonstrate how the combination of conserved PP2A-interacting modules with diverse C-terminal functional units enables these effectors to achieve different biochemical functions, despite sharing a common PP2A-binding capability.

The example of PP2A-interacting effectors suggests 1:) the binding surface to host targets may reside in the groove between two adjacent (L)WY units, which as a functional module to interact with host targets. 2:) Different combinations of (L)WY units can recruit distinct host proteins to form varied protein complexes.

Based on these observations, we hypothesize that LWY effectors employ specific functional modules to associate with specific host proteins. We further propose that recombination events can promote module shuffling, generating diverse functional modules capable of recruiting different host proteins. The combinations of different functional modules in LWY effectors enable the formation of diverse protein complexes by recruiting different host targets, facilitating the expansion of virulence targets and effector functional divergence.

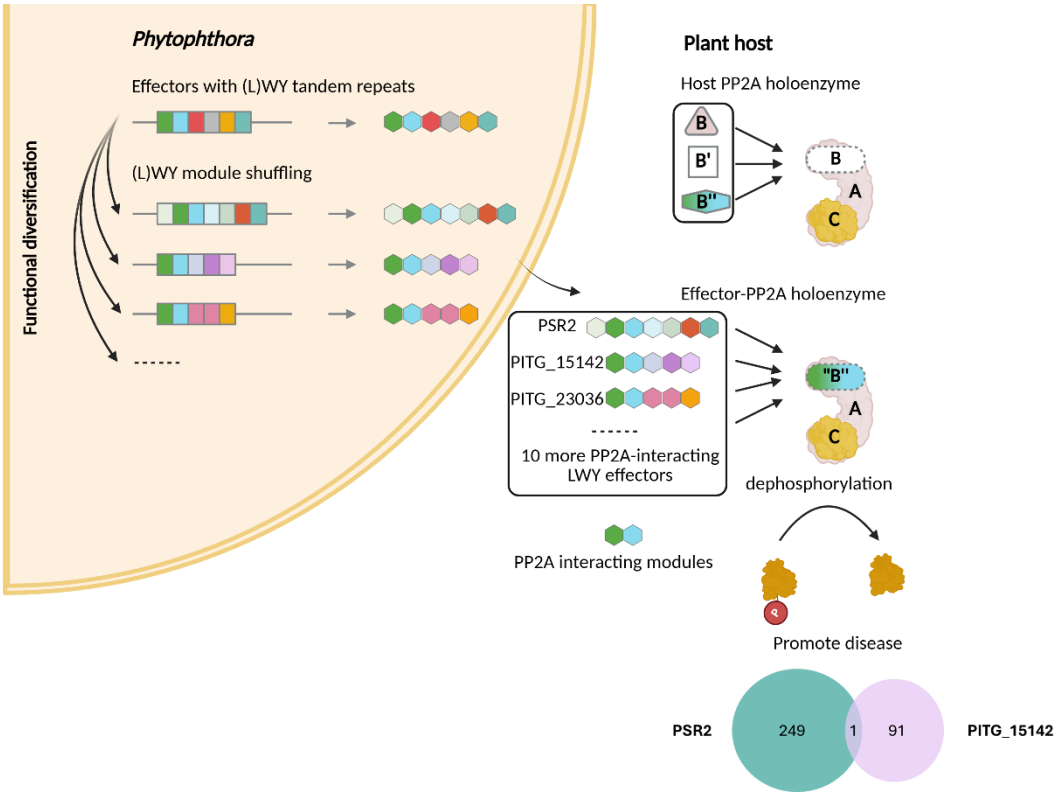

Figure 3.1 PP2A-interacting effectors regulate host protein phosphorylation.

The discovery of the PP2A-interacting module raises an important question: Do additional functional modules exist that benefit *Phytophthora* infection?

In this chapter, I carried out a systematic analysis of (L)WY-LWY unit combinations to identify potential functional modules. I focus on (L)WY unit combinations, rather than individual units because PP2A-interacting residues reside in the grooves of two adjacent (L)WY units and we're looking for similar patterns that could potentially recruit host proteins.

Using the (L)WY repertoire predicted in the five *Phytophthora* species (*P. infestans*, *P. mirabilis*, *P. sojae, P. melonis* and *P. pisi*) analysed in Chapter 2, I first classified individual (L)WY units into 65 clusters based on their surface exposed residues. The cluster definition was further used to identify co-occurring unit-unit combinations that are enriched in the (L)WY protein repertoire. Analysis of two-unit combinations revealed 45 potential functional modules, with 13 co-occurred modules specifically enriched in LWY effectors with SP and RxLR motifs.

Our findings suggest that (L)WY units or unit combinations serve as functional modules that may mediate specific interactions with host molecules, especially proteins. Functional modules that mediate critical host interactions can be adopted by multiple effectors. Combining these conserved modules with variable (L)WY units further enables LWY effectors to interact with both common and specific host proteins to form dynamic protein complexes, thereby facilitating the expansion of virulence activity.

3.2 Results

3.2.1 The pipeline to cluster exposed residues from 2168 (L)WY units.

Previously I identified 568 LWY effectors in five *Phytophthora* species (*P. infestans*, *P. mirabilis*, *P. sojae*, *P. melonis* and *P. pisi*). Using protein secondary structures and sequence features from each (L)WY unit, 2168 (L)WY units extracted from the 568 LWY effectors were further studied using a bioinformatic pipeline (Figure 3.2). Since the exposed residues on the surface of each (L)WY unit are presumed to determine specific interaction capacity with host molecules, these residues were extracted from each unit while the buried residues were replaced as methionine so that the alignment of exposed residues would be in the correct structural positions (Figure 3.2). This modification enabled us to analyze the potentially interaction-determining residues while maintaining structural context.

Multi-sequence alignments were then performed to align approximately 2168 sequences. A sequence similarity matrix was constructed from the alignments and subsequently converted into a distance matrix, which was then used as input for hierarchical clustering (Figure 3.2).

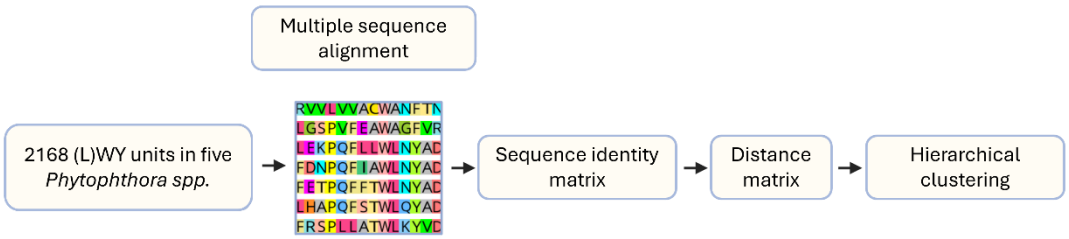

Figure 3.2 The pipeline for hierarchical clustering of (L)WY units

The preparation of input for hierarchical clustering involves in sequence alignment-based similarity matrix.

3.2.2 2168 (L)WY units were classified into 65 clusters.

The crystal structures of PP2A A subunit and PSR2 indicated the interfaces reside in the grooves between two adjacent (L)WY units. Therefore, we hypothesized that two-unit combinations in LWY effectors might serve as important platforms to mediate host protein interactions.

With this rationale, I mapped the clusters for each unit back to the individual LWY proteins and extracted and quantified the frequency of cluster combinations between adjacent (L)WY unit pairs across the entire dataset (Figure 3.3). 2168 units were grouped into distinct clusters based on sequence similarities of exposed residues. From the total 2,168 individual units, 1,596 (L)WY-LWY pairs were identified. 2168 individual units were classified into different clusters, leading to further characterization of distinct unit combinations that contain clustering information. These combinations were represented in the format n1_n2, where n1 and n2 denote the cluster classification of the first and second units, respectively. For example, 16_9 indicates that the first unit is a member of Cluster 16, while the second unit belongs to Cluster 9 (Figure 3.3). The abundance of each unit combination will be determined. The frequently occurring unit-unit combinations will be prioritized as candidate functional modules for further characterization.

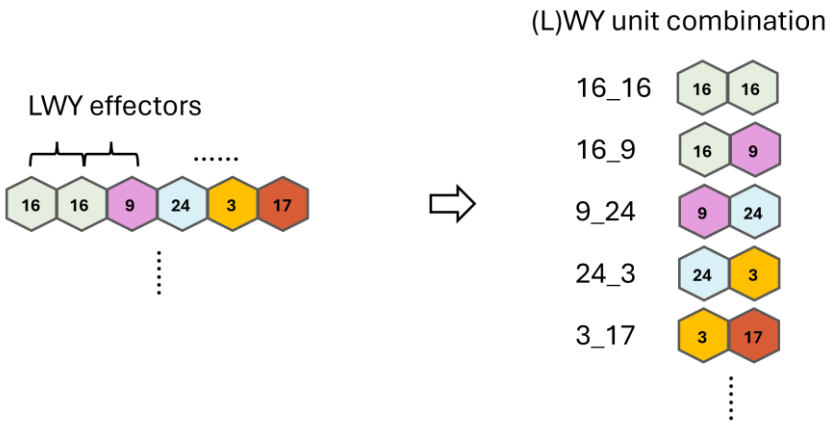

Figure 3.3 Workflow for identifying enriched (L)WY-LWY co-occurrence patterns.

(L)WY units from LWY effector proteins were hierarchically clustered and mapped back to individual LWY effectors. The cluster information of every two adjacent (L)WY units

was extracted and ranked by how frequently detected from the whole pool of unit-unit combinations. Unit combinations are denoted as n1_n2, where n1 and n2 represent the cluster numbers of first and second adjacent units, respectively.

Here I classified 2168 (L)WY units into different groups (22, 40, 65, and 99 clusters) to identify optimal clustering granularity that would reveal meaningful co-occurrence patterns, particularly for abundant combinations that may represent functional modules (Figure 3.4).

The optimal clustering granularity should achieve two key objectives: first, to maintain the co-occurrence patterns observed in positive controls, i.e. PP2A interacting modules, to serve as validated benchmarks, and second, to preserve distinct subgroups that show similar co-occurrence frequencies of (L)WY unit combinations to the positive control. This balanced approach ensures both reliability through positive control validation and proper resolution of biologically relevant subgroups.

To visualize the distribution patterns of (L)WY unit combinations across different clustering levels, I generated polar bar plots representing the 20 most frequent combinations in four different groups of clustering granularity (22, 40, 65, and 99 clusters) (Figure 3.4).

Initial analysis using 22 and 99 clusters proved suboptimal, as 22 clusters were too broad and 99 too granular to meet our objectives for optimal clustering. Using 22 clusters, I found that PP2A-interacting modules were distributed across several combinations, with the majority (six modules) appearing in combination 6_6 (where both units belonged to Cluster 6) (Figure 3.4). The remaining modules were dispersed across combinations 11_6, 13_6, 19_6, and 4_6 (Figure 3.4A). However, combination 6_6 contained 205 unit pairs while PP2A-interacting effectors only harbour 6 pairs of them. This poor resolution indicates the clustering level of 22 merged too many unit pairs into one single combination, which is insufficient to effectively discriminate unit combinations based on our hypothesized one module-one target hypothesis.

In contrast, a stringent 99 cluster revealed enrichment of two combinations: 27_27 and 21_21 (Figure 3.4B). Notably, combination 21_21 included four PP2A-interacting modules. However, at this high level, I observed only one combination (27_27) as abundant as the PP2A-interacting units (Figure 3.4B). This suggests that a cluster of

99 may be overly stringent, as it could split potential functional modules into multiple combinations. Such fragmentation complicates the investigation of which specific combinations may be important for interactions with host targets.

To optimize the balance between sensitivity and specificity in identifying distinct functional modules, I evaluated two intermediate clustering granularities: 40 and 65. Analysis using 40 clusters revealed a high frequency of the 8_8 combination in 120 unit pairs (Figure 3.4C). However, like clustering into 22 groups, using 40 clusters still failed to adequately separate unit combinations, with many remaining merged in a single combination. This indicates that clustering individual (L)WY units in 40 clusters lacked the specificity needed to identify candidates for further examination (Figure 3.4C).

Analysis of 2,168 sequences identified 65 clusters containing four main paired patterns: 16_16 (45 pairs), 18_18 (32 pairs), 9_9 (30 pairs), and 16_25 (21 pairs) (Figure 3.4D). Among the 32 pairs showing the 18_18 pattern, 5 pairs were present in PP2A-interacting effectors (Figure 3.4D). Furthermore, I observed 11 additional combinations that occurred more than 10 times. The identification of multiple frequently occurring (L)WY unit combinations in the effector repertoire suggests that these combinations may serve as functional modules that confer important host-interacting capacity.

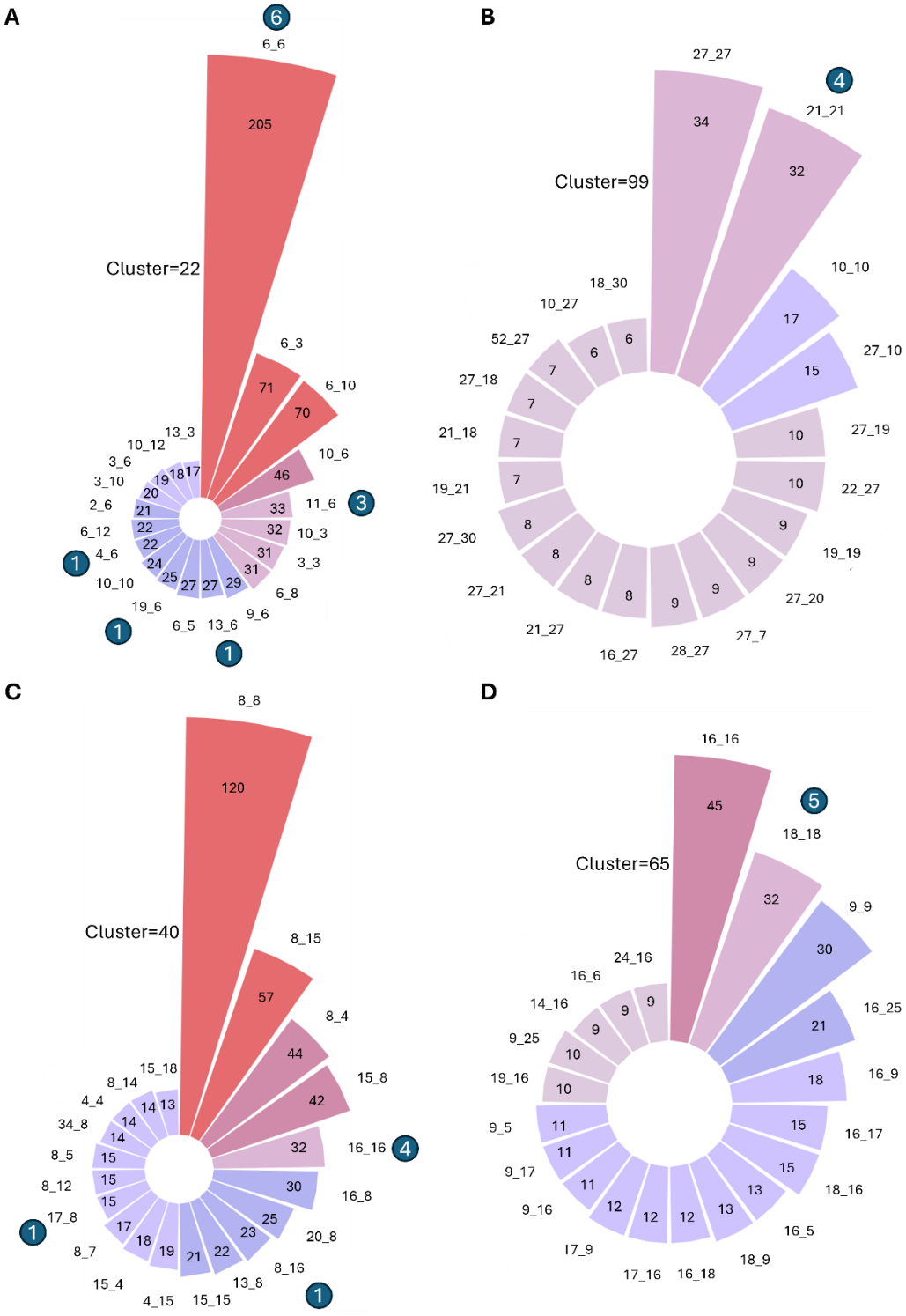

Figure 3.4 Comparison of (L)WY unit co-occurrence patterns across different clustering granularities.

(**A-D**) Polar bar plots display the frequency distribution of unit combinations, arranged in descending order, using different cluster threshold values: 22 clusters (**A**), 99 clusters (**B**), 40 clusters (**C**), and 65 clusters (**D**). The common combinations were annotated adjacent to their respective bars, while numerical abundance values were indicated

within each bar segment. Numbers within circles indicate the frequency of PP2A-interacting modules.

3.2.3 Identification of (L)WY candidate functional modules.

I determined that 65 clusters provided optimal specificity and sensitivity for further investigation (Figure 3.5A). Analysis of module distribution revealed that Cluster 16 contained the highest number of frequency (Figure 3.5A). Notably, the top six clusters alone accounted for 37% of all units identified from the five *Phytophthora* genomes (Figure 3.5A). The high representation of these top six units suggests they have an enhanced capacity for integration with other units.

To investigate evolutionary relationships among the 65 clusters, I constructed a phylogenetic tree based on exposed residues from individual (L)WY units. The tree was simplified by collapsing branches according to the 65 cluster designations, with circle sizes indicating the number of units within each cluster (Figure 3.5B). The resulting phylogeny revealed eight distinct clades, providing insights into the evolutionary correlations of these units.

Notably, five of the six most abundant clusters of (L)WY units were found within Clade 4. The three most prevalent Clusters (16, 9, and 18) formed a subclade, while Clusters 17 and 25 were positioned in another branch (Figure 3.5B). In contrast, (L)WY units from the remaining clusters showed a dispersed distribution across the phylogenetic tree, indicating substantial sequence divergence during evolution (Figure 3.5B). This diversity suggests that LWY effectors incorporating these variable LWY units may expand interaction capacity with host proteins, potentially enabling broad modulation of host physiology and cell signalling pathways.

65 clusters of 2168 (L)WY units lead to 739 distinct combinations of (L)WY-LWY pairs (Figure 3.5). Overall, 45 unit combinations were detected more than five times, corresponding to 496 two-unit pairs (~30% of the two-unit pairs). These commonly occurring unit combinations are called common modules.

Analysis of cluster distribution revealed that Cluster 16, while comprising 9.8% of individual units and participating in 10.3% of all unit combinations, was notably enriched in common modules, representing 51.1% of these combinations, a five-fold increase compared to its frequency among all 739 combinations (Table 2.1). Similar enrichment patterns were observed for the remaining top six (L)WY units, with their representation being two to three times higher, on average, than their occurrence in the

total 739 combinations (Table 2.1). In contrast, Clusters 6 and 24, which were relatively abundant but outside of the top six, showed uniform distribution across all 739 combinations (Table 2.1). Notably, these prevalent top six units formed common modules not only with each other but also with units from less abundant clusters. This pattern suggests that the top six clusters play a central role in generating diverse potential functional modules.

Table 2.1 Distribution of individual unit cluster in two-unit combinations.

65 Cluster (Top 8)	No. individual units	Combination frequency in all 739 combinations	Combination frequency in common modules (Top 45)
Cluster 16	212 (9.8%)	76 (10.3%)	23 (51.1%)
Cluster 9	166 (7.8%)	67 (9.1%)	12 (26.7%)
Cluster 18	112 (5.2%)	54 (7.3%)	9 (20.0%)
Cluster 17	109 (5.0%)	62 (8.4%)	8 (17.8%)
Cluster 5	106 (4.9%)	48 (6.5%)	5 (11.1%)
Cluster 25	101 (4.7%)	58 (7.8%)	7 (15.6%)
Cluster 6	76 (3.5%)	48 (6.5%)	2 (4.4%)
Cluster 24	64 (3.0%)	38 (5.1%)	1 (2.2%)

As a control to decide the optimal clustering granularity for hierarchical clustering, the PP2A-interacting modules were successfully characterized as 18_18, 18_9 and 23_18 using 65 clusters, which means that the first and second unit in the combinations come from Cluster 18, 9 or 23 (Figure 3.5C). Three module combinations, 16_16, 18_18, and 9_9 were similarly represented in the top three abundant combinations, which include the aforementioned PP2A-interacting module 18_18. Above the 19_16 combination, 15 module pairs occurred at high frequency (>10 occurrences each) (Figure 3.5C). These findings suggest that this clustering approach, which assigned 2168 (L)WY units into 65 clusters, effectively revealed potential functional modules that may mediate different host protein interactions.

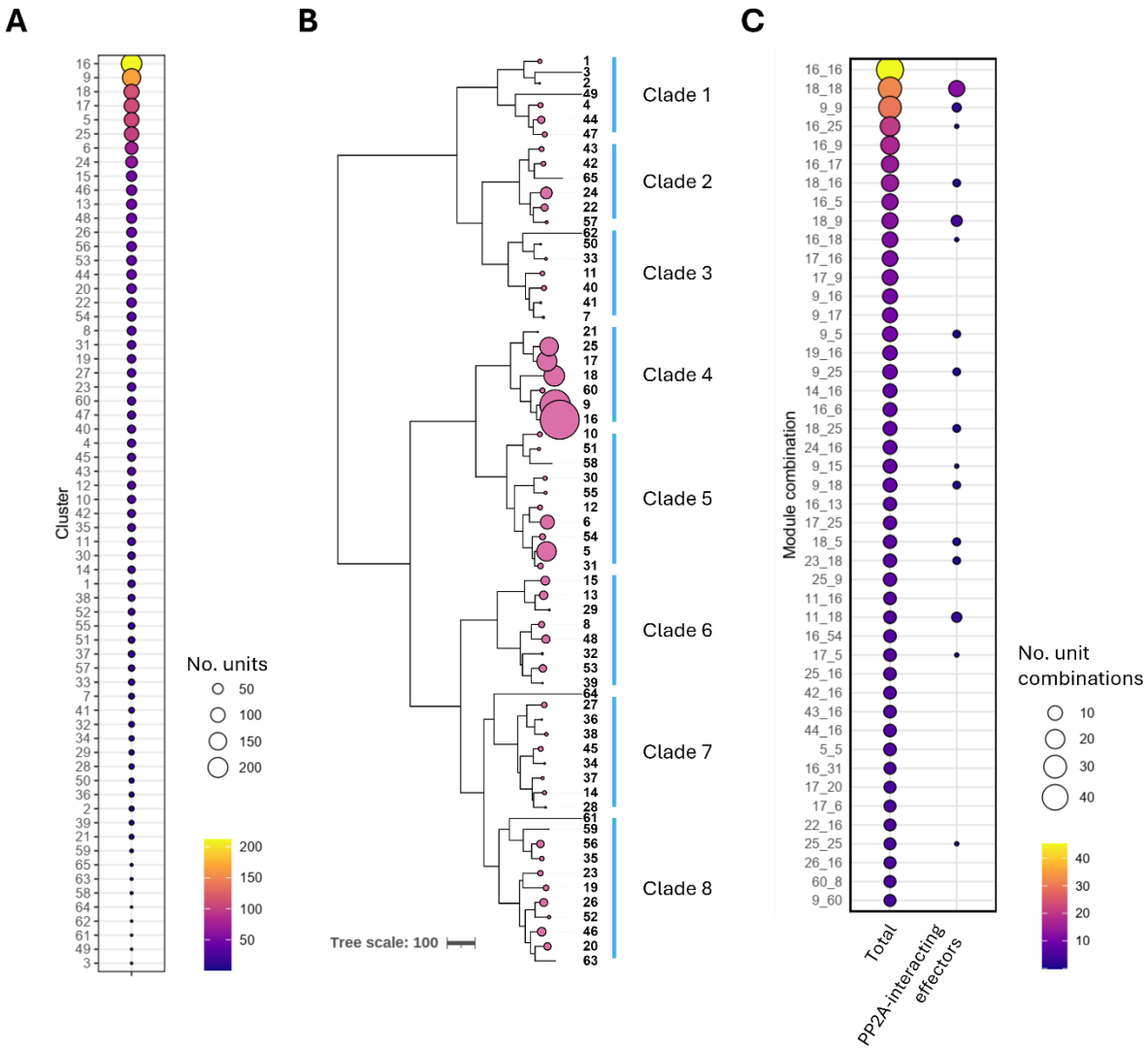

Figure 3.5 Potential functional modules are identified.

(**A**) Clusters are arranged in descending order by unit abundance, with both circle diameter and color intensity indicating abundance levels. (**B**) The phylogenetic tree displays eight major clades, constructed using exposed residues of individual (L)WY units. Units belonging to the same cluster are consolidated, with circle sizes representing the number of units per cluster. (**C**) Module combination patterns are shown for both complete unit pair datasets and experimentally validated PP2A-interacting LWY effectors, where circle dimensions and color gradients represent the frequency of occurrence.

3.2.4 LWY effectors contain multiple putative functional modules.

Understanding the preferential adoption of specific unit combinations by LWY effectors to benefit pathogen infection is crucial. This rationale came from co-evolution with hosts may drive the pathogens to adopt effectors that effectively target "hub" host proteins for the pathogens' benefit. Therefore, I analysed the percentage of LWY effectors contained with or without SP and/ or RxLR motifs in each combination (Figure 3.6A). This revealed for 37 common combinations (combinations detected more than seven times), there were more than 50% of LWY effectors contain signal peptides (Figure 3.6A). Notably, 13 of these 37 potential functional modules showed enrichments of >70% in LWYs with signal peptides, with combination 11_16 occurring in 6 out of 7 and 19_16 in 9 out of 10 SP+RxLR LWYs. These patterns suggest that these most promising functional modules may mediate direct interactions with host molecules.

Among 222 SP+RxLR LWY effectors, 105 (47.3%) contained at least one potential functional module from the top 45 module combinations, with 62 (27.9%) harboring multiple modules and a maximum of six modules per effector (Figure 3.6B). The PP2A-interacting effectors PITG_15142 (WY1-(LWY)4) and PsPSR2 (WY1-(LWY)6) demonstrate functional divergence in substrate dephosphorylation, likely due to their distinct C-terminal (L)WY units (H. Li et al. 2023). Both effectors contain PP2A-interacting modules: combination 23_18 in PITG_15142 and 18_18 in PsPSR2. PITG_15142 contains an additional module (17_5) at LWY4-LWY5, while PsPSR2 harbors three modules (18_16, 16_18, and 18_5) spanning LWY4 to LWY7. This variation in C-terminal module composition may contribute to their differential substrate specificity (Figure 3.6C). Similar modular arrangements appear in other PP2A-interacting effectors, including PITG_15032 and PITG_15038, potentially enabling the formation of diverse effector-PP2A holoenzymes targeting different substrates (Figure 3.6C).

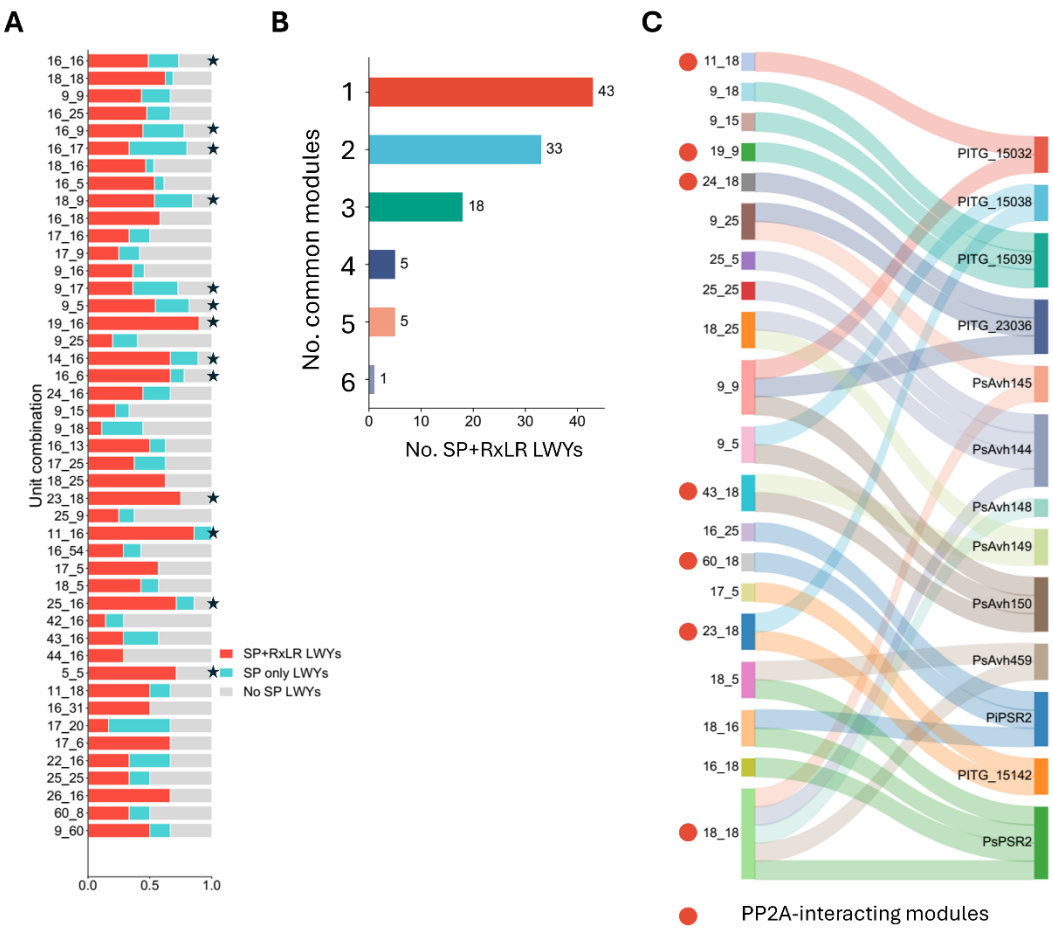

Figure 3.6 LWY effectors adopt multiple functional modules.

(**A**) The percentage of SP+RxLR LWYs, SP only LWYs and No SP LWYs in each combination was indicated in red, blue and grey bars, respectively. Combinations have more than 70% LWYs with Signal Peptides were labeled with stars. (**B**) Frequency of common modules in SP+RxLR LWY effectors. (**C**) Distribution of functional modules across PP2A-interacting effectors. Individual effector genes are shown on the right, with each uniquely color-coded. Colored lines connect each effector to its constituent functional modules (unit combinations), using matching colors to indicate the association. Modules known to interact with PP2A are highlighted with red circles. This visualization demonstrates the distribution and overlap of functional modules among PP2A-interacting effectors.

As stated previously, 13 PP2A-interacting effectors are identified from two *Phytophthora* species *P. sojae* and *P. infestans* (H. Li et al. 2023). To understand how widely these common modules are employed by five *Phytophthora* pathogens, I analysed the distribution of the top 45 unit combinations from Figure 3.5C to evaluate their presence across five *Phytophthora* species (*P. infestans*, *P. mirabilis*, *P. sojae, P. melonis* and *P. pisi*) (Figure 3.7).

The results suggest that 14 out of the 45 common unit combinations were adopted by the five *Phytophthora* species (Figure 3.7). The combination 18_18, which includes PP2A-interacting modules, showed uniform distribution across LWYs in all five *Phytophthora* species. This indicates that these modules may target similar proteins in various host species. Additionally, I observed that several combinations showed preferential distribution among specific species. In particular, six combinations (19_16, 25_9, 17_20, 17_6, 60_8, and 9_60) were specifically distributed between *P. infestans* and its sister species *P. mirabilis*. Interestingly, *P. mirabilis*, which encodes the largest number of LWY effectors, contained all 45 enriched common modules.

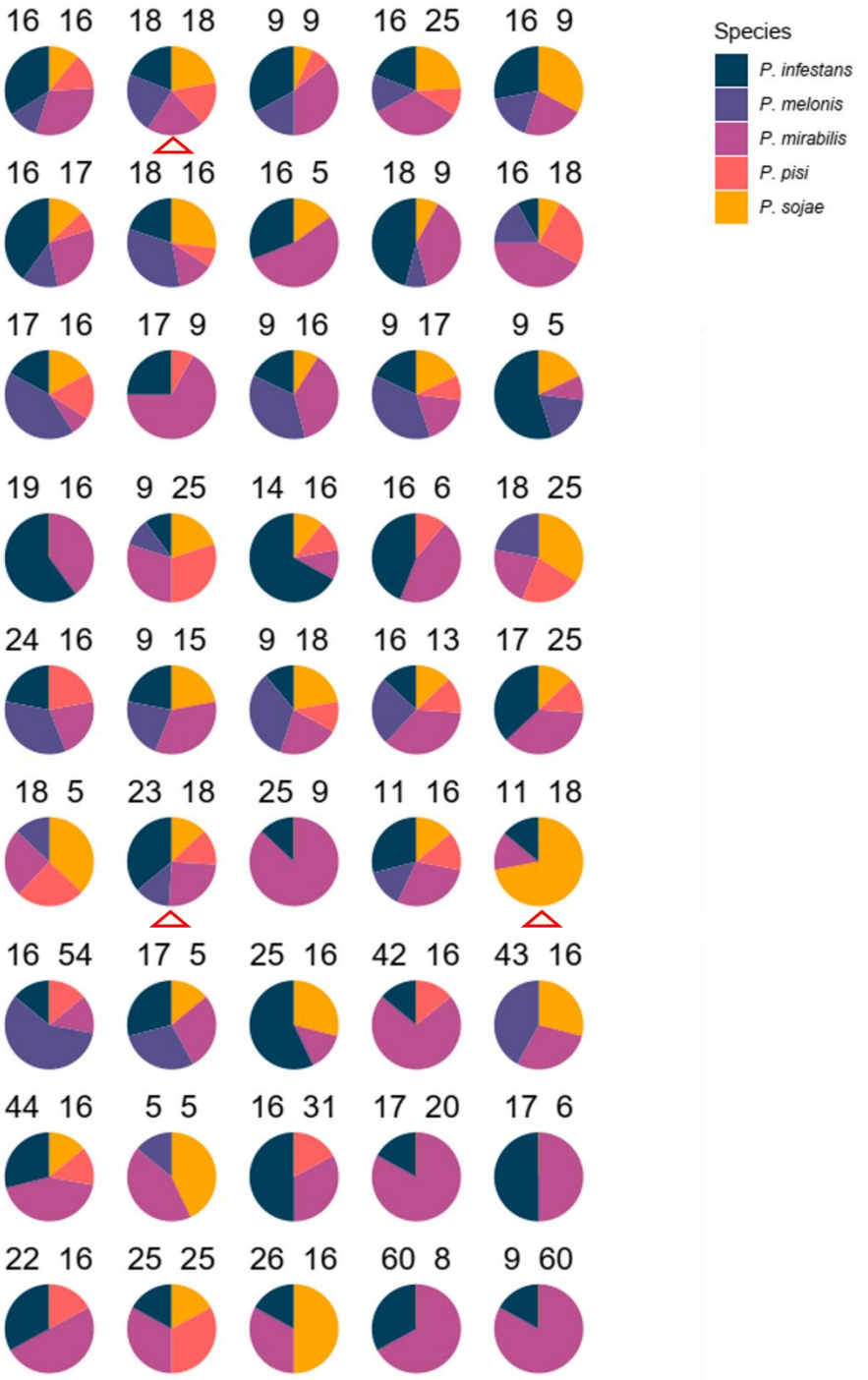

Figure 3.7 The distribution of enriched combinations across five *Phytophthora* species.

The pie chart illustrated the relative abundance of forty-five common modules across five *Phytophthora* species, with distinct colors representing each individual species. This visualization enables a direct comparison of module distribution patterns among the analyzed *Phytophthora* species. PP2A-interacting modules in the top 45 combinations are labelled with a triangle.

3.3 Methods

3.3.1 Hierarchical clustering

Surface-exposed residues from 2,168 individual (L)WY units were extracted and subjected to pairwise sequence alignment to generate comprehensive similarity and distance matrices. These matrices were used to perform hierarchical clustering. To determine optimal clustering parameters, I evaluated four different clustering granularity levels (k = 22, 40, 65, and 99). The optimal number of 65 clusters was determined based on two key criteria: (1) preservation of validated PP2A-interacting module patterns serving as positive controls, and (2) retention of distinct subgroups showing co-occurrence frequencies similar to these positive controls. This clustering granularity balanced biological validation through known PP2A-interacting modules while maintaining sufficient resolution to detect functionally relevant subgroups.

3.3.2 (L)WY module co-occurrence analysis

The 65 cluster classifications were mapped to their corresponding positions within each LWY effector gene sequence. Adjacent unit pairs were analyzed to identify co-occurring module patterns. Combinations occurring five or more times across the dataset were designated as common modules.

The frequency of common module combinations in SP+RxLR LWY effectors or among five *Phytophthora* species was calculated as (number of SP+RxLR LWY effectors containing the combination)/(total occurrences of the combination). N-terminal signal features (SP and RxLR motif) were derived from previous analyses (Chapter 2). PP2A-interacting modules were identified based on previously reported PP2A-binding pockets (H. Li et al. 2023).

3.4 Discussion

In this chapter, I aim to identify putative functional modules formed by specific LWY-LWY combinations in *Phytophthora*, which may directly contribute to host interactions. With that goal, I extracted the exposed residues from each (L)WY unit in five *Phytophthora* species for hierarchical clustering and classifying the individual (L)WY units into subsets. Using a cluster of 65, I identified 45 potential functional modules, with 13 showing enrichment in SP+RxLR LWY effectors, implying an important role in host manipulation. Additionally, I found that 14 enriched unit combinations were present in all five *Phytophthora* species, despite that these pathogens colonize different host plants. This conservation suggests that the functional modules may mediate interactions with common targets in different host species.

Shuffling of these various functional modules may combine different functional modules, which was hypothesized to drive the neofunctionality of LWY effectors. Supporting this hypothesis, of the total SP+RxLR LWY effector population (222 total), 105 (47.3%) contained at least one common module combination, with 62 of them (27.9%) harboring multiple modules, suggesting these SP+RxLR LWY effectors may form complex, dynamic interactions with host proteins. This observation aligns with our understanding of the PP2A-interacting effectors, which utilize conserved PP2A-interacting modules to bind the host PP2A A subunit while regulating distinct phosphoproteins through varied C-terminal LWY units (H. Li et al. 2023).

LWY effectors with predicted common modules may mediate interactions with common host targets, where the incorporation of multiple functional modules enables interactions with several host proteins to form diverse complexes, promoting novel functions despite shared modules. The identification of LWY effectors with conserved module combinations may reveal how pathogens evolve to optimize their fitness by targeting specific host proteins by deploying LWY effectors with common functional units or unit combinations. Mass spectrometry analysis, combined with experimental validation, could identify common virulence targets of LWY effectors and elucidate how their shared modules mediate interactions with host proteins.

Despite having a smaller genome (200 Mb vs 228.5 Mb), *P. mirabilis* contains more LWY effectors (173) than *P. infestans* (114), while having fewer RxLR effectors (397

vs 563). Notably, *P. mirabilis* incorporated all 45 enriched common combinations of LWY modules, which may be attributed to its larger LWY effector repertoire that represents approximately 30% of LWY effectors across the five studied *Phytophthora* species. This expansion is especially interesting given that *P. mirabilis* underwent a host jump from Solanaceous plants to *Mirabilis jalapa* (Raffaele et al. 2010). However, limited research studies effector evolution upon host jump. One of the studies suggests regressive evolution of a *P. mirabilis* WY effector PexRD54, losing the binding to host autophagy-related 8 (ATG8) protein due to sequence polymorphisms (Zess et al. 2022). However, the polymorphism occurs at the ATG8-interacting motif (AIM) but not the WY units. The wide employment of potential functional modules might promote efficient suppression of host immune responses and manipulation of host physiology for successful colonization on new hosts. More experiments would need to evaluate the contributions of LWY effectors to *P. mirabilis* infection.

Together, the approaches applied in this chapter layout the framework to understand effector evolution and functions and assign the functional dynamics to LWY unit combinations.

3.5 Reference

Guo, B., et al. (2019), 'Phytophthora sojae Effector PsAvh240 Inhibits Host Aspartic Protease Secretion to Promote Infection', *Mol Plant,* 12 (4), 552-64.

King, S. R., et al. (2014), 'Phytophthora infestans RXLR effector PexRD2 interacts with host MAPKKK epsilon to suppress plant immune signaling', *Plant Cell,* 26 (3), 1345-59.

Li, H., et al. (2023), 'Pathogen protein modularity enables elaborate mimicry of a host phosphatase', *Cell,* 186 (15), 3196-207 e17.

Raffaele, Sylvain., Farrer, Rhys A. ., and Liliana M. Cano, 1* David J. Studholme, 1‡ Daniel MacLean,1 Marco Thines,1,2,3 Rays H. Y. Jiang,4 Michael C. Zody,4 Sridhara G. Kunjeti,5 Nicole M. Donofrio,5 Blake C. Meyers,5 Chad Nusbaum,4 Sophien Kamoun1§ (2010), 'Genome Evolution Following Host Jumps in the Irish Potato Famine Pathogen Lineage', *Science,* 330.

Zess, E. K., et al. (2022), 'Regressive evolution of an effector following a host jump in the Irish potato famine pathogen lineage', *PLoS Pathog,* 18 (10), e1010918.

Chapter 4: A recombination event that may generate a novel LWY effector

4.1 Introduction

Recombination is a major driving force shaping the evolution of genomes by breaking up linkage between alleles of different loci and generating genetic variability in populations (Hill and Robertson 2009; Otto and Barton 1997). This process does not occur uniformly across the genome. Instead, recombination tends to concentrate in specific chromosomal regions known as recombination hotspots, which exhibit significantly elevated recombination rates (Jensen-Seaman et al. 2004; A. Kong et al. 2002). As a consequence, recombination hotspots are strongly associated with low linkage disequilibrium (Otto and Lenormand 2002).

In the context of microbe-plant molecular interactions (MPMI), recombination serves as a crucial evolutionary mechanism in the arms race between hosts and pathogens. Pathogens face strong selective pressure to evade host recognition, and recombination enables them to generate novel combinations of virulence alleles that can promote disease development. A notable example comes from bacterial effector proteins AvrBs3 and AvrBs4, which contain tandem arrays each encoding 34 amino acids and are recognized by the pepper Bs3 and tomato Bs4 proteins, respectively (Lahaye and Bonas 2001; Pierre et al. 2000; Schornack et al. 2004). These AvrBs3-like effectors display repeat unit variability at specific positions, likely arising through both intra- and intergenic recombination events (Schornack et al. 2006; Yang and Gabriel 1995; Yang et al. 2005).

The tandem repeated central amino acids, first identified in AvrBs3 and AvrBs4, are characteristic of the well-studied TAL (Transcription activator-like) effectors or TALEs, which are secreted by *Xanthomonas* bacteria. These effectors bind to target promoters and act as transcriptional activators of plant susceptibility (S) genes, including SWEET sugar transporters (Cox et al. 2017; Perez-Quintero and Szurek 2019; Romer et al. 2010; Streubel et al. 2013). Their DNA binding specificity is determined by repeat variable

diresidues (RVDs), pairs of amino acids at positions 12 and 13 within each repeat unit of the central domain, which contains 33-35 amino acid repeats (Boch et al. 2009; Moscou and Bogdanove 2009). Experimental evolution of four non-functional designer TALEs containing RVD mismatches to PthA4 drove repeat recombination, generating new variants with enhanced binding affinity to the *CsLOB1* promoter and restoring virulence function (Teper and Wang 2021). This highlights the evolutionary importance of recombination in pathogen adaptation.

Fungal pathogens provide compelling evidence for the presence of recombination hotspots, which are enriched with effector genes (Croll et al. 2015; Muller et al. 2019; Pierre et al. 2000; Stukenbrock and Dutheil 2018). Repetitive elements are also reported to facilitate genome rearrangement of non-allele repeats, particularly resulting in intra-chromosome inversion, inter-chromosome rearrangement and non-allelic sister chromatid rearrangement (Cordaux et al. 2006; Hedges and Deininger 2007). These findings collectively suggest that the localization of effector genes within gene-sparse, repeat-rich genomic compartments might encode recombination hotspots, potentially contributing to effector diversity and evolution.

In *Phytophthora ramorum*, five subfamilies of RxLR effectors, homologous to the 27-member PexRD2 protein family in *P. infestans*, exhibited substantial evidence of recombination (Goss et al. 2013; Haas et al. 2009). PexRD2 is a WY effector containing a single WY unit, forming dimers in planta to suppress MAPKKK activity (Boutemy et al. 2011; King et al. 2014). Similarly, *P. sojae* CRN effectors exhibit recombination breakpoints near their conserved HVLVVVP motifs using nucleotide-based recombination program RDP3 (Shen et al. 2013). These observations suggest that recombination serves as a crucial mechanism for both RxLR and CRN effectors to generate variability among paralogs (Goss et al. 2013).

A central question in microbe-plant molecular interactions is: how do effectors evolve novel functions? As stated in previous chapters, (L)WY effectors contain structurally conserved tandem repeats but execute divergent activities, including hijacking host PP2A-holoenzyme, suppressing host NRC network, interacting with host mitogen-activated protein kinase (MAPK or MAP kinase) (Bentham et al. 2024; Bos et al. 2010; Boutemy et al. 2011; Derevnina et al. 2021; Kim et al. 2024; King et al. 2014; H. Li et al. 2023). Studies in Chapter 2 suggested a similar genomic distribution between RxLR effectors and LWY effectors in *P. sojae* genome. Hence, it is likely that, these (L)WY

effectors also reside in repeat-rich genome regions that are more tolerant of evolutionary dynamics, such as gene duplication, recombination, deletion, insertion, and point mutations.

As mentioned in Chapters 2 and 3, LWY effectors contain mosaic patterns of units. A notable example is that PP2A-interacting effectors that regulate distinct phospho-proteins despite interacting with the host PP2A core enzyme through a conserved functional module. The difference between these effectors relies on the diversified C terminal interspersed units, which were proposed to be the products of module shuffling. The linear arrangement of the LWY units in effectors raises the possibility that recombination may facilitate domain shuffling, thereby generating novel combinations of (L)WY tandem repeats.

To test the hypothesis that recombination can give rise to new combinations of (L)WY units, I used a computational pipeline to identify LWYs that share sequence homology with potential "parent" genes. Analysis of predicted LWY datasets from five *Phytophthora* species studied in Chapters 2 and 3 revealed LWY effectors that display potential module shuffling. PmRxLR1, a *P. mirabilis* LWY protein with an RxLR motif, appears to be a recombinant of two *P. infestans* (L)WY effectors PITG_10341 and PITG_10347 with a breakpoint identified at the junction of two adjacent LWY units. This observation indicates that recombination could drive module shuffling in LWY effectors to form novel unit combinations.

Using immunoprecipitation and mass spectrometry, I characterized the host-interacting proteins of PmRxLR1 and its homolog PITG_10347 from *P. infestans*, along with Pm15069 from *P. mirabilis*. Analysis revealed both conserved and unique interaction partners between PmRxLR1 and its parent effector PITG_10347, demonstrating that LWY module shuffling enables the recruitment of distinct host targets. These findings suggest that the recombination of LWY modules drives functional divergence through the formation of different protein complexes, ultimately leading to the evolution of novel effector functions.

4.2 Results

4.2.1 A pipeline to identify potential recombination.

In Chapter 2, I discussed two pairs of LWY effectors in *P. sojae* (*JSPS_021759* and *JSPS_021762*; *JSPS_030430* and *JSPS_030434*) that showed patterns of module shuffling, which share highly conserved N-terminal units but exhibit significant divergence in their remaining units. This observation aligns with the PP2A-interacting effectors, where the conserved module that mediates PP2A interaction is combined with variable C-terminal units that are presumed to determine substrate specificity.

To investigate whether recombination can give rise to new unit combinations of LWY effectors, I developed a pipeline, which was applied to two comparisons: *P. infestans* with its sister species *P. mirabilis*, and two *P. sojae* isolates (JS2 and P6497). The pipeline was specifically designed to facilitate the visualization of sequence exchanges between LWY units during alignment analysis (Figure 4.1).

This analytical pipeline consisted of sequential steps, beginning with the construction of a protein database for each target *Phytophthora* species (Figure 4.1). Annotated LWY sequences were then subjected to BLAST analysis against these databases, followed by pairwise alignment of LWY sequences. The BLAST results were subsequently extracted and mapped back to the aligned LWY sequences. To identify potential recombination candidates, sequences were filtered using identity thresholds between 50% and 95%.

The selection of candidates for module shuffling was based on specific alignment patterns. For instance, a sequence was considered a candidate if its first two LWY units and last LWY unit showed alignment to corresponding regions in two different sequences as potential parents (A and B). Nucleotide-level alignments of these candidates were then analyzed using specialized recombination detection software Simplot 3.5, enabling highly sensitive detection of even minor sequence variations between putative "child" and "parent" sequences.

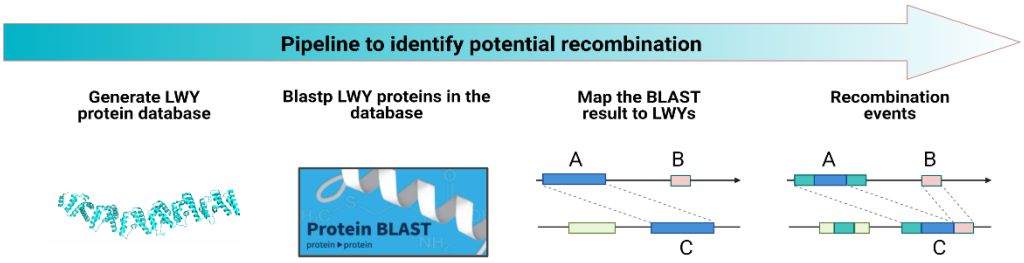

Figure 4.1 A pipeline to identify potential recombination of LWY effectors.

A computational pipeline was developed to identify potential recombination events among LWY effectors across *Phytophthora* species. LWY protein sequences from published datasets were compiled into a reference database. LWY-containing sequences from *P. infestans*, *P. mirabilis*, and *P. sojae* were subjected to BLAST analysis against this database. BLAST results were mapped back to identify homologous sequences. Candidate recombination events were identified when sequence C showed distinct regions of homology to two potential parent sequences (A and B), suggesting potential recombination. These candidate recombination events were subsequently validated through additional analyses. This figure was created using Biorender.

In Chapter 2, I identified seven conserved sets of LWY effectors shared among five *Phytophthora* species, designated as "core" LWY effectors. Using the pipeline described above, a potential recombination event was identified within three LWY genes from Core set 4, PITG_10341 and PITG_10347 from *P. infestans* and PmRxLR1 from *P. mirabilis*.

Comparative analysis between two *P. sojae* strains identified 13 insertion/deletion (indel) events among their LWY sequences, while the majority of LWY sequences remained identical between these two strains (Table 3.1). Although four sets of LWYs were identified as potential recombination candidates (Table 3.1), subsequent analysis using the recombination detection program Simplot 3.5 failed to confirm these as a result of recombination.

Table 3.1 Summary of observed indel events or recombination candidates in *P. sojae*.

Indel events	Sequence identity (%)	Recombination candidates	Sequence Identity (%)
JSPS_000134, EGZ22907.1	87.9	JSPS_013130, PsAvh168	93.2
JSPS_000138, EGZ22920.1	87.4	JSPS_021506, EGZ13785.1	79.5
JSPS_011671, EGZ19963.1	97.5	JSPS_027573, PsAvh379	74.1
JSPS_021612, EGZ13689.1	96.9	JSPS_030724, EGZ14590.1	67.4
JSPS_021758, EGZ13620.1	79.6		
JSPS_021762, EGZ13618.1	88.4		
JSPS_021900, EGZ13463.1	72.8		
JSPS_025518, PsAvh345	87.9		
JSPS_029100, EGZ07885.1	84.4		
JSPS_029125, EGZ07908.1	90		
JSPS_029218, EGZ07986.1	84		
JSPS_030216, EGZ15124.1	93.6		
JSPS_030359, EGZ15003.1	87.6		

4.2.2 *PmRxLR1* is homologous to *P. infestans* LWY effectors *PITG_10341* and *PITG_10347*.

The recombination event identified from the comparison between *P. infestans* and *P. mirabilis* includes three genes, two "parent" genes in *P. infestans* (PITG_10341 and PITG_10347) and one "child" gene in *P. mirabilis* (PmRxLR1) (Figure 4.2). Domain architecture analysis according to annotated gene models reveals that PITG_10341, PITG_10347 and PmRxLR1 share a common architecture, comprising five tandem repeats: one Y unit, three LWY units and a terminal L unit. another *P. mirabilis* LWY effector Pm15069 is a homolog of PITG_10347, which has the architecture of Y1-(LWY)3.

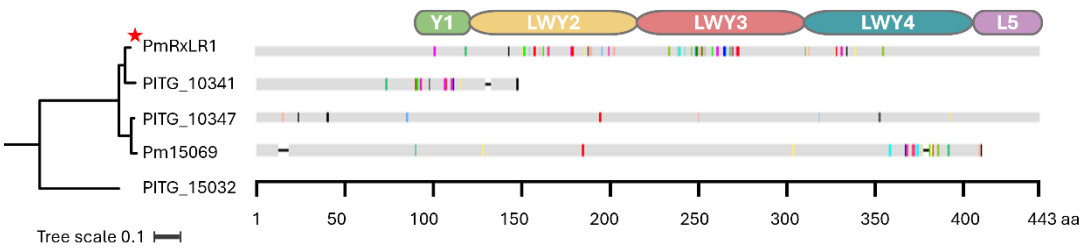

Figure 4.2 PmRxLR1 is homologous to PITG_10341 and PITG_10347.

Maximum likelihood phylogenetic analysis of full-length PmRxLR1, Pm15069, PITG_10341, and PITG_10347, with PITG_15032 as an outgroup. The phylogenetic tree is accompanied by amino acid alignments showing the modular organization of LWY units, with different colors representing distinct amino acids.

Sequence analysis demonstrates that PITG_10341 is the homolog of PmRxLR1 with a 92% nucleotide identity across positions 1 to 1218 bp, which covered N terminal first four (L)WY units in PmRxLR1 (Figure 4.3). Interestingly, the fifth L unit (positions 1219-1329 bp) in PmRxLR1 shows homology to another *P. infestans* LWY effector PITG_10347 (Figure 4.3). This indicates that PmRxLR1 shares sequence homology with two *P. infestans* LWY effectors. The absence of the L5 motif in Pm15069 terminal LWY unit, which is present in PITG_10347, precluded its inclusion in the L5 phylogenetic analysis (from 1218 bp to the end).

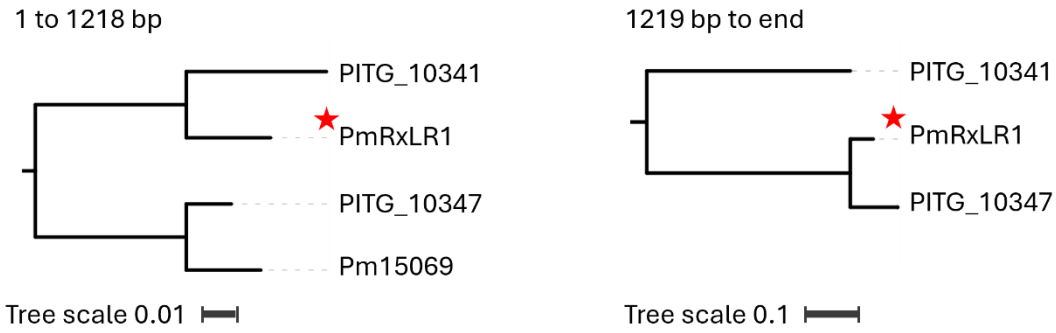

Figure 4.3 *P. infestans* and *P. mirabilis* LWY effectors exhibit evidence of recombination.

Maximum likelihood phylogenetic analysis highlighting sequence homology between specific regions (1 -1218 bp and 1219 bp to the end) of PmRxLR1 and its putative parent proteins PITG_10341 and PITG_10347.

However, the cloned DNA from *P. infestans* isolates indicated a 13-nucleotide deletion in PITG_10341 compared to the original gene model, resulting in a pre-mature stop codon in PITG_10341 and a truncated protein product (containing the first Y unit and partial LWY2 unit) (Figure 4.4). The truncated PITG_10341 might indicate gene pseudogenization, which affects the function of mature proteins. However, whether it still contributes to potential module shuffling remains to be determined. Primers used for cloning four LWY genes are listed in Table S1.

Figure 4.4 A 13-nucleotide deletion in PITG_10341 from *P. infestans* isolates leads to protein truncation.

Nucleotide sequence alignment was generated using ClustalW and visualized with ESpript 3. Conserved nucleotides are shown in red, while non-conserved positions remain uncolored, illustrating the patterns of sequence conservation and divergence among these LWY effectors. The 13-nucleotide deletion site is highlighted by a blue box.

4.2.3 PmRxLR1 is a recombinant of PITG_10341 and PITG_10347 at the junction of two C-terminal units.

Recombination analysis was performed using the RDP5 software and visualized through Simplot 3.5 to investigate whether PmRxLR1 originated as a recombination product of PITG_10341 (truncated version) and PITG_10347. The analysis revealed that PITG_10341, despite lacking 13 nucleotides compared to the gene model, serves as the major parent sequence of PmRxLR1 whereas PITG_10347 acts as the minor parent. Nucleotides around the Y1 unit display sequence divergence between the "parents" and "child". A similar pattern was seen at the end of LWY4, where a breakpoint located at 1214 bp was identified, supporting that PmRxLR1 is a hybrid of PITG_10341 and PITG_10347 at the junction of LWY4 and L5 (Figure 4.5). This also suggests that the gene PITG_10341 may have undergone pseudolization but can still serve as a donor for recombination and (L)WY unit rearrangement. Notably, Pm_15069, the *P. mirabilis* homolog of PITG_10347, shows no evidence of this recombination pattern, likely due to its lack of the L5 unit that serves as the recombination junction in PmRxLR1 (Figure 4.5).

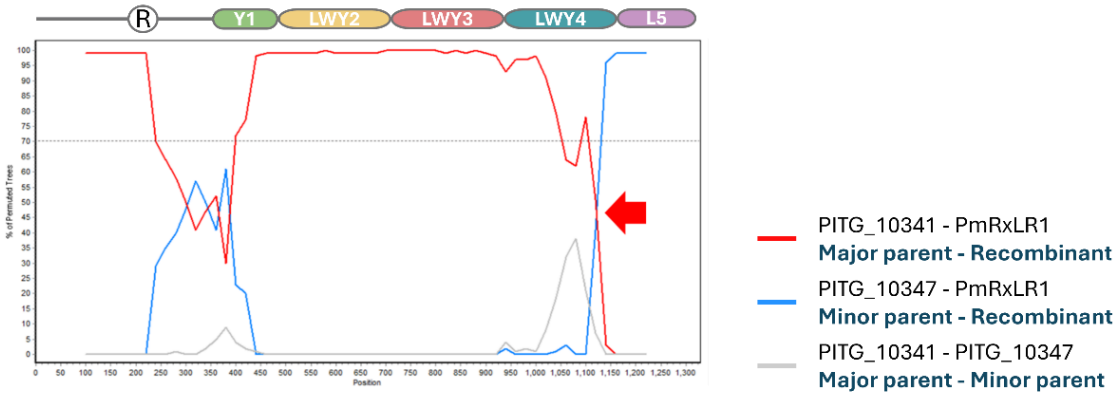

Figure 4.5 PmRxLR1 is a recombinant of PITG_10341 and PITG_10347.

The recombination event was identified using nucleotides. Simplot 3.5 was employed to identify the recombined events, with corresponding (L)WY units in PmRxLR1 aligned above the plot. The dotted line indicates sequence similarity exceeding 70%, and the red arrow marks the identified recombination breakpoint.

4.2.4 PmRxLR1, PITG_10341, and PITG_10347 form gene clusters with adjacent LWY effectors.

Gene clusters are derived from gene duplication and recombination. Since multi-gene clusters were identified in *the P. sojae* genome, it's intriguing to investigate if the three LWYs involved in recombination are arranged in gene clusters. Indeed, four LWYs are in proximity to other LWY genes with an average spacing of 2.4 kb to form gene clusters.

Building upon the individual (L)WY unit classification based on exposed residues described in Chapter 3, the units in four LWYs that undergo potential recombination were labelled according to their respective clusters. The units in PITG_10341 (except the first one) were labelled with the dashed box since it doesn't produce full-length proteins (Figure 4.6A). Consistent with the result from the recombination program, the first four units in PmRxLR1 had the same pattern of unit clusters with PITG_10341 while the L5 belonged to the same cluster of units with PITG_10347 (Figure 4.6A). In addition, sequence conservation in the left flanking regions was observed between PITG_10341 and PmRxLR1, as well as between PITG_10347 and Pm15069, indicating that homology between these gene pairs extends beyond their coding sequences.

I further performed structural modeling using AlphaFold2 (Jumper et al. 2021; Varadi et al. 2024) for PITG_10347, PmRxLR1, and Pm15069. The models showed high overall structural similarity among all three LWY proteins, but with particularly precise overlap between the L5 units of PmRxLR1 and PITG_10347 (Figure 4.6B). The conserved structure of the L5 unit in PmRxLR1 derived from PITG_10347 suggests PmRxLR1 may interact with some host protein targets of PITG_10347 but can also interact with host proteins that are not targeted by PITG_10347.

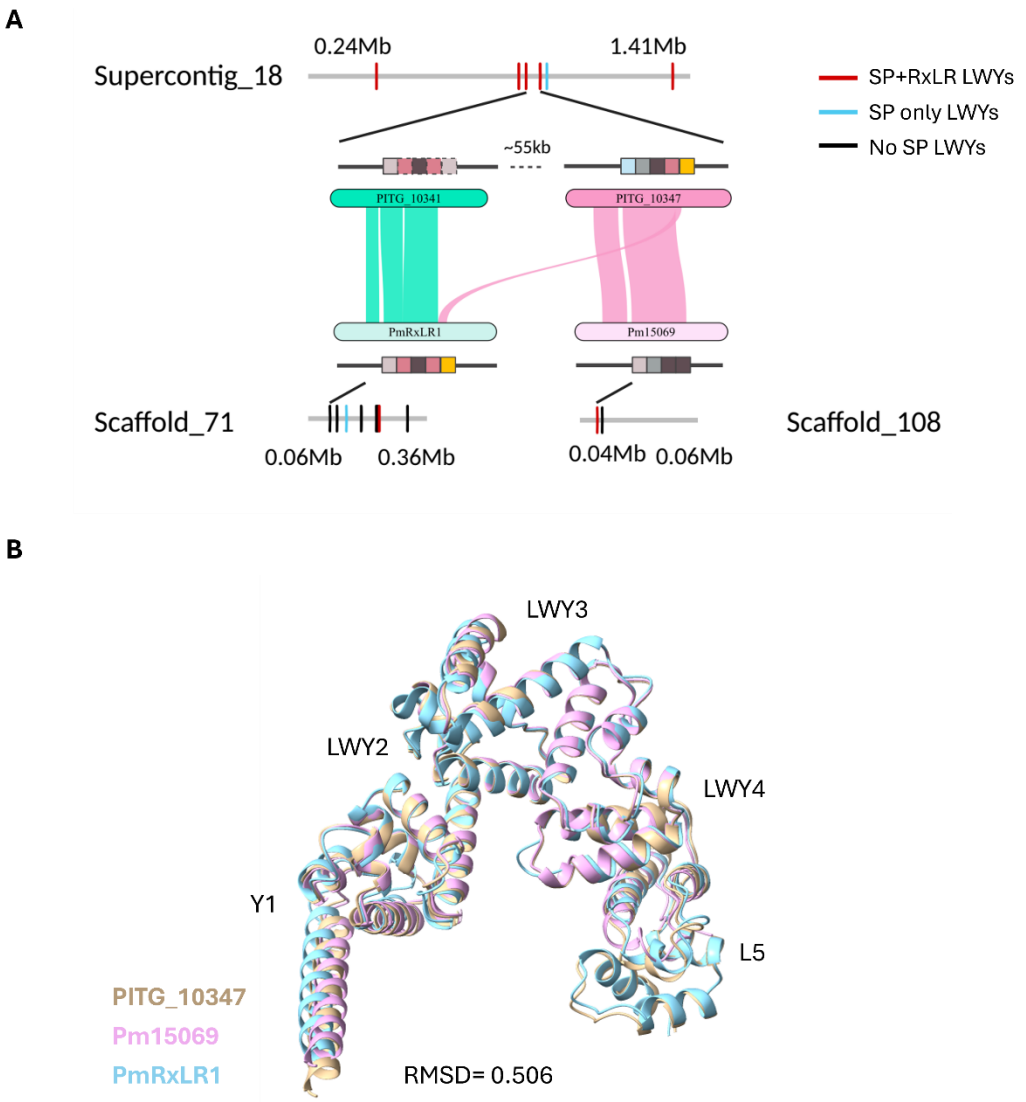

Figure 4.6 PmRxLR1, PITG_10341, and PITG_10347 distributed in LWY multi-gene clusters.

(**A**) Genome arrangement of LWY genes containing PmRxLR1, Pm_15069, PITG_10341, and PITG_10347. Colored sticks indicate the presence/absence of signal peptide (SP) and/or RxLR motifs. Synteny analysis includes gene bodies and 1 kb flanking regions. Units sharing sequence similarity are shown in matching colors in the boxed scheme and aligned to their corresponding positions in the genome synteny diagram. Dashed boxes in PITG_10341 represent the predicted unit organization based on the original gene model, though cloned sequences terminate before the LWY2 unit. (**B**) Structural comparison of predicted protein models generated by AlphaFold2. Structures were aligned using ChimeraX (RMSD = 0.506). Different colors distinguish the three LWY proteins, with individual units labelled accordingly.

4.2.5 PmRxLR1 associates with specific and common host proteins compared to PITG_10347.

To investigate whether the recombination of the L5 unit from PITG_10347 into PmRxLR1 affects host protein interactions, I performed a comparative interactome analysis. I transiently expressed PmRxLR1, PITG_10341, PITG_10347, and Pm15069 in *N. benthamiana* using GFP as the negative control. The effectors were expressed with an N-terminal GFP tag, and the proteins were immunoprecipitated from leaf tissues using anti-GFP antibody. Western blot confirmed the expression of proteins at their expected sizes, except for PITG_10341 which showed truncation (Figure 4.7). The enriched proteins from PmRxLR1, PITG_10347, and Pm15069 were analyzed by IP-mass spectrometry (IP-MS).

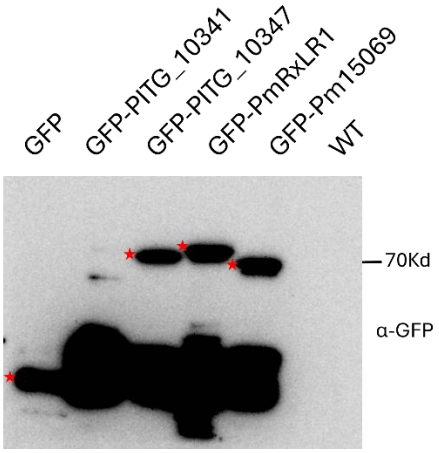

Figure 4.7 Protein expression of LWYs undergoing module rearrangement.

Transient expression of N-terminally GFP-tagged LWY proteins in *N. benthamiana* leaves using Agrobacterium-mediated infiltration. Protein samples were collected 2 days post-infiltration and analyzed by Western blot using anti-GFP antibodies. Red asterisks indicate the expected protein band.

Mass spectrometry analysis, using a threshold of 5 spectrum counts, identified distinct interaction profiles for each LWY protein. PmRxLR1 showed the most extensive interaction network with 101 interacting proteins, while PITG_10347 and its homolog Pm15069 each bound approximately 30 proteins (Figure 4.8). Among these interactions,

75 *N. benthamiana* proteins were unique to PmRxLR1, while three proteins were shared between PmRxLR1 and PITG_10347. 18 proteins were shared by all three LWY interactomes. Substantial overlap was observed in host protein interactors between PITG_10347 and its homolog Pm15069, suggesting that maintain similar host protein binding capabilities.

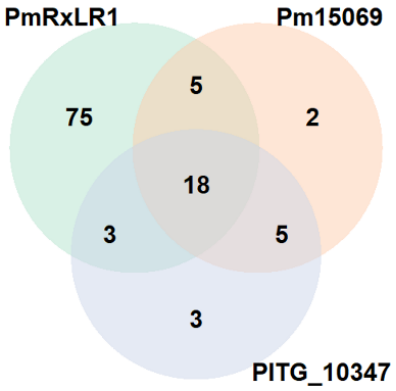

Figure 4.8 PmRxLR1 shares common interacting proteins with PITG_10347 but also has unique interactors.

Venn diagram showing common and unique interacting proteins of PmRxLR1, PITG_10347, and Pm15069 in *N. benthamiana*. Numbers indicate protein counts.

To further analyse the interactomes, I generated heatmaps displaying specific and common interactors across the three LWY interactomes. The interaction patterns were visualized using log2-transformed spectrum counts from three biological replicates for each effector (Figure 4.9). Additionally, I performed Gene Ontology (GO) enrichment analysis to identify functional pathways represented among the interacting proteins (Figure 4.9).

Among the shared interactors, lipoxygenase was shared between PITG_10347 and PmRxLR1 but absent in Pm15069, potentially due to the shared L5 unit in PmRxLR1 and its parent PITG_10347 (Figure 4.9A). GO analysis revealed that lipoxygenase is associated with oxidoreductase activity (GO:0016702) and lipid oxidation (GO:0034440) (Figure 4.9D and 4.9E).

Additionally, 75 interactors were found to specifically interact with PmRxLR1 (Figure 4.9B). These include Ankyrin repeat domain-containing proteins for protein

binding (GO:0005515), nuclear proteins for small-subunit processome (GO:0032040), cell division proteins for GTPase activity (GO:0003924) and GTP binding (GO:0005525) etc (Figure 4.9D and 4.9E).

It's likely the N terminal (L)WY units in PmRxLR1 might mediate the interactions with its specific targets while the recombined L5 might recruit lipoxygenase similar to PITG_10347. Therefore, I conclude the combinations of lipoxygenase and PmRxLR1-specific interactors, such as Ankyrin repeat domain-containing proteins (which are reported to promote protein-protein interactions), may generate novel protein complexes distinct from its "parent" PITG_10347 protein. The novel protein complexes formed by PmRxLR1 may confer new functionality through the recruitment of lipoxygenase, potentially modulating its stability and activity.

Furthermore, 18 host targets were commonly present in the three LWY interactomes. Among them, peroxisomal hydroxy acid oxidase and ATP synthase subunits were enriched in the effector interactomes but not negative control (Figure 4.9C). Hydroxy acid oxidase catalyses glycolate into glyoxylate and converts oxygen into hydrogen peroxide (Dellero et al. 2015). ATP synthase generates ATP from ADP, utilizing the proton gradient across the membrane as an energy source (Ko et al. 1999). In fact, oxidoreductase (GO:0016491) and ATP synthase activities (GO:0046933) are particularly prominent in the global GO term analysis of molecular functions across all interactors from the three LWYs (Figure 4.9D). Correspondingly, the peroxisome (GO:0005777) is prominently featured in the cellular component GO terms except for the organism involved in translation and protein transporting, supporting that hydroxy acid oxidase could be a potential interactor of three LWY effectors (Figure 4.9E).

Comparative proteome analysis revealed that the recombined LWY protein PmRxLR1 maintains dual interaction capabilities: it inherits host protein recruitment patterns from its parent PITG_ 10347 while also interacting with host proteins that are not targeted by PITG_10347. These PmRxLR1-specific interactors may be attributed to four N-terminal units inherited from the other parent. This demonstrates how modularity enables effector functional divergence through diverse host protein interactions.

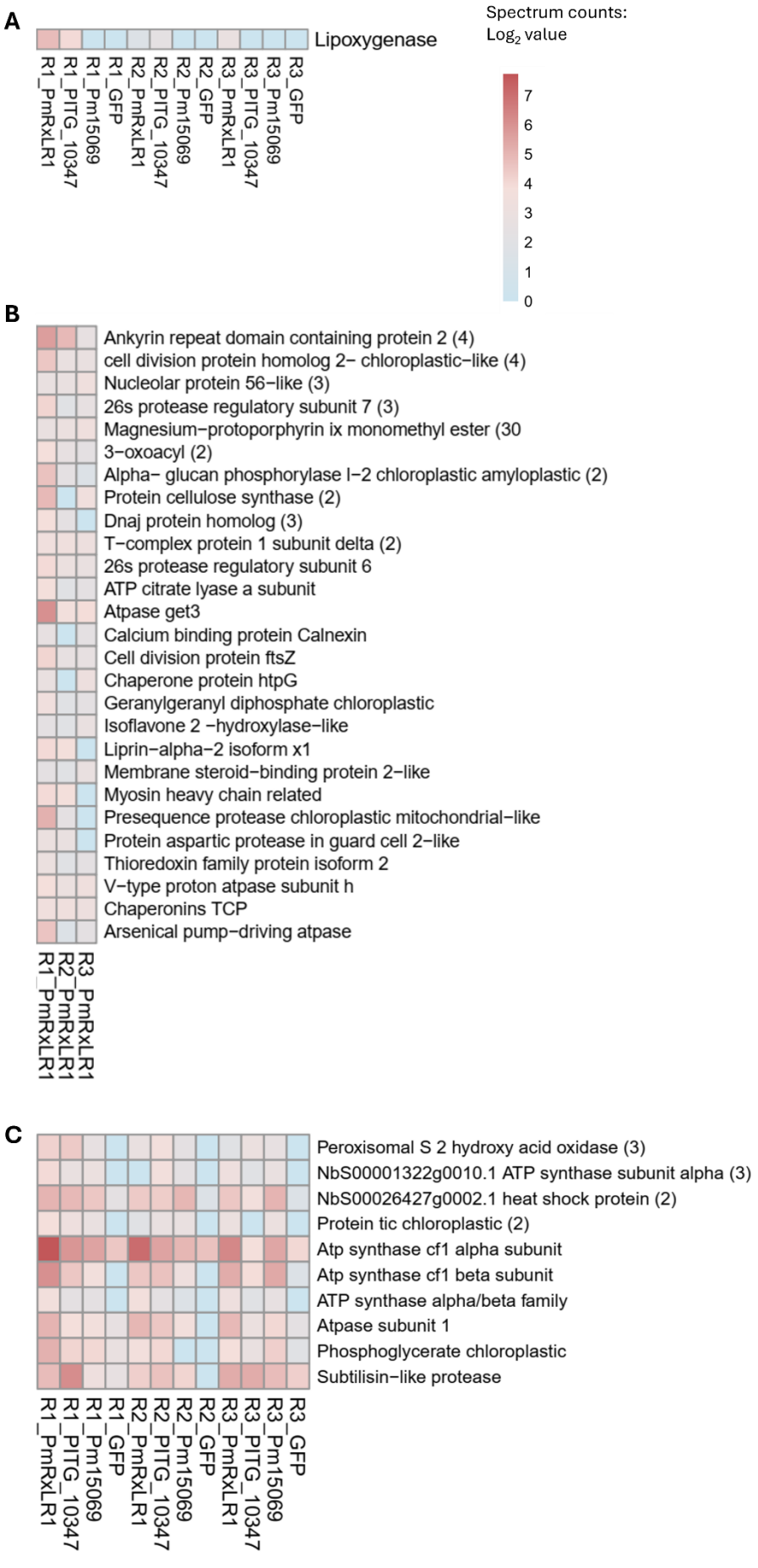
A
Lipoxygenase
R1_PmRxLR1
R1_PITG_10347
R1_Pm15069
R1_GFP
R2_PmRxLR1
R2_PITG_10347
R2_Pm15069
R2_GFP
R3_PmRxLR1
R3_PITG_10347
R3_Pm15069
R3_GFP
Spectrum counts:
Log2 value
7
6
5
4
3
2
1
0
B
Ankyrin repeat domain containing protein 2 (4)
cell division protein homolog 2− chloroplastic−like (4)
Nucleolar protein 56−like (3)
26s protease regulatory subunit 7 (3)
Magnesium−protoporphyrin ix monomethyl ester (30
3−oxoacyl (2)
Alpha− glucan phosphorylase l−2 chloroplastic amyloplastic (2)
Protein cellulose synthase (2)
Dnaj protein homolog (3)
T−complex protein 1 subunit delta (2)
26s protease regulatory subunit 6
ATP citrate lyase a subunit
Atpase get3
Calcium binding protein Calnexin
Cell division protein ftsZ
Chaperone protein htpG
Geranylgeranyl diphosphate chloroplastic
Isoflavone 2 −hydroxylase−like
Liprin−alpha−2 isoform x1
Membrane steroid−binding protein 2−like
Myosin heavy chain related
Presequence protease chloroplastic mitochondrial−like
Protein aspartic protease in guard cell 2−like
Thioredoxin family protein isoform 2
V−type proton atpase subunit h
Chaperonins TCP
Arsenical pump−driving atpase
R1_PmRxLR1
R2_PmRxLR1
R3_PmRxLR1
C
Peroxisomal S 2 hydroxy acid oxidase (3)
NbS00001322g0010.1 ATP synthase subunit alpha (3)
NbS00026427g0002.1 heat shock protein (2)
Protein tic chloroplastic (2)
Atp synthase cf1 alpha subunit
Atp synthase cf1 beta subunit
ATP synthase alpha/beta family
Atpase subunit 1
Phosphoglycerate chloroplastic
Subtilisin−like protease
R1_PmRxLR1
R1_PITG_10347
R1_Pm15069
R1_GFP
R2_PmRxLR1
R2_PITG_10347
R2_Pm15069
R2_GFP
R3_PmRxLR1
R3_PITG_10347
R3_Pm15069
R3_GFP

D

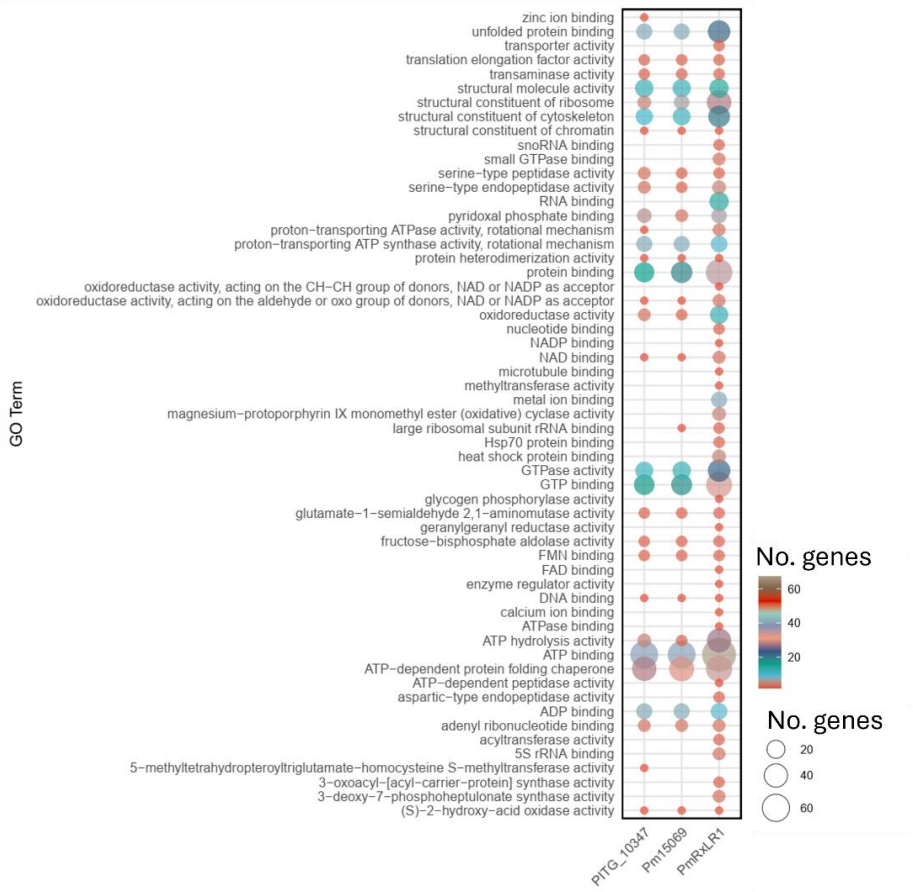
GO Term
zinc ion binding
unfolded protein binding
transporter activity
translation elongation factor activity
transaminase activity
structural molecule activity
structural constituent of ribosome
structural constituent of cytoskeleton
structural constituent of chromatin
snoRNA binding
small GTPase binding
serine−type peptidase activity
serine−type endopeptidase activity
RNA binding
pyridoxal phosphate binding
proton−transporting ATPase activity, rotational mechanism
proton−transporting ATP synthase activity, rotational mechanism
protein heterodimerization activity
protein binding
oxidoreductase activity, acting on the CH−CH group of donors, NAD or NADP as acceptor
oxidoreductase activity, acting on the aldehyde or oxo group of donors, NAD or NADP as acceptor
oxidoreductase activity
nucleotide binding
NADP binding
NAD binding
microtubule binding
methyltransferase activity
metal ion binding
magnesium−protoporphyrin IX monomethyl ester (oxidative) cyclase activity
large ribosomal subunit rRNA binding
Hsp70 protein binding
heat shock protein binding
GTPase activity
GTP binding
glycogen phosphorylase activity
glutamate−1−semialdehyde 2,1−aminomutase activity
geranylgeranyl reductase activity
fructose−bisphosphate aldolase activity
FMN binding
FAD binding
enzyme regulator activity
DNA binding
calcium ion binding
ATPase binding
ATP hydrolysis activity
ATP binding
ATP−dependent protein folding chaperone
ATP−dependent peptidase activity
aspartic−type endopeptidase activity
ADP binding
adenyl ribonucleotide binding
acyltransferase activity
5S rRNA binding
5−methyltetrahydropteroyltriglutamate−homocysteine S−methyltransferase activity
3−oxoacyl−[acyl−carrier−protein] synthase activity
3−deoxy−7−phosphoheptulonate synthase activity
(S)−2−hydroxy−acid oxidase activity
PITG_10347
Pm15069
PmRxLR1
No. genes
60
40
20
No. genes
20
40
60

E

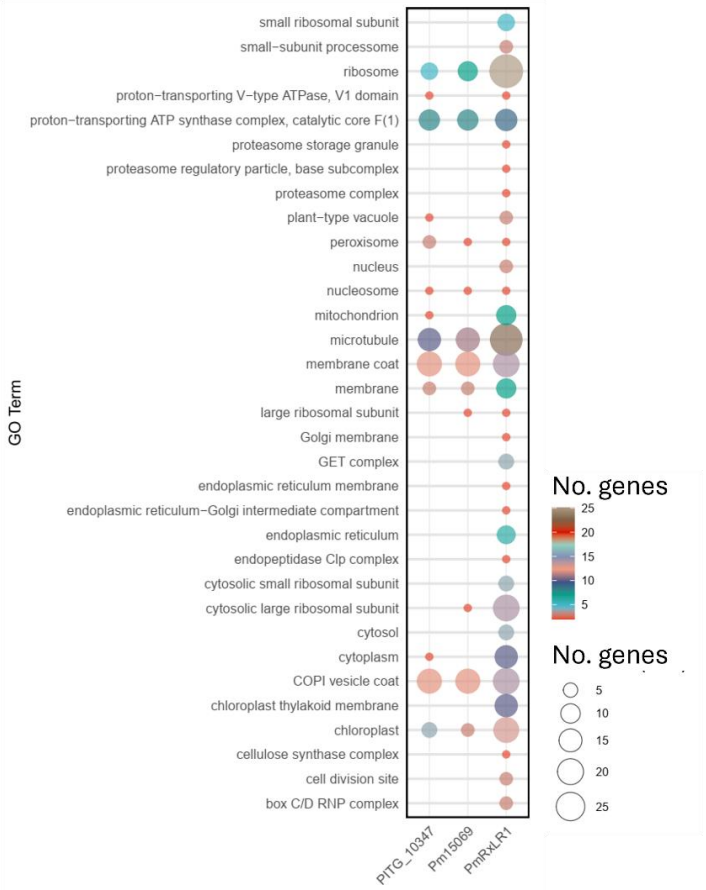
GO Term
small ribosomal subunit
small−subunit processome
ribosome
proton−transporting V−type ATPase, V1 domain
proton−transporting ATP synthase complex, catalytic core F(1)
proteasome storage granule
proteasome regulatory particle, base subcomplex
proteasome complex
plant−type vacuole
peroxisome
nucleus
nucleosome
mitochondrion
microtubule
membrane coat
membrane
large ribosomal subunit
Golgi membrane
GET complex
endoplasmic reticulum membrane
endoplasmic reticulum−Golgi intermediate compartment
endoplasmic reticulum
endopeptidase Clp complex
cytosolic small ribosomal subunit
cytosolic large ribosomal subunit
cytosol
cytoplasm
COPI vesicle coat
chloroplast thylakoid membrane
chloroplast
cellulose synthase complex
cell division site
box C/D RNP complex
PITG_10347
Pm15069
PmRxLR1
No. genes
25
20
15
10
5
No. genes
5
10
15
20
25

Figure 4.9 PmRxLR1 associated with specific interactors and share common interactors with PITG_10347.

(**A-C**) The heatmap showed host interactors that are specifically associated with PmRxLR1 (**A**), shared by PITG_10347 and PmRxLR1 (**B**) or recruited by all three LWYs (**C**). Heatmap colors represent log2-transformed spectrum counts, with the same scale applied across all panels. Numbers in parentheses indicate the frequency of proteins detected within each protein family. (**D-E**) Gene Ontology (GO) enrichment analysis of LWY interactomes showing molecular functions (**D**) and cellular components (**E**). Bubble size and color intensity correspond to the number of host interactors enriched in each GO term.

4.3 Methods

4.3.1 Phylogeny tree

Phylogenetic analyses were conducted using MEGA11. For *Phytophthora* species trees, concatenated sequences from five genetic markers were aligned using the ClustalW algorithm, followed by Neighbor-Joining (NJ) analysis with 1,000 bootstrap replicates. BBB protein phylogeny was constructed using maximum likelihood (ML) analysis with 1,000 bootstrap replicates following ClustalW alignment. For BBBs involved in recombination events, a separate phylogenetic tree was constructed using nucleotide sequences through ML analysis with 1,000 bootstrap replicates.

4.3.2 Recombination analysis

A local BLAST database was constructed using predicted LWY protein sequences to identify potential recombination events through changes in amino acid sequences of individual (L)WY units. BlastP searches were performed using the following criteria: >90% sequence identity and >95% coverage, either globally or locally, depending on gene body alterations. Candidate sequences meeting these criteria were further analyzed for rearrangements using Simplot 3.5 with nucleotide sequences (Lole et al. 1999).

4.3.3 Structural modelling

The structures of presented LWYs here, including PITG_10347, PmRxLR1 and Pm15069 were modeled using Alphafold2 (Jumper et al. 2021; Varadi et al. 2024). Structural alignments and similarity assessments were performed using ChimeraX (Pettersen et al. 2021). The structure of PsPSR2 (5GNC) was downloaded from the PDB database.

4.3.4 Gene clone

The genes *PmRxLR1* and *Pm15069* were cloned from the genomic DNA from *P. mirabilis* strain Pm3010 while *PITG_10341* and *PITG_10347* were cloned from *P. infestans* strain T30-4. All four LWYs were tagged with N terminal GFP (green fluorescent protein). SP was removed from the sequences where present. Primers used for PCR cloning are listed in Table S1. The constructs were generated by Golden Gate assembly of the Level 0 module into binary vector pICSL86955OD with 35S promoter. All constructs were verified by sequencing. Construct used are indicated in Table S2.

4.3.5 IP-MS

The vectors are transformed into Agrobacterium. Total proteins were extracted from *N. benthamiana* leaves 2 days after agroinfiltration of GFP (control), GFP::PITG_10341, GFP::PITG_10347, GFP::PmRxLR1, or GFP::Pm15069. Immunoprecipitation was performed using GFP_Trap_A beads (Chromotek, Munich, Germany), with three independent replicates. The immunoprecipitated samples were separated by SDS-PAGE using a 10% gradient gel (Biorad, United Kingdom). Enriched protein samples were excised from the gel and digested with trypsin.

4.3.6 Mass spectrometry data processing

Following the protocol described (Petre et al. 2021), peptide lists were extracted from raw data using MS Convert and identified on Mascot server 2.4.1 using Mascot Daemon (Matrix Science) (Chambers et al. 2012). The list of peptides was searched against the *N. benthamiana* genome database Nbv6tr_plus_SGNUniq_20170321, with common contaminants annotated. Protein identification was performed using Scaffold 4.4.0 (Proteome Software) to combine the Mascot results. The analysis required peptide sequence matches above 95.0%, inferred protein confidence above 99%, Mascot ions scores exceeding 39, and a minimum of 2 unique peptides per protein.

4.3.7 Gene Ontology (GO) term analysis

InterProScan was used to search for GO IDs of host proteins and extract their corresponding GO IDs (P. Jones et al. 2014). GO-term analysis was performed using the biocManager package ViSEAGO v.1.4.0, focusing on Cellular Component (CC) and Molecular Function (MF) functions. The frequency of detected GO terms across the three BBB interactomes was visualized using bubble plots.

4.4 Discussion

This study addressed a fundamental question in effector evolution: can recombination events generate new combinations that lead to novel functionalities compared to their parent proteins? Using a sequence-based recombination analysis pipeline, I identified a recombination event within gene clusters in *P. infestans* and *P. mirabilis* (Figure 4.10). Mass spectrometry analysis of the LWYs involved in this unit rearrangement revealed both common and specific interactors between the "parent" PITG_10347 and the "child" PmRxLR1. Notably, these interactions were absent in the PITG_10347 homolog Pm15069, which lacks the recombined L5 unit (Figure 4.10). These findings demonstrate that individual LWY units can facilitate associations with distinct host molecules, and the shuffling of these units leads to the formation of novel effector-host target protein complexes, contributing to the emergence of effector neo-functions. Our research highlights modularity can serve as a powerful evolutionary drive to shape effector evolution and offer a valuable framework to advance our understanding of effector biology.

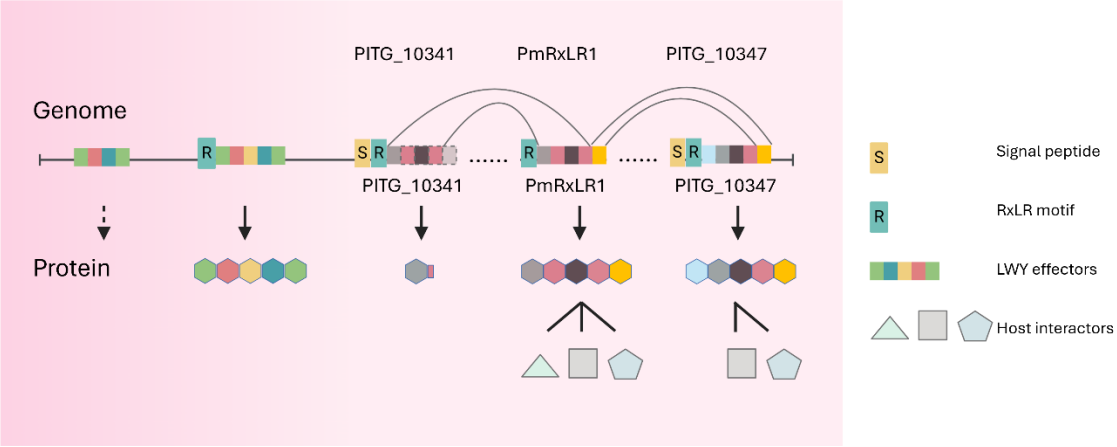

Figure 4.10 Model: recombination promotes functional diversity through formation of novel protein complexes.

Phytophthora genomes encode a reservoir of (L)WY tandem repeats, many of which form multi-gene clusters. A recombination event involving three (L)WYs was identified in *P. infestans* and *P. mirabilis*, with each in proximity to other LWY effectors in the genome. The first four units in PmRxLR1 recombined from PITG_10341 (a pseudo-LWY gene producing a truncated protein product) whereas the last unit was derived from PITG_10347. The N terminal four units from the “parent” PITG_10341 enable PmRxLR1

to recruit its specific host interactors, allowing it to potentially form distinct protein complexes while maintaining some common interactors with PITG_10347. This study illustrates that module shuffling driven the new combinations of LWY effectors, thereby promoting the diversification of the protein complex formed with host molecules and ultimately enabling novel functions distinct from the original “parent” LWY effectors. This figure was created using Biorender.

In PmRxLR1 interactomes, two sets of host interactors are observed, including specific proteins (such as nuclear proteins and ankyrin repeat domain-containing) and common interactors (including lipoxygenase and hydroxy acid oxidase). However, it remains unclear whether these host targets bind simultaneously to PmRxLR1 effectors to form functionally distinct complexes compared to their parents.

Notably, PmRxLR1 recruits over 70 host proteins specifically, compared to its recombination “parent” PITG_10347. Differences in the N-terminal tandem units of PmRxLR1 likely play a role in determining this increase in host protein-binding capacity. It remains unclear whether the enhanced binding compatibility is inherited from its primary parent, PITG_10341, as this gene is truncated. These findings suggest that tandem functional modules could potentially affect protein-binding compatibility. This enhanced compatibility may increase the possibility of forming novel protein complexes with distinct biological roles, ultimately contributing to neo-functionalization and/or multi-functionality.

Based on the identified recombination events and mosaic patterns of effector functional modules in *Phytophthora* species, we proposed that the highly organized (L)WY repeats in *Phytophthora* genomes facilitate effector evolution through (L)WY unit rearrangement. The effector repertoires can expand and develop divergent functional modules through recombination, residue polymorphisms, and indels. (L)WY effectors containing these mosaic modules may function as mediators by recruiting different host targets and forming dynamic complexes (Figure 4.11). Future experiments will be needed to determine whether proteins recruited by shuffled common modules form functionally distinct protein complexes.

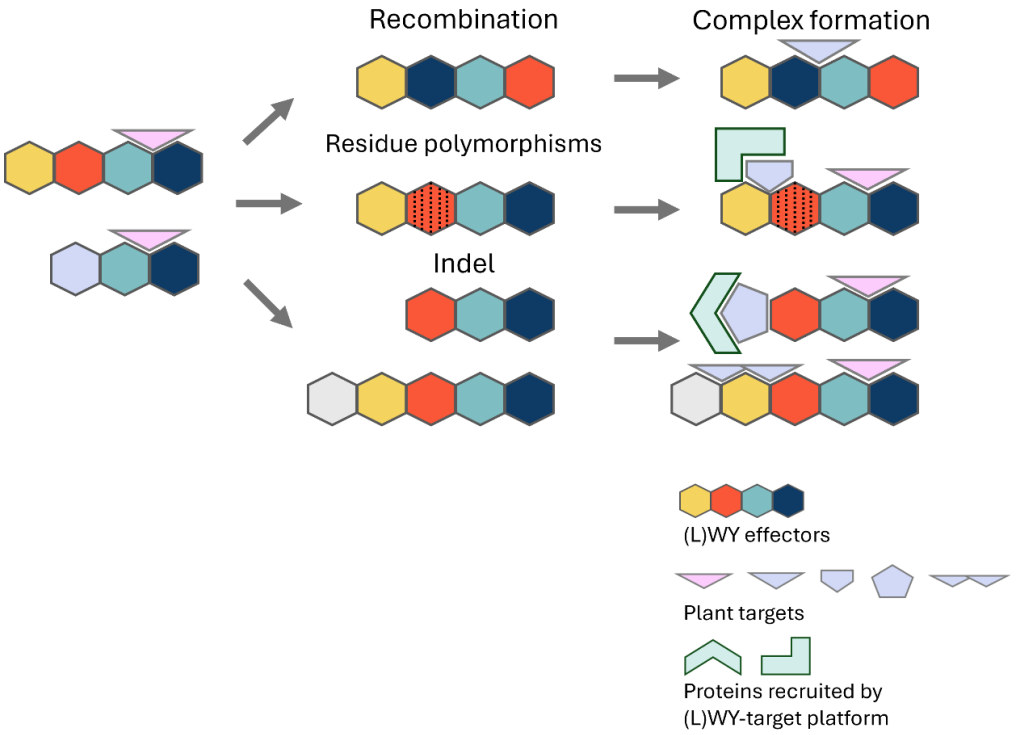

Figure 4.11 working model: (L)WY units facilitate rapid evolution of *Phytophthora* effectors.

It has been hypothesized that (L)WY functional modules were preserved and frequently adopted by effectors as the outcome of natural selection during the *Phytophthora*-host interactions. Recombination, residue polymorphisms, and insertion-deletion events allow (L)WY effectors to diversify, displaying a variety of modular patterns and expanding their functional repertoires. (L)WY effectors containing this mosaic (L)WY units may serve as a platform to recruit different host proteins and form large dynamic complexes. This modularity-driven effector evolution can facilitate pathogen rapid adaption to hosts by giving rise to novel functions.

In summary, our investigation of *Phytophthora* LWY repertoires has revealed modularity as a crucial drive of effector evolution. The observed potential for LWY module rearrangement highlights the capacity of LWY effectors to evolve through recombination. This provides a defined and efficient framework for studying effector evolution and function, offering promising applications for enhancing host resistance in the future.

4.5 Reference

Bentham, A. R., et al. (2024), 'The WY Domain of an RxLr Effector Drives Interactions with a Host Target Phosphatase to Mimic Host Regulatory Proteins and Promote *Phytophthora* infestans Infection', *Mol Plant Microbe Interact,* 37 (3), 239-49.

Boch, Jens., et al. (2009), 'Breaking the Code of DNA Binding

Specificity of TAL-Type III Effectors', *Science,* 326.

Bos, J. I., et al. (2010), '*Phytophthora* infestans effector AVR3a is essential for virulence and manipulates plant immunity by stabilizing host E3 ligase CMPG1', *Proc Natl Acad Sci U S A,* 107 (21), 9909-14.

Boutemy, L. S., et al. (2011), 'Structures of *Phytophthora* RXLR effector proteins: a conserved but adaptable fold underpins functional diversity', *J Biol Chem,* 286 (41), 35834-42.

Chambers, M. C., et al. (2012), 'A cross-platform toolkit for mass spectrometry and proteomics', *Nat Biotechnol,* 30 (10), 918-20.

Cordaux, Richard., et al. (2006), 'Birth of a chimeric primate gene by capture of the transposase gene from a mobile element', *PNAS,* 106.

Cox, K. L., et al. (2017), 'TAL effector driven induction of a SWEET gene confers susceptibility to bacterial blight of cotton', *Nat Commun,* 8, 15588.

Croll, D., et al. (2015), 'The Impact of Recombination Hotspots on Genome Evolution of a Fungal Plant Pathogen', *Genetics,* 201 (3), 1213-28.

Dellero, Y., et al. (2015), 'Experimental evidence for a hydride transfer mechanism in plant glycolate oxidase catalysis', *J Biol Chem,* 290 (3), 1689-98.

Derevnina, L., et al. (2021), 'Plant pathogens convergently evolved to counteract redundant nodes of an NLR immune receptor network', *PLoS Biol,* 19 (8), e3001136.

Goss, E. M., Press, C. M., and Grunwald, N. J. (2013), 'Evolution of RXLR-class effectors in the oomycete plant pathogen *Phytophthora* ramorum', *PLoS One,* 8 (11), e79347.

Haas, B. J., et al. (2009), 'Genome sequence and analysis of the Irish potato famine pathogen *Phytophthora* infestans', *Nature,* 461 (7262), 393-8.

Hedges, D. J. and Deininger, P. L. (2007), 'Inviting Instability: Transposable elements, Double-strand breaks, and the Maintenance of Genome Integrity', *Mutat Res,* 616.

Hill, W. G. and Robertson, Alan (2009), 'The effect of linkage on limits to artificial selection', *Genetical Research,* 8 (3), 269-94.

Jensen-Seaman, M. I., et al. (2004), 'Comparative recombination rates in the rat, mouse, and human genomes', *Genome Res,* 14 (4), 528-38.

Jones, P., et al. (2014), 'InterProScan 5: genome-scale protein function classification', *Bioinformatics,* 30 (9), 1236-40.

Jumper, J., et al. (2021), 'Highly accurate protein structure prediction with AlphaFold', *Nature,* 596 (7873), 583-89.

Kim, D. S., et al. (2024), 'ATR2(C) (ala2) from Arabidopsis-infecting downy mildew requires 4 TIR-NLR immune receptors for full recognition', *New Phytol,* 243 (1), 330-44.

King, S. R., et al. (2014), '*Phytophthora* infestans RXLR effector PexRD2 interacts with host MAPKKK epsilon to suppress plant immune signaling', *Plant Cell,* 26 (3), 1345-59.

Ko, Y. H., Hong, S., and Pedersen, P. L. (1999), 'Chemical mechanism of ATP synthase. Magnesium plays a pivotal role in formation of the transition state where ATP is synthesized from ADP and inorganic phosphate', *J Biol Chem,* 274 (41), 28853-6.

Kong, A., et al. (2002), 'A high-resolution recombination map of the human genome', *Nat Genet,* 31 (3), 241-7.

Lahaye, Thomas. and Bonas, Ulla. (2001), 'Molecular secrets of bacterial type III effector proteins', *TRENDSin Plant Science,* 6.

Li, H., et al. (2023), 'Pathogen protein modularity enables elaborate mimicry of a host phosphatase', *Cell,* 186 (15), 3196-207 e17.

Lole, KAVITA. S., et al. (1999), 'Full-Length Human Immunodeficiency Virus Type 1 Genomes from Subtype C-Infected Seroconverters in India, with Evidence of Intersubtype Recombination', *JOURNAL OF VIROLOGY,* 73.

Moscou, Matthew J. and Bogdanove, Adam J. (2009), 'A Simple Cipher Governs DNA Recognition by TAL Effectors', *Science,* 326.

Muller, M. C., et al. (2019), 'A chromosome-scale genome assembly reveals a highly dynamic effector repertoire of wheat powdery mildew', *New Phytol,* 221 (4), 2176-89.

Otto and Barton, Nick. H. (1997), 'The Evolution of Recombination: Removing the Limits to Natural Selection', *Genetics Society of America,* 147.

Otto and Lenormand, T. (2002), 'Resolving the paradox of sex and recombination', *Nat Rev Genet,* 3 (4), 252-61.

Perez-Quintero, A. L. and Szurek, B. (2019), 'A Decade Decoded: Spies and Hackers in the History of TAL Effectors Research', *Annu Rev Phytopathol,* 57, 459-81.

Petre, B., et al. (2021), 'Host-interactor screens of *Phytophthora* infestans RXLR proteins reveal vesicle trafficking as a major effector-targeted process', *Plant Cell,* 33 (5), 1447-71.

Pettersen, E. F., et al. (2021), 'UCSF ChimeraX: Structure visualization for researchers, educators, and developers', *Protein Sci,* 30 (1), 70-82.

Pierre, M., Noël , L., and Bonas, T. Lahaye · A. Ballvora J. Veuskens · M. Ganal · U. (2000), 'High-resolution genetic mapping of the pepper resistance locus Bs3governing recognition of the Xanthomonas campestris pv vesicatora AvrBs3 protein', *Theor Appl Genet,* 101.

Romer, P., et al. (2010), 'Promoter elements of rice susceptibility genes are bound and activated by specific TAL effectors from the bacterial blight pathogen, Xanthomonas oryzae pv. oryzae', *New Phytol,* 187 (4), 1048-57.

Schornack, S., et al. (2006), 'Gene-for-gene-mediated recognition of nuclear-targeted AvrBs3-like bacterial effector proteins', *J Plant Physiol,* 163 (3), 256-72.

Schornack, S., et al. (2004), 'The tomato resistance protein Bs4 is a predicted non-nuclear TIR-NB-LRR protein that mediates defense responses to severely truncated derivatives of AvrBs4 and overexpressed AvrBs3', *Plant J,* 37 (1), 46-60.

Shen, D., et al. (2013), 'Gene duplication and fragment recombination drive functional diversification of a superfamily of cytoplasmic effectors in *Phytophthora* sojae', *PLoS One,* 8 (7), e70036.

Streubel, J., et al. (2013), 'Five phylogenetically close rice SWEET genes confer TAL effector-mediated susceptibility to Xanthomonas oryzae pv. oryzae', *New Phytol,* 200 (3), 808-19.

Stukenbrock, E. H. and Dutheil, J. Y. (2018), 'Fine-Scale Recombination Maps of Fungal Plant Pathogens Reveal Dynamic Recombination Landscapes and Intragenic Hotspots', *Genetics,* 208 (3), 1209-29.

Teper, D. and Wang, N. (2021), 'Consequences of adaptation of TAL effectors on host susceptibility to Xanthomonas', *PLoS Genet,* 17 (1), e1009310.

Varadi, M., et al. (2024), 'AlphaFold Protein Structure Database in 2024: providing structure coverage for over 214 million protein sequences', *Nucleic Acids Res,* 52 (D1), D368-D75.

Yang and Gabriel, DEAN. W. (1995), 'Intragenic Recombination of a Single Plant Pathogen Gene Provides a Mechanism for the Evolution of New Host Specificities', *JOURNAL OF BACTERIOLOGY,* 177.

Yang, Sugio, Akiko., and White, Frank. F. (2005), 'Avoidance of Host Recognition by Alterations in the Repetitive and C-Terminal Regions of AvrXa7, a Type III Effector of Xanthomonas oryzae pv. oryzae', *MPMI,* 18.

Chapter 5 Modular commonality drives common host protein targeting by LWY effectors

5.1 Introduction

Effectors are secreted virulence factors that pathogens deploy to actively interfere with host immune response and manipulate cellular processes to facilitate pathogen infection (Lo Presti et al. 2015). These molecules are highly sequence-diverse molecules, normally lineage-specific, lacking conserved protein domains and may not share sequence similarity with closely related species, making functional prediction challenging (Franceschetti et al. 2017; Lovelace et al. 2023; McGowan and Fitzpatrick 2017).

Despite this diversity, some effector families maintain conserved structural folds that correspond to similar functions. For example, proteins containing lysin motif (LysM) domains, such as Ecp6, sequester chitin oligosaccharides while Necrosis and Ethylene-inducing Peptide 1 (Nep1)-like proteins function as microbe-associated molecular patterns (MAMPs) that trigger immune responses across various plant pathogens including oomycetes, fungi, and bacteria (Oome et al. 2014; Sanchez-Vallet et al. 2013; H. Tian et al. 2022).

Recent advances in crystallography and computational structural prediction have revealed shared structural folds within specific effector families across plant pathogens. These include the Fol dual-domain (FOLD) effector family, *Magnaporthe oryzae* Avrs and ToxB (MAX) effectors and the RNase-like proteins associated with haustoria (RALPH) effectors (Bialas et al. 2021; Cao et al. 2023; L. Guo et al. 2018; Pennington et al. 2019; Seong and Krasileva 2023; D. S. Yu et al. 2024). The common folds in MAX effectors are recognized by the intracellular immune receptors (NLRs) integrated heavy metal-associated (HMA) domains while the variations in binding interfaces between effectors and NLR HMA domains determine recognition specificity (De la Concepcion et al. 2018; L. Guo et al. 2018).). This suggests that specific residues

within conserved folds may define effector activities. However, our understanding of how effectors with similar folds evolve new functions remains limited.

In oomycetes, WY and LWY effectors represent an expansion of connected tandem repeats, with each unit containing 3-5 structurally conserved α-helices (Boutemy et al. 2011; Chou et al. 2011; B. Guo et al. 2019; He et al. 2019; Lovelace et al. 2023; Maqbool et al. 2016). In LWY effectors, WY units are connected by extended L units (Boutemy et al. 2011; He et al. 2019; Hou et al. 2019; H. Li et al. 2023). While the structural scaffold is conserved, the exposed residues on individual units show considerable divergence, allowing their classification into distinct clusters as demonstrated in Chapter 3. The recent identification of protein phosphatase 2A (PP2A)-interacting modules as functional modules (H. Li et al. 2023) raises two key questions for us to understand effector evolution:

1. Whether the deployment of functional modules represent a fundamental evolutionary strategy by LWY effectors, particularly in targeting common host proteins?
2. How do functional modules contribute to the acquisition of new functions or functional specifications in LWY effectors?

To address these questions, I analyzed two-unit combinations of (L)WY tandem repeats across all five *Phytophthora* species to identify potential functional modules. I selected 22 *P. infestans* LWY effectors for host interaction analysis in *Nicotiana benthamiana*, with 15 of them containing multiple common modules. Notably, 18 of these 22 effectors showed expression during infection, suggesting their functional relevance during pathogen colonization.

Mass spectrometry analysis of LWY effectors sharing common modules revealed several significant interaction patterns. The positive control PITG_15038 and AVRcap1b showed the association with previously identified host interactors in current mass-spectrometry data, confirming the reliability and sensitivity of our experimental approach. Besides, three additional unit combinations were identified to recruit common proteins: 9_5, 16_6, and 9_25.

The 9_5 combination, present in 11 LWY effectors, consistently showed three interactors across all three LWY effector interactomes. The 16_6 combination was found in 8 LWYs, with three *P. infestans* LWY effector interactomes being characterized. Among

these, two LWY effectors with combination 16_6 showed common associations with histone acetylases and bound to different protein phosphatase 2A (PP2A) subunits.

While previous studies identified numerous LWY effectors interacting with PP2A, the specific downstream substrates of effector-PP2A holoenzymes remained largely unexplored. Our investigation focused on PITG_23036, a *P. infestans* LWY effector containing five tandem repeats and promoted *P. capsici* infection. Similar to two PP2A-interacting effectors PSR2 and PITG_15142, PITG_23036 recruits PP2A A and C subunits, effectively mimicking the PP2A B subunit to hijack the PP2A holoenzyme. Additionally, PITG_23036 contains the common module 9_25, which was demonstrated to be responsible for binding to three ubiquitin-conjugating enzymes (E2). Published data identified phosphorylation sites within the C-terminal intrinsically disordered region of an E2 ubiquitin ligase. These phosphorylation sites are conserved between E2 ligase orthologs from different plant species, suggesting they may be substrates for PITG_23036-PP2A holoenzyme.

This study provides a new resolution to effector evolution by categorizing LWY effectors based on their modularity. The employment of different potential functional modules in an LWY effector appears to be a source of increasing complexity in LWY effector protein interactions, highlighting how modularity drives the functional divergence of these effectors.

5.2 Results

5.2.1 Selection of *P. infestans* LWY effectors for host target identification.

To identify host interactors of LWY effectors, I established specific selection criteria focusing on module combinations that appeared more than seven times across LWY genes. I specifically focused on *P. infestans* LWY effectors containing both signal peptides (SP) and RxLR motifs. This systematic screening identified 22 LWY effectors with different patterns of common modules (Figure 5.1A). These candidates were interconnected through shared common modules, represented by the same-coloured links (Figure 5.1A).

Our analysis identified 14 distinct module combinations that appear in multiple LWY effectors, suggesting these combinations may enable different LWY effectors to recruit the same host protein interactors. For instance, the 23_18 combination was identified in two PP2A-interacting effectors PITG_15038 and PITG_23035 (H. Li et al. 2023). In the PITG_15038, this combination is located in WY1-LWY2 and was predicted to form PP2A-interacting pockets. PITG_23035 also showed an association with PP2A A subunit in the mass-spectrometry data in Figure 5.5A, suggesting 23_18 might be a functional module mediating PP2A A subunit association.

In addition, 15/22 LWYs contain more than one common module (Figure 5.1A). Four LWY effectors exhibited exceptional complexity, containing four or more "popular" modules: PITG_15105, PITG_23035, a reported NRC network suppressor AVRcap1b (Derevnina et al. 2021), and PITG_15038 (a PP2A-interacting effector), implying an expanded capacity to engage with multiple host targets. Therefore, it's hypothesized that LWY effectors sharing common modules may interact with similar host targets, while the combination of different common modules could enhance their ability to recruit multiple host proteins into functional complexes. Future comparative analysis of interactomes from effectors sharing common modules will facilitate the identification of genuine host interactors.

To investigate whether these LWY effectors potentially modulate host physiology during infection, I analysed transcriptomic data from two *P. infestans* isolates (1306 and 3928A) during both vegetative growth and potato tuber infection (unpublished data) (Ah-Fong et al. 2017) (Figure 5.1B and 5.1C). Expression patterns were visualized using $\log_{10}$-transformed counts per million (CPM) for isolate 1306 and Fragments Per Kilobase of transcript per Million mapped reads (FPKM) for isolate 3928A. Hierarchical clustering of the transcriptome data revealed similarities in expression patterns across different stages of samples.

The analysis revealed that 16 LWY effectors showed expression during infection in both isolates. These included three known PP2A-interacting effectors (PiPSR2, PITG_15038, and PITG_23036) and an NRC network suppressor (AVRCap1b) (Figure 5.1B). Some LWY effectors displayed isolate-specific expression patterns: for example, PITG_12791 and PITG_10116 showed infection-induced expression in isolate 3928A but were not expressed in isolate 1306 (Figure 5.1C). These variations may reflect differences in infection strategies between isolates or variations in sequencing depth between experiments. Nevertheless, the data indicate that most LWY effectors containing these potential functional modules are induced during infection, suggesting their potential contribution to *Phytophthora* host colonization.

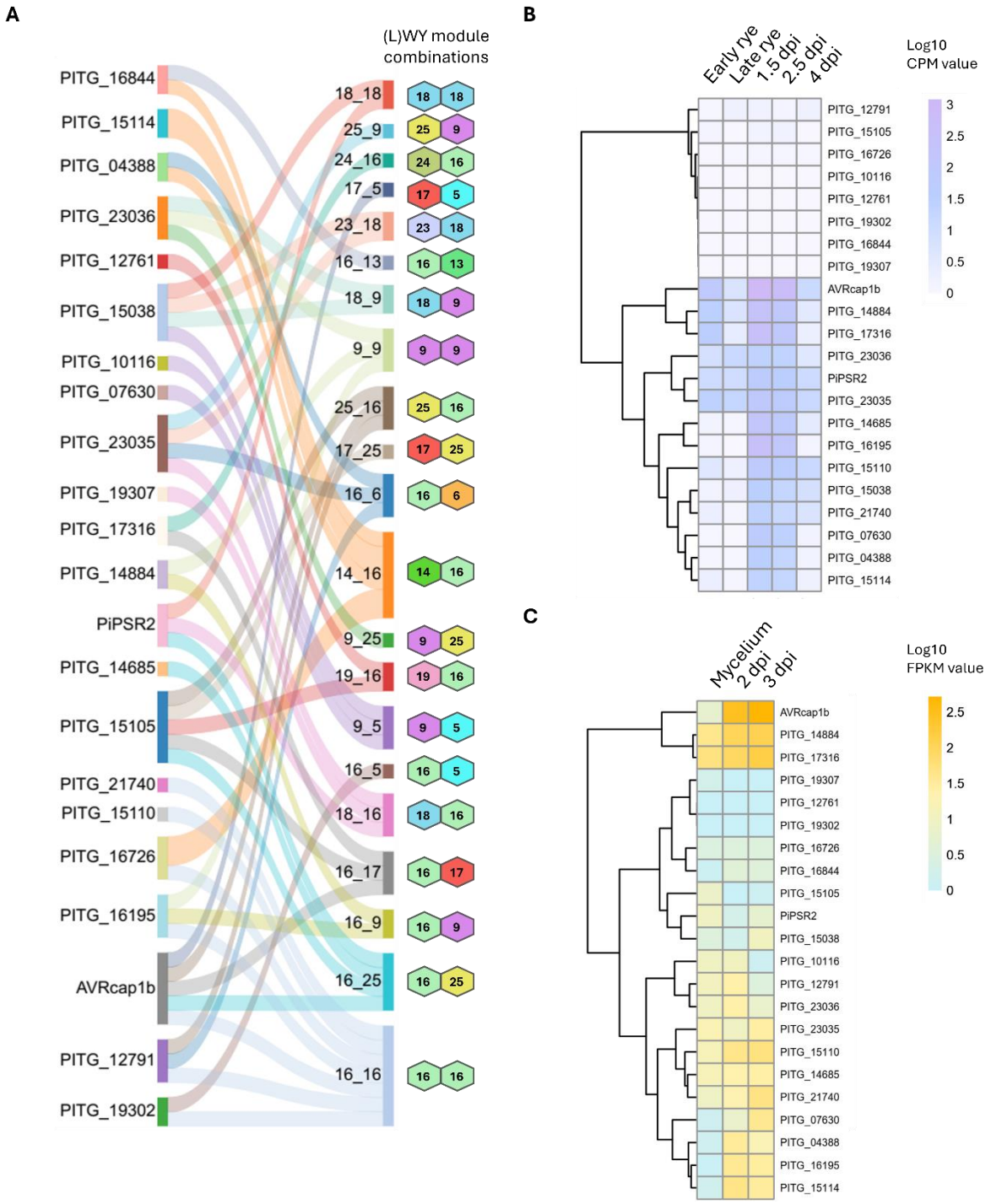

Figure 5.1 Selection of 22 P. infestans LWY effector candidates for host target analysis.

(**A**) Sankey diagram illustrating the distribution of common modules (right) across 22 LWY effectors (left) as identified in Chapter 3. Colores indicate distinct clusters of (L)WY units. (**B, C**) Transcriptional profiles of LWY effectors during vegetative growth and infection stages in *P. infestans* isolates 1306 (**B**) and 3928A (**C**). Expression values were normalized by gene length and $\log_{10}$-transformed, represented as counts per million

reads mapped (CPM) or fragments per kilobase million (FPKM). Dendrograms show hierarchical clustering based on expression pattern similarity across developmental stages.

5.2.2 Overview of 20 *P. infestans* LWY effector interactomes in *Nicotiana benthamiana*.

To investigate whether LWY effectors adopt the common modules for interacting with common host proteins, I expressed LWY effectors individually in *N. benthamiana* to identify effector interactomes. Due to ongoing experimental analysis of PiPSR2 and insufficient biological replication for PITG_14884 (n=1), these two LWY effectors were excluded from the analysis. Twenty LWY effectors were individually expressed with C-terminal GFP tags, using AVRcap1b and PITG_15038 as positive controls and free GFP as a negative control (Figure 5.2). Western blot analysis using GFP antibodies confirmed the expression of all effector proteins at their expected molecular weights (Figure 5.2). At least two independent replicates for each effector were then submitted for immunoprecipitation coupled with mass spectrometry (IP-MS) (Figure 5.2).

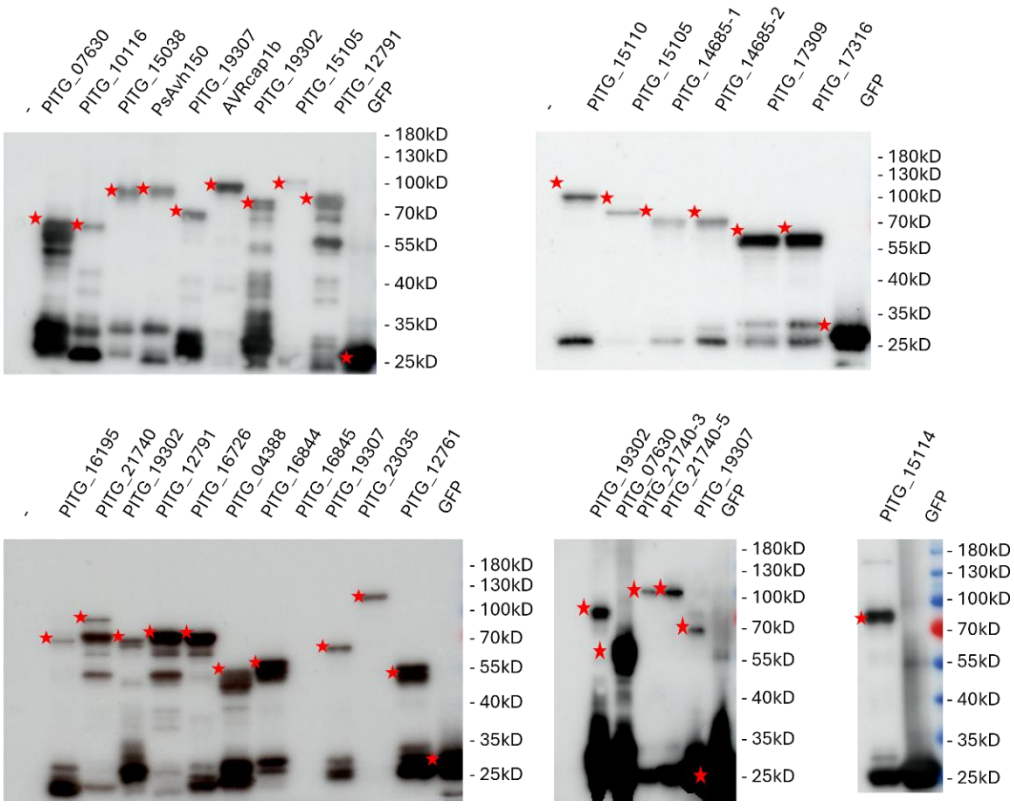

Figure 5.2 Western blot of LWY effectors for IP-MS.

Western blots were used to indicate the transient expression of GFP-tagged LWY effectors. Effector proteins (indicated by red asterisks) were detected using anti-GFP

antibodies. Free GFP served as a positive control for immunoblotting and a negative control for subsequent mass spectrometry analysis.

Initial analysis identified over 5,000 candidate host interactors across the 20 LWY effectors (Figure 5.3A). To ensure high-confidence interactions, contaminants (already known in the database) and previously reported sticky proteins were removed (Petre et al. 2021). Additional quality control steps included removing peptides with ion scores below 39 and confidence levels below 90%. Furthermore, interactors were only retained if they appeared in at least one replicate.

This filtering approach yielded 870 high-confidence host protein interactors. The number of interactors per effector ranged from 12 to 243, with an average of 43 host proteins per LWY effector (Figure 5.3B). 17 of the 20 tested effectors recruited more proteins than the average. Analysis of the unit cluster compositions for each LWY effector (highlighted by red boxes for common modules) revealed that PITG_15038 and PITG_07630 had the largest interactomes (Figure 5.3B). Intriguingly, these two effectors share the same patterns of modules in their final two-unit positions (Figure 5.3B). A third effector, PITG_10116, which contains the same module combination, showed the fourth-largest interactome with 150 host protein interactions. This pattern suggests that these shared C-terminal modules may enhance the capacity for effector-target interactions.

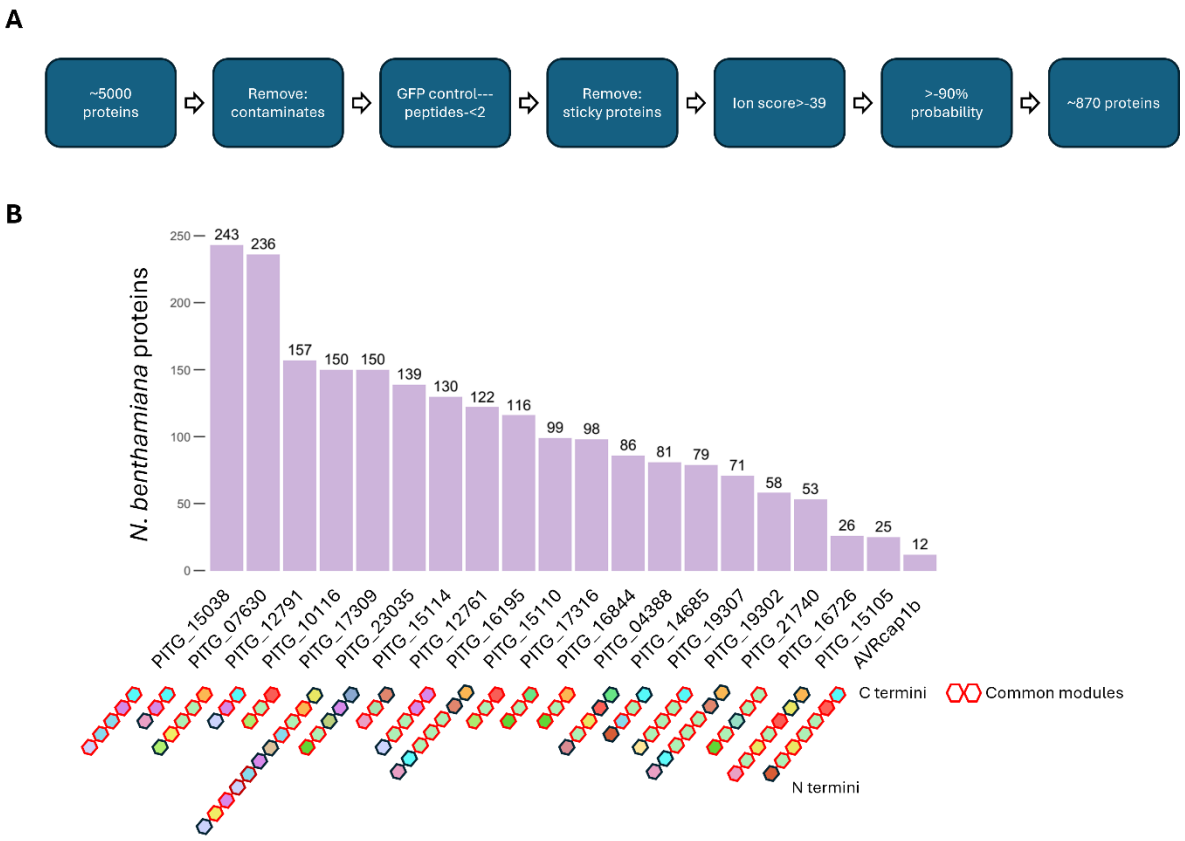

Figure 5.3 Identification LWY effector interactomes in *N. benthamiana*.

(**A**) The schematic workflow for mass spectrometry data processing and analysis. (**B**) Distribution of host protein interactors identified for individual LWY effectors. Module architectures are shown for each effector, with common modules highlighted by red borders.

To analyse the overlap between effector interactomes, I constructed a presence-absence matrix incorporating the 870 host proteins identified across all 20 LWY effectors. This matrix was transformed into an interaction network to visualize both shared and effector-specific host protein interactions (Figure 5.4). In the network visualization, effector-specific interactors are positioned along the edge, while proteins targeted by multiple effectors occupy central positions. Each effector-protein interaction is represented by color-coded links, with shared host proteins connected to multiple effectors by differently coloured links (Figure 5.4). This network analysis revealed extensive interconnectivity between LWY effector interactomes, suggesting the potential to identify common host targets that attribute to effector modularity-driven evolution.

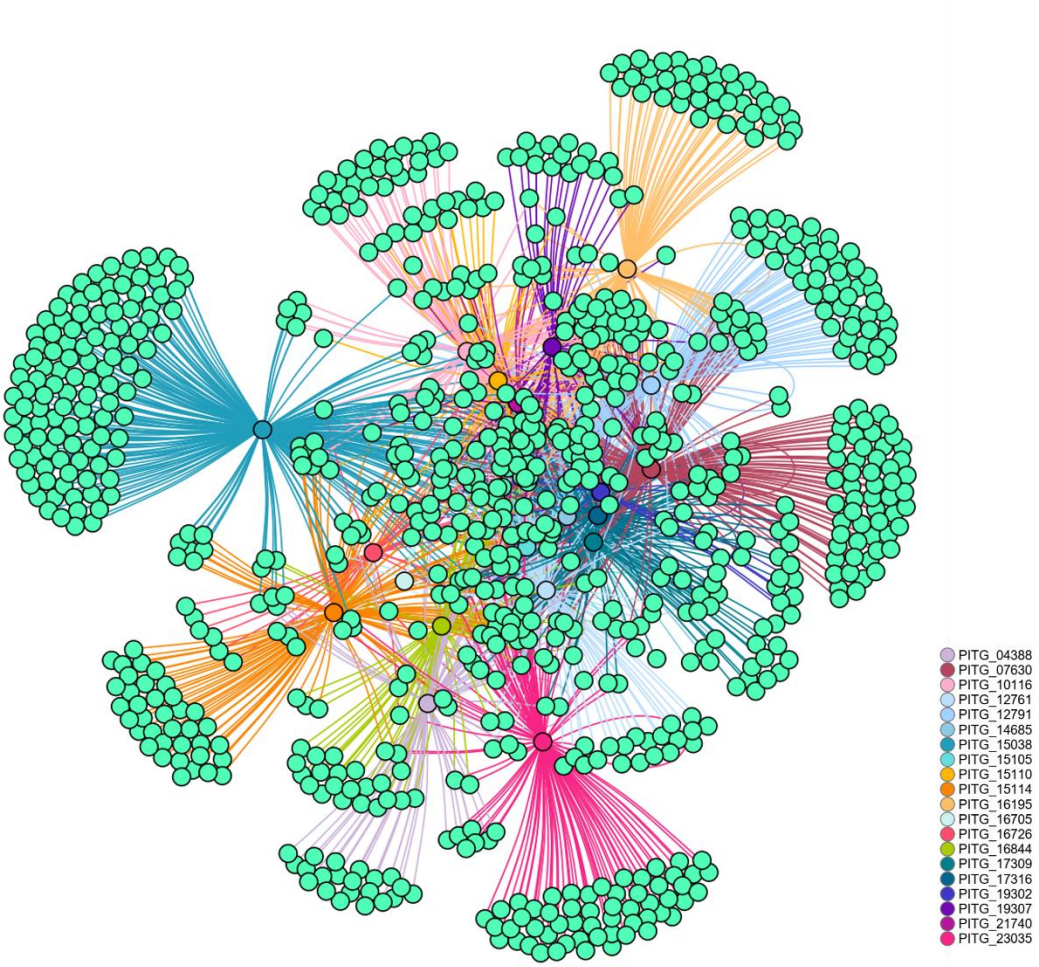

Figure 5.4 Overview of 20 LWY effector interactomes.

Network visualization of LWY effector-host protein interactions. Green nodes represent host interactors, with coloured edges indicating their associations with specific LWY effectors (n=20). The edge colours correspond to their respective LWY effectors.

5.2.3 LWY effectors with common modules recruit common host proteins.

To identify if module combinations that were frequently adopted bind the same host interactors, I compared the interactomes from LWY effectors with the same module combinations and visualized the presence of interactors in effector interactomes using heatmaps, with interaction intensities represented by log_2-transformed spectral counts from each biological replicate. This approach enabled quantitative assessment of host protein associations across effector interactome replicates.

5.2.3.1 LWY effectors with predicted PP2A-interacting modules associate with different combinations of PP2A subunits

Among the 20 *P. infestans* LWY effectors studied, PITG_15038, a five-repeat effector with a WY1-(LWY)4 structure, was previously shown to exhibit high PP2A phosphatase activity when transiently expressed in *N. benthamiana* (H. Li et al. 2023). Therefore, this PP2A-interacting effector PITG_15038 was used as a positive control for the IP-MS assay (Figure 5.5A). Hierarchical clustering and combination enrichment analysis identified common PP2A A subunit-interacting modules 23_18 in two effectors: WY1-LWY2 in PITG_15038 and LWY4-LWY5 in PITG_23035 (Figure 5.5A). PITG_23035 has eleven tandem repeats displayed as WY1-(LWY)2-WY4-(LWY)2-WY7-(LWY)4. Consistent with these predictions, PP2A A subunits were identified from two replicates of PITG_15038 and one replicate of PITG_23035 effector interactomes. Interestingly, two LWY effectors PITG_10116 and PITG_15114 lacking the predicted PP2A-interacting pockets were also showing an association with PP2A A subunits despite of lower spectrum counts identified than PITG_15038.

Despite of association with PP2A A subunits, these effectors displayed different patterns of recruiting PP2A regulatory or catalytic subunits. For example, PITG_15038 demonstrated interaction with complete PP2A holoenzymes (A, B and C subunits) while PITG_15114, which has a WY1-(LWY)3-LW domain organization, associated specifically with PP2A core enzymes (A and C subunits) (Figure 5.5A). The other two LWY effectors PITG_10116 (formatted as WY1-LWY2-LW3) and PITG_23035 however mediate the

interaction with PP2A A subunits exclusively. Furthermore, the interactome analysis revealed that effectors PITG_04388 (arranged as WY1-LWY2-LW3) uniquely associate with PP2A B and C subunits (Figure 5.5A). These diverse interaction patterns with PP2A subunits, which correlate with the distinct unit compositions of these effectors, suggest extensive functional diversification in their ability to form complexes with host PP2A components.

Although PITG_10116 and PITG_15114 lack predicted PP2A-interacting pockets, our analysis detected PP2A A subunits in their interactomes. Previous research identified that interaction with the PP2A A subunit PDF1 in *Arabidopsis thaliana* requires 12 specific residues across LWY2-LWY3 in PSR2, with the REQ triad being essential for this interaction (H. Li et al. 2023). Importantly, the PP2A A subunit beta isoform in *N. benthamiana* is a homolog of *A. thaliana* PDF1 with 93% sequence identity, suggesting the potential for conserved interaction interfaces between these organisms.

To survey whether these newly identified PP2A-interacting effectors (PITG_10116 and PITG_15114) form similar interfaces, I compared their exposed residues from each pair of adjacent units with the 12 key residues identified in PSR2, a known PP2A-interacting effector (Figure 5.5B). The analysis mapped these residues to their corresponding positions in each protein, with amino acids color-coded based on their chemical properties. While all four LWY effectors showed similar numbers of interacting residues overall, PITG_15038 and PITG_23035 displayed the highest similarity to PSR2's REQ triad within their predicted PP2A-interacting modules (Figure 5.5B). In contrast, PITG_10116 and PITG_15114 showed greater variations in their REQ triads within their first two units, which may explain their absence from initial screens and low PP2A activities in a previous publication (Figure 5.5B) (H. Li et al. 2023).

The successful identification of known PP2A-interacting effectors through our analysis validates the reliability of our (L)WY unit clustering approach and common module prediction.

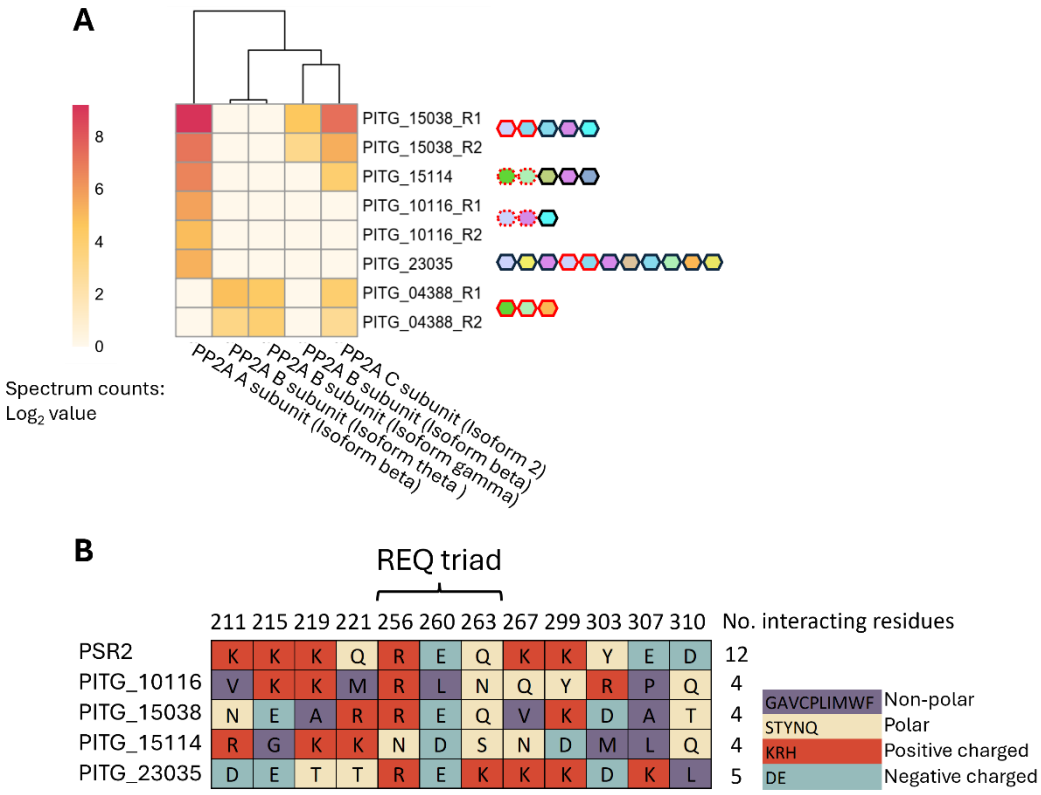

Figure 5.5 LWY effector PP2A-binding modules specify distinct subunit interactions.

(**A**) A heatmap showed LWY effector interactomes with host PP2A A, B and C subunits using transformed log_2 spectrum counts. Hierarchical clustering groups LWY effectors based on their PP2A subunit interaction patterns. Red borders indicate modules predicted to interact with PP2A subunit A (solid lines) or modules containing putative interaction interfaces based on the presence/absence of 12 key residues (dashed lines). (**B**) Two-unit exposed residues from each LWY effector were aligned with PSR2 to extract PP2A binding interfaces. The top row shows the 12 critical residues from PSR2. Amino acid polarity is indicated for each position.

5.2.3.2 Two LWY effectors with 16_16 suggested a common association with NbTOL9

Analysis from Chapter 3 revealed Cluster 16 includes the most abundant units, which form diverse two-unit combinations with units from other clusters. The most enriched two-unit combination, designated as 16_16, was found in 31 LWY effectors, including 14 LWY effectors with Signal Peptide (SP) and RxLR motifs. To characterize the sequence diversity of these 16_16 common modules, I conducted a phylogenetic analysis using exposed residues from the 16_16 (L)WY-LWY module. The resulting neighbor-joining tree was validated using bootstrap values, with combinations labelled by their relative positions and accompanied by aligned LWY domain architectures showing 16_16 common modules highlighted in green (Figure 5.6). This analysis revealed that 16_16 combinations predominantly occur in the middle regions of effector domains.

Of the effectors analysed by mass spectrometry, seven *P. infestans* LWY effectors containing the combination 16_16 are located in the upper portion of the heatmap: AVRcap1b formatting as WY1-(LWY)6, PITG_12791 organizing as WY1-(LWY)3-L5, PITG_15110 and PITG_21740 showing as Y1-(LWY)4-LW6-LWY7, PITG_16195, PITG_16726 and PITG_19302 arranging as WY1-(LWY)4. Every 16_16 combination in the seven LWY effectors was indicated in the red branch on the phylogeny tree (Figure 5.6). The phylogenetic analysis revealed that 16_16 common modules form five clades. The seven *P. infestans* LWY effectors represent four of these clades, with Clades 1, 2, and 4 containing 16_16 modules exclusively from *P. infestans* and its sister species. In contrast, Clades 3 and 5 comprise 16_16 combinations from five different *Phytophthora* species (Figure 5.6).

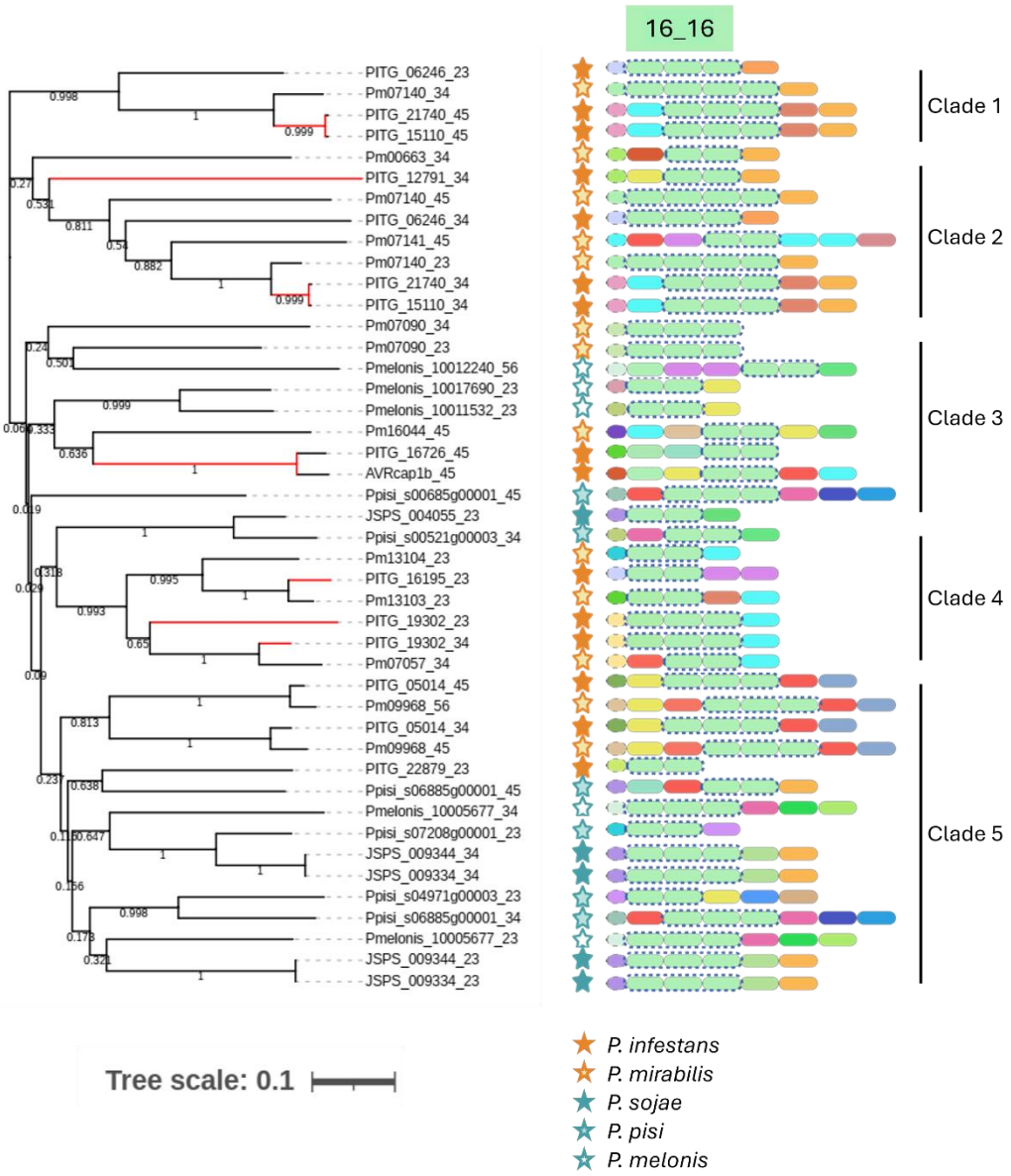

Figure 5.6 Phylogeny tree of (L)WY-LWY from combination 16_16.

Neighbour-joining phylogenetic tree of LWY effectors based on exposed residues of two-unit 16_16 combinations. Red branches indicate effectors tested for immunoprecipitation-mass spectrometry (IP-MS) analysis. Individual unit compositions are shown for each effector. Two-unit 16_16 combinations (marked by dashed outlines) are grouped by *Phytophthora* species of origin.

Comparative analysis of LWY effectors with 16_16 common modules indicated five candidate host interactors (Figure 5.7A). LWY effectors lacking the 16_16 common module appeared in the lower region of the heatmap. Among the seven effectors studied, AVRcap1b contains seven tandem (L)WY repeats, which was previously shown to interact with the membrane trafficking-associated Target of Myb 1-like protein 9 (TOL9) in *N. benthamiana* to suppress NRC networks (Derevnina et al. 2021) (Figure 5.7A). Additionally, our mass spectrometry analysis revealed that analysis revealed that PITG_16726, another LWY effector containing 16_16 common modules, also associates with NbTOL9 across three replicates, suggesting NbTOL9 role as a potential hub for effector targeting (Figure 5.7A). Notably, these two NbTOL9-interacting effectors contain highly similar 16_16 combinations within Clade 3 (Figure 5.5A). A sequence similarity analysis was conducted between these two LWY effectors. The overall sequence alignment revealed a 69.8% similarity between AVRcap1b and PITG_16726 (Figure 5.7B). Noticeably, AVRcap1b has two additional LWY units than PITG_16726. When analyzing the first five units specifically, the sequence similarity increases to 89%, with 16_16 positioned at the LWY4-LWY5 region (Figure 5.7B). The high degree of conservation in the first five units suggests they may play a crucial role in NbTOL9 targeting.

Further analysis revealed that both PITG_19302 and PITG_16195, with 16_16 common modules from Clade 4 (Figure 5.5A), interact with magnesium protoporphyrin IX monomethyl ester, a key enzyme in chlorophyll biosynthesis (Figure 5.7A). This interaction was also observed with two additional LWY effectors, PITG_17316 and PITG_19307, which contain 24_16 and 18_16 combinations rather than 16_16. The presence of Cluster 16 units in the second position across these four effectors suggests that interfaces mediating interaction with magnesium protoporphyrin IX monomethyl ester may primarily reside within Cluster 16 LWY units. Beyond this interaction, PITG_16195 also associates with ABC transporters, a characteristic shared with three other LWY effectors: PITG_15110, PITG_21740 and PITG_14685 (which contains a 16_25 common module) (Figure 5.7A).

PITG_12791, which contains 16_16 modules from Clade 2, demonstrated consistent interaction across three replicates with two trafficking-related proteins: SEC16, a COPII coat assembly protein essential for protein transport from the endoplasmic reticulum (ER) to Golgi, and TPLATE, a protein involved in vesicle trafficking (Figure 5.7A).

These findings reveal several key insights into LWY effector function and evolution. First, the targeting of NbTOL9 by two LWY effectors sharing similar 16_16 combinations from the same clade suggests functional conservation within this clade. Second, the 16_16 combination represents a broadly diversified module family, with different variants potentially enabling distinct host protein interactions. This functional diversification appears to allow LWY effectors to interfere with multiple cellular processes, including chlorophyll biosynthesis, vesicle trafficking, and ER-to-Golgi protein transport. Such diversity in targeting capabilities suggests that variations in 16_16 combinations may have facilitated the expansion of effector function across different cellular pathways and processes.

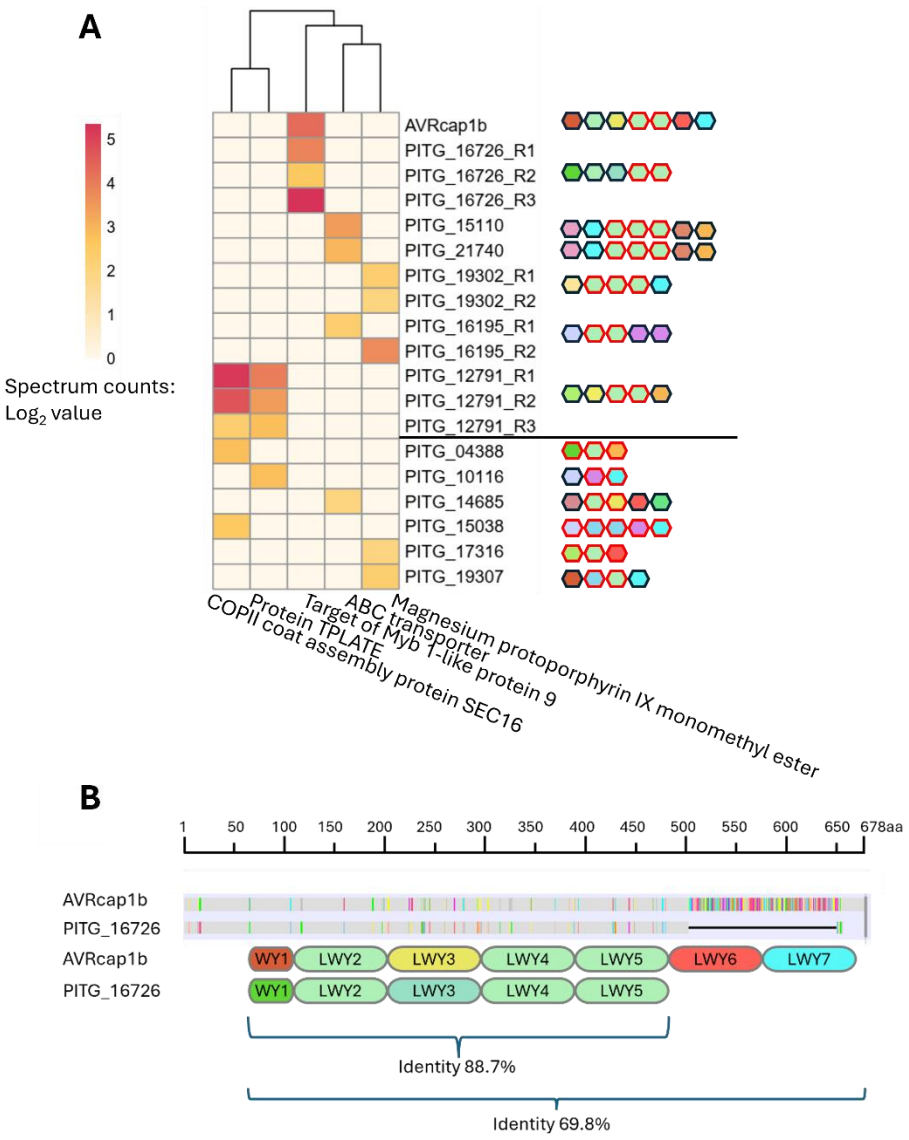

Figure 5.7 AVRcap1b and PITG_16726 with combination 16_16 share a common association with NbTOL9.

(**A**) Comparative interaction profile of host proteins with LWY effectors. The heatmap depicts log2-transformed spectrum counts of proteins interacting with 16_16 module-containing effectors (upper panel) versus effectors lacking 16_16 combinations (lower panel). (**B**) Sequence alignment comparing AVRcap1b and PITG_16726, highlighting their unit compositions. Conserved residues between the two sequences are shown in grey, while divergent residues are indicated by distinct colours. The unit composition of each protein is displayed alongside the alignment.

5.2.3.3 9_5 modular LWY effectors share diverse common proteins

Further analysis revealed another significant common module shared between PP2A-interacting effectors PITG_15038 and PITG_10116 (Figure 5.8A). While both effectors may contain the first two (L)WY units for PP2A interaction, they also share a 9_5 combination located at LWY4-LWY5 in PITG_15038 or LWY2-LWY3 in PITG_10116. This 9_5 module combination was identified in 11 LWY effectors in total, consistently appearing in the terminal two-unit positions (Figure 5.8A).

Our interactome analysis included three LWY effectors containing 9_5 module combinations: PITG_07630 (formatting as WY1-(LWY)2), PITG_10116 (WY1-LWY2-LW3), and PITG_15038 (WY1-(LWY)4) (Figure 5.8B). These effectors shared 21 candidate interactors, including Myosin XI, Serrate RNA effector molecule, and CDC48 homolog. PITG_07630 and PITG_10116, which share similar three interspersed repeat architectures, both interact with proteasome activator subunit and calcium-sensing proteins. PITG_10116 and PITG_15038 showed a common association with the E3 ligase KEG (Figure 5.8B). Additionally, PITG_15038 exhibited unique interactions with various proteins, including Importin subunits, NAC domain proteins, and outer envelope proteins, possibly due to the presence of other common combinations (18_9) within this effector (Figure 5.8B).

These findings suggest that effectors containing 9_5 common modules can recruit a shared set of host proteins, potentially enabling interference with diverse cellular processes including Golgi-mediated protein trafficking, membrane fusion, and pre-mRNA splicing.

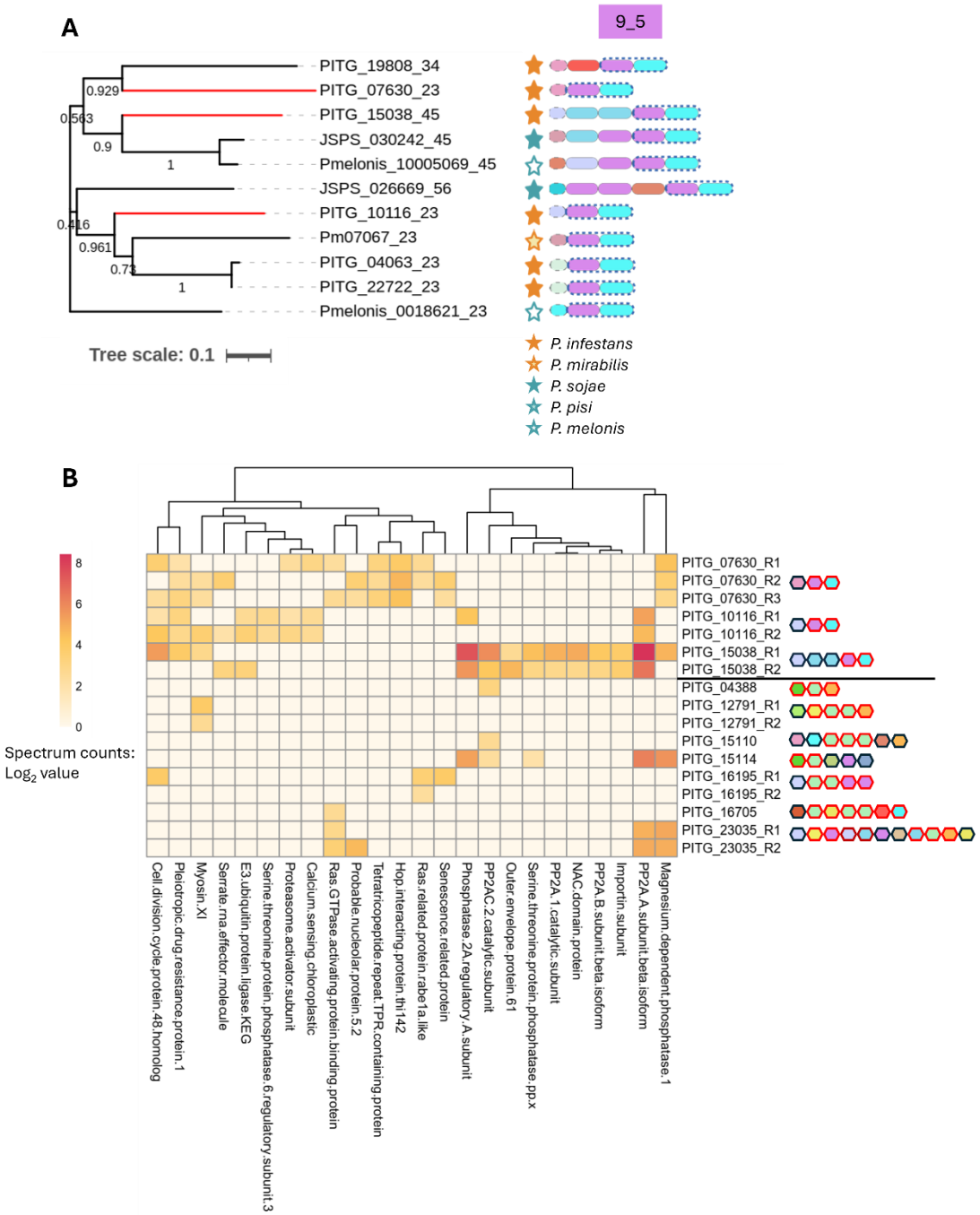

Figure 5.8 Phylogenetic distribution and interactome analysis of LWY effectors with 9_5 combination.

(**A**) Neighbour-joining phylogenetic tree constructed from exposed residues of two-unit 9_5 combinations. LWY effectors selected for immunoprecipitation-mass spectrometry (IP-MS) analysis are highlighted with red branches. Individual unit compositions are shown for each effector. Two-unit 9_5 combinations (marked by dashed outlines) are grouped by *Phytophthora* species of origin. (**B**) Comparative interaction profile of host proteins with LWY effectors. The heatmap depicts log2-transformed spectrum counts of

proteins interacting with 9_5 module-containing effectors (upper panel) versus effectors lacking 9_5 combinations (lower panel).

5.2.3.4 Two 16_6 modular LWY Effectors interacting with host HDACs, ZFPs, and PEX2-like Proteins.

The analysis identified eight LWY effectors enriched for the 16_6 combination, with three of these presenting among the 20 *P. infestans* LWY effectors tested for interactomes (Figure 5.9A). Phylogenetic analysis revealed that the 16_6 common modules in these three effectors were distributed across different branches in the phylogeny tree (Figure 5.9A).

Comparative proteomics across these three LWY effectors indicated most similar protein profiling between PITG_23035 (arranged as WY1-(LWY)2-WY4-(LWY)2-WY7-(LWY)4) and PITG_04388 (presented as WY1-LWY2-LW3), including Histone deacetylases (HDACs), Zinc finger proteins (ZFPs) and Protein exordium-like 2 (PEX2) proteins etc (Figure 5.9B). While PITG_23035 and PITG_12791 shared interaction with Chaperonin Cpn60/GroEL, this protein was also detected in the interactomes of two LWY effectors lacking the 16_6 combination, suggesting its interaction is not specifically mediated by the 16_6 module (Figure 5.9B).

Notably, our earlier analysis identified PP2A subunit associations for both PITG_23035 and PITG_04388 though with distinct patterns: PITG_23035 was associated with the PP2A A subunit, while PITG_04388 bonded to PP2A B and C subunit. It's likely that PITG_23035 and PITG_04388 are forming different complexes despite the presence of common module 16_6 that may confer the binding to the same host targets. The diverse interactors of these effectors suggest roles in multiple cellular processes, including histone lysine deacetylation, DNA binding, and BIIDXI-mediated regulation of cell wall pectin status (Figure 5.9B).

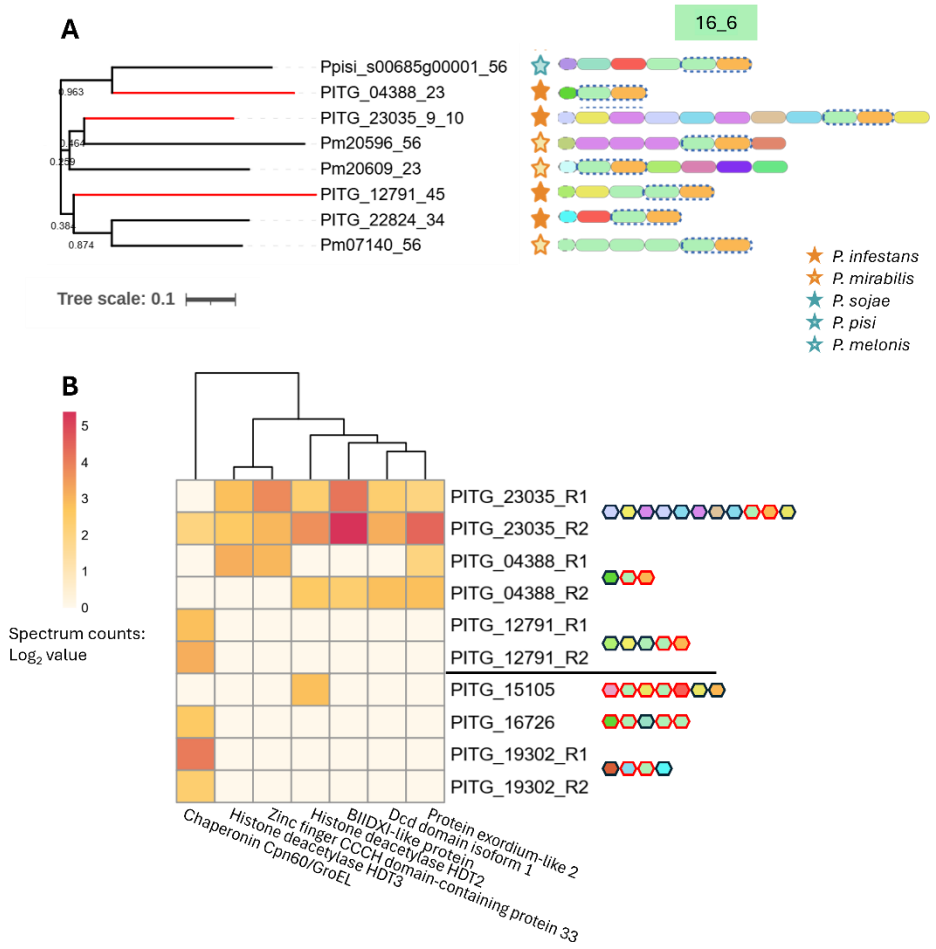

Figure 5.9 Phylogenetic and interatomic profiling of 16_6 modular LWY effectors.

(**A**) Phylogenetic tree constructed by neighbour-joining method based on surface-exposed residues of dual-unit 16_6 combinations. LWY effectors subjected to IP-MS analysis are depicted in red branches. Each effector is labelled with its unit composition. Dashed boxes denote 16_6 combinations, grouped according to *Phytophthora* species origin. (**B**) Heatmap representation of protein interactions showing 16_6-containing LWY effectors and their specific interaction partners (above), contrasted with their detection in LWY effectors without 16_6 combinations (below), displayed as log2-transformed spectrum counts.

5.2.4 Common combination 9_25 confers to LWY effector virulence function.

Previous research identified 13 PP2A-interacting effectors containing specific modules that enable the hijacking of host PP2A core enzymes to form effector-PP2A holoenzymes (H. Li et al. 2023). One of these effectors, PITG_23036, contains a predicted common module 9_25 at its C-terminus, suggesting this combination might be involved in substrate binding of the PITG_23036-PP2A holoenzyme. To test this hypothesis, I employed IP-MS, Co-IP, and virulence assays.

5. 2. 4. 1 A PP2A-interacting LWY effector PITG_23036 promotes Phytophthora capsici infection.

PITG_23036 consists of five tandem repeats arranged as WY1-(LWY)3-LW5, with the conserved PP2A-interacting residues present in between WY1-LWY2. Each unit was labelled according to the cluster they belonged to. AlphaFold-multimer analysis predicted interaction between PITG_23036 and *A. thaliana* PP2A A subunit PDF1 in the first two units, with a predicted template modelling (pTM) score of 0.6, validating the structural predictions. The interface quality was supported by an interface predicted template modelling (ipTM) score of 0.5, while the predicted aligned error (PAE) plot indicated low positional errors at the interfaces (Figure 5.10A). Six residues especially the essential REQ triad identified from 12 binding residues in PSR2 with PDF1, is conserved in PITG_23036 WY1-LWY2 (Figure 5.10B).

To further explore the function of LWY effector PITG_23036 in planta, Dr. Hui Li generated PITG_23036-Turbo-YFP *A. thaliana* transgenic lines and screened three independent lines (lines 3, 15 and 31) (Figure 5.10C). Pathogenicity assays using *Phytophthora capsici* LT263 revealed enhanced disease development in all three PITG_23036 transgenic lines, comparable to PSR2 transgenic lines and significantly higher than wild-type *A. thaliana* and Turbo-YFP transgenic controls (Figure 5.10C).

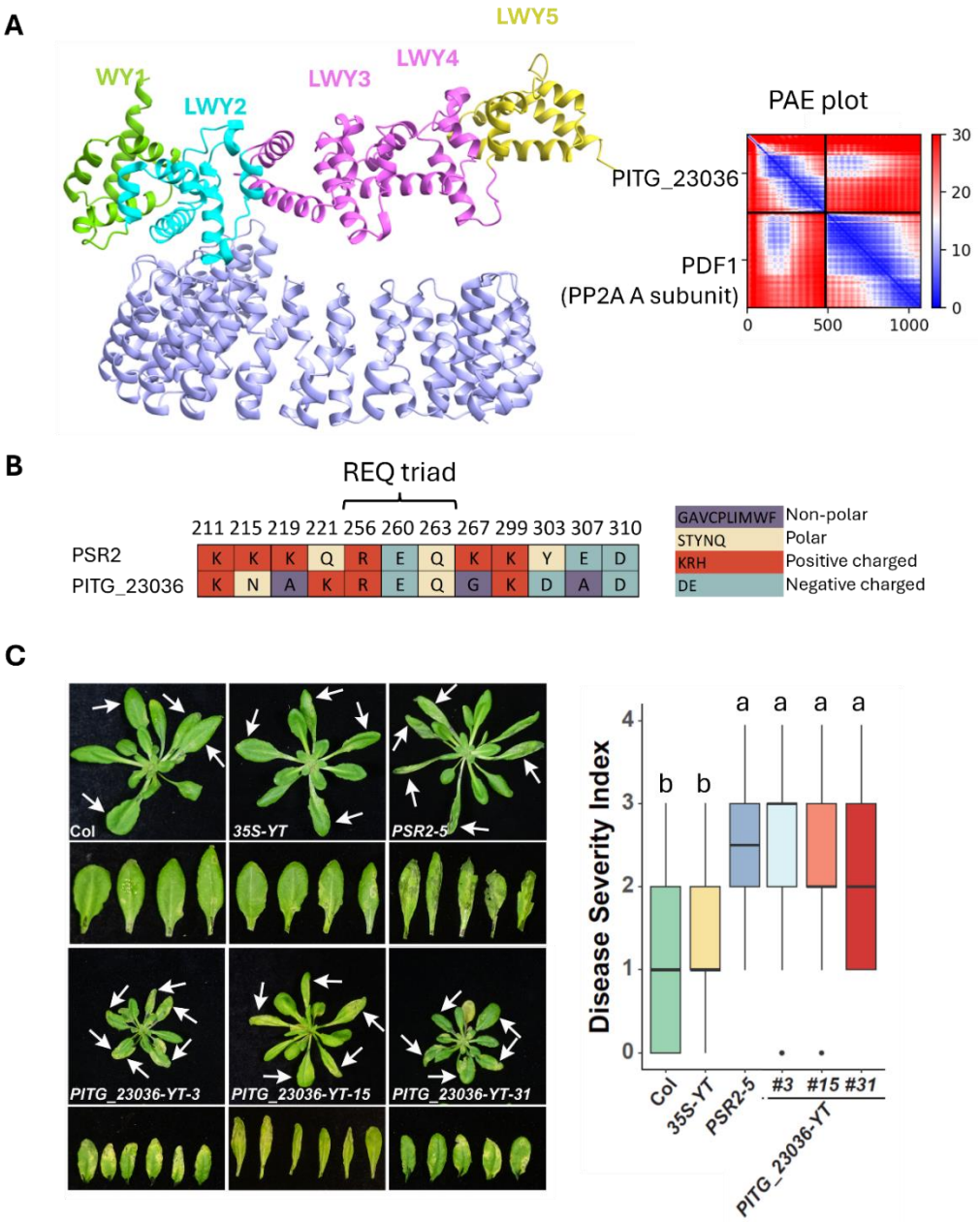

Figure 5.10 PITG_23036 promotes *P. capsici* infection on Arabidopsis.

(**A**) Predicted interaction interfaces between PITG_23036 and PDF1 generated using AlphaFold-multimer. The predicted aligned error (PAE) plot (right) indicates confidence levels of structural predictions. (L)WY units from distinct clusters are annotated within the PITG_23036 structure. (**B**) Sequence alignment comparing potential PP2A-interacting residues between PITG_23036 and PSR2, based on PSR2-PDF1 interaction. The REQ triad is highlighted, with amino acid polarity indicated for each position. (**C**) 4-week-old PITG_23036, PSR2 and YFP-Turbo transgenic Arabidopsis lines were infected by *P. capsici* LT263. Disease symptoms were recorded 3 days after inoculation with arrows indicating inoculated leaves.

5. 2. 4. 2 PITG_23036 and PsAvh145 encode PP2A-interacting pockets and the most similar 9_25 LWY module combination

To investigate potential additional PP2A-interacting pockets in PITG_23036, I analysed its (L)WY unit combinations. This analysis revealed a common module, designated as 9_25, located at the C-terminus of PITG_23036 (Figure 5.11). This 9_25 combination appears in 10 LWY effectors across five *Phytophthora* species. Phylogenetic analysis of the 9_25 modules from 10 LWY effectors revealed that a *P. sojae* LWY effector, PsAvh145, contains a 9_25 common module that's similar to that of PITG_23036 (Figure 5.11). Furthermore, three LWY effectors (indicated by red branches) share a common unit arrangement: PP2A-interacting pockets at their N-terminus (shown as red dashed units) and the 9_25 modular pair in their final two units (Figure 5.11). This similarity suggests these three effectors may form functional complexes that facilitate the colonization of respective host plants by different *Phytophthora* pathogens.

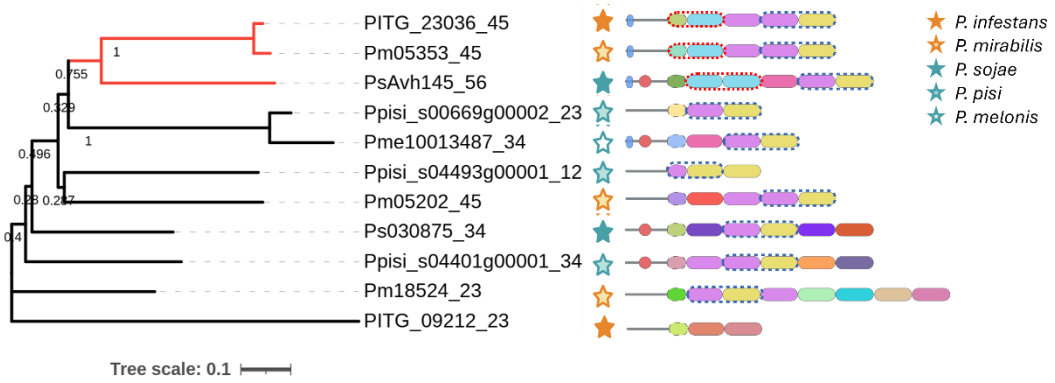

Figure 5.11 Phylogenetic analysis of surface-presented residues in 9_25-containing LWY effectors.

Neighbour-joining phylogenetic analysis derived from surface-accessible residues in 9_25 combinations. Red branches indicate LWY effectors with predicted PP2A-interacting pockets. Unit compositions are annotated for individual effectors. 9_25 combinations are highlighted by dashed frames in colour blue and organized by *Phytophthora* species. The PP2A-interacting modules were indicated in dashed red borders.

5. 2. 4. 3 Mass-spectrometry data for PITG_23036 transgenic Arabidopsis lines identified UBC5 and UBC6.

To identify the host interactors that PITG_23036 binds to promote disease, Dr. Hui Li performed the IP-MS of PITG_23036 using *p35S::PITG_23036* Arabidopsis transgenic lines. PP2A-interacting LWY interactors are showing a mosaic pattern of tandem repeats, which result in the regulation of distinct phosphoproteins by two PP2A-interacting LWY interactors PSR2 and PITG_15142 (H. Li et al. 2023). Therefore, PSR2 transgenic lines and YFP lines were included as controls to refine our target identification. Three independent biological repeats were included in the mass-spectrometry (Figure 5.12).

Mass spectrometry data analysis, visualized in a heatmap, revealed the presence of three PP2A A subunits and five PP2A C subunits in both PITG_23036 and PSR2 samples. This finding aligns with previous observations that PP2A-interacting effectors function by mimicking PP2A B subunits and hijacking PP2A core enzymes (A and C subunits). Notably, the PITG_23036 interactomes uniquely contained two ubiquitin-conjugating enzymes (UBCs or E2 ligases), suggesting that PITG_23036 may form a complex with these UBCs and PP2A core enzymes to execute its virulence function.

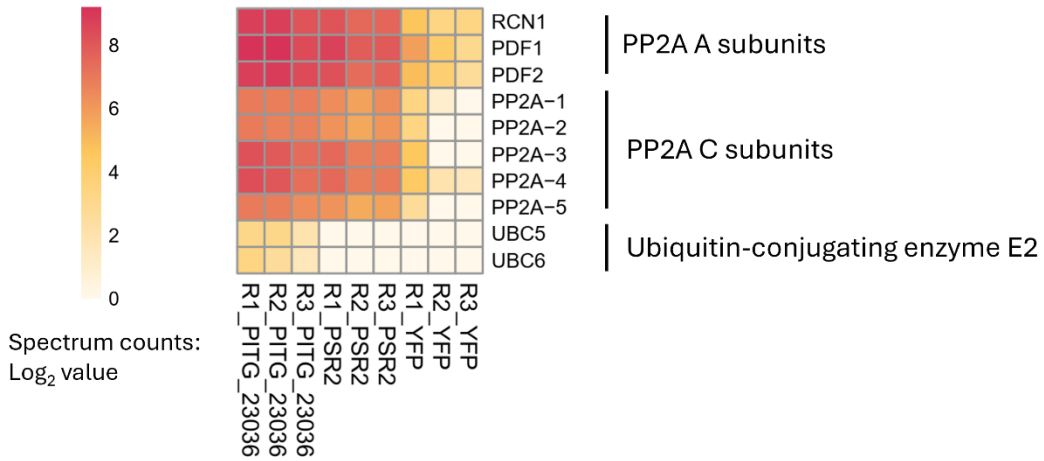

Figure 5.12 PITG_23036 associated with PP2A core enzymes and two UBC proteins.

The interaction profile heatmap depicts associations PITG_23036 and its interacting proteins, represented by log2-transformed spectrum counts.

5. 2. 4. 4 PITG_23036 interacts with UBC4, UBC5 and UBC6 through LWY5 in N. benthamiana.

Protein ubiquitination is orchestrated by three enzyme classes: E1, E2, and E3. E2 ligases serve as intermediaries, transferring ubiquitin from E1 to E3 ligases, which then facilitate the ubiquitination of downstream substrates. E1 and E2 ligases are normally quite conserved (Stewart et al. 2016). Plants normally have one to two E1 ligases, about forty E2 ligases and hundreds of E3 ligases. In *Arabidopsis thaliana*, the 37 E2 ligases are categorized into 16 subclades (Turek et al. 2018). UBC4, UBC5, and UBC6 belong to clade IV, suggesting functional redundancy in their E3 ligase pairing and substrate regulation (Turek et al. 2018). Based on this relationship, I selected these three UBC proteins from *A. thaliana* for further investigation.

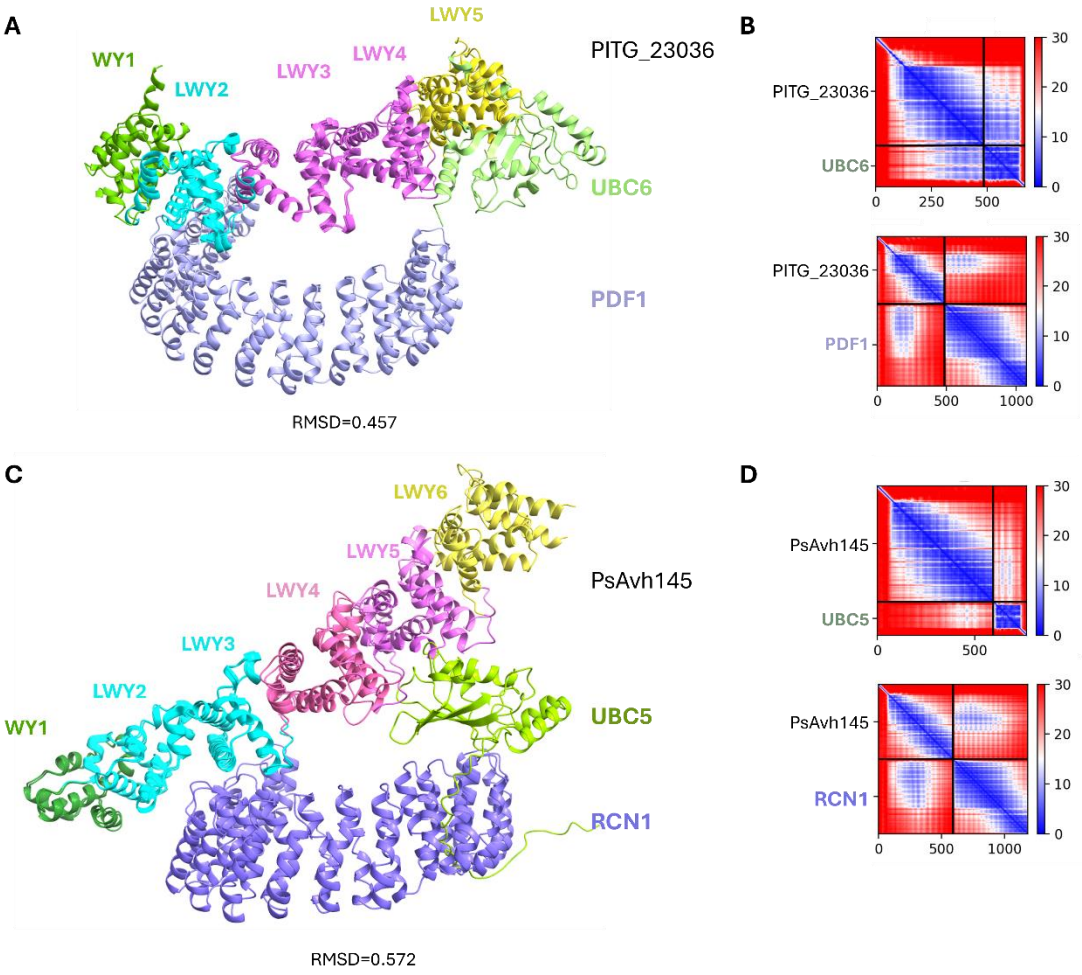

Figure 5.13 AlphaFold-multimer prediction of PITG_23036 with and PsAvh145 with two E2 ligases and PP2A A subunits.

(**A**) and (**C**) Structural models showing the superimposed predicted binding interfaces between effector-UBC and effector-PP2A A subunit complexes. (**B**) and (**D**) Confidence assessment of protein complex predictions using predicted aligned error (PAE) plots, with blue colouring indicating regions of high prediction confidence (low error values).

To validate the predicted interactions between PITG_23036/PsAvh145 and UBC4/5/6, as well as their ability to form complexes with PP2A A subunits, I conducted co-immunoprecipitation (co-IP) by co-expression of each LWY effector together with three UBCs. Based on the prediction that LWY4-LWY5 in PITG_23036 mediates its interaction with UBC6, I generated truncated versions of PITG_23036 (ΔLWY5 and ΔLWY4-LWY5) to evaluate their contribution to host target interactions. The effectors and their mutants were GFP-tagged, while UBCs were tagged with mCherry. PP2A A subunit recruitment was detected using PP2A antibody in both input and co-IP samples.

PITG_23036 showed strong interaction with AtUBC4 after IP, while efficiently enriching PP2A A subunits in the PITG_23036-GFP pull-down samples (Figure 5.14A). This suggests the formation of a complex containing PITG_23036, PP2A A subunit, and AtUBC4. Deletion of either LWY5 or LWY4-LWY5 abolished the interaction with AtUBC4, indicating LWY5 is crucial for UBC4 binding. Notably, while PITG_23036$^{\triangle 5}$ maintained PP2A A subunit recruitment, PITG_23036$^{\triangle 45}$ lost this ability, demonstrating that the LWY4-LWY5 module is essential for forming the complete protein complex with both PP2A A subunits and UBC4 (Figure 5.14A). PsAvh145, when co-expressed with AtUBC4, showed no interaction with AtUBC4 and only weak interaction with PP2A A subunits (Figure 5.14A).

PITG_23036 also demonstrated LWY5-dependent interactions with AtUBC5 and AtUBC6, suggesting that all three UBCs are likely to interact with similar interfaces in PITG_23036 (Figures 5.14B and 5.14C). The requirement of both LWY4 and LWY5 for PP2A A subunit recruitment remained consistent across all three UBC co-infiltration experiments, confirming PITG_23036's ability to form complexes with PP2A A subunits and all three UBCs. PsAvh145 exhibited weak interaction with AtUBC5, comparable to the level observed with PITG_23036$^{\triangle 45}$ (Figure 5.14B), likely due to its specificity for soybean rather than *A. thaliana* proteins. No interaction was detected between PsAvh145 and UBC6 (Figure 5.14C).

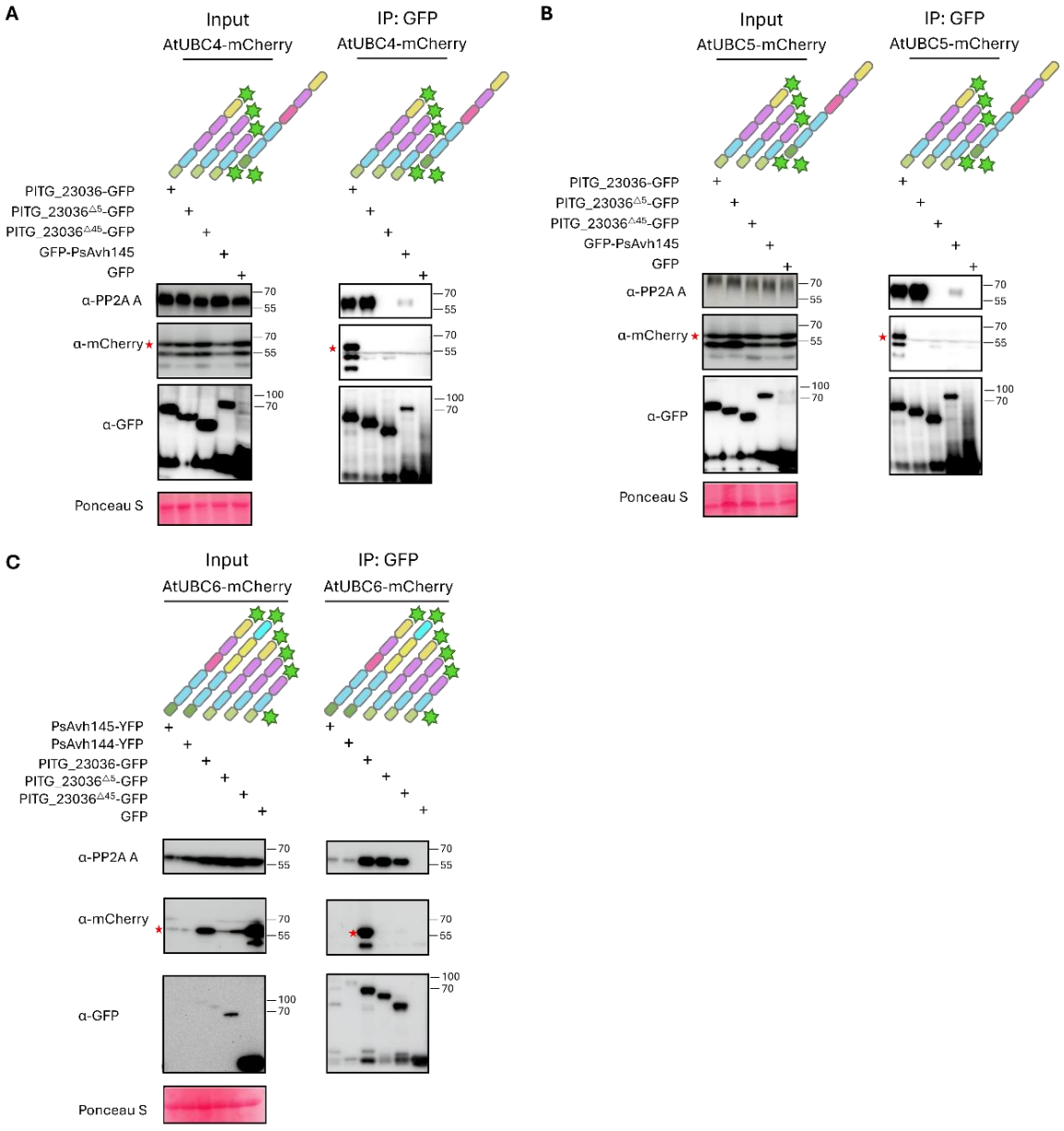

Figure 5.14 PITG_23036 interacts with UBC4, UBC5 and UBC6 through LWY5 in *N. benthamiana*.

(**A**-**C**) Co-immunoprecipitation assay showing interaction between UBC4 (**A**), UBC5 (**B**) and UBC6 (**C**) with PITG_23036, PITG_23036△5, PITG_23036△45, PsAvh145, PsAvh144 and GFP (negative control) in *N. benthamaiana*. The modular patterns were indicated above each sample. Total proteins were extracted from leaves harvested 2 days after agroinfiltration. Protein interactions were analysed by immunoprecipitation (IP) using anti-GFP agarose beads. Input (total protein extracts) and IP (pulled-down proteins) samples were immunoblotted with specific antibodies: anti-PP2A A to detect *N. benthamiana* PP2A A subunit, anti-mCherry for UBC proteins, and anti-GFP for LWY

effectors. Expected protein bands are marked with asterisks to distinguish them from non-specific signals. Ponceau S staining served as the protein loading control. The experiment was performed in three independent biological replicates.

5. 2. 4. 5 Conservations in binding interfaces of PITG_23036 with UBC4, UBC5 and UBC6 and phosphorylation sites

To investigate whether three UBCs interact with PITG_23036 in a conserved manner, seven key interacting residues were identified in UBC6 based on interaction distances of less than 4 Angstroms. These residues were also present in UBC4 and UBC5 (indicated by asterisks in black) (Figure 5.15A). Furthermore, two functionally critical residues reported by (Wu et al. 2003) are also common to E2 ligases: a cysteine residue that serves as the catalytic active site, and an upstream asparagine that stabilizes the E2 structure (marked with asterisks in red) (Figure 5.15A).

The structural alignment of the three UBCs revealed high conservation in their overall architecture. The PITG_23036 interacting residues reside in the one α-helix of three UBCs (Figure 5.15B), suggesting that three UBCs interact with PITG_23036 in the same manner. The catalytic residue cysteine and an asparagine residue for E2 structure stabilization are labelled in red.

A key question that emerged was the biological significance of PITG_23036 ability to recruit both PP2A core enzymes and E2 ligases. One hypothesis suggests that the three E2s serve as substrates for the PITG_23036-PP2A holoenzyme complex, which regulates downstream signalling through substrate dephosphorylation. To test this hypothesis, I searched for phosphorylation evidence of the three E2s in the Eukaryotic Phosphorylation Sites Database (EPSD), which catalogs experimentally identified phospho-peptides. AtUBC4 appeared in two phospho-proteomics studies: one examining wild-type and abscisic acid (ABA)-treated seedlings, and another comparing wild-type and G-protein deficient Arabidopsis root samples (G. Song et al. 2018; P. Wang et al. 2013). These studies identified five potential phosphorylation sites (157S, 158S, 163S, 167Y, and 169S) in EPSD, all with phospho-probability scores exceeding 0.5 (Figure 5.15C). These five phospho-sites are all labelled in Figure 5.15B.

To investigate whether phosphorylation represents a conserved regulatory mechanism across the three E2s and their orthologs in different host species, I conducted a comparative sequence analysis of phospho-sites found in the aforementioned studies (Figure 5.15C). Phylogenetic analysis of *A. thaliana* UBC4, UBC5 and UBC6 orthologs in *Glycine max* (soybean), *N. benthamiana* and *Solanum lycopersicum* (tomato) revealed several patterns (Figure 5.15C). *G. max* showed general

duplication of all three UBCs. UBC4 and UBC5 orthologs in these four plant species are closer related than UBC6. Most of the UBC4 and UBC5 orthologs displayed identical phosphorylation sites, with one *G. max* gene being the exception (Figure 5.15C). In contrast, AtUBC6 and SlUBC6 showed less conservation of phosphorylation sites. These sites in *A. thaliana* UBCs are distributed in the C terminal disorder region (Figure 5.15B). This suggests that UBC4 and UBC5 are more likely to function as substrates of PITG_23036-PP2A holoenzyme while residue divergence in UBC6 implies a less conserved pattern for being dephosphorylated at analysed five sites.

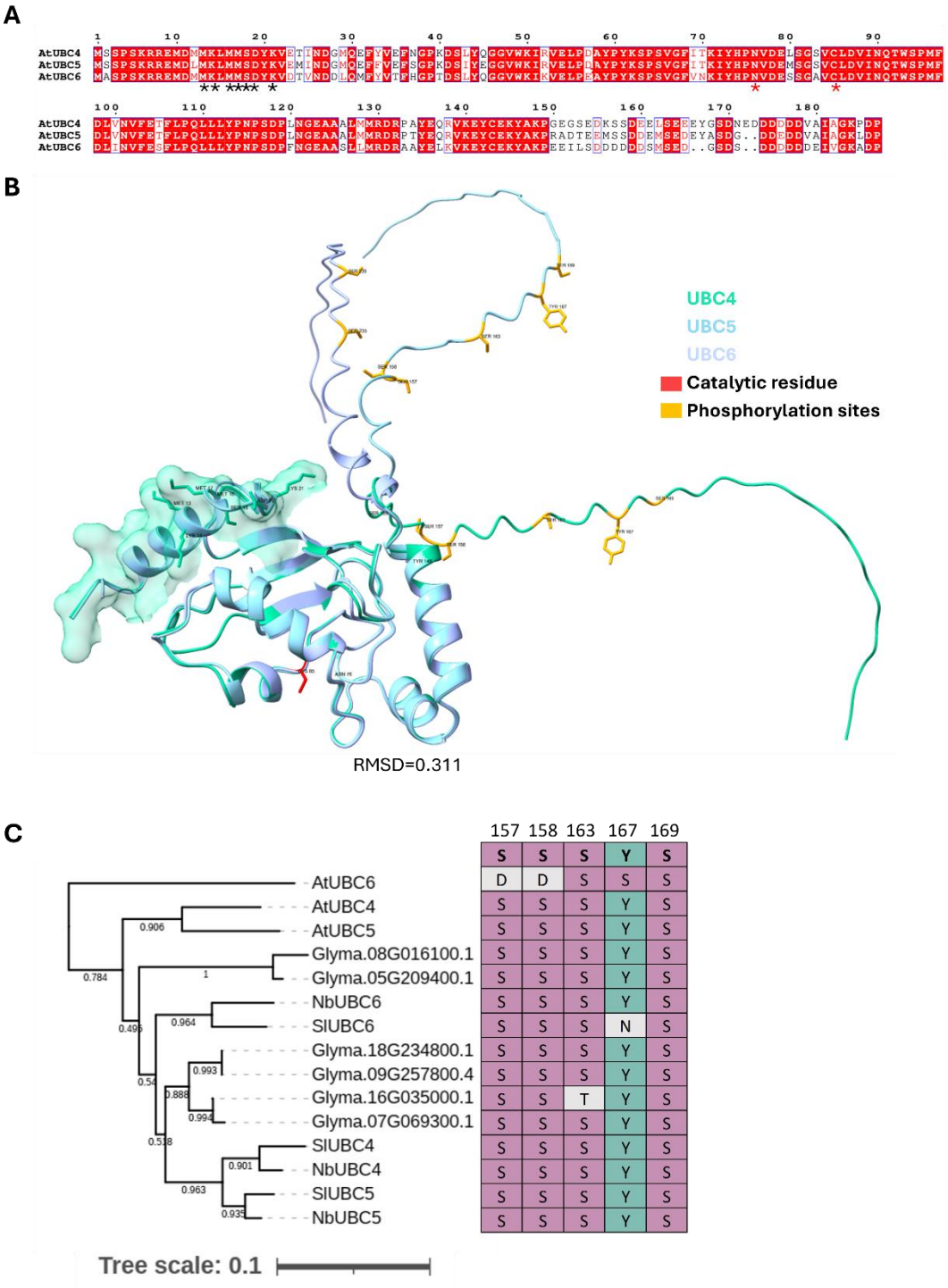

Figure 5.15 Conservations in binding interfaces of PITG_23036 with UBC4, UBC5 and UBC6 and phosphorylation sites.

(**A**) Protein sequence alignment of UBC4, UBC5 and UBC6. Predicted binding residues with PITG_23036 in confidence were labelled in black asterisks. The first red asterisk is an important asparagine residue, and the second one is the conserved catalytic cysteine residues in E2 ligases. (**B**) Super-imposition of three UBC predicted structures, with the PITG_23036 binding interface labelled in transparent surfaces, a catalytic residue in red

and potential phosphorylated sites in orange. (**C**) The orthologs of three UBCs were searched in another three plant species *Glycine max* (soybean), *N. benthamiana* and *Solanum lycopersicum* (tomato). The conservation of five phosphorylation sites was indicated by the same colours.

5. 2. 4. 6 LWY4-LWY5 contributes to PITG_23036 promoted P. infestans infection on N. benthamiana.

Previous research has established that interaction with PP2A A subunits is crucial for pathogen-promoted infection. PITG_23036 as a PP2A-interacting effector, enhances *Phytophthora capsici* infection in *A. thaliana*, indicating its importance as a virulence factor in *Phytophthora* host colonization. Our earlier experiments confirmed that the newly identified common module 9_25, located in the last two units, is essential for interactions with both E2 ligases and PP2A A subunits.

To evaluate whether the interactions with UBC proteins are also critical for PITG_23036 virulence, I conducted infection assays to inoculate *P. infestans* on *N. benthamiana* leaves. I tested the full-length PITG_23036, its mutant variants, and GFP as a negative control, with each construct independently infiltrated into *N. benthamiana* leaves (Figure 5.16).

The results demonstrated that PITG_23036 enhanced *P. infestans* infection after 6 days post-infection (dpi). PITG_23036△5 mutant showed partial, though not statistically significant, attenuation of disease development, suggesting that interference with UBC4/5/6 contributes partially to virulence (Figure 5.16). However, mutation of both LWY4-LWY5 completely abolished *P. infestans* virulence, demonstrating that the 9_25 combination represents an essential functional module for PITG_23036 virulence.

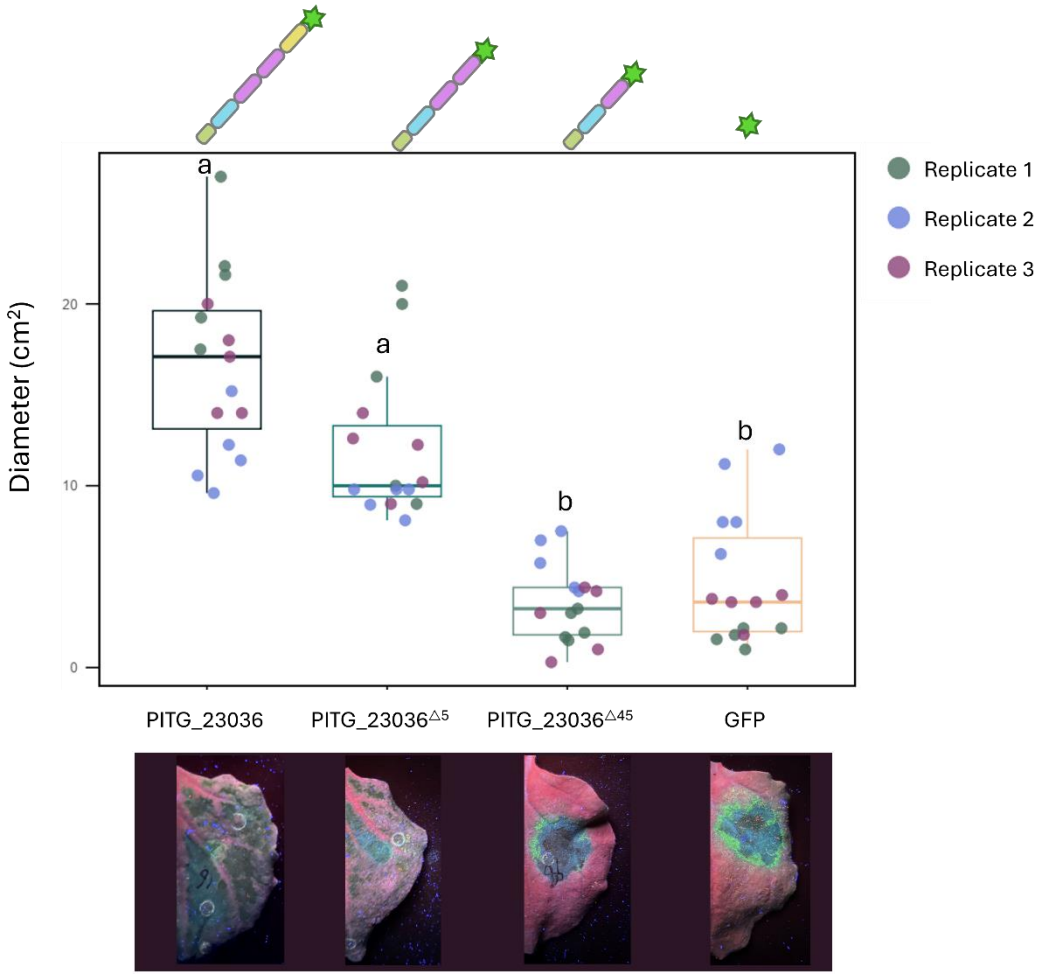

Figure 5.16 LWY4-LWY5 contributes to PITG_23036 promoted *P. infestans* infection in *N. benthamiana*.

PITG_23036, PITG_23036$^{\triangle 5}$, PITG_23036$^{\triangle 45}$, and GFP (negative control) were transiently expressed in *N. benthamiana*. Leave samples were taken 2 days after *P. infestans* zoospore inoculation. The pictures of lesion sizes were recorded at 6 dpi. Three independent replicates were included in this assay.

5.3 Methods

5.3.1 Transcriptome analysis

As stated in Chapter 2, the transcriptomic data for *P. infestans* 1306 included two vegetative growth stages (Early rye and late rye) and three infection time points (1.5 dpi, 2.5 dpi and 4 dpi) (Ah-Fong et al. 2017). To enhance comparative analysis, transcriptomic data from an additional *P. infestans* isolate (3928A) was incorporated. Expression patterns of target effectors were visualized using heatmaps, with values transformed to $\log_{10}$ scale of Counts Per Million (CPM) or Fragments Per Kilobase Million (FPKM). Hierarchical clustering was performed based on similarities in expression patterns.

5.3.2 Gene clone and vector construction

All the *P. infestans* LWY effectors for IP-MS in *N. benthamiana* were cloned and constructed into Level 0 module into binary vector pICSL86977OD with 35S promoter. Each LWY effectors were tagged C terminal GFP (green fluorescent protein). Constructs used in this study are listed in Table S2.

5.3.3 Agro-infiltration and protein expression

The vectors are transformed into Agrobacterium. Total proteins were extracted from *N. benthamiana* leaves 2 days after agroinfiltration of GFP (control). Proteins were enriched using GFP_Trap_A beads, with a minimum of two replicates for each LWY effector. In-gel trypsin digestion for immunoprecipitation mass spectrometry (IP-MS) was performed as described in Chapter 4.

5.3.4 Mass spectrometry data processing

Raw mass spectrometry data were processed using MS Convert to extract peptide information. Peptide identification was performed using Mascot server 2.4.1, searching against the *Nicotiana benthamiana* genome database with annotated contaminants. Protein identification was conducted using Scaffold 4.4.0 with the

following criteria: Peptide sequence confidence >95.0%; Protein confidence >99%; Mascot ion score >39; Minimum unique peptides per protein as 2.

For effector interacting network analysis, host proteins with valid peptides from at least one replicate were included to generate an interacting matrix for all 20 LWY effectors. To assess the specificity of host protein recruitment by LWY effectors containing common modules, I first performed cross-comparisons of interactomes among LWY effectors sharing common combinations. I then examined the presence of each identified host target across all LWY effector interactomes. Host protein specificity was visualized using heatmaps of log2-transformed spectrum counts.

5.3.5 Phospho-sites analysis

Phosphorylation sites in E2 ligases were identified through searches in the Eukaryotic Phosphorylation Sites Database (EPSD), which contains experimentally validated phosphorylation sites from 68 eukaryotic species (S. Lin et al. 2021a). Each potential phosphorylation site was assigned a localization probability (LP) score ranging from 0 to 1, indicating the confidence of phosphorylation prediction. LP scores were categorized into four classes: class I (>0.75), class II (≤0.75 and >0.5), class III (≤0.5 and ≥0.25) and class IV (<0.25).

5.3.6 *P. infestans* infection assay

PITG_23036-GFP, PITG_23036$^{\triangle 5}$-GFP, PITG_23036$^{\triangle 45}$-GFP and GFP (negative control) were transiently expressed on *N. benthamiana*. After two days of agro infiltration, detached leaves were challenged with *P. infestans* isolate 88069. For the infection, 20 µL droplets of *P. infestans* zoospore solution (100,000 zoospores/mL) were placed on the detached leaves. Disease progression was monitored by measuring lesion diameters (cm^2) and documenting with photographs at 6 days post-infection (6 dpi).

5.4 Discussion

In this study, I aim to investigate two aspects of *Phytophthora* LWY effector modularity: First, whether common functional modules within these effectors facilitate interactions with common host proteins. Second, the potential for effectors containing multiple functional modules to develop new functions through the formation of protein complexes with distinct host targets.

Our analysis focused on 20 *P. infestans* LWY effectors containing diverse common modules to identify host interactors in *N. benthamiana*. The comparative comparison of interacting proteins in LWY effectors suggests effectors with five common modules shared common interactors listed as PP2A-interacting pockets (positive control), 16_16 (two effectors associate with NbTOL9), 9_5 (interacting with Myosin XI), 16_6 (two effectors bound to Histone deacetylases) and 9_25 (in association with UBCs).

Notably, 9_25 together with PP2A-interacting pocket were found commonly present in three LWY effectors: PITG_23036, PsAvh145 and Pm05353. Correspondingly, the comparative interactomes from two PP2A-interacting effectors PITG_23036 and PSR2 suggested a common presence of PP2A core enzyme (PP2A scaffolding and catalytic subunits) and specific interactors as two E2 ligases exclusively recruited by PITG_23036, suggesting the dynamic protein complexes formation despite sharing the PP2A core enzyme interaction in these two effectors. Co-immunoprecipitation experiments demonstrated PITG_23036 forming complexes with host PP2A A subunits and three UBCs. Deletion of the 9_25 module significantly reduced both the recruitment of PP2A A subunits and UBC proteins and PITG_23036 virulence function, establishing 9_25 as a crucial functional module.

This research highlights the potential of mass spectrometry cross-comparison for identifying functional modules among LWY effectors with common module combinations. The study demonstrates how different combinations of multiple functional modules in LWY effectors can promote interactions with distinct host proteins, forming varied protein complexes, as exemplified by PITG_23036 interactions with PP2A A subunits and UBCs (Figure 5.17). These findings emphasize that the shuffling of functional LWY modules facilitates effector association with specific host

targets in distinct protein complexes, thereby driving the evolution of novel functions to enhance disease progression in effector repertoires.

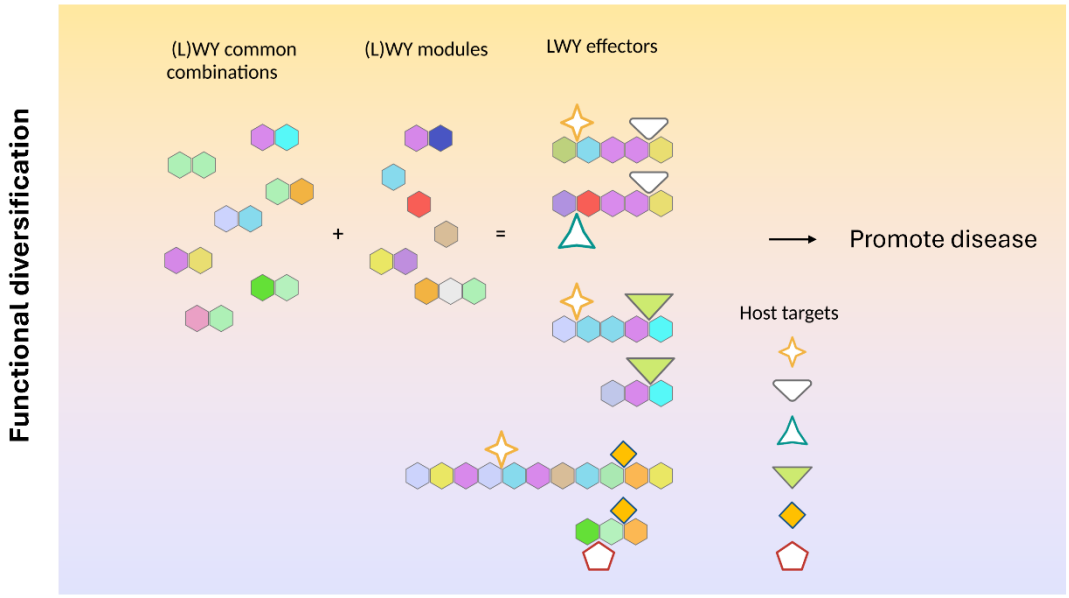

Figure 5.17 Model: different combinations of functional modules drive functional diversification of (L)WY effectors.

In Chapter 3, 45 enriched combinations of two-unit pairs were identified as potential functional modules. The present chapter extends this analysis by comparing LWY effector interactomes based on the presence of common modules. The 16_16 modules emerged as the most enriched combination, present in seven selected LWY effectors for interactome characterization. Among these, AVRcap1b is known to suppress the NRC network through interaction with NbTOL9. Notably, PITG_16726, which contains a highly similar 16_16 combination, also showed interaction with NbTOL9. However, the tested five *P. infestans* LWY effectors containing 16_16 unit combination did not show NbTOL9 association in their interactomes, indicating substantial sequence divergence within the same unit combination.

This pattern of functional divergence within shared combinations parallels observations in PP2A-interacting effectors. While the 18_18 combination is considered the primary PP2A-interacting pocket, not all effectors use this combination for PP2A interaction. For example, PITG_15142 interacts with PDF1 (PP2A A subunit) through its 23_18 combination, despite also containing the 18_18 combination.

Our findings suggest two critical directions for future research. First, validating how LWY effectors with shared combinations from the same clades target host proteins would enhance our interpretation of the mass spectrometry data. This validation would better characterize conserved modules across *Phytophthora* species. The PSR2-PDF1 interaction illustrates this concept, where three key residues REQ proved essential for the interaction. The identification of common modules thus provides a powerful approach to discovering key residues within these structurally conserved folds.

Second, our analysis of *P. infestans* LWY effectors likely captures only a subset of common modules, as some functional modules may be underrepresented in *P. infestans*. A more comprehensive understanding of these interactions, particularly those involving conserved host proteins like PP2A, requires a broader characterization of LWY effector functional modules across a wider range of *Phytophthora* species.

In our current mass-spec data, numerous effectors were showing diverse patterns of associations with PP2A A, B and C subunits. PITG_15038 was reported with PP2A activity in a previous study (H. Li et al. 2023). In our data here, PITG_15038 showed an association with PP2A scaffolding A, regulatory B and catalytic C subunit. The experimental observation that PITG_15038 retains PP2A-holoenzyme activity when transiently expressed in plants suggests it may inefficiently compete with host PP2A B subunits.

PITG_15114 exhibited interactions with PP2A A and C subunits, a pattern consistent with PSR2 and PITG_15142 interactomes, suggesting its role in B subunit mimicry, as reported in many PP2A-interacting effectors. PITG_10116 and PITG_23035 showed exclusive interaction with the PP2A A subunit. PITG_10116, containing one predicted common module, associates with E3 ligase KEG, suggesting potential targeting of PP2A A subunit for degradation. PITG_23035 might function by sequestering PP2A A subunits or blocking binding sites for B and C subunits.

Notably, both PITG_23035 and PITG_04388 contain 16_6 common modules and interact with host histone deacetylases. In mammalian systems, histone deacetylase 5 (HDAC5) was reported to directly interact and deacetylate PP2A C subunit and inactivate PP2A activity (Xu et al. 2021). So, it's likely that PITG_23035 might lock PP2A in an inactive state. PITG_04388 shows a unique interaction pattern, recruiting B and C subunits without A subunit association, potentially functioning as a PP2A inhibitor through mechanisms distinct from PITG_23035.

These findings demonstrate that mosaic module combinations in PP2A-interacting effectors enable recruitment of different host proteins and interaction with various PP2A subunits, suggesting diverse evolutionary strategies for PP2A activity manipulation. This evolution of LWY effector toward PP2A binding, while maintaining diverse targeting capabilities, suggests that PP2A modulation represents a crucial pathogen strategy for robust *Phytophthora* infection. Further experimental validation is needed to confirm these hypothesized mechanisms of effector function through interactions with various PP2A subunits and other host targets.

E2 ubiquitin-conjugating enzymes undergo various forms of regulatory control, including phosphorylation, which affects their ubiquitin charging capacity, E3 ligase activation for ubiquitin transfer, and selective E2-E3 pairing (Chrustowicz et al. 2024; Coccetti et al. 2008; Sarcevic et al. 2002). Phosphorylation is reversible through phosphatase activity. In this study, I propose that three E2 ligases (UBC4, UBC5, and UBC6) may serve as substrates for the effector-PP2A holoenzyme complex, potentially undergoing dephosphorylation.

Among them, UBC5 was reported to couple with plant U-box protein 13 (PUB13) and PUB22, two E3 ligases contributing the regulation of drought stress, flowering time, plant hormone signalling and immune signalling (Chrustowicz et al. 2024; Furlan et al. 2017; Jacobs et al. 2011; L. Kong et al. 2015; W. Li et al. 2012; Liao et al. 2017; Stegmann et al. 2012; Trujillo et al. 2008; Zhou et al. 2018). UBC6 has been identified to interact with transcription repressors MYB7 and MYB32, directly mediating their degradation and thereby regulating secondary cell wall (SCW) thickening, although the specific E3 ligases involved remain unidentified (Q. Wang et al. 2023b).

The dephosphorylation of E2 ligases can affect E2 protein stability or specific E2-E3 pairing (Chang et al. 2011; Chrustowicz et al. 2024). Therefore, it's likely that the dephosphorylation of these UBCs is likely to stabilize UBC proteins or selective pairing with E3 ligases to regulate downstream signalling pathways. Further investigation using dephosphorylation assays to compare UBC activity or protein stability in the presence and absence of effectors will be necessary to test this hypothesis.

This study demonstrates that LWY effectors contain common unit combinations that enable them to target common host proteins. Through analysis of PITG_23036, we provide evidence that these common modules likely represent functional modules. Shuffling of these multiple functional modules can thereby facilitate the association of

different host proteins into protein complexes, hence promoting the fast evolution of effector neo-functionality and evolutionary adaptability.

5.5 Contributions to research

I extend my gratitude to Dr. Hui Li for his substantial contributions to this work. His efforts included generating PITG_23036 transgenic Arabidopsis lines, conducting pathogen infection assays on these lines, and performing mass spectrometry analyses of PITG_23036 interactomes.

5.6 Reference

Ah-Fong, A. M. V., Shrivastava, J., and Judelson, H. S. (2017), 'Lifestyle, gene gain and loss, and transcriptional remodeling cause divergence in the transcriptomes of Phytophthora infestans and Pythium ultimum during potato tuber colonization', *BMC Genomics,* 18 (1), 764.

Bialas, A., et al. (2021), 'Two NLR immune receptors acquired high-affinity binding to a fungal effector through convergent evolution of their integrated domain', *Elife,* 10.

Boutemy, L. S., et al. (2011), 'Structures of Phytophthora RXLR effector proteins: a conserved but adaptable fold underpins functional diversity', *J Biol Chem,* 286 (41), 35834-42.

Cao, Y., et al. (2023), 'Structural polymorphisms within a common powdery mildew effector scaffold as a driver of coevolution with cereal immune receptors', *Proc Natl Acad Sci U S A,* 120 (32), e2307604120.

Chang, S. W., et al. (2011), 'NRIP, a novel calmodulin binding protein, activates calcineurin to dephosphorylate human papillomavirus E2 protein', *J Virol,* 85 (13), 6750-63.

Chou, S., et al. (2011), 'Hyaloperonospora arabidopsidis ATR1 effector is a repeat protein with distributed recognition surfaces', *Proc Natl Acad Sci U S A,* 108 (32), 13323-8.

Chrustowicz, J., et al. (2024), 'Multisite phosphorylation dictates selective E2-E3 pairing as revealed by Ubc8/UBE2H-GID/CTLH assemblies', *Mol Cell,* 84 (2), 293-308 e14.

Coccetti, P., et al. (2008), 'The CK2 phosphorylation of catalytic domain of Cdc34 modulates its activity at the G1 to S transition in Saccharomyces cerevisiae', *Cell Cycle,* 7 (10), 1391-401.

De la Concepcion, J. C., et al. (2018), 'Polymorphic residues in rice NLRs expand binding and response to effectors of the blast pathogen', *Nat Plants,* 4 (8), 576-85.

Derevnina, L., et al. (2021), 'Plant pathogens convergently evolved to counteract redundant nodes of an NLR immune receptor network', *PLoS Biol,* 19 (8), e3001136.

Franceschetti, M., et al. (2017), 'Effectors of Filamentous Plant Pathogens: Commonalities amid Diversity', *Microbiol Mol Biol Rev,* 81 (2).

Furlan, G., et al. (2017), 'Changes in PUB22 Ubiquitination Modes Triggered by MITOGEN-ACTIVATED PROTEIN KINASE3 Dampen the Immune Response', *Plant Cell,* 29 (4), 726-45.

Guo, B., et al. (2019), 'Phytophthora sojae Effector PsAvh240 Inhibits Host Aspartic Protease Secretion to Promote Infection', *Mol Plant,* 12 (4), 552-64.

Guo, L., et al. (2018), 'Specific recognition of two MAX effectors by integrated HMA domains in plant immune receptors involves distinct binding surfaces', *Proc Natl Acad Sci U S A,* 115 (45), 11637-42.

He, J., et al. (2019), 'Structural analysis of Phytophthora suppressor of RNA silencing 2 (PSR2) reveals a conserved modular fold contributing to virulence', *Proc Natl Acad Sci U S A,* 116 (16), 8054-59.

Hou, Y., et al. (2019), 'A Phytophthora Effector Suppresses Trans-Kingdom RNAi to Promote Disease Susceptibility', *Cell Host Microbe,* 25 (1), 153-65 e5.
Jacobs, S., et al. (2011), 'Broad-spectrum suppression of innate immunity is required for colonization of Arabidopsis roots by the fungus Piriformospora indica', *Plant Physiol,* 156 (2), 726-40.
Kong, L., et al. (2015), 'Degradation of the ABA co-receptor ABI1 by PUB12/13 U-box E3 ligases', *Nat Commun,* 6, 8630.
Li, H., et al. (2023), 'Pathogen protein modularity enables elaborate mimicry of a host phosphatase', *Cell,* 186 (15), 3196-207 e17.
Li, W., et al. (2012), 'The U-Box/ARM E3 ligase PUB13 regulates cell death, defense, and flowering time in Arabidopsis', *Plant Physiol,* 159 (1), 239-50.
Liao, D., et al. (2017), 'Arabidopsis E3 ubiquitin ligase PLANT U-BOX13 (PUB13) regulates chitin receptor LYSIN MOTIF RECEPTOR KINASE5 (LYK5) protein abundance', *New Phytol,* 214 (4), 1646-56.
Lin, S., et al. (2021), 'EPSD: a well-annotated data resource of protein phosphorylation sites in eukaryotes', *Brief Bioinform,* 22 (1), 298-307.
Lo Presti, L., et al. (2015), 'Fungal effectors and plant susceptibility', *Annu Rev Plant Biol,* 66, 513-45.
Lovelace, A. H., et al. (2023), 'Effector Identification in Plant Pathogens', *Phytopathology,* 113 (4), 637-50.
Maqbool, A., et al. (2016), 'Structural Basis of Host Autophagy-related Protein 8 (ATG8) Binding by the Irish Potato Famine Pathogen Effector Protein PexRD54', *J Biol Chem,* 291 (38), 20270-82.
McGowan, Jamie. and Fitzpatrick, David. A. (2017), 'Genomic, Network, and Phylogenetic Analysis of the Oomycete Effector Arsenal', *mSphere,* 2 (6).
Oome, S., et al. (2014), 'Nep1-like proteins from three kingdoms of life act as a microbe-associated molecular pattern in Arabidopsis', *Proc Natl Acad Sci U S A,* 111 (47), 16955-60.
Pennington, H. G., et al. (2019), 'The fungal ribonuclease-like effector protein CSEP0064/BEC1054 represses plant immunity and interferes with degradation of host ribosomal RNA', *PLoS Pathog,* 15 (3), e1007620.
Petre, B., et al. (2021), 'Host-interactor screens of Phytophthora infestans RXLR proteins reveal vesicle trafficking as a major effector-targeted process', *Plant Cell,* 33 (5), 1447-71.
Sanchez-Vallet, A., et al. (2013), 'Fungal effector Ecp6 outcompetes host immune receptor for chitin binding through intrachain LysM dimerization', *Elife,* 2, e00790.
Sarcevic, Boris., et al. (2002), 'Regulation of the ubiquitin-conjugating enzyme hHR6A by CDK-mediated phosphorylation', *The EMBO Journal,* 21.
Seong, K. and Krasileva, K. V. (2023), 'Prediction of effector protein structures from fungal phytopathogens enables evolutionary analyses', *Nat Microbiol,* 8 (1), 174-87.
Song, G., et al. (2018), 'Heterotrimeric G-Protein-Dependent Proteome and Phosphoproteome in Unstimulated Arabidopsis Roots', *Proteomics,* 18 (24), e1800323.

Stegmann, M., et al. (2012), 'The ubiquitin ligase PUB22 targets a subunit of the exocyst complex required for PAMP-triggered responses in Arabidopsis', *Plant Cell,* 24 (11), 4703-16.
Stewart, M. D., et al. (2016), 'E2 enzymes: more than just middle men', *Cell Res,* 26 (4), 423-40.
Tian, H., et al. (2022), 'Fungal dual-domain LysM effectors undergo chitin-induced intermolecular, and not intramolecular, dimerization', *Plant Physiol,* 190 (3), 2033-44.
Trujillo, M., et al. (2008), 'Negative regulation of PAMP-triggered immunity by an E3 ubiquitin ligase triplet in Arabidopsis', *Curr Biol,* 18 (18), 1396-401.
Turek, I., et al. (2018), 'Multi-tiered pairing selectivity between E2 ubiquitin-conjugating enzymes and E3 ligases', *J Biol Chem,* 293 (42), 16324-36.
Wang, P., et al. (2013), 'Quantitative phosphoproteomics identifies SnRK2 protein kinase substrates and reveals the effectors of abscisic acid action', *Proc Natl Acad Sci U S A,* 110 (27), 11205-10.
Wang, Q., et al. (2023), 'UBC6, a ubiquitin-conjugating enzyme, participates in secondary cell wall thickening in the inflorescence stem of Arabidopsis', *Plant Physiol Biochem,* 205, 108152.
Wu, Pei-Ying., et al. (2003), 'A conserved catalytic residue in the ubiquitin-conjugating enzyme family', *The EMBO Journal,* 22.
Xu, C., et al. (2021), 'Histone deacetylase 5 deacetylates the phosphatase PP2A for positively regulating NF-kappaB signaling', *J Biol Chem,* 297 (6), 101380.
Yu, D. S., et al. (2024), 'The structural repertoire of Fusarium oxysporum f. sp. lycopersici effectors revealed by experimental and computational studies', *Elife,* 12.
Zhou, J., et al. (2018), 'Regulation of Arabidopsis brassinosteroid receptor BRI1 endocytosis and degradation by plant U-box PUB12/PUB13-mediated ubiquitination', *Proc Natl Acad Sci U S A,* 115 (8), E1906-E15.

Chapter 6 General discussion

The solved crystal structures and structural modelling using AlphaFold enable the classification of sequence unrelated effectors into structural subfamilies, including the RNase-like proteins associated with haustoria (RALPH) effectors, *Magnaporthe oryzae* Avrs and ToxB (MAX) effectors, *Leptosphaeria* Avirulence and Suppressing (LARS) effectors, Fol dual-domain (FOLD) effectors and ToxA family (de Guillen et al. 2015; De la Concepcion et al. 2018; Di et al. 2017; Franceschetti et al. 2017; Lazar et al. 2022; Ortiz et al. 2017; Outram et al. 2022; Sarma et al. 2005; Seong and Krasileva 2021; Spanu 2017; Teulet et al. 2023). Despite significant advances implicated by structural biology on effector evolution, the mechanism of effector evolving diversified functions is still poorly understood.

In oomycetes, WY effectors or LWY effectors form similarly folded structural families. These (L)WY effectors display the format of WY1-(WY)n or WY1-(LWY)n architectures. Each WY or LWY motif forms a similar bundle with 3 a-helices or 5 a-helices (Boutemy et al. 2011; Chou et al. 2011; B. Guo et al. 2019; He et al. 2019; Lovelace et al. 2023; Maqbool et al. 2016). One *Phytophthora ramorum* subfamily, which is homologous to *P. infestans* WY effector PexRD2 protein family, was proposed to evolve from a single ancestral gene in the common ancestor of three *Phytophthora* species (*P. hibernalis*, *P. lateralis*, and *P. ramorum*) through recombination with clear breakpoints detected (Goss et al. 2013). This suggests that these (L)WY effectors might undergo recombination to evolve new combinations of tandem repeats. Therefore, we attempted to use (L)WY effectors as probes to understand effector evolution.

Two fundamental biological questions drive this research:

1. Can new combinations of LWY tandem repeats emerge through recombination events, and do these recombined proteins acquire novel functions distinct from their "parent" proteins?

2. If recombination serves as an evolutionary drive of (L)WY effector evolution, are functional modules conserved across multiple (L)WY effectors to facilitate common host protein recruitment?

In this thesis, I studied whether recombination could generate novel LWY unit combinations and develop new functions by identifying a recombination event between PITG_10347 and PmRxLR1 that leads to different host protein interactions. Additionally, I demonstrated that more functional modules across LWY effectors, such as the 23_18 and 9_25 modules in PITG_23036, serve as an evolutionary strategy to target common host proteins like PP2A and UBCs for promoting virulence.

In Chapter 2, I analysed LWY effectors across five *Phytophthora* genomes, classifying them based on the presence of Signal Peptide (SP) and RxLR motifs. While 22-54% of LWYs contained both SP and RxLR motifs, a substantial portion lacked either or both components: 4-30% had SP without RxLR motifs, and 15-63% lacked SP and/or RxLR motifs. These LWY genes, regardless of encoding SP and RxLR motifs or not, physically co-localize to form multi-gene clusters. This suggests that these diverse LWY effectors may serve as a genetic reservoir for recombination to generate new module combinations in LWY effectors.

In Chapter 3, I analysed functional modules across five *Phytophthora* species. Using hierarchical clustering of exposed residues from (L)WY units, I combined the information of every two adjacent LWY units to indicate potential host protein binding interfaces around the groove of two units, which identified 45 combinations with 13 highly enriched in LWY effectors with SP and RxLR motifs, serving as a pool to identify potential functional modules. Importantly, 62 SP+RxLR LWY effectors contain two or more potential functional modules, suggesting the possibility for LWY effectors to form protein complexes with host targets recruited by multiple functional modules.

In Chapter 4, I leveraged my findings on the prediction of LWY repertoires to identify recombination analysis, where I identified a specific recombination event within gene clusters in *P. infestans* and *P. mirabilis*. Through mass spectrometry analysis, I discovered both common and specific interactors between the recombination "parent" PITG_10347 and "child" PmRxLR1, while these interactions were absent in the PITG_10347 homolog Pm15069 (lacking the recombined unit). This study revealed that recombination events enable module shuffling in effector proteins, as demonstrated by PmRxLR1, which maintains interactions inherited from its parent PITG_10347 while acquiring the ability to interact with additional host proteins not targeted by PITG_10347. These PmRxLR1-specific interactions may be attributed to its four N-terminal units

which were inherited from another parent PITG_10341. This implies how module shuffling enables effectors to expand their host protein interaction network.

In my final investigation in Chapter 5, I examined two key aspects: whether common functional modules facilitate heteromeric interactions of LWY effectors and common host proteins, and if LWY effectors with multiple functional modules can develop new functions through forming protein complexes with distinct host targets. Through detailed analysis of PITG_23036, I discovered a key mechanistic insight into effector function, demonstrating how two different functional modules within an individual effector can coordinate the assembly of protein complexes through the simultaneous recruitment of different host proteins, specifically PP2A A subunits and UBCs.

Our research established a broader conceptual framework for understanding effector evolution, demonstrating that recombination can generate novel combinations to form diverse functional modules within LWY effectors. Through unit rearrangement, LWY effectors containing multiple functional modules can maintain interactions with their original protein targets while acquiring new interactions through their shuffled modules, enabling the formation of dynamic protein complexes and driving effector functional divergence. Such modularity-driven evolution of novel functionality serves as a fundamental mechanism that could enhance pathogen rapid adaptation to hosts, providing valuable insights on the evolutionary advantage of functional modules and shedding light on a rational framework for engineering durable disease resistance.

6.1 Surface-encoded specificity: How conserved effector folds achieve diverse functions.

With the advances of structural biology in effector biology, increasing cases of sequence-unrelated structural similar effectors are reported, assigning these virulence factors to different structural subfamilies. These effectors, while sharing structural foundations, often exhibit diverse functions by presenting specific residues on the protein surface during host-protein interactions.

The LWY effector family exemplifies this principle, with each effector comprising multiple (L)WY units that form 3-5 α-helical hydrophobic bundles. 12 residues reside in the groove the two adjacent (L)WY units contribute direct interaction to host PP2A core enzymes. Our research on LWY effectors further demonstrates two-unit can serve as functional modules to recruit other host proteins. Our experimental studies revealed that PITG_23036, an LWY effector containing five tandem units, exhibits dual interactions through distinct interaction surfaces. While the first two units engage with PP2A, the last two units specifically interact with E2 ligases through a distinct set of exposed residues. This finding demonstrates how different surfaces within the same structural scaffold can mediate distinct host-protein interactions. These structural units are therefore serving as functional units.

This phenomenon extends beyond LWY effectors to fungal pathogens. The Fol dual-domain (FOLD) effector family, comprising secreted in xylem (SIX) effector proteins, represents another class of structurally similar effectors with dual domains (Outram et al. 2021b; Outram et al. 2021a). FOLD-like structures appear across various plant pathogens and symbionts (D. S. Yu et al. 2024). A notable example is FonSIX4, a homolog of Avr1(SIX4) from *F. oxysporum* f. sp. *niveum* (*Fon*), which is recognized by the immunity receptor in moneymaker tomato cultivar through seven exposed residues in its C-domain (Catanzariti et al. 2017; D. S. Yu et al. 2024).

The MAX effector family provides another compelling example with the characteristic β-sandwich structures. Two MAX effectors, AVR1-CO39 and AVR-PikD, interact with heavy metal-associated (HMA) domains integrated into the immune receptors RGA5 and Pikp-1. Intriguingly, these effectors bind to opposite interfaces of the HMA domain (Cesari et al. 2013; Ortiz et al. 2017). Furthermore, Pikp1-HMA can

interact with an additional MAX effector, AVR-Pia, through distinct binding interfaces compared to AVR-PikD, contributing to partial resistance against *M. oryzae* infection (Varden et al. 2019).

The effector repertoire of *Blumeria graminis* demonstrates how host receptors can recognize pathogen proteins with high specificity despite structural conservation among effectors. Despite limited sequence similarity, multiple AVR effectors in this pathogen share the RALPH (RNase-like effector family) scaffold structure. Notably, different surfaces of these RALPH scaffolds are recognized by distinct CNL (coiled-coil) NLR immune receptors (Cao et al. 2023).

This recurring pattern of conserved structural scaffolds coupled with polymorphic binding surfaces appears to be a widespread evolutionary strategy among plant pathogens. By maintaining common structures while varying interaction interfaces, pathogens can evolve diverse host protein associations that enhance their adaptive fitness. This mechanistic insight suggests new approaches for engineering durable plant resistance, particularly through targeted modification of effector-binding interfaces or by engineering novel recognition specificities in plant immune receptors.

6.2 Engineering durable defence against *Phytophthora* infection.

Recent structural insights into effector-target complexes have created new opportunities for the rational design of disease-resistant plants. In particular, crystallography and structural modelling have revealed functional units within common effector folds, suggesting novel strategies for engineering durable resistance through precise modification of key interaction determinants.

Significant progress has been made in manipulating pathogen-host interactions through targeted modification of crucial binding surfaces. A breakthrough example is the engineering of novel recognition specificity in the RGA5 immune receptor. The RGA5-HMA domain recognizes the MAX effector AVR-pia but not AvrPib. Through strategic substitution of two residues critical for AVR-pia interaction, researchers created RGA5-HMA2, which inverted this specificity, enabling AvrPib recognition while abolishing AVR-pia binding. Importantly, transgenic rice expressing RGA5-HMA2 demonstrated functional resistance against *M. oryzae* strains carrying AvrPib (Liu et al. 2021).

Another example involves the *Mildew locus a 6* (*Mla6*) immune receptor, which recognizes the RALPH effector AVRA6 but not its family member CSEP0333. By integrating the central region of AVRA6 into CSEP0333, a successfully engineered CSEP0333 triggers MLA6-mediated immune responses, effectively converting a non-recognized effector into one that activates host immunity (Cao et al. 2023). These examples demonstrate how structural understanding of recognition specificity can be translated into functional disease resistance.

Site-directed mutagenesis can be effectively applied to engineer plant resistance against pathogens by modifying host proteins that are common targets of pathogen effectors. One example is the PP2A protein, which functions as a conserved host phosphatase targeted by thirteen different LWY effectors to facilitate pathogen infection. This widespread targeting makes PP2A an excellent candidate for engineering durable disease resistance.

Several strategic approaches can be implemented to modify PP2A functionality. First, mutations can be introduced into common effector binding sites on PP2A regulatory or scaffolding subunits, while maintaining the essential phosphatase activity and substrate recognition of the PP2A complex. Second, an inducible defense system

can be engineered wherein pathogen infection triggers the expression of decoy proteins that sequester effectors away from PP2A. This can be achieved by designing synthetic mini-binding domains that mimic natural targets but exhibit a higher binding affinity for LWY effectors. These binding domains can be further enhanced by integration with either proteasome-targeting domains to facilitate effector degradation or with Pikobody systems (Kourelis et al. 2023) to activate resistance responses against *Phytophthora* pathogens upon effector binding. These engineering strategies are broadly applicable and can be implemented to modify various host proteins that serve as targets for pathogen effectors.

Taken together, understanding the evolutionary dynamics of effector modularity provides valuable insights that can help predict effector functions and inform the development of more effective disease resistance strategies. This knowledge base continues to expand our capability to engineer durable plant immunity against pathogens.

6.3 Future perspectives

This thesis investigates the evolution of LWY effectors through recombination-based mechanisms and demonstrates that LWY effectors target host proteins through conserved mechanisms, wherein surface residues on functional modules determine binding specificity to host targets.

While significant progress has been made in understanding how LWY effectors evolve the ability to recruit different proteins through module shuffling, several critical questions remain unresolved. One fundamental question concerns PP2A, a crucial phosphatase: given the widespread occurrence of PP2A-targeting modules in pathogen effectors, what plant-evolved defence mechanisms might counteract these interactions? Specifically, do plants possess endogenous inhibitors that could prevent pathogen effectors from accessing PP2A regulatory subunits?

The interaction between PITG_23036 and host proteins raises important structural and functional questions. Having demonstrated the PP2A activity of PITG_23036 and its association with both the PP2A core enzyme and UBC4/5/6, we need to elucidate: (1) the structural basis of the PITG_23036-PP2A-UBC4/5/6 complex, (2) whether PITG_23036-PP2A holoenzymes dephosphorylate UBC4/5/6 at predicted phosphorylation sites, and (3) whether these UBCs functionally couple with known E3 ligases such as PUB13 and PUB22 to regulate plant immunity.

Additionally, the diverse interactions between LWY effectors and PP2A subunits needs further investigation. For instance, PITG_23035 and PITG_04388, while both containing 16_6 common modules and associating with host histone deacetylases, exhibit distinct PP2A interaction patterns. PITG_23035, with eleven tandem repeats, exclusively interacts with the PP2A A subunit, while PITG_04388, containing three repeats, associates with PP2A B and C subunits. This is particularly noteworthy given that in mammalian systems, histone deacetylase 5 (HDAC5) has been shown to inactivate PP2A through direct interaction and deacetylation of the PP2A C subunit (Xu et al. 2021). The unique interaction pattern in PITG_04388 by recruiting B and C subunits but not A subunit suggests it may function as a PP2A inhibitor through mechanisms distinct from PITG_23035, which might lock PP2A in an inactive state. These observations raise several questions: What are the distinct functions of these effectors?

How do their mechanisms differ from PP2A B-mimicking effectors? Do they have PP2A-independent functions?

A WY effector PsAvh240 forms a functional homodimer essential for suppressing GmAP1 secretion in soybean (B. Guo et al. 2019), which raises intriguing questions about the broader role of oligomerization in (L)WY effector function. The functional diversification (L)WY effectors may be achieved not only through (L)WY unit variation but also through the formation of various oligomeric states, either as homo-oligomers or potentially as hetero-oligomers with other (L)WY effectors.

A notable pattern emerging from our analyses is the prevalence of odd-numbered modules within LWY effectors. This consistent feature may have implications for host target binding or protein stability, etc. Understanding the distribution pattern of odd-numbered modules in LWY effectors could provide insights into host-pathogen coevolution and inform strategies for developing sustainable disease resistance in crops.

Furthermore, the observation that certain LWY effectors lacking SP are upregulated during infection raises questions about their potential regulatory roles in this process. These proteins might serve as modulators of endogenous cellular processes in *Phytophthora* species, adding another layer of complexity to pathogen-host interactions.

Our systematic investigation of LWY effectors has illuminated fundamental principles underlying how pathogens evolve to acquire novel functionality through recombination. We demonstrated that while these LWY units share structural homology, they serve as distinct functional modules for recruiting different host proteins due to employing different surface residues. Identification of conserved surface residues that mediate common target recognition can provide new opportunities for engineering enhanced disease resistance in agricultural crops. This work establishes a foundation for future research directions, including detailed structural characterization of effector-target binding interfaces and mechanisms of differential host protein recruitment. These insights contribute to the broader goal of developing more resilient agricultural systems with durable disease resistance.

6.4 Reference

Ah-Fong, A. M. V., Shrivastava, J., and Judelson, H. S. (2017), 'Lifestyle, gene gain and loss, and transcriptional remodeling cause divergence in the transcriptomes of Phytophthora infestans and Pythium ultimum during potato tuber colonization', *BMC Genomics,* 18 (1), 764.

Ahn, H. K., et al. (2023), 'Effector-dependent activation and oligomerization of plant NRC class helper NLRs by sensor NLR immune receptors Rpi-amr3 and Rpi-amr1', *EMBO J,* 42 (5), e111484.

Ai, G., et al. (2020), 'Prediction and Characterization of RXLR Effectors in Pythium Species', *Mol Plant Microbe Interact,* 33 (8), 1046-58.

Albert, I., et al. (2015), 'An RLP23-SOBIR1-BAK1 complex mediates NLP-triggered immunity', *Nat Plants,* 1, 15140.

Altschu, Stephen. F. , et al. (1990), 'Basic Local Alignment Search Tool', *J Mol Biol,* 215.

Anderson, R. G., et al. (2015), 'Recent Progress in RXLR Effector Research', *Mol Plant Microbe Interact,* 28 (10), 1063-72.

Anderson, T, R. (1985), 'Plant Losses and Yield Responses to Monoculture of Soybean Cultivars Susceptible, Tolerant and Resistant to Phytophthora megasperma f. sp. glycinea', *Plant Disease,* 70.

Anna-Liisa Fabritius, Howard S. Judelson (1997), 'Mating-type loci segregate aberrantly in Phytophthora infestans but normally in Phytophthora parasitica: implications for models of mating-type determination', *Curr Genet,* 32.

Armstrong, M. R., et al. (2005), 'An ancestral oomycete locus contains late blight avirulence gene Avr3a, encoding a protein that is recognized in the host cytoplasm', *PNAS,* 102.

Ascurra, Yerisf C. Torres., et al. (2023), 'Functional diversification of a wild potato immune receptor at its center of origin', *Science,* 381.

Bao, J., et al. (2017), 'PacBio Sequencing Reveals Transposable Elements as a Key Contributor to Genomic Plasticity and Virulence Variation in Magnaporthe oryzae', *Mol Plant,* 10 (11), 1465-68.

Beakes, G. W., Glockling, S. L., and Sekimoto, S. (2012), 'The evolutionary phylogeny of the oomycete "fungi"', *Protoplasma,* 249 (1), 3-19.

Bentham, A. R., et al. (2024), 'The WY Domain of an RxLr Effector Drives Interactions with a Host Target Phosphatase to Mimic Host Regulatory Proteins and Promote Phytophthora infestans Infection', *Mol Plant Microbe Interact,* 37 (3), 239-49.

Bialas, A., et al. (2021), 'Two NLR immune receptors acquired high-affinity binding to a fungal effector through convergent evolution of their integrated domain', *Elife,* 10.

Bian, C., et al. (2020), 'Protein phosphatase 2A promotes stomatal development by stabilizing SPEECHLESS in Arabidopsis', *Proc Natl Acad Sci U S A,* 117 (23), 13127-37.

Bienapfl , J. C. and Balci, Y. (2013), 'Movement of Phytophthora spp. in Maryland's Nursery Trade', *Plant Disease,* 98.

Blackman, L. M., et al. (2015), 'RNA-Seq Analysis of the Expression of Genes Encoding Cell Wall Degrading Enzymes during Infection of Lupin (Lupinus angustifolius) by Phytophthora parasitica', *PLoS One,* 10 (9), e0136899.

Bleecker, Shin-Han Shiu and Anthony B. (2001), 'Receptor-like kinases from Arabidopsis form a monophyletic gene family related to animal receptor kinases', *PNAS,* 98.

Boch, Jens., et al. (2009), 'Breaking the Code of DNA Binding

Specificity of TAL-Type III Effectors', *Science,* 326.

Boller, T. and He, S. Y. (2009), 'Innate immunity in plants: an arms race between pattern recognition receptors in plants and effectors in microbial pathogens', *Science,* 324 (5928), 742-4.

Bos, J. I., et al. (2010), 'Phytophthora infestans effector AVR3a is essential for virulence and manipulates plant immunity by stabilizing host E3 ligase CMPG1', *Proc Natl Acad Sci U S A,* 107 (21), 9909-14.

Boutemy, L. S., et al. (2011), 'Structures of Phytophthora RXLR effector proteins: a conserved but adaptable fold underpins functional diversity', *J Biol Chem,* 286 (41), 35834-42.

Bouwmeester, K., et al. (2011), 'The lectin receptor kinase LecRK-I.9 is a novel Phytophthora resistance component and a potential host target for a RXLR effector', *PLoS Pathog,* 7 (3), e1001327.

Brasier, C., et al. (2022), 'Phytophthora: an ancient, historic, biologically and structurally cohesive and evolutionarily successful generic concept in need of preservation', *IMA Fungus,* 13 (1), 12.

Brautigan, D. L. (2013), 'Protein Ser/Thr phosphatases--the ugly ducklings of cell signalling', *FEBS J,* 280 (2), 324-45.

Brefort, T., et al. (2014), 'Characterization of the largest effector gene cluster of Ustilago maydis', *PLoS Pathog,* 10 (7), e1003866.

Bruinsma, Nikos Alexandratos and Jelle (2012), 'WORLD AGRICULTURE TOWARDS 2030/2050'.

Brunner, FreÂdeÂric., Rosahl, Sabine., and Lee, Justin. (2002), 'Pep-13, a plant defense-inducing pathogenassociated pattern from Phytophthora transglutaminases', *EMBO J,* 21.

Canham, J., et al. (2024), 'GetGenome: Overcoming inequalities in access to genomics technology', *PLoS Biol,* 22 (8), e3002804.

Cao, Y., et al. (2023), 'Structural polymorphisms within a common powdery mildew effector scaffold as a driver of coevolution with cereal immune receptors', *Proc Natl Acad Sci U S A,* 120 (32), e2307604120.

Catanzariti, A. M., et al. (2017), 'The tomato I gene for Fusarium wilt resistance encodes an atypical leucine-rich repeat receptor-like protein whose function is nevertheless dependent on SOBIR1 and SERK3/BAK1', *Plant J,* 89 (6), 1195-209.

Cesari, S., et al. (2013), 'The rice resistance protein pair RGA4/RGA5 recognizes the Magnaporthe oryzae effectors AVR-Pia and AVR1-CO39 by direct binding', *Plant Cell,* 25 (4), 1463-81.

Chambers, M. C., et al. (2012), 'A cross-platform toolkit for mass spectrometry and proteomics', *Nat Biotechnol,* 30 (10), 918-20.

Champouret, Nicolas., Bouwmeester, Klaas., and Rietman, Hendrik. (2009), 'Phytophthora infestans Isolates Lacking Class I ipiO Variants Are Virulent on Rpi-blb1 Potato', *MPMI,* 22.

Chang, S. W., et al. (2011), 'NRIP, a novel calmodulin binding protein, activates calcineurin to dephosphorylate human papillomavirus E2 protein', *J Virol,* 85 (13), 6750-63.

Chen, Hanbo. and Boutros, Paul. C. (2012), 'VennDiagram: a package for the generation of highly-customizable Venn and Euler diagrams in R', *BMC Bioinformatics,* 12.

Chen, S., et al. (2021), 'Arabidopsis downy mildew effector HaRxLL470 suppresses plant immunity by attenuating the DNA-binding activity of bZIP transcription factor HY5', *New Phytol,* 230 (4), 1562-77.

Chen, X. R., et al. (2019), 'The RXLR Effector PcAvh1 Is Required for Full Virulence of Phytophthora capsici', *Mol Plant Microbe Interact,* 32 (8), 986-1000.

Chinchilla, D., et al. (2007), 'A flagellin-induced complex of the receptor FLS2 and BAK1 initiates plant defence', *Nature,* 448 (7152), 497-500.

Chou, S., et al. (2011), 'Hyaloperonospora arabidopsidis ATR1 effector is a repeat protein with distributed recognition surfaces', *Proc Natl Acad Sci U S A,* 108 (32), 13323-8.

Chrustowicz, J., et al. (2024), 'Multisite phosphorylation dictates selective E2-E3 pairing as revealed by Ubc8/UBE2H-GID/CTLH assemblies', *Mol Cell,* 84 (2), 293-308 e14.

Chuma, I., et al. (2011), 'Multiple translocation of the AVR-Pita effector gene among chromosomes of the rice blast fungus Magnaporthe oryzae and related species', *PLoS Pathog,* 7 (7), e1002147.

Coccetti, P., et al. (2008), 'The CK2 phosphorylation of catalytic domain of Cdc34 modulates its activity at the G1 to S transition in Saccharomyces cerevisiae', *Cell Cycle,* 7 (10), 1391-401.

Cordaux, Richard., et al. (2006), 'Birth of a chimeric primate gene by capture of the transposase gene from a mobile element', *PNAS,* 106.

Cox, K. L., et al. (2017), 'TAL effector driven induction of a SWEET gene confers susceptibility to bacterial blight of cotton', *Nat Commun,* 8, 15588.

Croll, D. and McDonald, B. A. (2012), 'The accessory genome as a cradle for adaptive evolution in pathogens', *PLoS Pathog,* 8 (4), e1002608.

Croll, D., et al. (2015), 'The Impact of Recombination Hotspots on Genome Evolution of a Fungal Plant Pathogen', *Genetics,* 201 (3), 1213-28.

Dagdas, Y. F., et al. (2016), 'An effector of the Irish potato famine pathogen antagonizes a host autophagy cargo receptor', *Elife,* 5.

de Groot, Grecia Stefanía, et al. (2021), 'Large-scale monoculture reduces honey yield: The case of soybean expansion in Argentina', *Agriculture, Ecosystems & Environment,* 306.

de Guillen, K., et al. (2015), 'Structure Analysis Uncovers a Highly Diverse but Structurally Conserved Effector Family in Phytopathogenic Fungi', *PLoS Pathog,* 11 (10), e1005228.

de Jonge, R., et al. (2013), 'Extensive chromosomal reshuffling drives evolution of virulence in an asexual pathogen', *Genome Res,* 23 (8), 1271-82.

De la Concepcion, J. C., et al. (2018), 'Polymorphic residues in rice NLRs expand binding and response to effectors of the blast pathogen', *Nat Plants,* 4 (8), 576-85.
Dellero, Y., et al. (2015), 'Experimental evidence for a hydride transfer mechanism in plant glycolate oxidase catalysis', *J Biol Chem,* 290 (3), 1689-98.
Derevnina, L., et al. (2021), 'Plant pathogens convergently evolved to counteract redundant nodes of an NLR immune receptor network', *PLoS Biol,* 19 (8), e3001136.
Di, X., et al. (2017), 'Structure-function analysis of the Fusarium oxysporum Avr2 effector allows uncoupling of its immune-suppressing activity from recognition', *New Phytol,* 216 (3), 897-914.
Doehlemann, G., et al. (2009), 'Pep1, a secreted effector protein of Ustilago maydis, is required for successful invasion of plant cells', *PLoS Pathog,* 5 (2), e1000290.
Dong, S., Raffaele, S., and Kamoun, S. (2015), 'The two-speed genomes of filamentous pathogens: waltz with plants', *Curr Opin Genet Dev,* 35, 57-65.
Dong, S., et al. (2011), 'Sequence variants of the Phytophthora sojae RXLR effector Avr3a/5 are differentially recognized by Rps3a and Rps5 in soybean', *PLoS One,* 6 (7), e20172.
Du, Y., et al. (2021), 'Phytophthora infestans RXLR effector PITG20303 targets a potato MKK1 protein to suppress plant immunity', *New Phytol,* 229 (1), 501-15.
Dutheil, J. Y., et al. (2016), 'A Tale of Genome Compartmentalization: The Evolution of Virulence Clusters in Smut Fungi', *Genome Biol Evol,* 8 (3), 681-704.
Dye, Sara M. and Bostock, Richard M. (2021), 'Eicosapolyenoic fatty acids induce defense responses and resistance to Phytophthora capsici in tomato and pepper', *Physiological and Molecular Plant Pathology,* 114.
Fabro, G. (2022), 'Oomycete intracellular effectors: specialised weapons targeting strategic plant processes', *New Phytol,* 233 (3), 1074-82.
Feehan, J. M., et al. (2020), 'Plant NLRs get by with a little help from their friends', *Curr Opin Plant Biol,* 56, 99-108.
FLOR, H. H. (1971), 'CURRENT STATUS OF THE GENE-FOB-GENE CONCEPT', *Annu. Rev. Phytopathol,* 9.
Fouché, Simone., Plissonneau, Clémence., and Croll, Daniel. (2018), 'The birth and death of effectors in rapidly evolving filamentous pathogen genomes', *Current Opinion in Microbiology,* 46.
Franceschetti, M., et al. (2017), 'Effectors of Filamentous Plant Pathogens: Commonalities amid Diversity', *Microbiol Mol Biol Rev,* 81 (2).
Fry, W. (2008), 'Phytophthora infestans: the plant (and R gene) destroyer', *Mol Plant Pathol,* 9 (3), 385-402.
Furlan, G., et al. (2017), 'Changes in PUB22 Ubiquitination Modes Triggered by MITOGEN-ACTIVATED PROTEIN KINASE3 Dampen the Immune Response', *Plant Cell,* 29 (4), 726-45.

Gaulin, E., et al. (2006), 'Cellulose binding domains of a Phytophthora cell wall protein are novel pathogen-associated molecular patterns', *Plant Cell,* 18 (7), 1766-77.
Gomez-Gomez, Lourdes . and Boller, Thomas. (2000), 'FLS2: An LRR Receptor–like Kinase Involved in the Perception of the Bacterial Elicitor Flagellin in Arabidopsis', *Molecular Cell,* 5.
Goodwin, S. B., et al. (2011), 'Finished genome of the fungal wheat pathogen Mycosphaerella graminicola reveals dispensome structure, chromosome plasticity, and stealth pathogenesis', *PLoS Genet,* 7 (6), e1002070.
Goritschnig, S., et al. (2016), 'Structurally distinct Arabidopsis thaliana NLR immune receptors recognize tandem WY domains of an oomycete effector', *New Phytol,* 210 (3), 984-96.
Goss, E. M., Press, C. M., and Grunwald, N. J. (2013), 'Evolution of RXLR-class effectors in the oomycete plant pathogen Phytophthora ramorum', *PLoS One,* 8 (11), e79347.
Grandaubert, Jonathan., Lowe, Rohan. GT., and Soyer, Jessica. L. (2014), 'Transposable element-assisted evolution and adaptation to host plant within the Leptosphaeria maculans-Leptosphaeria biglobosa species complex of fungal pathogens', *BMC Genomics,* 15.
Green, Sarah, et al. (2021), 'PHYTO-THREATS: Addressing Threats to UK Forests and Woodlands from Phytophthora; Identifying Risks of Spread in Trade and Methods for Mitigation', *Forests,* 12 (12).
Guo, B., et al. (2019), 'Phytophthora sojae Effector PsAvh240 Inhibits Host Aspartic Protease Secretion to Promote Infection', *Mol Plant,* 12 (4), 552-64.
Guo, L., et al. (2018), 'Specific recognition of two MAX effectors by integrated HMA domains in plant immune receptors involves distinct binding surfaces', *Proc Natl Acad Sci U S A,* 115 (45), 11637-42.
Haas, B. J., et al. (2009), 'Genome sequence and analysis of the Irish potato famine pathogen Phytophthora infestans', *Nature,* 461 (7262), 393-8.
Hardham, A. R. (2005), 'Phytophthora cinnamomi', *Mol Plant Pathol,* 6 (6), 589-604.
Hardham, A. R. and Blackman, L. M. (2018), 'Phytophthora cinnamomi', *Mol Plant Pathol,* 19 (2), 260-85.
He, J., et al. (2019), 'Structural analysis of Phytophthora suppressor of RNA silencing 2 (PSR2) reveals a conserved modular fold contributing to virulence', *Proc Natl Acad Sci U S A,* 116 (16), 8054-59.
Hedges, D. J. and Deininger, P. L. (2007), 'Inviting Instability: Transposable elements, Double-strand breaks, and the Maintenance of Genome Integrity', *Mutat Res,* 616.
Heese, Antje ., et al. (2007), 'The receptor-like kinase SERK3/BAK1 is a central regulator of innate immunity in plants', *PNAS,* 104.
Hein, I., et al. (2009), 'The zig-zag-zig in oomycete-plant interactions', *Mol Plant Pathol,* 10 (4), 547-62.

Henricot, B., Pérez Sierra, A., and Jung, T. (2014), 'Phytophthora pachypleura sp. nov., a new species causing root rot of Aucuba japonica and other ornamentals in the United Kingdom', *Plant Pathology,* 63 (5), 1095-109.
Hill, W. G. and Robertson, Alan (2009), 'The effect of linkage on limits to artificial selection', *Genetical Research,* 8 (3), 269-94.
Hogenhout, Saskia A., Hoorn, Renier A. L. Van der., and Terauchi, Ryohei and Sophien Kamoun4 (2009), 'Emerging Concepts in Effector Biology of Plant-Associated Organisms', *MPMI,* 22.
Hoie, M. H., et al. (2022), 'NetSurfP-3.0: accurate and fast prediction of protein structural features by protein language models and deep learning', *Nucleic Acids Res,* 50 (W1), W510-W15.
Hou, Y., et al. (2019), 'A Phytophthora Effector Suppresses Trans-Kingdom RNAi to Promote Disease Susceptibility', *Cell Host Microbe,* 25 (1), 153-65 e5.
Huang, S., et al. (2005), 'Comparative genomics enabled the isolation of the R3a late blight resistance gene in potato', *Plant J,* 42 (2), 251-61.
Huppi, K., Martin, S. E., and Caplen, N. J. (2005), 'Defining and assaying RNAi in mammalian cells', *Mol Cell,* 17 (1), 1-10.
Irieda, H., et al. (2019), 'Conserved fungal effector suppresses PAMP-triggered immunity by targeting plant immune kinases', *Proc Natl Acad Sci U S A,* 116 (2), 496-505.
Jacobs, S., et al. (2011), 'Broad-spectrum suppression of innate immunity is required for colonization of Arabidopsis roots by the fungus Piriformospora indica', *Plant Physiol,* 156 (2), 726-40.
Jensen-Seaman, M. I., et al. (2004), 'Comparative recombination rates in the rat, mouse, and human genomes', *Genome Res,* 14 (4), 528-38.
Ji, Z., et al. (2016), 'Interfering TAL effectors of Xanthomonas oryzae neutralize R-gene-mediated plant disease resistance', *Nat Commun,* 7, 13435.
Jiang, H. Y., et al. (2008), 'RXLR effector reservoir in two Phytophthora species is dominated by a single rapidly evolving superfamily with more than 700 members', *PNAS,* 105 (12).
Jones, J. D. and Dangl, J. L. (2006), 'The plant immune system', *Nature,* 444 (7117), 323-9.
Jones, J. D. G., Staskawicz, B. J., and Dangl, J. L. (2024), 'The plant immune system: From discovery to deployment', *Cell,* 187 (9), 2095-116.
Jones, P., et al. (2014), 'InterProScan 5: genome-scale protein function classification', *Bioinformatics,* 30 (9), 1236-40.
Judelson, H. S. and Ah-Fong, A. M. V. (2019), 'Exchanges at the Plant-Oomycete Interface That Influence Disease', *Plant Physiol,* 179 (4), 1198-211.
Jumper, J., et al. (2021), 'Highly accurate protein structure prediction with AlphaFold', *Nature,* 596 (7873), 583-89.
Kamper, J., et al. (2006), 'Insights from the genome of the biotrophic fungal plant pathogen Ustilago maydis', *Nature,* 444 (7115), 97-101.
Kearney, Brain. and Staskawicz, B. J. (1990), 'Widespread distribution and fitness contribution of Xanthomonas campestris avirulence gene avrBs2', *Nature,* 346.

Kim, D. S., et al. (2024), 'ATR2(C) (ala2) from Arabidopsis-infecting downy mildew requires 4 TIR-NLR immune receptors for full recognition', *New Phytol,* 243 (1), 330-44.
King, S. R., et al. (2014), 'Phytophthora infestans RXLR effector PexRD2 interacts with host MAPKKK epsilon to suppress plant immune signaling', *Plant Cell,* 26 (3), 1345-59.
Klarzynski, Olivier., et al. (2000), 'Linear β-1,3 Glucans Are Elicitors of Defense Responses in Tobacco', *plant Physiol,* 124.
Ko, Y. H., Hong, S., and Pedersen, P. L. (1999), 'Chemical mechanism of ATP synthase. Magnesium plays a pivotal role in formation of the transition state where ATP is synthesized from ADP and inorganic phosphate', *J Biol Chem,* 274 (41), 28853-6.
Kong, A., et al. (2002), 'A high-resolution recombination map of the human genome', *Nat Genet,* 31 (3), 241-7.
Kong, L., et al. (2015), 'Degradation of the ABA co-receptor ABI1 by PUB12/13 U-box E3 ligases', *Nat Commun,* 6, 8630.
Kourelis, Jiorgos., et al. (2023), 'NLR immune receptor–nanobody fusions confer plant disease resistance', *Science,* 379.
Kovacs, K., et al. (2011), 'Predicting the economic costs and property value losses attributed to sudden oak death damage in California (2010-2020)', *J Environ Manage,* 92 (4), 1292-302.
Kronmiller, B. A., et al. (2023), 'Comparative Genomic Analysis of 31 Phytophthora Genomes Reveals Genome Plasticity and Horizontal Gene Transfer', *Mol Plant Microbe Interact,* 36 (1), 26-46.
Lahaye, Thomas. and Bonas, Ulla. (2001), 'Molecular secrets of bacterial type III effector proteins', *TRENDSin Plant Science,* 6.
Lamour, K. H., et al. (2012), 'Genome sequencing and mapping reveal loss of heterozygosity as a mechanism for rapid adaptation in the vegetable pathogen Phytophthora capsici', *Mol Plant Microbe Interact,* 25 (10), 1350-60.
Langner, T., et al. (2021), 'Genomic rearrangements generate hypervariable mini-chromosomes in host-specific isolates of the blast fungus', *PLoS Genet,* 17 (2), e1009386.
Lapin, D., Bhandari, D. D., and Parker, J. E. (2020), 'Origins and Immunity Networking Functions of EDS1 Family Proteins', *Annu Rev Phytopathol,* 58, 253-76.
Latorre, S. M., et al. (2020), 'Differential loss of effector genes in three recently expanded pandemic clonal lineages of the rice blast fungus', *BMC Biol,* 18 (1), 88.
Lazar, N., et al. (2022), 'A new family of structurally conserved fungal effectors displays epistatic interactions with plant resistance proteins', *PLoS Pathog,* 18 (7), e1010664.
Li, H., et al. (2023), 'Pathogen protein modularity enables elaborate mimicry of a host phosphatase', *Cell,* 186 (15), 3196-207 e17.
Li, Q., et al. (2020), 'A Phytophthora capsici effector suppresses plant immunity via interaction with EDS1', *Mol Plant Pathol,* 21 (4), 502-11.

Li, T., et al. (2022), 'A Phytophthora capsici RXLR effector manipulates plant immunity by targeting RAB proteins and disturbing the protein trafficking pathway', *Mol Plant Pathol,* 23 (12), 1721-36.
Li, W., et al. (2012), 'The U-Box/ARM E3 ligase PUB13 regulates cell death, defense, and flowering time in Arabidopsis', *Plant Physiol,* 159 (1), 239-50.
Liang, X., et al. (2021), 'A Phytophthora capsici RXLR effector targets and inhibits the central immune kinases to suppress plant immunity', *New Phytol,* 232 (1), 264-78.
Liao, D., et al. (2017), 'Arabidopsis E3 ubiquitin ligase PLANT U-BOX13 (PUB13) regulates chitin receptor LYSIN MOTIF RECEPTOR KINASE5 (LYK5) protein abundance', *New Phytol,* 214 (4), 1646-56.
Lin, S., et al. (2021a), 'EPSD: a well-annotated data resource of protein phosphorylation sites in eukaryotes', *Brief Bioinform,* 22 (1), 298-307.
Lin, X., et al. (2020), 'Identification of Avramr1 from Phytophthora infestans using long read and cDNA pathogen-enrichment sequencing (PenSeq)', *Mol Plant Pathol,* 21 (11), 1502-12.
Lin, X., et al. (2022), 'A potato late blight resistance gene protects against multiple Phytophthora species by recognizing a broadly conserved RXLR-WY effector', *Mol Plant,* 15 (9), 1457-69.
Lin, Y., et al. (2021b), 'Phytophthora sojae effector Avr1d functions as an E2 competitor and inhibits ubiquitination activity of GmPUB13 to facilitate infection', *Proc Natl Acad Sci U S A,* 118 (10).
Liu, Y., et al. (2021), 'A designer rice NLR immune receptor confers resistance to the rice blast fungus carrying noncorresponding avirulence effectors', *Proc Natl Acad Sci U S A,* 118 (44).
Lo Presti, L., et al. (2015), 'Fungal effectors and plant susceptibility', *Annu Rev Plant Biol,* 66, 513-45.
Lole, KAVITA. S., et al. (1999), 'Full-Length Human Immunodeficiency Virus Type 1 Genomes from Subtype C-Infected Seroconverters in India, with Evidence of Intersubtype Recombination', *JOURNAL OF VIROLOGY,* 73.
Lovelace, A. H., et al. (2023), 'Effector Identification in Plant Pathogens', *Phytopathology,* 113 (4), 637-50.
Ma, L. J., et al. (2010), 'Comparative genomics reveals mobile pathogenicity chromosomes in Fusarium', *Nature,* 464 (7287), 367-73.
Ma, Z., et al. (2017), 'A paralogous decoy protects Phytophthora sojae apoplastic effector PsXEG1 from a host inhibitor', *Science,* 355.
Ma, Z., et al. (2015), 'A Phytophthora sojae Glycoside Hydrolase 12 Protein Is a Major Virulence Factor during Soybean Infection and Is Recognized as a PAMP', *Plant Cell,* 27 (7), 2057-72.
Maqbool, A., et al. (2016), 'Structural Basis of Host Autophagy-related Protein 8 (ATG8) Binding by the Irish Potato Famine Pathogen Effector Protein PexRD54', *J Biol Chem,* 291 (38), 20270-82.
Matson, M. E. H., et al. (2022), 'Karyotype variation, spontaneous genome rearrangements affecting chemical insensitivity, and expression level polymorphisms in the plant pathogen Phytophthora infestans revealed

using its first chromosome-scale assembly', *PLoS Pathog,* 18 (10), e1010869.
McCoy, A. G., et al. (2023), 'A global-temporal analysis on Phytophthora sojae resistance-gene efficacy', *Nat Commun,* 14 (1), 6043.
McDonald, B. A. and Stukenbrock, E. H. (2016), 'Rapid emergence of pathogens in agro-ecosystems: global threats to agricultural sustainability and food security', *Philos Trans R Soc Lond B Biol Sci,* 371 (1709).
McGowan, Jamie. and Fitzpatrick, David. A. (2017), 'Genomic, Network, and Phylogenetic Analysis of the Oomycete Effector Arsenal', *mSphere,* 2 (6).
Miao, VIVIAN. P., Covert, SARAH. F. , and Vanetten, HANs. D. (1991), 'A Fungal Gene for Antibiotic Resistance on a Dispensable ("B") Chromosome', *Science,* 254.
Moscou, Matthew J. and Bogdanove, Adam J. (2009), 'A Simple Cipher Governs DNA

Recognition by TAL Effectors', *Science,* 326.
Muller, M. C., et al. (2019), 'A chromosome-scale genome assembly reveals a highly dynamic effector repertoire of wheat powdery mildew', *New Phytol,* 221 (4), 2176-89.
Na, R., et al. (2013), 'Deletion of the Phytophthora sojae avirulence gene Avr1d causes gain of virulence on Rps1d', *Mol Plant Microbe Interact,* 26 (8), 969-76.
Ngou, B. P. M., Ding, P., and Jones, J. D. G. (2022a), 'Thirty years of resistance: Zig-zag through the plant immune system', *Plant Cell,* 34 (5), 1447-78.
Ngou, B. P. M., Jones, J. D. G., and Ding, P. (2022b), 'Plant immune networks', *Trends Plant Sci,* 27 (3), 255-73.
Ngou, B. P. M., et al. (2021), 'Mutual potentiation of plant immunity by cell-surface and intracellular receptors', *Nature,* 592 (7852), 110-15.
Nielsen, H., et al. (2019), 'A Brief History of Protein Sorting Prediction', *Protein J,* 38 (3), 200-16.
O'Connor, C. M., et al. (2018), 'Therapeutic targeting of PP2A', *Int J Biochem Cell Biol,* 96, 182-93.
Oh, S. K., et al. (2009), 'In planta expression screens of Phytophthora infestans RXLR effectors reveal diverse phenotypes, including activation of the Solanum bulbocastanum disease resistance protein Rpi-blb2', *Plant Cell,* 21 (9), 2928-47.
Oome, S., et al. (2014), 'Nep1-like proteins from three kingdoms of life act as a microbe-associated molecular pattern in Arabidopsis', *Proc Natl Acad Sci U S A,* 111 (47), 16955-60.
Ortiz, D., et al. (2017), 'Recognition of the Magnaporthe oryzae Effector AVR-Pia by the Decoy Domain of the Rice NLR Immune Receptor RGA5', *Plant Cell,* 29 (1), 156-68.
Otto and Barton, Nick. H. (1997), 'The Evolution of Recombination: Removing the Limits to Natural Selection', *Genetics Society of America,* 147.
Otto and Lenormand, T. (2002), 'Resolving the paradox of sex and recombination', *Nat Rev Genet,* 3 (4), 252-61.

Outram, M. A., Solomon, P. S., and Williams, S. J. (2021a), 'Pro-domain processing of fungal effector proteins from plant pathogens', *PLoS Pathog,* 17 (10), e1010000.
Outram, M. A., et al. (2022), 'Seeing is believing: Exploiting advances in structural biology to understand and engineer plant immunity', *Curr Opin Plant Biol,* 67, 102210.
Outram, M. A., et al. (2021b), 'The crystal structure of SnTox3 from the necrotrophic fungus Parastagonospora nodorum reveals a unique effector fold and provides insight into Snn3 recognition and pro-domain protease processing of fungal effectors', *New Phytol,* 231 (6), 2282-96.
Pandey, P., et al. (2021), 'An oomycete effector subverts host vesicle trafficking to channel starvation-induced autophagy to the pathogen interface', *Elife,* 10.
Parada-Rojas, Camilo H., et al. (2021), 'A Diagnostic Guide for Phytophthora capsici Infecting Vegetable Crops', *Plant Health Progress,* 22 (3), 404-14.
Peng, Y., van Wersch, R., and Zhang, Y. (2018), 'Convergent and Divergent Signaling in PAMP-Triggered Immunity and Effector-Triggered Immunity', *Mol Plant Microbe Interact,* 31 (4), 403-09.
Peng, Z., et al. (2019), 'Effector gene reshuffling involves dispensable mini-chromosomes in the wheat blast fungus', *PLoS Genet,* 15 (9), e1008272.
Pennington, H. G., et al. (2019), 'The fungal ribonuclease-like effector protein CSEP0064/BEC1054 represses plant immunity and interferes with degradation of host ribosomal RNA', *PLoS Pathog,* 15 (3), e1007620.
Perez-Quintero, A. L. and Szurek, B. (2019), 'A Decade Decoded: Spies and Hackers in the History of TAL Effectors Research', *Annu Rev Phytopathol,* 57, 459-81.
Petre, B., et al. (2021), 'Host-interactor screens of Phytophthora infestans RXLR proteins reveal vesicle trafficking as a major effector-targeted process', *Plant Cell,* 33 (5), 1447-71.
Pettersen, E. F., et al. (2021), 'UCSF ChimeraX: Structure visualization for researchers, educators, and developers', *Protein Sci,* 30 (1), 70-82.
Pierre, M., Noël , L., and Bonas, T. Lahaye · A. Ballvora J. Veuskens · M. Ganal · U. (2000), 'High-resolution genetic mapping of the pepper resistance locus Bs3governing recognition of the Xanthomonas campestris pv vesicatora AvrBs3 protein', *Theor Appl Genet,* 101.
Prince, V. E. and Pickett, F. B. (2002), 'Splitting pairs: the diverging fates of duplicated genes', *Nat Rev Genet,* 3 (11), 827-37.
Pruitt, R. N., et al. (2021), 'The EDS1-PAD4-ADR1 node mediates Arabidopsis pattern-triggered immunity', *Nature,* 598 (7881), 495-99.
Qiao, Y., et al. (2015), 'Phytophthora effector targets a novel component of small RNA pathway in plants to promote infection', *Proc Natl Acad Sci U S A,* 112 (18), 5850-5.
Qiao, Y., et al. (2013), 'Oomycete pathogens encode RNA silencing suppressors', *Nat Genet,* 45 (3), 330-3.
Qiu, X., et al. (2023), 'The Phytophthora sojae nuclear effector PsAvh110 targets a host transcriptional complex to modulate plant immunity', *Plant Cell,* 35 (1), 574-97.

Qutob, D., Chapman, B. P., and Gijzen, M. (2013), 'Transgenerational gene silencing causes gain of virulence in a plant pathogen', *Nat Commun,* 4, 1349.

Qutob, D., et al. (2009), 'Copy number variation and transcriptional polymorphisms of Phytophthora sojae RXLR effector genes Avr1a and Avr3a', *PLoS One,* 4 (4), e5066.

Raffaele, Sylvain., Farrer, Rhys A. ., and Liliana M. Cano, 1* David J. Studholme, 1‡ Daniel MacLean,1 Marco Thines,1,2,3 Rays H. Y. Jiang,4 Michael C. Zody,4 Sridhara G. Kunjeti,5 Nicole M. Donofrio,5 Blake C. Meyers,5 Chad Nusbaum,4 Sophien Kamoun1§ (2010), 'Genome Evolution Following Host Jumps in the Irish Potato Famine

Pathogen Lineage', *Science,* 330.

Reams, A. B. and Neidle, E. L. (2004), 'Selection for gene clustering by tandem duplication', *Annu Rev Microbiol,* 58, 119-42.

Romer, P., et al. (2010), 'Promoter elements of rice susceptibility genes are bound and activated by specific TAL effectors from the bacterial blight pathogen, Xanthomonas oryzae pv. oryzae', *New Phytol,* 187 (4), 1048-57.

Rosa, C., et al. (2018), 'RNA Interference Mechanisms and Applications in Plant Pathology', *Annu Rev Phytopathol,* 56, 581-610.

Rouxel, T., et al. (2011), 'Effector diversification within compartments of the Leptosphaeria maculans genome affected by Repeat-Induced Point mutations', *Nat Commun,* 2, 202.

Sanchez-Vallet, A., et al. (2013), 'Fungal effector Ecp6 outcompetes host immune receptor for chitin binding through intrachain LysM dimerization', *Elife,* 2, e00790.

Sanchez-Vallet, A., et al. (2018), 'The Genome Biology of Effector Gene Evolution in Filamentous Plant Pathogens', *Annu Rev Phytopathol,* 56, 21-40.

Sarcevic, Boris., et al. (2002), 'Regulation of the ubiquitin-conjugating enzyme hHR6A by CDK-mediated phosphorylation', *The EMBO Journal,* 21.

Sarma, G. N., et al. (2005), 'Structure of Ptr ToxA: an RGD-containing host-selective toxin from Pyrenophora tritici-repentis', *Plant Cell,* 17 (11), 3190-202.

Savary, S., et al. (2019), 'The global burden of pathogens and pests on major food crops', *Nat Ecol Evol,* 3 (3), 430-39.

Schmidt, Sarah. M., Houterman, Petra. M., and Schreiver, Ines. (2013), 'MITEs in the promoters of effector genes allow prediction of novel virulence genes in Fusarium oxysporum', *BMC Genomics,* 14.

Schornack, S., et al. (2006), 'Gene-for-gene-mediated recognition of nuclear-targeted AvrBs3-like bacterial effector proteins', *J Plant Physiol,* 163 (3), 256-72.

Schornack, S., et al. (2004), 'The tomato resistance protein Bs4 is a predicted non-nuclear TIR-NB-LRR protein that mediates defense responses to severely truncated derivatives of AvrBs4 and overexpressed AvrBs3', *Plant J,* 37 (1), 46-60.

Schotanus, K., et al. (2015), 'Histone modifications rather than the novel regional centromeres of Zymoseptoria tritici distinguish core and accessory chromosomes', *Epigenetics Chromatin,* 8, 41.
Seong, K. and Krasileva, K. V. (2021), 'Computational Structural Genomics Unravels Common Folds and Novel Families in the Secretome of Fungal Phytopathogen Magnaporthe oryzae', *Mol Plant Microbe Interact,* 34 (11), 1267-80.
--- (2023), 'Prediction of effector protein structures from fungal phytopathogens enables evolutionary analyses', *Nat Microbiol,* 8 (1), 174-87.
Shan, L., et al. (2008), 'Bacterial effectors target the common signaling partner BAK1 to disrupt multiple MAMP receptor-signaling complexes and impede plant immunity', *Cell Host Microbe,* 4 (1), 17-27.
Sharp, J. K., Valent, B., and Albersheim, P. (1984), 'Purification and partial characterization of a beta-glucan fragment that elicits phytoalexin accumulation in soybean', *Journal of Biological Chemistry,* 259 (18), 11312-20.
Shen, D., et al. (2013), 'Gene duplication and fragment recombination drive functional diversification of a superfamily of cytoplasmic effectors in Phytophthora sojae', *PLoS One,* 8 (7), e70036.
Song, G., et al. (2018), 'Heterotrimeric G-Protein-Dependent Proteome and Phosphoproteome in Unstimulated Arabidopsis Roots', *Proteomics,* 18 (24), e1800323.
Song, T., et al. (2013), 'Two RxLR avirulence genes in Phytophthora sojae determine soybean Rps1k-mediated disease resistance', *Mol Plant Microbe Interact,* 26 (7), 711-20.
Spanu, P. D. (2017), 'Cereal immunity against powdery mildews targets RNase-Like Proteins associated with Haustoria (RALPH) effectors evolved from a common ancestral gene', *New Phytol,* 213 (3), 969-71.
Staskawicz, Brian. J., Dahlbeck, Douglas., and Keen, Noel T. (1984), 'Cloned avirulence gene of Pseudomonas syringae pv. glycinea determines race-specific incompatibility on Glycine max (L.) Merr.', *PNAS,* 81.
Stegmann, M., et al. (2012), 'The ubiquitin ligase PUB22 targets a subunit of the exocyst complex required for PAMP-triggered responses in Arabidopsis', *Plant Cell,* 24 (11), 4703-16.
Stewart, M. D., et al. (2016), 'E2 enzymes: more than just middle men', *Cell Res,* 26 (4), 423-40.
Streubel, J., et al. (2013), 'Five phylogenetically close rice SWEET genes confer TAL effector-mediated susceptibility to Xanthomonas oryzae pv. oryzae', *New Phytol,* 200 (3), 808-19.
Studholme, D. J., et al. (2019), 'Genome sequencing of oomycete isolates from Chile supports the New Zealand origin of Phytophthora kernoviae and makes available the first Nothophytophthora sp. genome', *Mol Plant Pathol,* 20 (3), 423-31.
Stukenbrock, E. H. and Dutheil, J. Y. (2018), 'Fine-Scale Recombination Maps of Fungal Plant Pathogens Reveal Dynamic Recombination Landscapes and Intragenic Hotspots', *Genetics,* 208 (3), 1209-29.

Tamura, K., Stecher, G., and Kumar, S. (2021), 'MEGA11: Molecular Evolutionary Genetics Analysis Version 11', *Mol Biol Evol,* 38 (7), 3022-27.
Temporini, E. D. and VanEtten, H. D. (2004), 'An analysis of the phylogenetic distribution of the pea pathogenicity genes of Nectria haematococca MPVI supports the hypothesis of their origin by horizontal transfer and uncovers a potentially new pathogen of garden pea: Neocosmospora boniensis', *Curr Genet,* 46 (1), 29-36.
Teper, D. and Wang, N. (2021), 'Consequences of adaptation of TAL effectors on host susceptibility to Xanthomonas', *PLoS Genet,* 17 (1), e1009310.
Teulet, A., et al. (2023), 'A pathogen effector FOLD diversified in symbiotic fungi', *New Phytol,* 239 (3), 1127-39.
Thulasi Devendrakumar, K., Li, X., and Zhang, Y. (2018), 'MAP kinase signalling: interplays between plant PAMP- and effector-triggered immunity', *Cell Mol Life Sci,* 75 (16), 2981-89.
Tian, H., et al. (2022), 'Fungal dual-domain LysM effectors undergo chitin-induced intermolecular, and not intramolecular, dimerization', *Plant Physiol,* 190 (3), 2033-44.
Tian, M., Benedetti, B., and Kamoun, S. (2005), 'A Second Kazal-like protease inhibitor from Phytophthora infestans inhibits and interacts with the apoplastic pathogenesis-related protease P69B of tomato', *Plant Physiol,* 138 (3), 1785-93.
Tian, M., et al. (2004), 'A Kazal-like extracellular serine protease inhibitor from Phytophthora infestans targets the tomato pathogenesis-related protease P69B', *J Biol Chem,* 279 (25), 26370-7.
Trujillo, M., et al. (2008), 'Negative regulation of PAMP-triggered immunity by an E3 ubiquitin ligase triplet in Arabidopsis', *Curr Biol,* 18 (18), 1396-401.
Tsai, I. J., Burt, A., and Koufopanou, V. (2010), 'Conservation of recombination hotspots in yeast', *Proc Natl Acad Sci U S A,* 107 (17), 7847-52.
Tsuda, K. and Katagiri, F. (2010), 'Comparing signaling mechanisms engaged in pattern-triggered and effector-triggered immunity', *Curr Opin Plant Biol,* 13 (4), 459-65.
Turek, I., et al. (2018), 'Multi-tiered pairing selectivity between E2 ubiquitin-conjugating enzymes and E3 ligases', *J Biol Chem,* 293 (42), 16324-36.
Turnbull, D., et al. (2017), 'RXLR Effector AVR2 Up-Regulates a Brassinosteroid-Responsive bHLH Transcription Factor to Suppress Immunity', *Plant Physiol,* 174 (1), 356-69.
Tyler, B. M. (2007), 'Phytophthora sojae: root rot pathogen of soybean and model oomycete', *Mol Plant Pathol,* 8 (1), 1-8.
van der Vossen, E., et al. (2003), 'An ancient R gene from the wild potato species Solanum bulbocastanum confers broad-spectrum resistance to Phytophthora infestans in cultivated potato and tomato', *Plant J,* 36 (6), 867-82.
Varadi, M., et al. (2024), 'AlphaFold Protein Structure Database in 2024: providing structure coverage for over 214 million protein sequences', *Nucleic Acids Res,* 52 (D1), D368-D75.

Varden, F. A., et al. (2019), 'Cross-reactivity of a rice NLR immune receptor to distinct effectors from the rice blast pathogen Magnaporthe oryzae provides partial disease resistance', *J Biol Chem,* 294 (35), 13006-16.
Vlaardingerbroek, I., et al. (2016), 'Dispensable chromosomes in Fusarium oxysporum f. sp. lycopersici', *Mol Plant Pathol,* 17 (9), 1455-66.
Vleeshouwers, V. G., et al. (2008), 'Effector genomics accelerates discovery and functional profiling of potato disease resistance and phytophthora infestans avirulence genes', *PLoS One,* 3 (8), e2875.
Wang, H., et al. (2021), 'An atypical Phytophthora sojae RxLR effector manipulates host vesicle trafficking to promote infection', *PLoS Pathog,* 17 (11), e1010104.
Wang, M. Y., et al. (2023a), 'The plant immune receptor SNC1 monitors helper NLRs targeted by a bacterial effector', *Cell Host Microbe,* 31 (11), 1792-803 e7.
Wang, P., et al. (2013), 'Quantitative phosphoproteomics identifies SnRK2 protein kinase substrates and reveals the effectors of abscisic acid action', *Proc Natl Acad Sci U S A,* 110 (27), 11205-10.
Wang, Q., et al. (2023b), 'UBC6, a ubiquitin-conjugating enzyme, participates in secondary cell wall thickening in the inflorescence stem of Arabidopsis', *Plant Physiol Biochem,* 205, 108152.
Wang, S., et al. (2023c), 'RxLR Effectors: Master Modulators, Modifiers and Manipulators', *Mol Plant Microbe Interact,* 36 (12), 754-63.
Wang, S., et al. (2017), 'Delivery of cytoplasmic and apoplastic effectors from Phytophthora infestans haustoria by distinct secretion pathways', *New Phytol,* 216 (1), 205-15.
Wang, Z., et al. (2023d), 'A Phytophthora infestans RXLR effector targets a potato ubiquitin-like domain-containing protein to inhibit the proteasome activity and hamper plant immunity', *New Phytol,* 238 (2), 781-97.
Wang., et al. (2020), 'Effector gene silencing mediated by histone methylation underpins host adaptation in an oomycete plant pathogen', *Nucleic Acids Res,* 48 (4), 1790-99.
Win, J., et al. (2012), 'Sequence divergent RXLR effectors share a structural fold conserved across plant pathogenic oomycete species', *PLoS Pathog,* 8 (1), e1002400.
Win, J., et al. (2007), 'Adaptive evolution has targeted the C-terminal domain of the RXLR effectors of plant pathogenic oomycetes', *Plant Cell,* 19 (8), 2349-69.
Witek, K., et al. (2016), 'Accelerated cloning of a potato late blight-resistance gene using RenSeq and SMRT sequencing', *Nat Biotechnol,* 34 (6), 656-60.
Witek, K., et al. (2021), 'A complex resistance locus in Solanum americanum recognizes a conserved Phytophthora effector', *Nat Plants,* 7 (2), 198-208.
Wood, K. J., et al. (2020), 'Effector prediction and characterization in the oomycete pathogen Bremia lactucae reveal host-recognized WY domain

proteins that lack the canonical RXLR motif', *PLoS Pathog,* 16 (10), e1009012.
Wrather, J. A and Koenning, S.R. (2006), 'Estimates of Disease Effects on Soybean Yields in the United States 2003 to 2005', *JOURNAL OF NEMATOLOGY,* 38.
Wu, Pei-Ying., et al. (2003), 'A conserved catalytic residue in the ubiquitin-conjugating enzyme family', *The EMBO Journal,* 22.
Xiong, Q., et al. (2014), 'Phytophthora suppressor of RNA silencing 2 is a conserved RxLR effector that promotes infection in soybean and Arabidopsis thaliana', *Mol Plant Microbe Interact,* 27 (12), 1379-89.
Xu, C., et al. (2021), 'Histone deacetylase 5 deacetylates the phosphatase PP2A for positively regulating NF-kappaB signaling', *J Biol Chem,* 297 (6), 101380.
Yang and Gabriel, DEAN. W. (1995), 'Intragenic Recombination of a Single Plant Pathogen Gene Provides a Mechanism for the Evolution of New Host Specificities', *JOURNAL OF BACTERIOLOGY,* 177.
Yang, Sugio, Akiko., and White, Frank. F. (2005), 'Avoidance of Host Recognition by Alterations in the Repetitive and C-Terminal Regions of AvrXa7, a Type III Effector of Xanthomonas oryzae pv. oryzae', *MPMI,* 18.
Yang, B., et al. (2017), 'Distinct regions of the Phytophthora essential effector Avh238 determine its function in cell death activation and plant immunity suppression', *New Phytol,* 214 (1), 361-75.
Yang, B., et al. (2019), 'The Phytophthora sojae RXLR effector Avh238 destabilizes soybean Type2 GmACSs to suppress ethylene biosynthesis and promote infection', *New Phytol,* 222 (1), 425-37.
Ye, W., et al. (2016), 'Sequencing of the Litchi Downy Blight Pathogen Reveals It Is a Phytophthora Species With Downy Mildew-Like Characteristics', *Mol Plant Microbe Interact,* 29 (7), 573-83.
Yu, D. S., et al. (2024), 'The structural repertoire of Fusarium oxysporum f. sp. lycopersici effectors revealed by experimental and computational studies', *Elife,* 12.
YU, LLOYD M. (1995), 'Elicitins from Phytophthora and basic resistance in tobacco', *PNAS,* 92.
Yuan, M., et al. (2021), 'PTI-ETI crosstalk: an integrative view of plant immunity', *Curr Opin Plant Biol,* 62, 102030.
Zess, E. K., et al. (2022), 'Regressive evolution of an effector following a host jump in the Irish potato famine pathogen lineage', *PLoS Pathog,* 18 (10), e1010918.
Zhang, F., et al. (2021), 'Genome Analysis of Two Newly Emerged Potato Late Blight Isolates Sheds Light on Pathogen Adaptation and Provides Tools for Disease Management', *Phytopathology,* 111 (1), 96-107.
Zhang, L., et al. (2014), 'Fungal endopolygalacturonases are recognized as microbe-associated molecular patterns by the arabidopsis receptor-like protein RESPONSIVENESS TO BOTRYTIS POLYGALACTURONASES1', *Plant Physiol,* 164 (1), 352-64.

Zhang, P., et al. (2019), 'The WY domain in the Phytophthora effector PSR1 is required for infection and RNA silencing suppression activity', *New Phytol,* 223 (2), 839-52.
Zhang, Z., et al. (2024), 'Complete telomere-to-telomere genomes uncover virulence evolution conferred by chromosome fusion in oomycete plant pathogens', *Nat Commun,* 15 (1), 4624.
Zheng, X., et al. (2018), 'Phytophthora infestans RXLR effector SFI5 requires association with calmodulin for PTI/MTI suppressing activity', *New Phytol,* 219 (4), 1433-46.
Zheng, X., et al. (2014), 'Functionally redundant RXLR effectors from Phytophthora infestans act at different steps to suppress early flg22-triggered immunity', *PLoS Pathog,* 10 (4), e1004057.
Zhou, J., et al. (2018), 'Regulation of Arabidopsis brassinosteroid receptor BRI1 endocytosis and degradation by plant U-box PUB12/PUB13-mediated ubiquitination', *Proc Natl Acad Sci U S A,* 115 (8), E1906-E15.
Zhu, X., et al. (2023), 'Phytophthora sojae effector PsAvh113 associates with the soybean transcription factor GmDPB to inhibit catalase-mediated immunity', *Plant Biotechnol J,* 21 (7), 1393-407.
Zipfel, C., et al. (2006), 'Perception of the bacterial PAMP EF-Tu by the receptor EFR restricts Agrobacterium-mediated transformation', *Cell,* 125 (4), 749-60.

Appendix

Table S1 Primers used for cloning PmRxLR1, Pm15069, PITG_10341 and PITG_10347.

Primer name	Sequence	Purpose in this study
10341-F	ATGATGCGTCTCTTTTCAGTCGTATTGCTG	Clone the gene
10341-R	CTATAAAAATGGTAAATTTAGTGATAAGCT	Clone the gene
10347-F	ATGATGCATCTCTTTTCAGTCGTATTGCTG	Clone the gene
10347-R	TCAGTTTAGCT(L)WYTGAATTGCGTGCGTAA	Clone the gene
PmRxLR1-F	ATGGCCTCGGTCGAGTCGCTTTCATTTCGC	Clone the gene
PmRxLR1-R	TCAATTTAGTT(L)WYCGAATTGCGCACGTAG	Clone the gene
Pm15069-F	ATGATGCATCTCTTTTCAGTCGTATTGCTG	Clone the gene
Pm15069-R	TCACGAAGCGCCAACCAACGTTTCGTCTGC	Clone the gene

Table S2 Constructs used in this thesis.

Gene	Made by	Construct name	Tag	Antibiotic resistance
PITG_15038	H.L	pGWB514	GFP	Hygromycin/Rif
PITG_15105	Y.L	pGWB514	GFP	Hygromycin/Rif
PITG_19307	Y.L	pGWB514	GFP	Hygromycin/Rif
PITG_23035	H.L	pGWB514	GFP	Hygromycin/Rif
PITG_10341	Y.L	pICSL86955OD	GFP	Kan/Rif
PITG_10347	Y.L	pICSL86955OD	GFP	Kan/Rif
Pm15069	Y.L	pICSL86955OD	GFP	Kan/Rif
PmRxLR1	Y.L	pICSL86955OD	GFP	Kan/Rif
PsAvh145	Y.L	pICSL86955OD	GFP	Kan/Rif
AtUBC4	Y.L	pICSL86977OD	mCherry	Kan/Rif
AtUBC4	Y.L	pICSL86977OD	mCherry	Kan/Rif
AtUBC5	Y.L	pICSL86977OD	mCherry	Kan/Rif
AtUBC5	Y.L	pICSL86977OD	mCherry	Kan/Rif
AtUBC6	Y.L	pICSL86977OD	mCherry	Kan/Rif
AtUBC6	Y.L	pICSL86977OD	mCherry	Kan/Rif
AVRcap1b	M.P.C	pICH86988	GFP	Kan/Rif
PITG_04388	Y.L	pICSL86977OD	GFP	Kan/Rif
PITG_07630	Y.L	pICSL86977OD	GFP	Kan/Rif
PITG_10116	Y.L	pICSL86977OD	GFP	Kan/Rif
PITG_12761	Y.L	pICSL86977OD	GFP	Kan/Rif
PITG_12791	Y.L	pICSL86977OD	GFP	Kan/Rif
PITG_14685	Y.L	pICSL86977OD	GFP	Kan/Rif
PITG_15110	Y.L	pICSL86977OD	GFP	Kan/Rif
PITG_15114	Y.L	pICSL86977OD	GFP	Kan/Rif
PITG_16195	Y.L	pICSL86977OD	GFP	Kan/Rif
PITG_16195	Y.L	pICSL86977OD	GFP	Kan/Rif
PITG_16844	Y.L	pICSL86977OD	GFP	Kan/Rif
PITG_17309	Y.L	pICSL86977OD	GFP	Kan/Rif
PITG_17316	Y.L	pICSL86977OD	GFP	Kan/Rif
PITG_19302	Y.L	pICSL86977OD	GFP	Kan/Rif

PITG_19307	Y.L	pICSL86977OD	GFP	Kan/Rif
PITG_21740	Y.L	pICSL86977OD	GFP	Kan/Rif
PITG_23036	Y.L	pICSL86977OD	GFP	Kan/Rif
PITG_23036△^{45}	Y.L	pICSL86977OD	GFP	Kan/Rif
PITG_23036△^{5}	Y.L	pICSL86977OD	GFP	Kan/Rif